University of Alberta
Department of Civil &
Environmental Engineering

Structural Engineering Report No. 255

STRENGTH AND BEHAVIOUR OF MULTI-ORIENTATION FILLET WELD CONNECTIONS

by

Logan J. Callele

Gilbert Y. Grondin

and

Robert G. Driver

March, 2005

Strength and Behaviour of Multi–Orientation Fillet Weld Connections

by

Logan J. Callele

Gilbert Y. Grondin

and

Robert G. Driver

Structural Engineering Report No. 255

Department of Civil and Environmental Engineering
University of Alberta
Edmonton, Alberta, Canada

February 2005

ABSTRACT

The fact that the difference in deformation ductility can be quite large for welds of different orientations could have a significant impact on the behaviour of connections that combine fillet welds of multiple orientations (MOFW connection). Because of the difference in deformation ductility, there is potential for MOFW connections to fail before the full capacity of all of the welds in the connection reach their full capacity. A test series on welded lapped splice connections containing a transverse weld in combination with either longitudinal or 45° welds was conducted to investigate the effect of weld ductility on MOFW connections. The MOFW connection's capacity is dependent on whether or not the connection will undergo enough deformation in order to mobilize the full capacities of each of the weld segments. The MOFW tests conducted indicate a that a strength lower than the sum of the strengths of the individual weld segments is achieved. A method that incorporates fillet weld load deformation response and addresses the differences in ductilities is presented. This method yields a prediction of any MOFW connection's capacity. A reliability analysis completed for this method indicates that it results in an acceptable safety index.

ACKNOWLEDGEMENTS

Funding for this research project was provided by the Natural Sciences and Engineering Research Council of Canada and the American Institute of Steel Construction.

The assistance of Mr. Andre Blanchard, undergraduate student in the Department of Civil & Environmental Engineering of the University of Alberta, with the testing of the complementary specimens presented in this report is acknowledged.

TABLE OF CONTENTS

LIST OF TABLES

LIST OF FIGURES

LIST OF SYMBOLS

A_{throat}, A_w	Theoretical throat area of the weld (mm^2)
a_i	Weld response equation coefficient
CRF	Combination reduction factor
CRF(θ)	Represents an equation that predicts the combination reduction factor for any fillet weld orientation, θ.
CRF_X^Y	Combination reduction factor for a MOFW connection with critical segment orientation "Y" and non-critical segment orientation "X"
CRF_X^{90}	Combination reduction factor for a MOFW connection with a transverse fillet weld segment and a non-critical segment orientation "X"
d	Average measured weld leg size (mm)
d*	Adjusted fillet weld leg size (mm)
MPL	The main plate leg is the fillet weld leg that is on the main plate of the specimen (mm)
LPL	The lap plate leg is the fillet weld leg that is on the lap plate of the specimen (mm)
MTD	Minimum throat dimension
MOFW	Multi-orientation fillet weld
SOFW	Single orientation fillet weld
Normalized P_m/A_{throat}	The value of the term (P_m/A_{throat}) divided by the ultimate tensile strength of the weld metal
P_m	Maximum applied load (kN)
R_{ult}	Maximum fillet weld capacity (kips/in.)
R	Capacity of a fillet weld that has undergone a certain deformation (kips/in.)
$R_{wl.}$	Nominal strength of a longitudinal fillet weld

R_{wt}	Nominal strength of a transverse fillet weld with no increase in strength because of orientation
V_G	Coefficient of variation for the measured-to-nominal theoretical throat area of the weld
V_{M1}	Coefficient of variation for the measured-to-nominal ultimate tensile strength of the filler metal
V_{M2}	Coefficient of variation for the measured-to-predicted ultimate shear strength of the filler metal
V_P	Coefficient of variation for the test-to-predicted weld capacity
V_R	Coefficient of variation for the resistance of the weld
V_θ	Shear strength of a fillet weld of any orientation, θ
V_o	Shear strength of a longitudinal fillet weld
$\frac{P_\theta}{P_{u\theta}}$	Fraction of the strength that a fillet weld of any orientation is at
X_u	Nominal ultimate tensile strength of the filler metal (MPa)
α_R	Coefficient of separation
β	Reliability index
Δ	Fillet weld deformation given in millimetres except for Section 2.3.1 where it is given in inches
Δ_f	Fillet weld deformation at weld fracture (mm)
Δ_{ult}	Fillet weld deformation at ultimate load (mm)
Δ_{Max}	Maximum fillet weld deformation (inch)
μ	Regression coefficient used to characterize fillet weld response
λ	Regression coefficient used to characterize fillet weld response

θ	Angle between the axis of the fillet weld and the direction of the applied load (degrees)
ρ	Normalized weld deformation
ρ_G	Bias coefficient for the theoretical weld throat area
ρ_{M1}	Bias coefficient for the ultimate tensile strength of the filler metal
ρ_{M2}	Bias coefficient for the ultimate shear strength of the filler metal
ρ_P	Mean test-to-predicted weld capacity
ρ_R	Bias coefficient for the resistance of the weld
τ_u	Measured ultimate shear strength for a longitudinal fillet weld (MPa)
ϕ	Resistance factor
ϕ_w	Weld resistance factor
ϕR	A factored resistance
αD	A factored load effect
Φ_β	Adjustment factor for the weld resistance factor
σ_{UTS}	Tensile strength of the weld metal

CHAPTER 1

INTRODUCTION

1.1 Background

The behaviour of fillet weld connections has been extensively researched over the past half century. This research has focused upon fillet weld connections containing fillet welds with only one orientation (angle between the line of action of the applied load and the axis of the fillet weld). The two most common fillet weld configurations are transverse (90°) and longitudinal (0°) fillet welds. Many tests on fillet weld connections of different orientations have shown that transverse and longitudinal fillet welds define the bounds of fillet weld strength and ductility. The transverse weld occupies the upper bound on strength but the lower bound on ductility, whereas the longitudinal weld represents the lower bound on strength but the upper bound on ductility.

Both the Canadian and American design standards, S16–01 (CSA, 2001) and LRFD 1999 (AISC, 1999) recognize the effect of weld orientation on weld strength. Work by Miazga and Kennedy (1989) and Lesik and Kennedy (1990) has led to both design standards recognizing that transverse fillet welds are 50% stronger than longitudinal fillet welds.

The work of Miazga and Kennedy (1989) was conducted using test specimens prepared with the shielded metal arc welding (SMAW) process and a filler metal without toughness requirement. Research by Ng *et al.* (2004b) and Deng *et al.* (2003), demonstrated that the current design equations provide an adequate level of safety for specimens prepared with the much more common flux cored arc welding (FCAW) process. However this research has only considered connections with single orientation fillet welds (SOFW).

Most of the fillet weld research has focused on single orientation welded connections with little research on connections containing fillet welds in multiple orientations. Joints with welds in multiple orientations are referred to herein as a multi-orientation fillet weld (MOFW) connections. Both the Canadian design standard and the American specification offer guidance on the design of connections which contain fillet welds of a single orientation. There is also some guidance offered on the design of eccentrically loaded fillet weld connections that contain welds in different directions within the same joint. However, neither the Canadian design standard nor the American specification offers clear guidance regarding the design of concentrically loaded MOFW connections. It is not clear whether or not the design equation that applies to single orientation fillet welded connections can be used to estimate the capacity of the connection by summing the capacities (as estimated by the design equation) of each segment (a portion of the fillet weld that has only a single orientation). Thus it seems that both research on and guidance for the design of MOFW connections is lacking.

When fillet welds of different orientations are combined in a MOFW connection the question arises as to whether the strongest, but least ductile, weld segment has sufficient ductility to develop the full strength of the other weld segments in the connection. For example, in a MOFW connection that combines both transverse and longitudinal fillet welds the transverse welds have significantly less ductility than the longitudinal welds, and this difference in ductility may mean that there is not sufficient ductility to develop the full capacity of the longitudinal welds. This strength and compatibility issue has been investigated in the analysis of eccentrically loaded weld groups. There have been two major research programs that investigated the behaviour and strength of eccentrically loaded weld groups: earlier work by Butler *et al.* (1972), which was later modified by Lesik and Kennedy (1990). Both research programs made use of weld load versus deformation curves obtained from tests on joints with welds in a single orientation and the method of instantaneous centre of rotation to calculate the ultimate capacity of eccentrically loaded joints. The two different fillet weld response curves proposed in these two research programs lead to significantly different capacities of concentrically loaded MOFW joints. This is discussed in more detail in Chapter 2.

1.2 Research Objectives and Scope

This research project is the third phase of a research program conducted at the University of Alberta to investigate the behaviour of fillet welds. In the first phase, Ng *et al.* (2004b) found that the design assumption that transverse fillet welds are 50% stronger than longitudinal fillet welds provided an acceptable level of safety for a variety of welding processes and electrode classifications. Deng *et al.* (2003) extended the work by Ng *et al.* (2004b) in the second phase to include two other weld orientations; 0° and 45°. More detail on both of these research programs is presented in Chapter 2. The work conducted in the first two phases of this research program indicated that the fillet weld design equation used in S16–01 (CSA, 2001) and LRFD 1999 (AISC, 1999) provide an adequate safety margin for connections that contain a single fillet weld orientation. However, the first two phases of the research program also indicated that fillet weld ductility can vary substantially.

This third phase of the research program was designed to investigate the strength and behaviour of welded joints where more than one fillet weld orientation are combined in a joint. More specifically, this research program investigates whether the least ductile segment in a concentrically loaded connection can deform sufficiently to develop the full strength of the more ductile segments. It also provides specific guidance on how to estimate the capacity of a concentrically loaded MOFW connection.

To investigate the capacity and behaviour of MOFW connections, 31 double lap-spliced connections that combined transverse welds with either longitudinal welds or 45° welds were tested. In addition, nine longitudinal and three transverse fillet weld connections were tested to define the fillet weld response curves required for the analysis of the MOFW connections. Several parameters were varied during testing in order to characterize their effect on the overall connection capacity: (1) fillet weld leg size, (2) number of weld passes, (3) fillet weld continuity at the corners, (4) fillet weld length, and (5) stress state of connection plates (yielded or elastic).

1.3 Units Used in this Report

SI units are used throughout this document with the exception of filler metal designation, which uses imperial units as implemented in the AWS classification. This exception was made because of the wide use of the AWS classification in industry.

CHAPTER 2

LITERATURE REVIEW

2.1 Introduction

Over the last several decades the behaviour of fillet welds has been extensively researched. In spite of this, there has been little work completed that investigates the behaviour of concentrically loaded multi–orientation fillet weld (MOFW) connections. A MOFW connection is a connection with a weld group that contains weld segments with different orientations. A segment is a portion of the weld group with only one orientation. This literature review will focus on fillet weld connection research conducted at the University of Alberta and the current North American design practice for concentrically loaded MOFW connections. The reader is referred to the literature review by Deng *et al.* (2003) for a summary of other fillet weld research.

2.2 Research on Concentrically Loaded Fillet Welded Joints

Although there has been extensive experimental research on concentrically loaded fillet weld connections only four research programs, Miazga and Kennedy (1989), Lesik and Kennedy (1990), Ng *et al.* (2004a), Deng *et al.* (2003) that investigated the behaviour of single orientation fillet weld (SOFW) connections, will be discussed here. Several researchers, including the aforementioned researchers from the University of Alberta, have found that the strength of SOFW connections increases with increasing angle between the axis of the weld and the line of action of the applied force, with the range in strength being bounded by longitudinal welds (lower) and transverse welds (upper). Test data from all these research programs will be used in the analysis of the MOFW test results of the current research. Research by Manuel and Kulak (2000) contains some information regarding the behaviour of MOFW connections and will be discussed here as well.

2.2.1 Miazga and Kennedy (1989)

Forty-two tests were carried out on fillet welded lap spliced connections (Miazga and Kennedy (1989)). The welds were fabricated using the shielded metal arc welding (SMAW) process and E7014 electrodes. Seven different fillet weld orientations were tested. Both strength and ductility of the welds were recorded. The plates forming the connections were composed of CAN/CSA-G40.21 300W steel and were designed to remain elastic. An analytical method was developed to predict the capacity of the fillet welds. This analytical method was later simplified by Lesik and Kennedy (1990) and adopted by both the Canadian (CAN/CSA S16.1-94) and American (AISC Load and Resistance Factor Design 1999) design standards, as will be discussed later.

2.2.2 *Ng et al. (2004a)*

The recent experimental investigation conducted by Ng *et al.* (2004a) has provided much information on the response of transverse fillet welds. A total of 102 transverse fillet weld lap spliced specimens were prepared using primarily the flux cored arc welding (FCAW) process, though nine specimens were prepared with the SMAW process in order to provide a direct comparison with the test results of Miazga and Kennedy (1989). Several parameters that were thought to influence the strength and/or the ductility of fillet weld connections were investigated by Ng *et al.*: (1) effect of filler metals with and without a toughness requirement, (2) variability between steel fabricators, (3) effect of electrode manufacturer, (4) effect of weld size and number of passes, (5) effect of root notch orientation, (6) effect of plate yielding, and (7) effect of test temperature.

In order to investigate these parameters, five different electrode types were used: E7014, E70T-4, E70T-7, E70T7-K2 and K71T8-K6. It was found that fillet welds fabricated with toughness requirements were more ductile than welds fabricated with filler metal without toughness requirements. Two different weld sizes were tested by Ng *et al.* (2004a), 6 mm (one pass) and 12 mm (three pass), and it was found that proportionally, the 6 mm welds were significantly stronger than the 12 mm welds, though the 6 mm welds showed somewhat less ductility.

One common feature of all of the specimens tested by Ng *et al.* (2004a) is that the connection main plates did not remain elastic, which was not the case for the fillet weld specimens tested by Miazga and Kennedy (1989).The weld deformations measured by Ng *et al.* (2004a) were significantly larger than those recorded by Miazga and Kennedy (1989) for transverse welds. It is believed that the effect of plate yielding had a significant impact on the large ductilities observed by Ng *et al.* (2004a). As such, the deformations recorded by Ng *et al.* (2004a) will be compared with the deformations of the transverse fillet weld specimens of this research program, all of which had main plates that remained elastic.

2.2.3 *Deng et al. (2003)*

Eighteen lap spliced fillet weld specimens were tested as part of the research program conducted by Deng *et al.* (2003). The specimens were prepared using the FCAW technique, with three different electrode classifications: E70T-4, E70T-7, and E71T8-K6. Specimens with both longitudinal and 45° fillet welds were tested to complement the test program reported by Ng *et al*. (2004a). However, unlike the test specimens of Ng *et al*. (2004a), all of the specimens had plates that remained elastic.

Deng *et al*. (2003) reported that the variation in filler metal classification and toughness requirements had no significant effect on fillet weld strength. However, like Ng *et al*. (2004a), the welds fabricated using electrodes with a toughness requirement were more ductile than welds fabricated using electrodes without a toughness requirement. As expected, the strength of fillet welds was seen to increase with increasing loading angle or orientation. However, the effect of orientation on weld ductility was not as expected since Deng *et al*. (2003) observed larger ductilities for the 45° specimens than the transverse specimen ductilities observed by Ng *et al*. (2004b). Again, the influence of plate yielding is believed to account for this unexpected result.

Together, the test programs of Deng *et al*. (2003) and Ng *et al*. (2004b) investigated the impact of weld classification, toughness, fabricator and leg size on the strength of fillet welds. It was found that the fillet weld design equation currently used in North America provides an adequate level of safety for SOFW.

2.2.4 Manuel and Kulak (2000)

Research conducted by Manuel and Kulak (2000) on connections that combine bolts and welds suggests that longitudinal welds contribute approximately 85% of their capacity to the connection strength when combined with transverse welds and bolts. The contribution of longitudinal segments is thus expected to be only 85% of their capacity as would be obtained if the connection were composed only of longitudinal segments. The value of 85% comes from an average of four tests on connections that combined 520 mm of transverse weld and 560 mm of longitudinal welds with four structural 19 mm (3/4 in.) bolts. The authors attributed the reduction in weld segment contribution from the expected SOFW capacity to the ductility incompatibility effect, which will be explained later.

2.3 Design Provisions

Currently, both the Canadian and American design standards provide guidance on the design of both weld group and SOFW connections. However, both S16–01 (CSA, 2001) and AISC LRFD (Load and Resistance Factor Design) 1999 (AISC, 1999) give no explicit guidance on the design of concentrically loaded MOFW connections. This should soon change as design provisions are being proposed for the 2005 LRFD AISC specification that will give guidance on the design of concentrically loaded MOFW connections that combine longitudinal and transverse welds only (Duncan, 2004; AISC, 2004). However, before presenting these proposed provisions, a review of the current standards will be presented.

Work by Lesik and Kennedy (1990) led to the following equation, which is incorporated into both S16–01 and AISC LRFD 1999:

$$\frac{V_\theta}{V_o} = 1.0 + 0.5\sin^{1.5}(\theta) \tag{2.1}$$

where V_θ is the shear strength of a fillet weld at an angle θ from the line of action of the applied load, and V_o is the shear strength of a longitudinal weld. This equation is an approximation of the rational approach proposed by Miazga and Kennedy (1989). In addition to the above strength equation, Lesik and Kennedy (1990) developed equations that describe the deformation of a fillet weld at both its ultimate capacity and at fracture. These equations are presented in Section 2.3.2. The three relationships proposed by Lesik and Kennedy were used to evaluate the capacity of eccentrically loaded fillet weld connections. They used the method of instantaneous center of rotation, used earlier by Butler *et al.* (1972), except that Lesik and Kennedy (1990) used different equations from Butler *et al.* (1972) to describe the fillet weld ultimate capacity, deformation, and response. Both the CISC Steel Design Handbook (CISC, 2004) and AISC LRFD 1999 use the procedure described by Lesik and Kennedy (1990) for the calculation of the strength of eccentrically loaded welded connections; however, the CISC Steel Design Handbook presents a description of the work of Butler and Kulak as a preamble for the eccentrically loaded welded joint design tables, when in fact the numbers presented in the design tables are calculated using the three equations developed by Lesik and Kennedy (1990). In light of this ambiguity, both methods will be reviewed here so that their differences may be examined.

2.3.1 Butler, Pal and Kulak (1972)

The procedure used by Butler *et al.* (1972) to calculate the capacities of eccentrically loaded fillet weld connections is called the method of instantaneous center of rotation. This method can also be used for calculating the capacity of eccentrically loaded bolted connections. For the purpose of this literature review it is not necessary to completely review the method of instantaneous center of rotation, a detailed summary is presented by several others including Butler *et al.* (1972), Tide (1980), and Lesik and Kennedy (1990). Rather, it is more important to review the equations used by Butler *et al.* (1972) for the description of fillet weld strength, deformation, and response. The work by Butler and Kulak (1971) forms the basis for the description of these three fillet weld parameters. The three fillet weld parameters are described using the following equations:

$$R_{ult.} = \frac{10+\theta}{0.92+0.0603\theta} \tag{2.2}$$

$$\Delta_{max} = 0.225\times(\theta+5)^{-0.47} \tag{2.3}$$

$$\mu = 75e^{0.0114\theta} \tag{2.4}$$

$$\lambda = 0.4e^{0.0146\theta} \tag{2.5}$$

$$R = R_{ult}(1-e^{-\mu\Delta})^{\lambda} \tag{2.6}$$

where R_{ult} is the predicted capacity of a fillet weld of orientation θ (expressed in degrees) given in kips/inch. Equation 2.3 predicts the ultimate deformation of fillet welds (in inches) for any angle θ. Equation 2.6 is used to predict the response of a fillet weld segment that has undergone a deformation Δ (in inches). The terms μ and λ are regression coefficients used to fit Equation 2.6 to the test data, and R is the load (given in kips/inch) that is mobilized by the deformation Δ. The values given by Equations 2.2 to 2.6 are derived from specimens prepared with single pass 6.4 mm (1/4 inch) fillet welds from E60XX electrodes.

2.3.2 Lesik and Kennedy (1990)

The method of instantaneous center of rotation was also used by Lesik and Kennedy (1990) in the calculation of capacities of eccentrically loaded fillet weld connections. However, as stated previously, Lesik and Kennedy (1990) use different equations to describe the fillet weld capacity, deformation, and response. These equations were derived from the test results of Miazga and Kennedy (1989). The equations take the following form:

$$P_{u\theta} = 0.67 X_u A_w (1.0 + 0.5 \sin^{1.5}(\theta)) \tag{2.7}$$

$$\frac{\Delta_{ult}}{d} = 0.209(\theta + 2)^{-0.32} \tag{2.8}$$

$$\frac{\Delta_f}{d} = 1.087(\theta + 6)^{-0.65} \tag{2.9}$$

$$\frac{P_\theta}{P_{u\theta}} = -13.29\rho + 457.32\rho^{1/2} - 3385.9\rho^{1/3} + 9054.29\rho^{1/4} - 9952.13\rho^{1/5} + 3840.71\rho^{1/6} \tag{2.10}$$

when $\rho \geq 0.0325$

$$\frac{P_\theta}{P_{u\theta}} = 8.23384\rho \tag{2.11}$$

when $\rho \leq 0.0325$

$$\rho = \frac{\Delta}{\Delta_{ult}} \tag{2.12}$$

Equation 2.7 predicts the capacity of a fillet weld segment in terms of the electrode tensile strength, X_u, the weld throat area, A_w, and the angle, θ. The constant 0.67 is the shear stress transformation factor adopted in S16-01. This constant is taken as 0.60 in the AISC LRFD specification. Equations 2.8 and 2.9 predict the deformations of the fillet weld at ultimate capacity and fracture, respectively. Lastly, Equations 2.10 and 2.11 are used to predict the response of the fillet weld as it undergoes a normalized deformation, ρ, taken as the ratio of weld deformation, Δ, to the ultimate deformation, Δ_{ult}, obtained from Equation 2.8. The American standard, AISC LRFD 1999, uses an approximation of Equations 2.10 and 2.11. The approximation, used for simplicity, takes on the following form:

$$\frac{P_\theta}{P_{u\theta}} = \left[\rho\left(1.9 - 0.9\rho\right)\right]^{0.3} \tag{2.13}$$

2.3.3 Implications on the Capacities of MOFW Connections

Both the Canadian and American standards have at different times in their history used both of the methods presented above. Because the two methods have such different implications on the capacity of MOFW connections, these implications will be explained in detail. The method of instantaneous center of rotation can be applied to the case of a MOFW connection that is concentrically loaded, i.e., for the special case of zero eccentricity. In this case, the method is greatly simplified and the capacity of the concentrically loaded MOFW connection is predicted using the following steps.

1) The least ductile weld segment in the weld group is identified.
2) The connection is assumed to reach its capacity at the ultimate capacity of the least ductile segment. Because of this assumption and compatibility, the deformations of the remaining segments are calculated to be exactly the same as the least ductile segments predicted deformation (see Equations 2.3 or 2.8, for example).
3) With all of the segment deformations calculated, the amount of load contributed to the connection capacity by each segment is determined using the fillet weld response equations, such as Equations 2.6, 2.10, 2.11, or 2.13. Here it is assumed that the instantaneous center of rotation is located at infinity (i.e., concentric loading).
4) The capacity of the concentrically loaded MOFW connection is the sum of contributions of all the segments that form the connection.

By considering an example of a MOFW connection that consists of transverse and longitudinal weld segments (referred to as a TL connection), the implications of the two methods on the strength of concentrically loaded MOFW connections becomes clear. The capacity of the TL MOFW connection is computed using the four steps previously described. The transverse weld is seen to be the least ductile segment in the TL connection. When the capacity of the TL connection is computed using the equations proposed by Butler and Kulak (1971) the contribution of the longitudinal weld is found to be 94% of its ultimate capacity (Equation 2.2). On the other hand, when the equations proposed by Lesik and Kennedy (1990) are used, the longitudinal weld is found to contribute 80% of its ultimate capacity (Equation 2.7). The calculations indicate that the longitudinal weld contributes less than its full capacity because the transverse weld lacks the ductility necessary to mobilize the ultimate capacity. This phenomenon is called the ductility incompatibility effect (see Figure 2.1). In Figure 2.1 the weld deformations, Δ, are divided by the fillet weld leg size, d, to give a non-dimensionalized deformation, Δ/d. The different fillet weld responses described by Butler and Kulak and Lesik and Kennedy are seen to predict significantly different contributions from the longitudinal weld.

2.3.4 AISC LRFD Draft Document Provisions for Concentric MOFW Connections

In the upcoming edition of the AISC LRFD specification, guidance on the design of concentrically loaded TL MOFW connections will be given (Duncan, 2004; AISC, 2004). The proposed guidance will take the following form:

$$\text{TL Connection Capacity} = R_{wl} + R_{wt} \text{ or } 0.85R_{wl} + 1.5R_{wt} \text{ (whichever is greater)} \quad (2.14)$$

Here, R_{wl} and R_{wt} are the nominal strengths of the longitudinal and transverse segments, respectively, without the orientation strength adjustment of Equation 2.1. The second part of Equation 2.14 assumes that the longitudinal segments contribute 85% of their ultimate capacity, whereas the first part of the equation assumes that the longitudinal segment contributes 100% of its capacity but the transverse segment's capacity is not increased because of its orientation as per Equation 2.1. These two parts of the equation seem to contradict each other because the first part ignores the increase in strength with orientation and the ductility incompatibility effect, while the second part takes both of these issues into consideration. The first part of the equation is also inconsistent with S16-01 and AISC LRFD 1999, both of which acknowledge, either explicitly or implicitly, the increase in strength with orientation and the ductility incompatibility effect. However, the second part of the equation, which predicts 85% of the longitudinal capacity is contributed to the TL connection capacity, which is seen to be between the value predicted by Butler and Kulak (94%) and Lesik and Kennedy (80%), but consistent with the value proposed by Manuel and Kulak (2000).

2.4 Summary and Conclusions

The literature review has shown that there has been no clear guidance on how to calculate the capacity of concentrically loaded MOFW connections. It is also seen that extending the work on eccentrically loaded fillet weld connections to concentric fillet weld connections can give large differences in connection capacities. In an attempt to deal with this problem, there is a proposal for the upcoming AISC LRFD specification, which will give guidance on the design of concentrically loaded MOFW connections that combine transverse and longitudinal fillet welds. However, the proposal seems inconsistent; one part of the equation agrees with Manuel and Kulak (2000) that the longitudinal weld will contribute 85% of its capacity, while the other part does not deal with the ductility incompatibility or the increase in strength for non-longitudinal welds. Because of this uncertainty about how to deal with concentrically loaded MOFW connections there is a need for a research in this area. The research should endeavour to provide clear guidance for the design of MOFW connections and assess whether the method used for eccentrically loaded connections can be safely extended to concentrically loaded connections that combined welds in various directions. It has also been demonstrated that different fillet weld responses can have significant implications in the calculation of concentrically loaded MOFW connection capacities. Several parameters have been shown to influence the response of single orientation fillet weld segments, such as weld leg size, number of passes, electrode type, etc. (Ng *et al.* 2004b; Deng *et al.* 2003) As MOFW connections' capacities are influenced by the fillet weld segment's response, the effect of these parameters on MOFW connections should also be investigated.

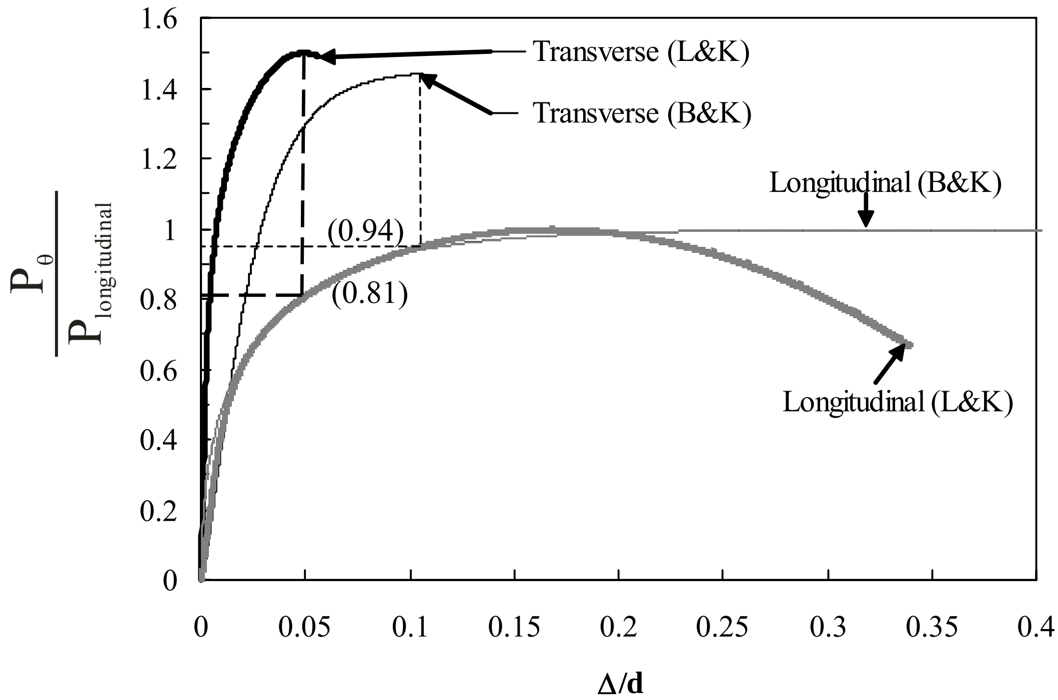

Figure 2.1 – Implications of Differences in Fillet Weld Response on the Capacity of MOFW Connections

CHAPTER 3

EXPERIMENTAL PROGRAM

3.1 Introduction

A total of 37 specimens were prepared and tested in this experimental program. The specimens were welded lap splice connections prepared with an E70T-7 electrode and the flux cored arc welding process. Both multi-orientation fillet weld specimens (MOFW) and single orientation fillet weld (SOFW) specimens were tested. A SOFW connection has only one weld orientation, whereas a MOFW connection is a weld group with more than one weld orientation. The orientation of a fillet weld is designated by the angle between the axis of the weld and the line of action of the applied load. In the following, a fillet weld segment in a MOFW connection consists of a fillet weld that has only one orientation. For example, two different types of MOFW connections were tested in this experimental program: MOFW connections composed of transverse and longitudinal segments and MOFW connections composed of transverse and 45° segments, as shown in Figures 3.1 and 3.2.

The MOFW test specimens are identified using an alphanumeric system. The specimen designations begin with either TL or TF, where TL indicates that the MOFW configuration consists of a combination of transverse and longitudinal weld segments and TF indicates that the connection consists of transverse and 45° segments. For the specimens containing transverse and longitudinal fillet welds, the nominal length of the longitudinal segment, given in millimetres, follows the TL. All the specimens incorporating 45° welds had two 62.2 mm long weld segments at 45° on each face (front and back). Other descriptors that follow the weld group configuration and longitudinal segment length are: "a" for an 8 mm single pass weld (the welds are nominally 12 mm by default, fabricated with 3 passes), "D" for welds discontinuous around the corner of the lap plate, and "SP" for single pass 12 mm welds.

The SOFW specimens are designated as either "T" for transverse or "L" for longitudinal. The nominal length of the longitudinal segments is added after the "L" for the longitudinal specimens. The descriptor "NY", which stands for no yielding, is added after the "T" for the transverse specimens. For both the SOFW and MOFW specimens, a dash and number between one and four follows the descriptors to indicate the test specimen number within a series of replicated specimens.

The test specimens fabricated for this research project were prepared in two consecutive summers. The specimens from sets TL50, TL50a, TF, and TFa were prepared during the summer of 2002. The remaining specimens were prepared during the summer of 2003. Both sets of test specimens were prepared by the same fabricator and same electrode classification, but from different spools.

3.2 Ancillary Tests

Six tension coupons were tested to establish the ultimate strength of the E70T-7 weld metal used in this research program. The specimens were fabricated using two different heats of electrodes. Three all-weld-metal tension coupons, with 50 mm gauge lengths, were fabricated in accordance with Clause 8 of ANSI/AWS A5.20 (AWS, 1995) for each electrode heat. Fillet weld specimens from sets TL50, TL50a, TF, and TFa were prepared using the E70T-7 electrode from heat 1 (prepared during 2002) and the remaining test specimens were prepared with the electrode from heat 2 (prepared during 2003).

3.3 Base Metal

The plate steel that was used in the preparation of the fillet weld specimens meets the requirements of ASTM A572 grade 50 steel and CAN/CSA-G40.21 350W. This grade of steel is suitable for welding but has no toughness requirement. Though five different plate thicknesses were used in preparing the test specimens fabricated during 2002, all of the plates of the same thickness were obtained from a single heat in order to minimize the variability in the test results. This is also true for the specimens fabricated during 2003.

3.4 Weld Metal

The specimens were prepared using the FCAW (Flux Cored Arc Welding) process. The AWS classification for the filler metal used is E70T-7. This type of filler metal is typically used in horizontal and flat positions and has a high deposition rate (AWS, 1995). The nominal tensile strength for E70T-7 electrodes is 480 MPa.

3.5 Test Parameters

3.5.1 Combination Weld Test Program

The objective of this research is to investigate the behaviour of MOFW connections. The most important parameter in the behaviour of MOFW connections is the ductility incompatibility effect, as discussed in Chapter 2. As such, the majority of the specimens were MOFW connections, with the SOFW connections being tested to assist in the analysis of the ductility incompatibility effect. However, three other test parameters were investigated: (1) number of passes/size of weld; (2) length of the longitudinal fillet weld; and (3) weld continuity around the corners of the lap plates. The third variable was included to investigate the influence of the interaction between the longitudinal weld and the transverse weld, such as propagation of cracks from the transverse to the longitudinal weld and the stress state at the intersection of the welds; this will be discussed in Chapter 5.

The effect of low temperature on fillet weld response was also part of the test parameters of this research program. Three TL100 specimens were tested at -50°C. Unfortunately, the specimens did not fail as expected. The lap plates of all three low temperature tests fractured rather than the fillet welds. Because the welds themselves did not fail in these specimens, the low temperature test results are not included in the analysis presented in Chapter 5. However, a discussion of the low temperature tests can be found in Appendix E.

3.5.2 Complementary Test Program

Results from SOFW tests were a necessary part of the analysis of the MOFW test results. SOFW tests results from Deng *et al.* (2003) and Ng *et al.* (2004a) were used in the analysis, but other test results were also required. These complementary tests were designed to complete the test results required for the analysis of the MOFW test data, and, therefore, had similar test parameters as given above. However, one unique parameter to the complementary tests is the effect of plate yielding on the weld deformation and strength. All of the test specimens of Ng *et al.* (2004a) yielded before the fillet welds fractured and larger than expected deformations were measured. It is believed that the stress state of the plates affects the fillet weld response. As such, the three transverse specimens tested here were prepared with plates that were designed to remain elastic. The longitudinal test specimens, as well as all the MOFW specimens, were also designed to have plates that remained elastic during testing. By using only test results from specimens that remained elastic, the SOFW results should then be directly applicable to the MOFW specimens.

3.6 Specimen Description

3.6.1 Combination Weld Tests

Thirty-one MOFW connections were fabricated and tested. Every specimen in the test program was fabricated as a double lap splice connection between two steel plates. The lap plates and main plates were welded together with an E70T-7 welding electrode. The physical dimensions of the specimens are shown in Figures 3.1 and 3.2 along with Table 3.1.

Once the specimens were fabricated they were inspected visually for weld quality and conformance to the design specifications. A decision as to which welds would be reinforced for the TF specimens was made during the visual inspection. These specimens were fabricated so that both sides of the joint were identical. Whichever side of the lap plate was determined to have better weld quality was taken as the test weld and the other side was reinforced by adding an additional five to six weld passes.

Initially, 12 specimens were prepared in the summer of 2002: TL50-1,2,3; TL50a-1,2,3; TF-1,2,3; and TF-1,2,3. However, upon receiving these specimens it was noted that there was light grinding on the face of the fillet welds. A specimen showing typical grinding is shown in Figure 3.3. In order to assess the effect of the grinding, one more specimen from each of the four types listed above was fabricated without any grinding of the fillet welds. This is the reason why there are four specimens for each of the above four specimen types only.

3.6.1.1 TL Specimens

The welds on only one end of the lap plate of the TL specimens were tested. The joint configuration was designed so that the weld length on one side of the joint was larger than the weld length on the test side of the joint, as shown in Figure 3.1. This proportion of weld length forced the test welds to fail, thus minimizing the required instrumentation and weld size measurements.

A 3 mm gap was left between the main plates of all TL specimens. The gap facilitated sawing through the fillet weld at the intersection of the two main plates. The length of the test weld, designated as "D_T" in Figure 3.1, was established by the location of the saw cut.

Some TL specimens were fabricated with a weld discontinuity at the corners of the lap plate. This discontinuity, shown in Figure 3.4, was introduced to investigate the interaction between weld segments in the weld group, as mentioned in Section 3.5.

3.6.1.2 TF Specimens

In order to mitigate the effect of weld termination, run-off tabs were used. A saw cut through the weld and run-off tab was made to remove the run-off tabs after welding. The cut was parallel to the line of action of the applied load and adjacent to the edge of the main plate. The saw cut was necessary to define the length of the 45-degree segments on the TF specimens since the segments were welded onto both the main plate of specimen and the run off tabs. Figures 3.5 and 3.6 illustrate the saw cut and the run off tabs.

3.6.2 Complementary Test Specimens

The complementary tests included longitudinal and transverse SOFW tests. Nine longitudinal and three transverse weld specimens were tested. The dimensions of the transverse weld specimens are given in Figure 3.7, and the dimensions of the longitudinal specimens are given in Figure 3.8 and Table 3.2.

Run-off tabs were tack welded to the longitudinal weld specimens as shown in Figure 3.9 in order to ensure that there was no stop or start in the test region. The longitudinal weld specimen test region is shown in Figure 3.8. Once the specimens were welded, the welds were cut at the locations indicated in Figure 3.9 in order to define the length of the longitudinal welds. This procedure is similar to that adopted by Deng *et al.* (2003).

The transverse weld assemblies were welded with three passes to produce a nominal 12 mm leg size (see Figure 3.7). An assembly consisted of three specimens and edge strips as shown in Figure 3.7. Once the transverse weld assembly was prepared, the welds were inspected and the side of the assembly with the poorest weld quality was reinforced with five to six additional weld passes in order to force failure in the test welds. Three 76 mm transverse specimens were cut out of the assembly, as depicted in Figure 3.7. The specimens were cut using a water jet. The edges of the specimens were then milled smooth to remove any notches left in the specimen from the water jet cutting.

3.7 Pre-Test Measurements

Four types of measurements were taken to characterize the fillet welds before testing: shear leg size (MPL dimension), tension leg size (LPL dimension), throat dimension, and length of the fillet weld. The definitions of the MPL (Main Plate Leg) dimension and the LPL (Lap Plate Leg) dimension are shown in Figure 3.10. The shear and tension leg measurements, along with the throat measurements, were taken at different frequencies depending on the specimen, varying from a measurement every 14 mm to a measurement every 19 mm.

The shear and tension leg sizes of the fillet welds were measured using a specially fabricated device and callipers. The device, illustrated in Figure 3.11, was used to measure the shear leg size. It consisted of a base and mast, a collar attached to the mast, and a shaft, which was constrained to move horizontally by the collar. Callipers were used to measure the distances “d1” and “d2” shown in Figure 3.11. A similar device was used for measuring the tension leg, and it is shown in Figure 3.12. The error in these measurements is conservatively estimated as ±0.15 mm.

The measured weld sizes are presented in Tables 3.3 through 3.7. Tables 3.3 through 3.5 contain the weld measurements of the MOFW specimens, and Tables 3.6 and 3.7 contain the measurements for the SOFW specimens.

Because each MOFW specimen has three distinct fillet weld segments, one transverse weld segment and two non-transverse weld segments, the transverse weld segment is always referred to as Segment 2, and the non-transverse welded segments are referred to as Segments 1 and 3. Figure 3.13 shows which non-transverse segments are Segments 1 and 3. The values presented in Tables 3.3 through 3.5 for the shear and tension fillet weld leg sizes are averages taken over the entire weld segment. There were five measurements taken on the transverse segment of all MOFW specimens. Four measurements were taken on all non-transverse segments except the “TL100” specimens, which had eight measurements taken on each longitudinal segment. The measurements on all segments were equally spaced.

The shear leg, tension leg, and throat measurements are an average of eight evenly spaced measurements for the longitudinal specimens with 100 mm nominal test length, and ten evenly spaced measurements for the longitudinal specimens with 150 mm nominal test length. The measurements of the transverse welds are averages of eight evenly spaced measurements.

3.8 Instrumentation and Test Procedures

The specimens were placed in a universal testing machine and loaded in concentric tension until rupture of the fillet welds. The specimens were oriented so that their long axis was vertical and so that the test section was positioned below the reinforced section. This orientation facilitated the instrumentation of the specimens with linear variable differential transformers (LVDTs). The overall test setup and instrumentation for all the specimens can be seen in Figures 3.16 through 3.18.

Special LVDT brackets were mounted on the test specimens as shown in Figures 3.16 and 3.17. The brackets consisted of a clamp attached to a small steel plate of dimensions 75 mm x 20 mm x 2mm. The LVDTs were secured in place using the clamp. Also attached to the plate were steel anchors, located at the front of the plate, and a wheel and axle set, located at the back of the plate. The anchors were set in shallow punch marks in the main plate of the specimen. These punch marks were located within 1 mm to 3 mm of the toe of the fillet weld on all the transverse welded segments and the forty-five degree welded segments. For the longitudinal weld segments the punch marks were located at the corner of the lap plate where the longitudinal weld and transverse weld meet (see Figure 3.16). The brackets were kept anchored to the punch marks during the test using elastic bands wrapped around the specimens.

Special measures were required to ensure that the LVDT probe would be properly positioned during the entire test for the LVDTs that measured the deformation of the non-transverse weld segments. Small tabs, consisting of angle section, were tack welded to the face of the lap plate of the TF specimens to create a bearing surface so that the extension from the LVDTs would not slip during a test. These tabs (angle sections) are depicted in Figure 3.17.

The specimens containing longitudinal welds were fabricated with the fillet weld continuous across the 3 mm gap between the two main plates. Using hacksaws and abrasive grinding discs the welds were cut at a right angle to the applied load as discussed in Section 3.6.1.1. Shallow punch marks were set in the sides of the lap plate such that the punch marks were in the same plane as the weld cut (see Figure 3.16). An angle section (referred to as a tab) with steel anchors was secured to these punch marks by setting the anchors in the punch marks and clamping the angles to the lap plate. The extensions from the LVDT cores were then able to rest on the face of these tabs as shown in Figure 3.16.

The test setup for the complementary test specimens was the same as the test setup described in Deng *et al.* (2003). Figure 3.18 shows photographs of the instrumentation for both longitudinal and transverse specimens of the complementary testing program.

The gauge length over which the weld deformations were measured varied with each segment of weld. For the transverse and 45° fillet welds, the gauge length was taken as the distance between the punch marks and the face of the lap plate. The punch marks were placed within one to three millimetres of the toe of the weld so that the amount of plate deformation captured within the gauge length was kept to a minimum. The longitudinal fillet weld gauge length extended from the corner of the lap plate where the longitudinal and transverse welds meet to the end of the main plate where the welds were cut as shown in Figure 3.16.

The specimens were loaded in concentric tension until the rupture of a fillet weld(s) occurred. The specimens were loaded with a 6000 kN universal testing machine. Because of size limitations of the testing machine hydraulic grips, the specimens could be no wider than 152 mm.

The specimens were loaded quasi-statically under displacement control. During the test, the load and displacements measured by the LVDTs were recorded in real time. Once a single segment of fillet weld ruptured, the test was terminated. The instrumentation was removed after rupture of any fillet weld segment(s), and if the whole connection wasn't ruptured it was loaded until all the fillet welds in the test section had ruptured. It was necessary to pull the specimen apart so that the post fracture measurements could be completed

After fracture of the transverse segment on the TL specimens, the longitudinal segment was sometimes observed to have a crack propagated along only part of the length. This observation led to the observation that first the transverse weld would fail; then either the rest of the fillet welds, or combinations of segments of fillet welds, would fail. It is believed that the fracture of the transverse weld resulted in a sudden release in the strain energy associated with the transverse segments which caused the other welds to fail. Where a partially propagated crack was observed in the longitudinal segments, it is believed that the release of the strain energy was insufficient to cause the crack to propagate through the entire length.

3.9 Post – Fracture Measurements

Once the specimens had failed, several other measurements were taken to assess the following three characteristics of the failed welds: (1) fracture angle, (2) weld penetration, and (3) fractured throat. Figure 3.19(a) shows a typical weld profile compared with the triangular approximation. The weld root penetration and face reinforcement shown in Figure 3.19(a) both make the fractured throat size larger than predicted by the triangular approximation as can be seen in Figure 3.19(b). The three measurements listed above are shown in Figure 3.19(c) and help to characterize the actual weld profile. However, it should be noted that the fracture surface depicted in Figure 3.19 is a simplification of the observed fracture surface, which was highly irregular. The fracture angle typically varied considerably over the length of a segment and even at one location. Though measurements were attempted at four different locations along a segment, not all the measurements were possible at a location because of facture surface abrasion. The surface abrasion was especially significant for the longitudinal weld segments and resulted from extensive rubbing of the fracture surfaces when the specimens were pulled apart. Where this occurred the fracture angle and fractured throat measurements were often not possible. Figure 3.20 shows an example of the fracture surface distortion.

Table 3.1 – Nominal Dimensions of TL Specimens

Nominal Dimensions*	TL50	TL50a	TL50D	TL100	TL100SP	TL100D
l	457	457	610	610	610	610
t	44	44	51	70	70	70
D_T	51	51	51	102	102	102
D_R	102	102	102	152	152	152
Number of Passes	3	1	3	3	1	3
Nominal Fillet Weld Size, S	12	8	12	12	12	12
Number of specimens	4	4	3	3	3	3

***** All dimensions given in millimetres. See Figure 3.1 for the dimension definitions.

Table 3.2 – Nominal Dimensions and Details for the Longitudinal Weld Specimens

Nominal Dimensions*	L100-1,2,3	L100-4,5,6	L150-1,2,3
D_T	102	102	152
D_R	203	203	254
t	41	41	70
Number of Passes	3	1	3

***** All dimensions given in millimetres. See Figure 3.8 for the dimension definitions.

Table 3.3 – Mean Measured Weld Size of TF Specimens

Specimen	Segment*	Front			Back		
		MPL Leg Size (mm)	LPL Leg Size (mm)	Segment † Length (mm)	MPL Leg Size (mm)	LPL Leg Size (mm)	Segment † Length (mm)
TF-1	1	12.9	10.5	66.1	14.4	11.6	64.6
	2	14.2	11.6	62.8	13.7	12.3	60.9
	3	14.4	11.0	62.9	14.9	13.2	69.6
TF-2	1	12.4	13.6	66.2	12.5	12.6	60.8
	2	15.0	13.6	61.2	13.6	12.7	66.0
	3	13.2	13.7	63.2	13.5	12.5	62.7
TF-3	1	13.9	12.1	64.7	12.2	12.0	68.0
	2	13.5	11.8	65.0	13.1	11.6	62.1
	3	13.2	11.2	61.5	12.4	11.3	60.7
TF-4	1	14.3	11.7	63.6	14.8	12.5	62.0
	2	17.1	11.7	65.9	16.8	12.6	65.7
	3	13.7	10.8	58.2	15.4	12.5	60.9
TFa-1	1	9.4	8.7	56.8	8.4	7.5	66.8
	2	9.2	9.2	64.9	9.6	8.2	60.8
	3	9.0	8.8	68.2	9.1	8.4	64.2
TFa-2	1	9.4	8.2	61.4	8.4	7.5	60.6
	2	9.5	8.0	62.5	8.9	7.7	61.1
	3	9.6	8.8	64.0	9.0	7.1	67.1
TFa-3	1	9.0	8.3	57.9	8.9	8.1	65.5
	2	9.0	8.5	65.8	9.2	7.7	61.0
	3	8.8	8.1	67.4	9.1	8.2	65.9
TFa-4	1	9.3	9.6	62.4	8.5	9.4	61.5
	2	9.6	9.9	64.8	8.8	9.2	65.5
	3	8.5	9.3	61.3	8.4	7.4	60.0

* Refer to Figure 3.13 for the definition of the segment numbers.
† Refer to Figure 3.14 for the definition of the segment lengths.

Table 3.4 – Mean Measured Weld Size of TL Specimens (2002)

Specimen	Segment*	Front			Back		
		MPL Leg Size (mm)	LPL Leg Size (mm)	Segment Length (mm)	MPL Leg Size (mm)	LPL Leg Size (mm)	Segment Length (mm)
TL50-1	1	15.7	11.5	51.4	14.1	10.1	51.3
	2	16.4	12.3	76.2	16.0	11.0	76.1
	3	12.9	12.9	51.2	12.8	11.6	51.2
TL50-2	1	13.7	12.2	51.4	13.5	10.3	50.2
	2	15.2	11.9	76.4	13.5	11.9	77.0
	3	14.9	12.2	51.2	13.1	11.9	52.5
TL50-3	1	14.2	10.7	52.1	14.0	11.1	50.6
	2	15.3	12.8	76.3	15.3	11.8	76.7
	3	12.0	12.9	51.7	12.8	9.8	50.8
TL50-4	1	17.1	10.2	53.0	13.1	11.3	52.4
	2	18.3	11.0	78.4	15.8	11.2	76.6
	3	13.7	11.8	51.5	14.6	11.8	51.6
TL50a-1	1	9.6	7.8	51.0	8.4	7.4	50.9
	2	10.7	8.3	75.8	10.7	8.2	76.2
	3	9.2	8.4	51.2	8.6	8.5	52.1
TL50a-2	1	9.6	7.8	51.2	9.3	8.5	50.8
	2	10.7	8.3	76.2	11.3	8.2	76.8
	3	9.8	8.2	51.0	10.0	8.4	51.4
TL50a-3	1	8.4	7.6	50.1	9.0	9.2	50.2
	2	10.7	8.2	76.5	10.1	9.0	75.6
	3	9.7	8.0	51.8	9.7	8.3	50.3
TL50a-4	1	10.0	8.5	52.7	10.8	8.7	50.3
	2	11.8	9.1	78.3	12.3	7.9	78.2
	3	9.1	9.6	51.7	10.0	9.5	51.4

* Refer to Figure 3.13 for the definition of the segment numbers.

Table 3.5 – Mean Measured Weld Size of TL Specimens (2003)

Specimen	SEGMENT*	Front MPL Leg Size (mm)	Front LPL Leg Size (mm)	Front Leg Length (mm)	Back MPL Leg Size (mm)	Back LPL Leg Size (mm)	Back Segment Length (mm)
TL100-1	1	13.9	12.9	97.9	14.6	12.9	96.9
	2	17.1	12.4	76.6	17.5	13.0	77.0
	3	15.2	13.9	98.1	16.4	13.9	100.9
TL100-2	1	14.1	10.6	98.8	15.4	12.6	98.7
	2	14.6	11.0	78.0	16.7	11.9	75.6
	3	13.5	10.6	99.4	15.3	11.5	100.8
TL100-3	1	13.8	12.5	98.9	12.5	11.5	102.0
	2	16.8	12.6	77.2	15.7	10.8	76.0
	3	13.7	13.0	99.3	14.0	10.3	101.9
TL100SP-1	1	12.9	10.6	98.7	11.7	9.3	101.3
	2	12.2	9.3	76.8	12.8	9.7	76.7
	3	11.9	9.7	98.5	13.9	11.7	101.9
TL100SP-2	1	11.9	9.9	100.3	11.9	10.8	97.1
	2	12.2	10.1	75.4	13.9	9.7	74.6
	3	14.0	11.6	98.5	14.1	10.7	95.2
TL100SP-3	1	14.3	10.0	99.2	13.4	9.6	98.8
	2	13.5	10.9	78.3	13.7	9.4	77.9
	3	12.8	10.6	100.3	13.9	10.3	98.7

Specimen	SEGMENT	Front MPL Leg Size (mm)	Front LPL Leg Size (mm)	Front Leg Length (mm)	Back MPL Leg Size (mm)	Back LPL Leg Size (mm)	Back Segment Length (mm)
TL100D-2	1	12.8	11.4	94.7	13.4	11.7	93.7
	2	12.3	11.3	73.8	13.9	11.7	76.3
	3	13.3	9.5	91.8	12.7	11.8	95.4
TL100D-3	1	14.4	13.6	99.9	15.6	13.8	97.5
	2	14.0	13.1	75.2	14.3	11.8	73.5
	3	15.3	13.7	100.1	15.6	12.5	97.9
TL50D-1	1	15.5	12.4	47.8	15.2	13.5	47.4
	2	13.8	12.6	72.5	14.3	14.0	72.2
	3	13.5	13.3	47.0	13.4	13.1	45.8
TL50D-2	1	12.4	13.5	46.3	15.0	13.4	46.3
	2	14.0	12.2	71.1	15.4	12.7	74.2
	3	13.0	13.3	48.6	14.2	12.9	50.0
TL50D-3	1	12.2	14.1	47.6	16.9	12.7	52.5
	2	16.7	11.8	71.5	14.9	10.5	74.5
	3	15.4	11.6	48.8	14.4	10.8	52.5

* Refer to Figure 3.13 for the definition of the segment numbers.

Table 3.6 – Mean Longitudinal Weld Measurements

Specimen	Front								Back							
	Weld 1*				Weld 2*				Weld 3*				Weld 4*			
	MPL (mm)	LPL (mm)	Throat (mm)	Weld Length (mm)	MPL (mm)	LPL (mm)	Throat (mm)	Weld Length (mm)	MPL (mm)	LPL (mm)	Throat (mm)	Weld Length (mm)	MPL (mm)	LPL (mm)	Throat (mm)	Weld Length (mm)
L100 – 1	12.9	12.2	9.8	98.2	12.3	11.3	9.7	98.9	12.3	11.6	9.8	100.8	12.9	12.0	9.8	99.7
L100 – 2	14.7	12.6	11.0	99.3	14.2	10.9	10.9	98.2	13.1	11.7	10.6	99.6	13.8	10.6	9.1	100.0
L100 – 3	13.4	12.8	10.7	101.6	13.7	12.7	11.2	103.3	12.3	13.0	10.9	102.0	13.1	12.9	11.1	101.2
L100 – 4	12.3	8.9	9.3	99.5	12.6	9.7	9.5	97.8	12.0	9.1	8.4	99.2	12.6	10.0	10.2	100.2
L100 – 5	11.9	10.4	9.9	99.2	12.3	9.2	10.2	98.9	14.1	10.4	10.5	99.5	12.9	9.9	10.7	99.2
L100 – 6	11.1	10.8	10.2	100.7	11.2	10.8	10.2	102.3	11.2	10.5	10.6	100.8	12.3	9.9	9.9	102.0
L150 – 4	13.3	11.1	9.4	149.7	13.7	10.2	10.0	151.1	13.1	10.8	9.4	151.6	13.3	10.4	9.0	150.8
L150 – 5	13.0	10.5	9.2	150.8	12.7	10.7	9.2	152.2	11.9	10.4	8.6	151.5	12.1	10.5	8.6	151.5
L150 – 6	12.0	9.6	8.2	152.6	12.0	11.2	9.1	150.9	12.9	10.7	10.1	151.1	12.6	11.3	9.3	151.2

* Refer to Figure 3.15 for the definition of the weld numbers.

Table 3.7 – Mean Transverse Weld Measurements

Specimen	Front Face				Back Face			
	MPL (mm)	LPL (mm)	Throat (mm)	Weld Length (mm)	Shear Leg (mm)	Tension Leg (mm)	Throat (mm)	Weld Length (mm)
TNY - 1	13.4	12.2	10.7	76.3	13.9	12.4	10.7	76.4
TNY - 2	13.9	12.0	11.4	76.2	14.1	12.1	10.7	76.3
TNY - 3	14.5	12.0	10.9	76.4	13.6	12.5	10.7	76.3

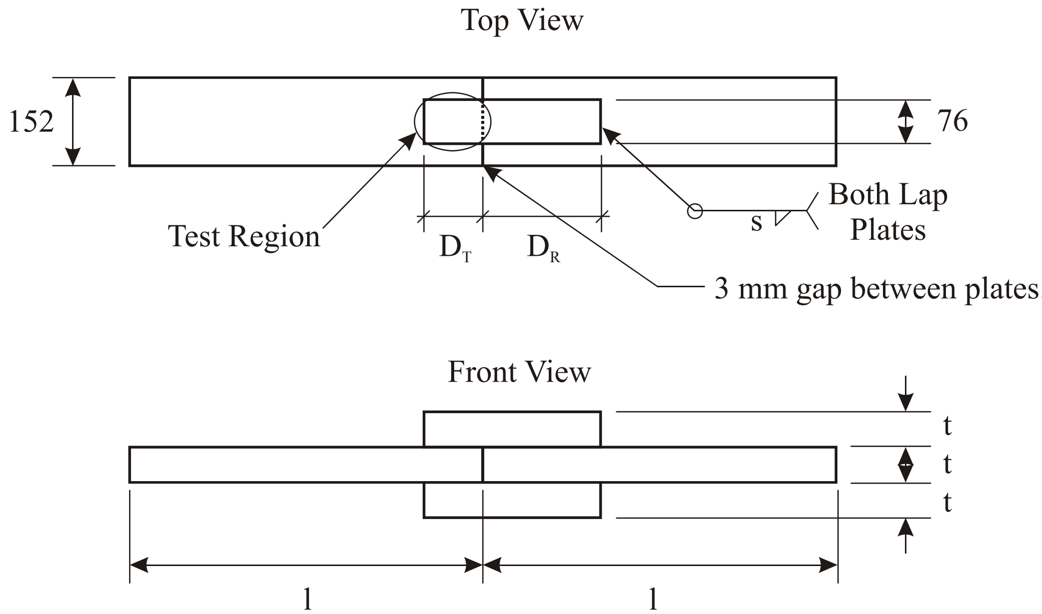

Figure 3.1 – Generic TL Specimen with Dimensions

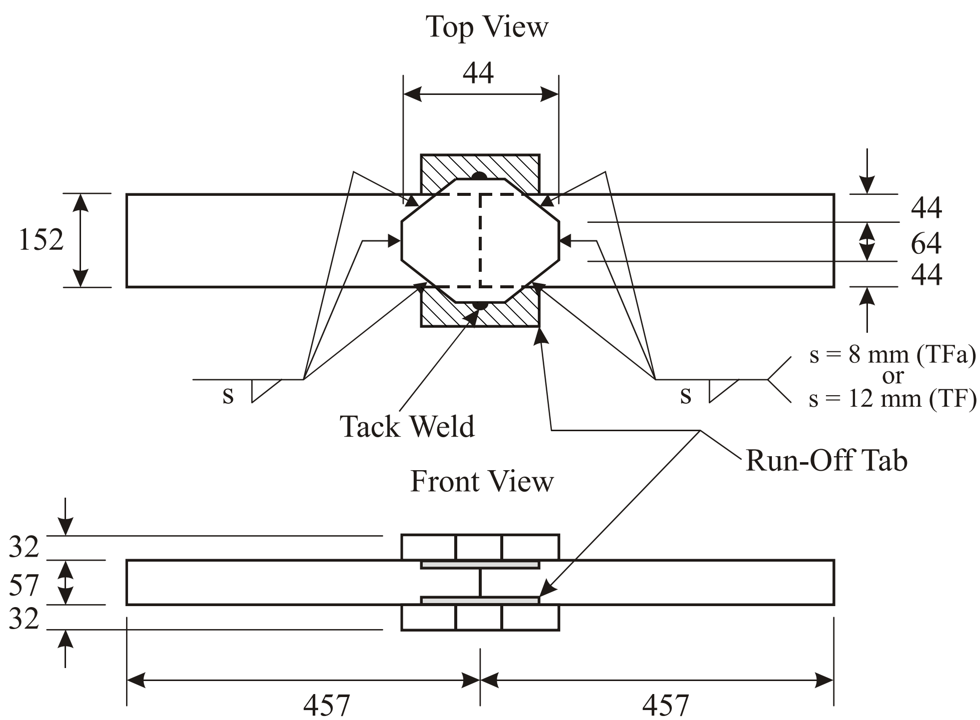

Note: Dimensions of Run-Off Tab are: 152 mm x 51 mm x 6 mm

Figure 3.2 – Generic TF Specimen with Dimensions

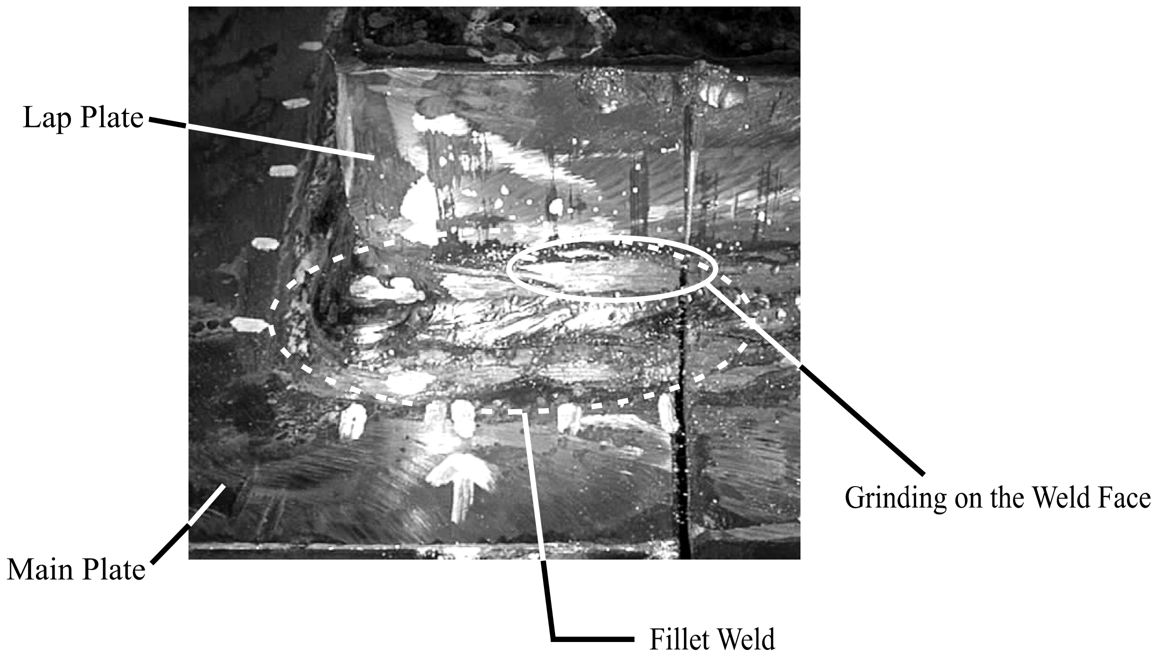

Figure 3.3 – Observed Light Grinding on Face of Fillet Weld

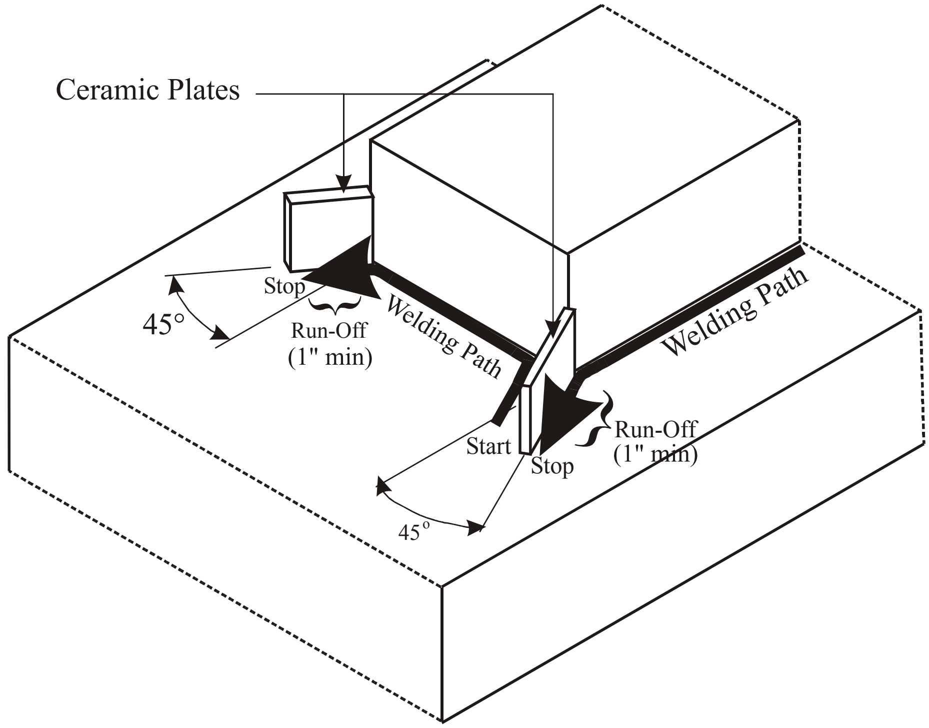

a) Discontinuous Detail

b) Discontinuous Specimen

Figure 3.4 – Discontinuous Corner Specimen Detail

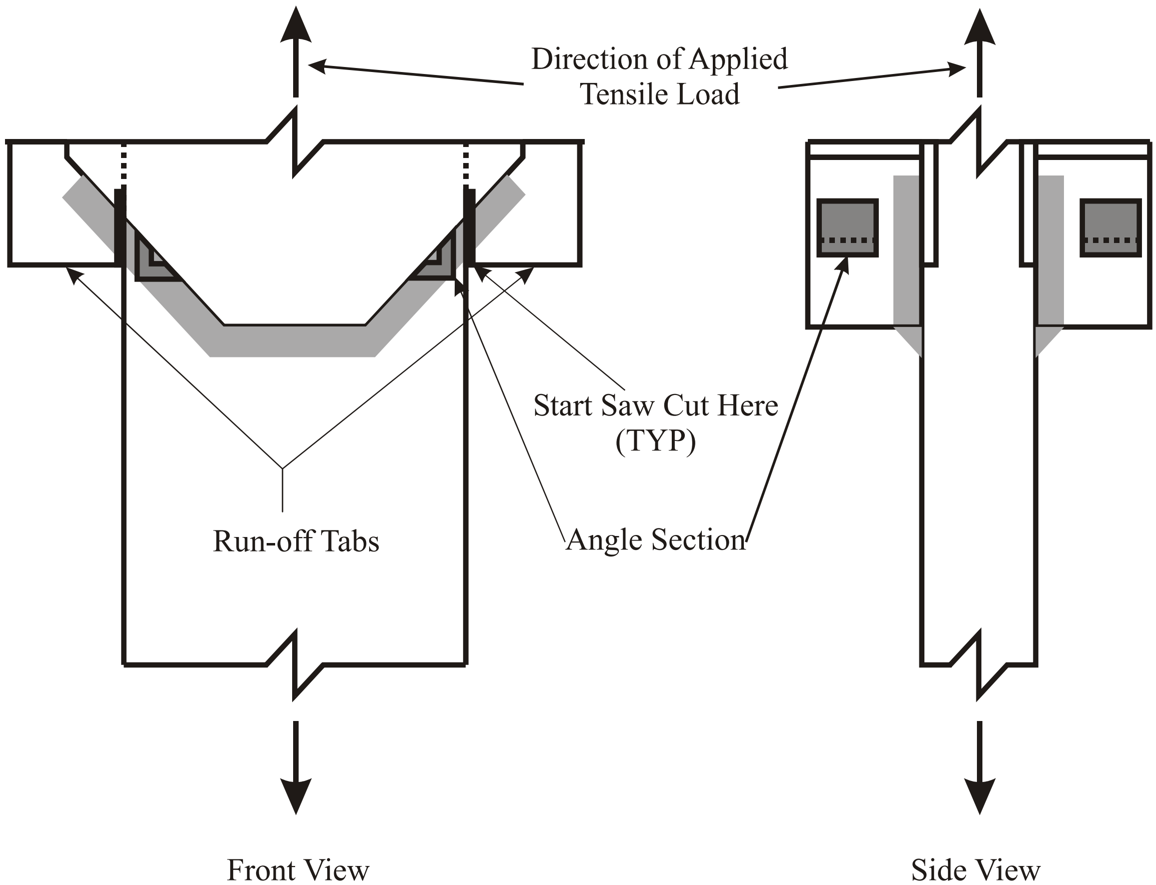

Figure 3.5 – Sketch Showing Generic TF Specimen Details

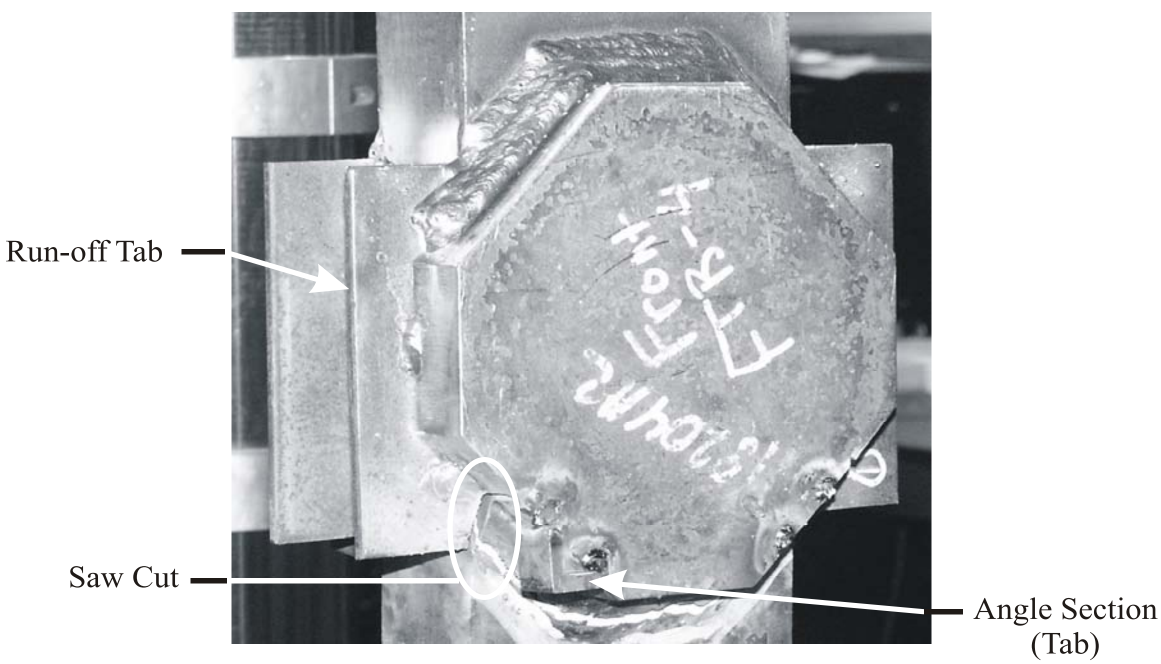

Figure 3.6 – TF Specimen With Details Shown

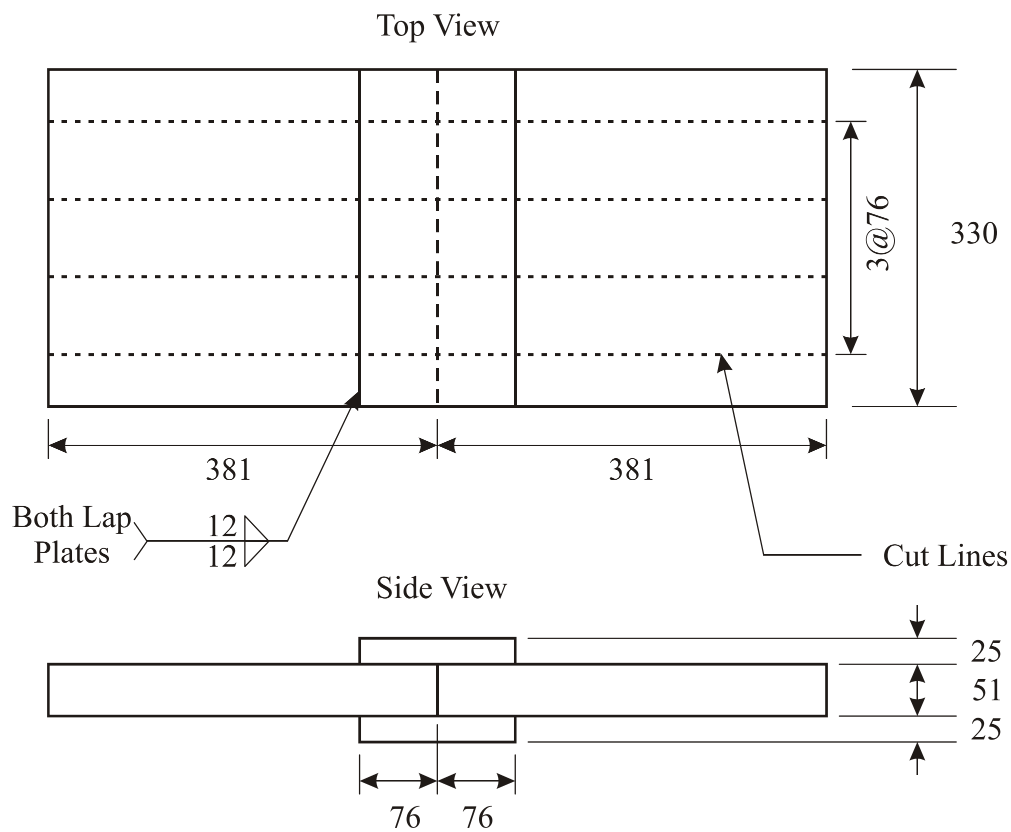

Figure 3.7 – Transverse Weld Specimen Dimensions

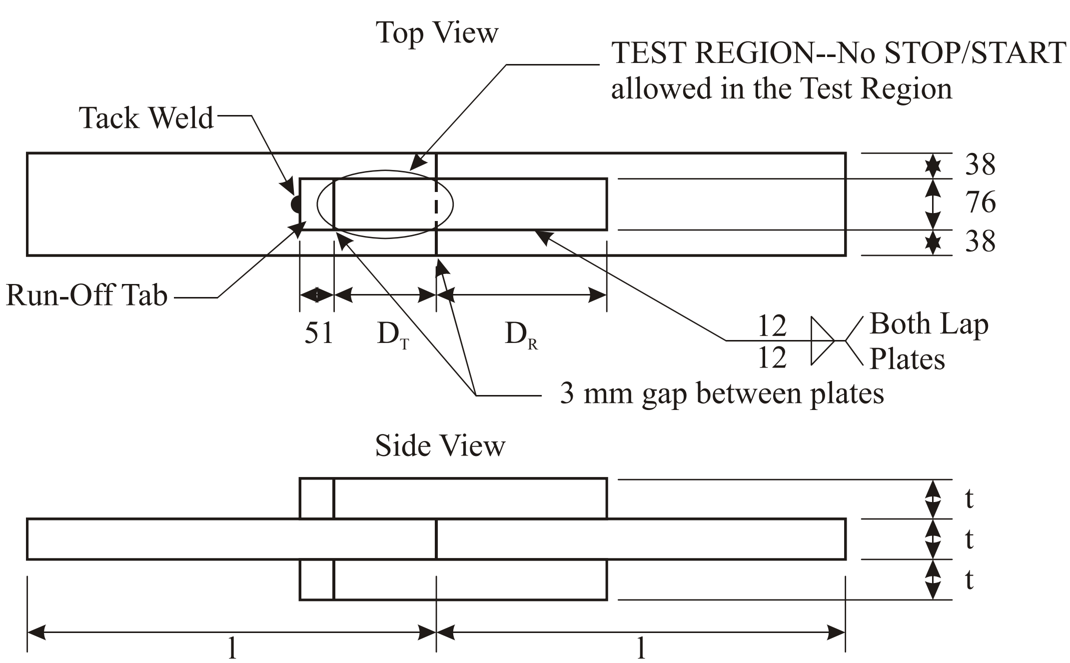

Figure 3.8 – Generic Longitudinal Weld Specimen with Dimensions

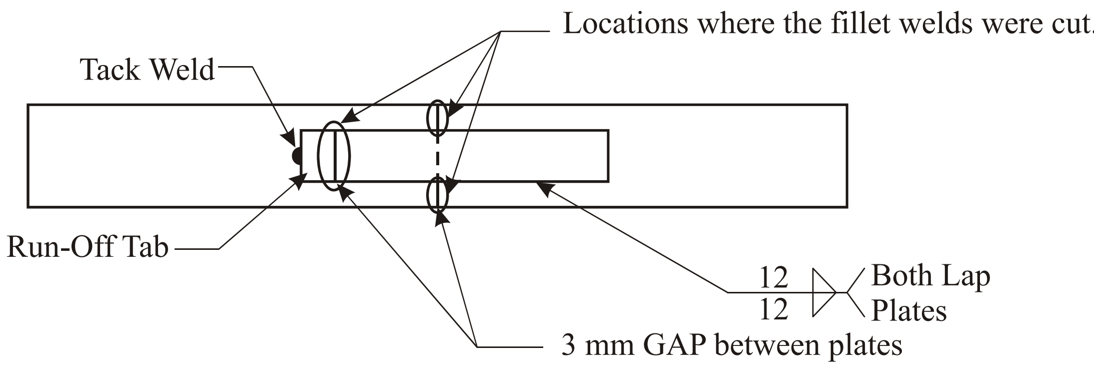

Figure 3.9 – Fillet Weld Cut Locations on the Longitudinal Weld Specimens

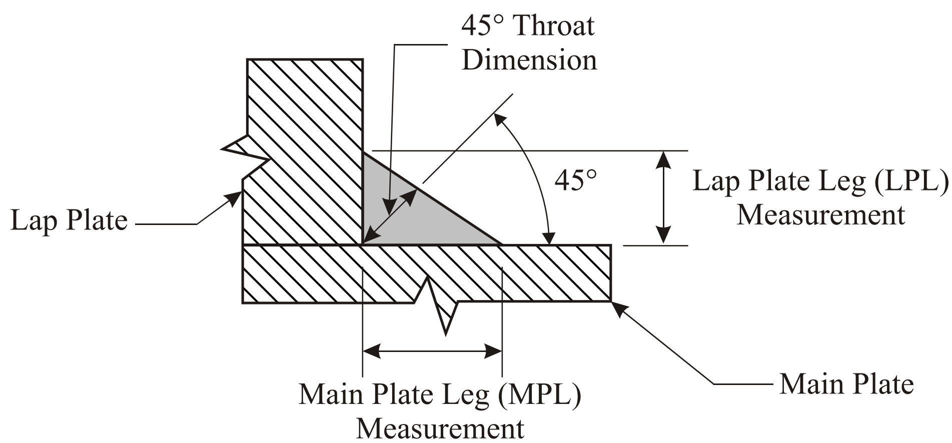

Figure 3.10 – Simplified Fillet Weld Cross-section with Measurement Definitions

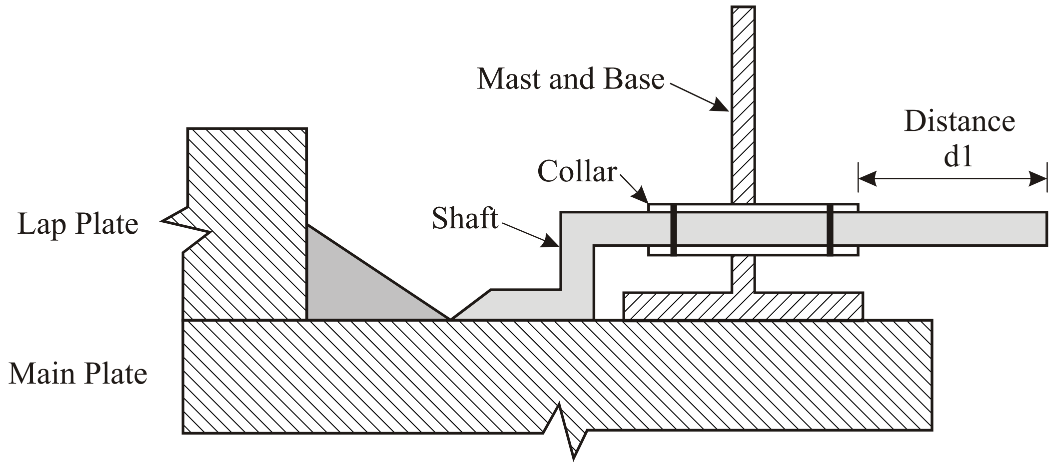

a) Step One - Zero Reading at Weld Toe

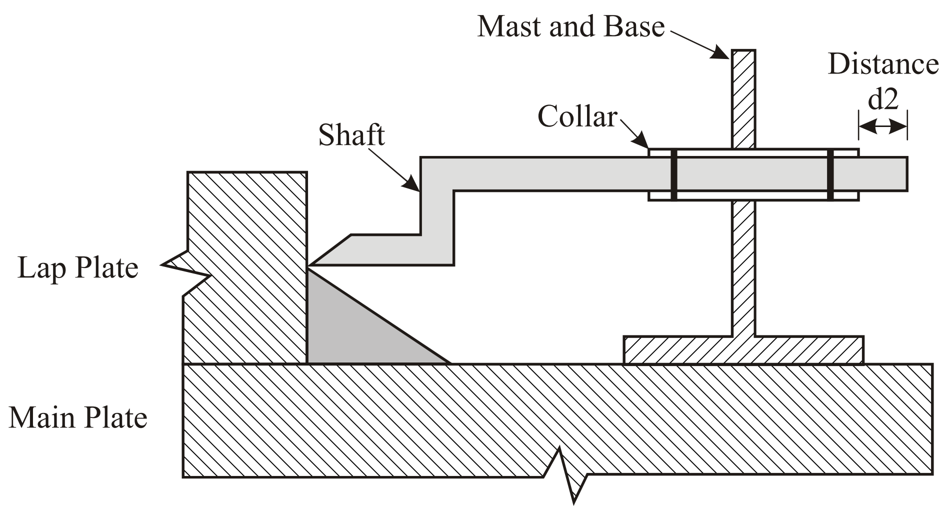

b) Step Two - Final Reading

c) Step Three - Calculation of MPL Dimension

MPL Dimension = d1 - d2

Figure 3.11 – Measurement of Shear Leg (MPL Dimension)

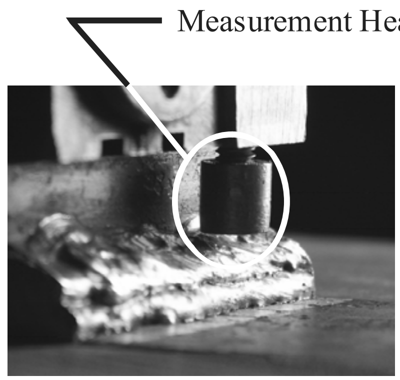

a) Initial Position of Measurement Head

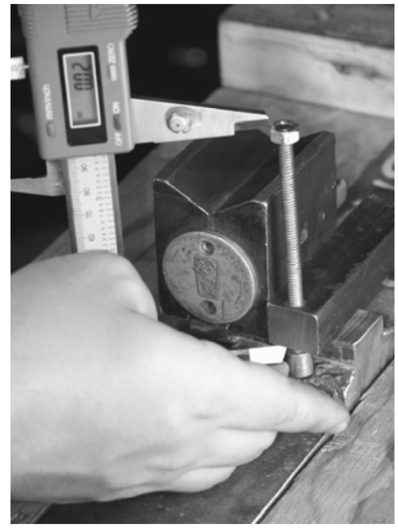

b) Zero Reading

c) Place Measurement Head on Main Plate

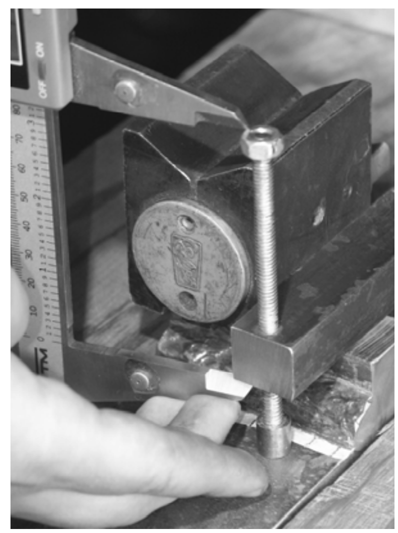

d) Final Measurement

Figure 3.12 – Measurement of Tension Leg (LPL Dimension)

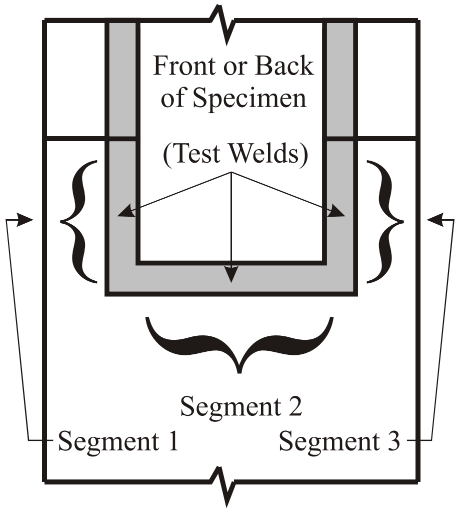

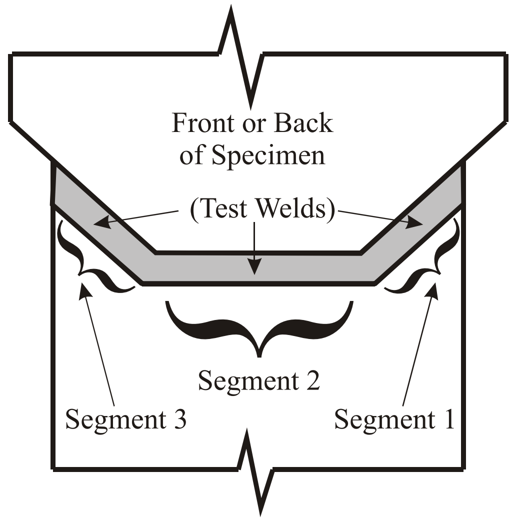

Figure 3.13 – Measurement Leg Definitions

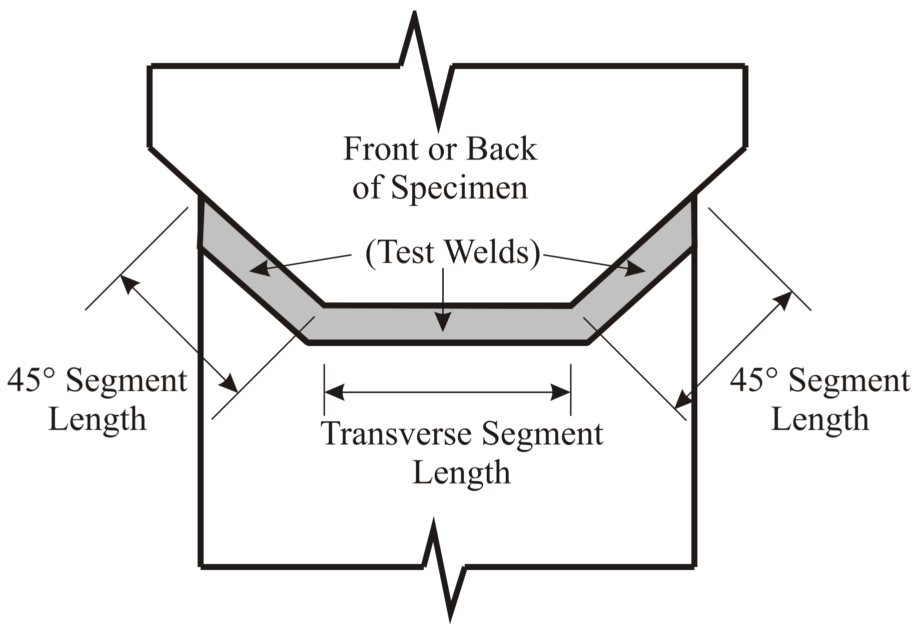

Figure 3.14 – 45° Segment Length Definition

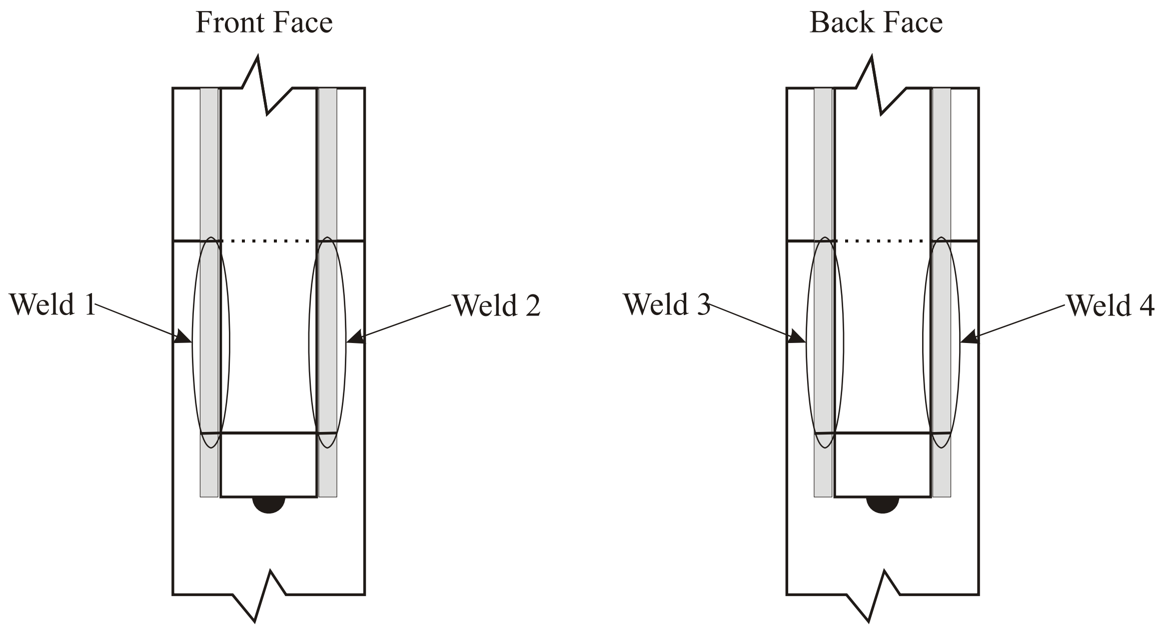

Figure 3.15 – Longitudinal Weld Leg Definitions for Measurement Purposes

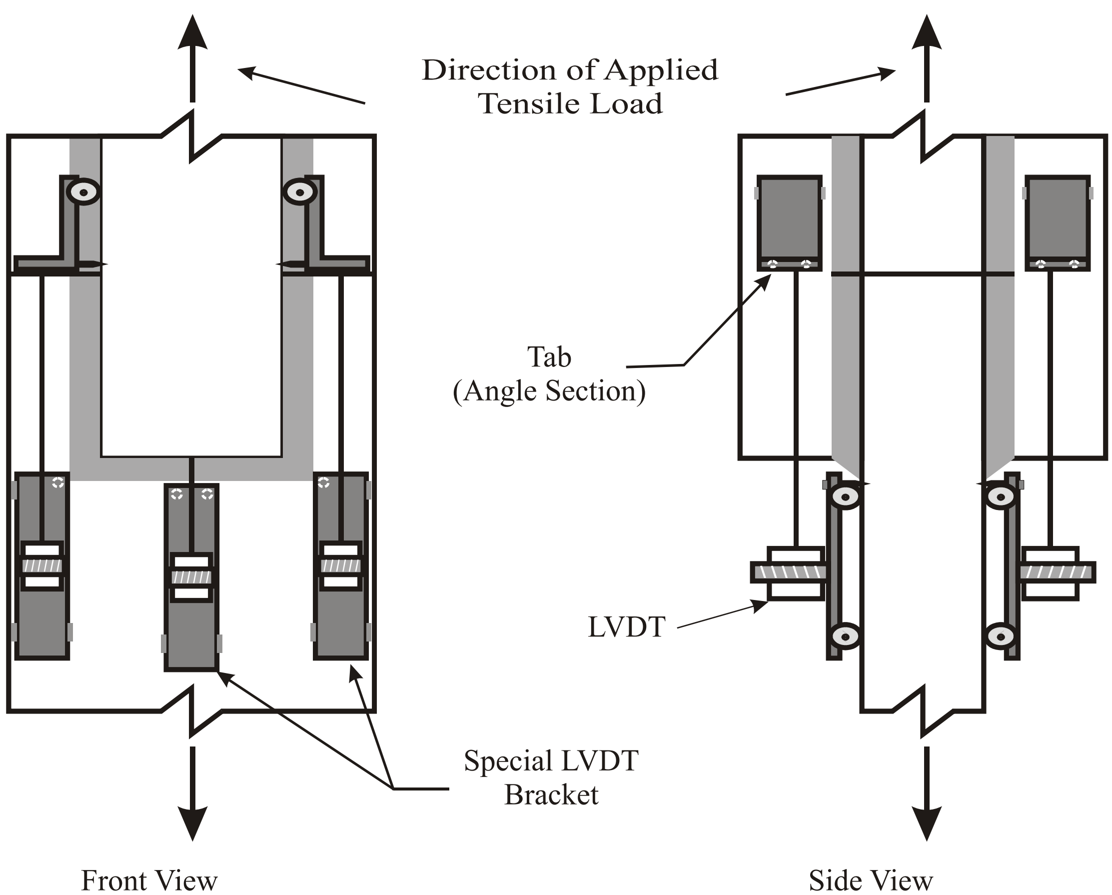

Figure 3.16 – Test Setup of the TL Specimens

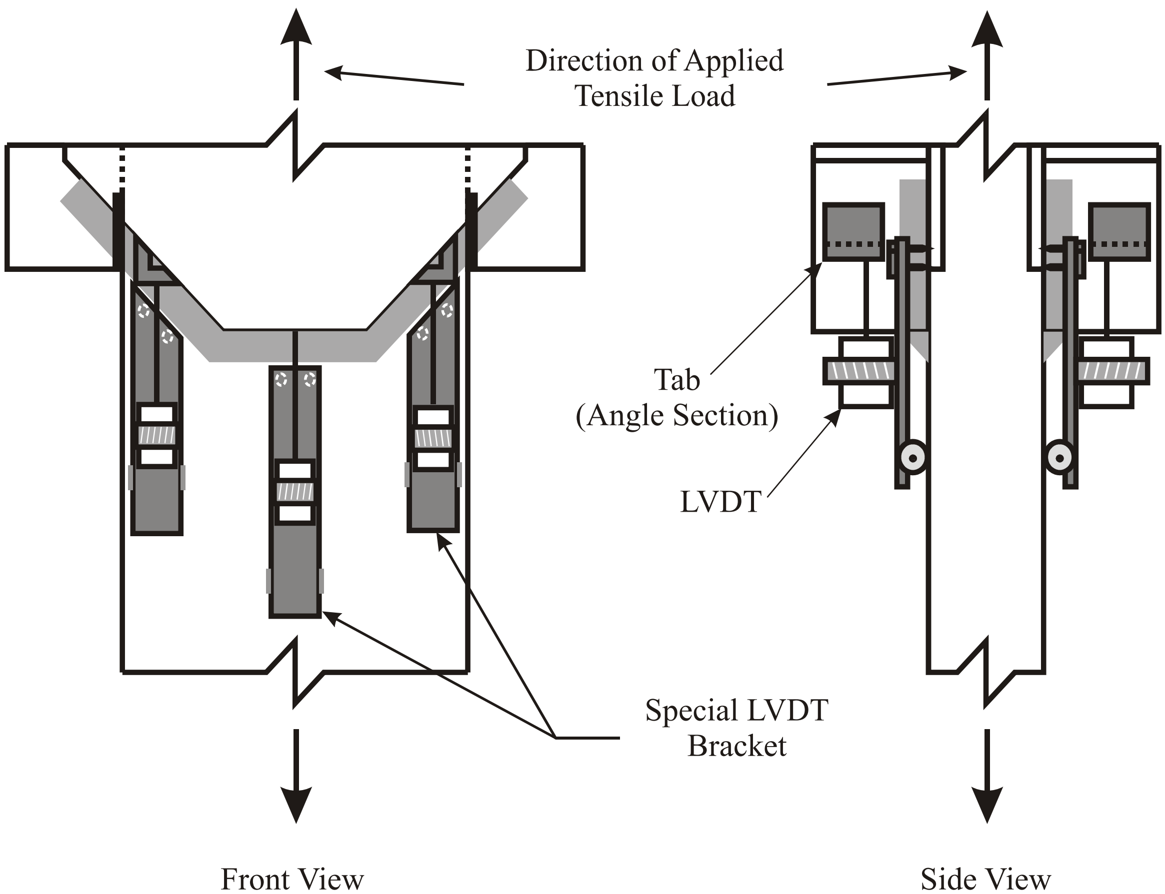

Figure 3.17 – Test Setup for the TF Specimens

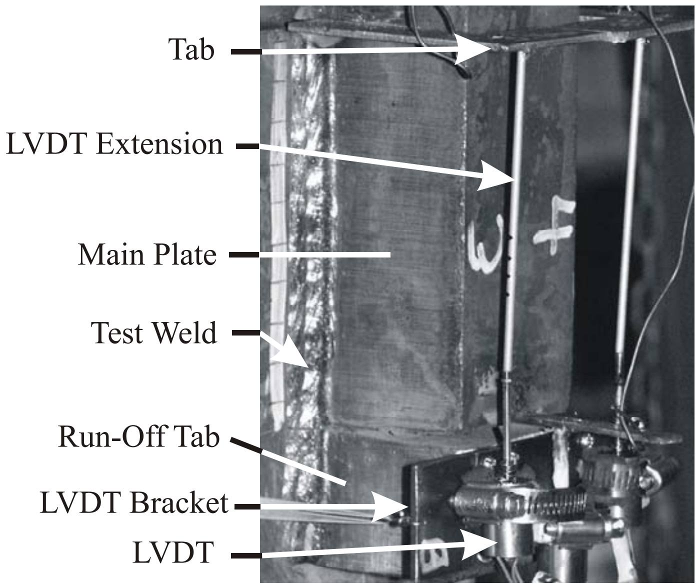

a) Longitudinal Weld Specimen Test Setup and Instrumentation

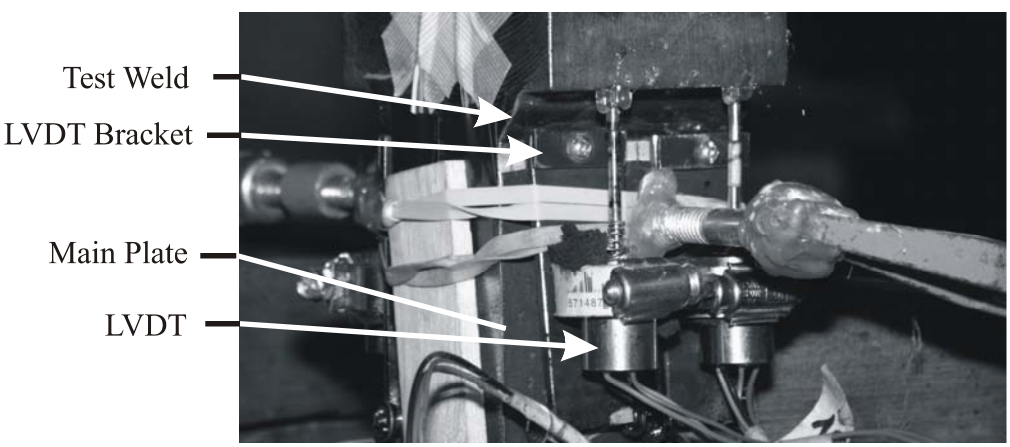

b) Transverse Weld Test Setup and Instrumentation

Figure 3.18 – Complementary Tests Instrumentation

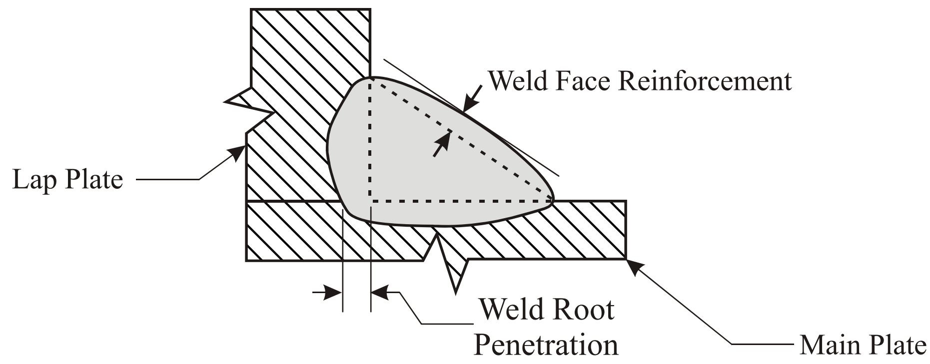

Note: Assumed triangular weld cross-section
shown by the dotted lines.

a) Cross-section of an Actual Fillet Weld Contrasted With the Triangular Aproximation

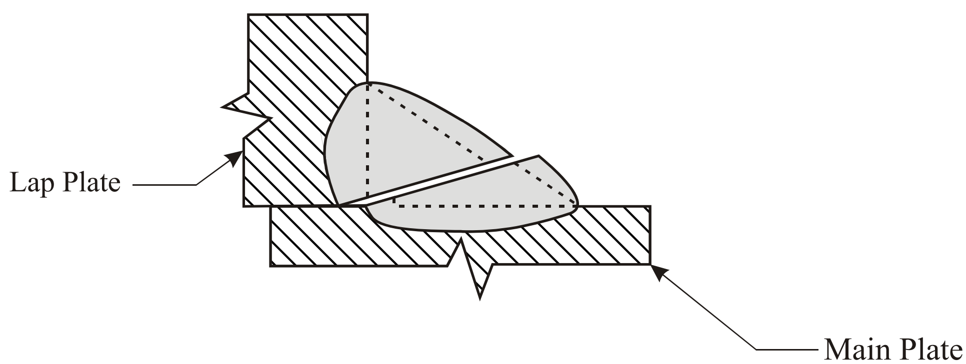

b) Fractured Weld

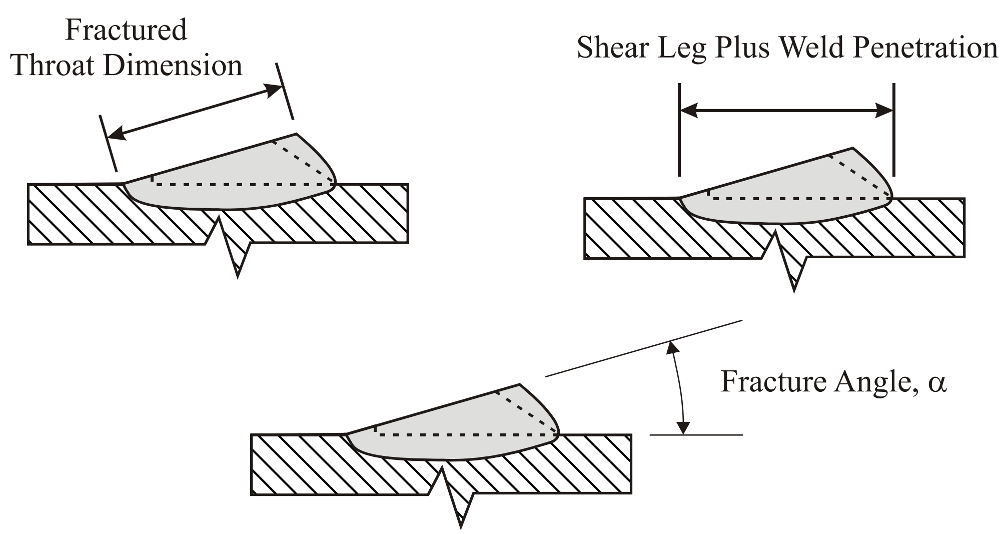

c) Fracture Surface Measurements

Figure 3.19 – Fractured Weld Characteristics

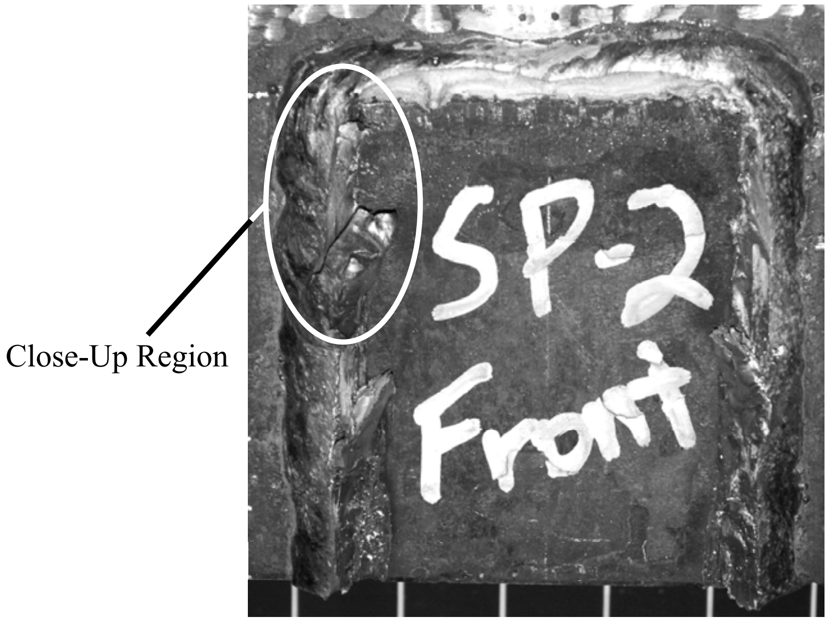

a) Fracture Surface of Specimen TL100SP-2

b) Close-Up of a Portion of the Fracture Surface that Has Been Distorted

Figure 3.20 – Uneven and Irregular Fracture Surface

CHAPTER 4

TEST RESULTS

4.1 Ancillary Test Results

Six all-weld-metal coupons were tested to determine the mechanical properties of the E70T-7 weld metal. Each coupon was fabricated in accordance with Clause 8 of ANSI/AWS A5.20 (AWS, 1995). The results of the six tests are shown in Table 4.1. The filler metal used in this test program originated from two different heats. Test specimens TF-1,2,3,4; TFa-1,2,3,4; TL50-1,2,3,4; and TL50a-1,2,3,4 were prepared using the electrode from heat 1, whereas the other test specimens were prepared with the electrode from heat 2. The static yield strengths reported correspond to the average value of the yield plateau of each specimen from the respective heat. A full description of the ancillary test results is found in Appendix C.

4.2 MOFW Test Results

4.2.1 Test Capacities

The ultimate static capacity of each test specimen is presented in Table 4.2. The capacities are normalized against the weld metal provided by each specimen by dividing by the calculated minimum throat area, A_{throat}. The minimum throat area of each segment is a function of the measured shear leg, or main plate leg (MPL), tension leg, or lap plate leg (LPL) dimensions, and the weld length. Figure 4.1 shows the minimum throat dimension for a typical fillet weld cross section. The minimum throat area is equal to the product of the minimum throat dimension and the weld segment length. The minimum throat dimension (MTD) is the smallest distance from the root of the fillet weld to the theoretical weld face for a cross section as shown in Figure 4.1 and it is calculated by means of the following equation.

$$\mathrm{MTD} = \frac{\mathrm{MPL} \times \mathrm{LPL}}{\sqrt{\mathrm{MPL}^2 + \mathrm{LPL}^2}} \tag{4.1}$$

The term P_m in Table 4.2 and Figure 4.2 refers to the ultimate load that a test specimen obtained. Figure 4.2 plots the mean P_m/A_{throat} data given in Table 4.2.

4.2.2 Measured Weld Strain

The deformations of the weld segments at the ultimate capacity and fracture of the MOFW specimens are reported in Table 4.3. The measured weld deformations in the applied load direction, Δ, are normalized by the main plate leg dimension, d, and a factor that is a function of θ.

$$\frac{\Delta}{d*} = \frac{\Delta}{d}(\sin(\theta) + \cos(\theta))^{-1} \tag{4.2}$$

Here θ is the angle between the axis of the weld and the line of action of the applied force. Figure 4.3 shows three different fillet welded lap plate connections. The axis of the dimension d* is seen to be parallel to the line of action of the applied force for both the transverse and 45 degree connections but perpendicular for the longitudinal connection. So even though the value of d* is equal to d for both longitudinal and transverse orientations, the type of deformation from each orientation is different. As θ varies from 0° to 90° the weld deformations change from consisting entirely of shear deformation to partial contributions from shear and tension. The necessity to modify d using Equation 4.2 will be explained during the analysis of the test results.

4.2.3 Fracture Angle

After testing, the fracture angle, α, shown in Figure 4.4 was measured for each segment that failed. The results of these measurements of the fracture angle are shown in Tables 4.4 and 4.5. Measurements of the fracture angle were taken at four locations along each segment. The results shown in Table 4.4 are the means of these measurements, typically averaged over the two non-transverse segments and one transverse segment on each face (front or back) of the specimens. The values reported in Table 4.5 are the means of the appropriate values from Table 4.4. Though one fracture angle is reported for each segment orientation from each face of each specimen, the fracture angle typically varied considerably even along a single segment.

The fracture angle near the junction between two segments of different orientations was found to be different than the fracture angles measured away from the junction. This, along with the comparison between the transverse segment fracture angles shown in Table 4.5, indicates the interaction between the individual segments forming the MOFW connection. This interaction will be discussed further in Chapter 5.

4.3 Results of Complementary Tests

As a continuation of this research program and the past fillet weld research that has been conducted at the University of Alberta, a complementary test program was developed to look at other fillet welded connection properties. The analysis of the test results from the current MOFW connection testing program requires data from the complementary testing program as well as the data reported by Deng *et al.* (2003)and Ng *et al.* (2004a).

The complementary testing program investigated the behaviour of both longitudinal and transverse fillet weld connections. Two parameters that effect fillet weld behaviour were investigated: (1) number of passes and (2) length of the longitudinal weld segment. Since the MOFW connection plates remained elastic, the transverse test data used here are from connections that had plates that remained elastic.

Three characteristics from both the longitudinal and transverse tests were used for the analysis of the present research. The three characteristics are (1) strength, (2) deformation at ultimate load, and (3) load versus deformation response. The measured load, A_{throat}, and ultimate deformations are reported in Table 4.6. The results are reported using the same notation as for reporting the MOFW test data. The values of A_{throat} are based upon the weld segment had fractured. The ultimate deformations reported are also only for those weld segments that fractured. The deformation response curves are reported in Appendix D.

Table 4.1 – Mechanical Properties of Weld Metal

Heat	Test ID	Static Yield Strength		Static Tensile Strength		Modulus of Elasticity		Rupture Strain	
		Test (MPa)	Mean of Heat (MPa)	Test (MPa)	Mean of Heat (MPa)	Test (MPa)	Mean of Heat (MPa)	Test (%)	Mean of Heat (%)
1	102-1	374	395	571	575	190 500	193 000	17.8	20.9
	102-2	405		572		194 000		21.6	
	102-3	406		575		194 400		23.1	
2	103-1	418	420	568	570	197 200	195 300	8.3	10.9
	103-2	431		566		195 900		9.0	
	103-3	410		573		192 700		15.6	

Table 4.2 – Combined Weld Test Results

Specimen	Ultimate Load (P_m) (kN)	Average Ultimate Load (kN)	Total Throat Area (A_{throat}) (mm^2)	P_m/A_{throat} (MPa)	Average P_m/A_{throat} (MPa)
TF-1	2003	2292	3476	576	659
TF-2	2508		3554	706	
TF-3	2228		3319	671	
TF-4	2429		3548	685	
TFa-1	1544	1705	2362	654	734
TFa-2	1734		2247	772	
TFa-3	1840		2316	794	
TFa-4	1704		2381	716	
TL50-1	1484	1605	3240	458	496
TL50-2	1664		3230	515	
TL50-3	1573		3200	492	
TL50-4	1700		3283	518	
TL50a-1	1299	1292	2215	586	561
TL50a-2	1186		2289	518	
TL50a-3	1213		2243	541	
TL50a-4	1472		2457	599	
TL100-1	2359	2184	5502	429	423
TL100-2	2218		4974	446	
TL100-3	1976		5013	394	
TL100SP-1	2032	1904	4357	466	431
TL100SP-2	1866		4401	424	
TL100SP-3	1813		4489	404	
TL100D-1	2077	2152	4603	451	448
TL100D-2	2040		4462	457	
TL100D-3	2341		5356	437	
TL50D-1	1486	1451	3213	462	453
TL50D-2	1455		3193	456	
TL50D-3	1412		3206	440	

Table 4.3 – Ultimate and Fracture Weld Deformations

Specimen	Non-Transverse Welds				Transverse Weld			
	Ultimate (mm)	Fracture (mm)	Ultimate (Δ/d*)	Fracture (Δ/d*)	Ultimate (mm)	Fracture (mm)	Ultimate (Δ/d*)	Fracture (Δ/d*)
TF-1	1.05	1.17	0.0510	0.0566	1.04	1.21	0.0747	0.0865
TF-2	0.73	1.10	0.0399	0.0600	0.75	1.08	0.0526	0.0764
TF-3	0.76	0.95	0.0423	0.0529	0.74	0.94	0.0560	0.0708
TF-4	0.44	0.44	0.0208	0.0208	0.46	0.46	0.0272	0.0272
TFa-1	0.42	0.45	0.0331	0.0354	0.42	0.46	0.0451	0.0487
TFa-2	0.69	0.91	0.0536	0.0707	0.72	0.96	0.0786	0.1046
TFa-3	0.71	0.92	0.0561	0.0731	0.68	0.91	0.0746	0.1004
TFa-4	0.54	0.76	0.0443	0.0616	0.53	0.75	0.0573	0.0817
TL50-1	0.72	0.92	0.0528	0.0673	0.63	0.83	0.0389	0.0512
TL50-2	1.00	1.30	0.0724	0.0939	0.83	1.14	0.0584	0.0797
TL50-3	0.85	1.08	0.0644	0.0818	0.68	0.96	0.0442	0.0626
TL50-4	1.07	1.30	0.0729	0.0891	0.97	1.22	0.0573	0.0723
TL50a-1	0.53	0.74	0.0596	0.0830	0.43	0.64	0.0404	0.0593
TL50a-2	0.62	0.88	0.0645	0.0918	0.51	0.77	0.0467	0.0702
TL50a-3	0.59	0.79	0.0641	0.0861	0.48	0.67	0.0457	0.0646
TL50a-4	0.72	1.14	0.0728	0.1152	0.63	1.05	0.0526	0.0875
TL100-1	0.92	1.07	0.0597	0.0697	0.60	0.74	0.0341	0.0424
TL100-2	1.02	1.18	0.0661	0.0768	0.76	0.95	0.0454	0.0570
TL100-3	0.57	0.70	0.0412	0.0507	0.44	0.55	0.0265	0.0326
TL100SP-1	1.03	1.38	0.0811	0.1082	0.79	1.10	0.0617	0.0859
TL100SP-2	0.76	1.11	0.0594	0.0864	0.61	0.96	0.0475	0.0747
TL100SP-3	1.01	1.15	0.0740	0.0843	0.82	0.98	0.0600	0.0720
TL100D-1	0.60	0.74	0.0475	0.0585	0.44	0.57	0.0342	0.0441
TL100D-2	0.39	0.42	0.0296	0.0325	0.25	0.27	0.0206	0.0222
TL100D-3	0.63	0.74	0.0427	0.0496	0.44	0.53	0.0315	0.0379
TL50D-1	0.64	1.02	0.0446	0.0715	0.57	0.98	0.0404	0.0697
TL50D-2	0.43	0.51	0.0297	0.0352	0.39	0.48	0.0253	0.0310
TL50D-3	0.66	1.21	0.0447	0.0567	0.60	1.21	0.0382	0.0495

Table 4.4 – Fracture Angle

Specimen	Mean Fracture Angle (Degrees) by Specimen			
	Front Face		Back Face	
	Transverse Weld	Non-Transverse Weld	Transverse Weld	Non-Transverse Weld
TF-1	13	N/A*	17	15
TF-2	62	33	23	28
TF-3	34	18	0	15
TF-4	19	16	N/A	N/A
TFa-1	0	24	26	23
TFa-2	30	14	36	58
TFa-3	8	31	11	11
TFa-4	5	8	6	23
TL50-1	78	38	71	42
TL50-2	63	37	66	39
TL50-3	77	47	73	25
TL50-4	31	71	19	73
TL50a-1	64	62	64	49
TL50a-2	61	65	78	44
TL50a-3	57	52	29	64
TL50a-4	65	69	27	66
TL100-1	15	66	N/A	N/A
TL100-2	29	72	N/A	N/A
TL100-3	N/A	N/A	23	64
TL100SP-1	45	71	N/A	N/A
TL100SP-2	30	52	57	62
TL100SP-3	55	66	N/A	N/A
TL100D-1	N/A	N/A	24	64
TL100D-2	N/A	N/A	61	57
TL100D-3	N/A	N/A	64	65
TL50D-1	28	49	24	49
TL50D-2	31	48	N/A	N/A
TL50D-3	41	46	38	62

* N/A = Weld did not fracture

Table 4.5 – Overall Mean Fracture Angles

Segment Orientation Combination	Transverse Segment Mean Fracture Angle (Degrees)	Non-Transverse Segment Mean Fracture Angle (Degrees)
Transverse and Longitudinal (TL Specimens)	48	56
Transverse and 45 Degrees (TF Specimens)	19	23

Table 4.6 – Complementary Test Results

Specimen	Side That Failed	Max Load, P_m (kN)	A_{throat} (mm^2)	P_m/A_{throat} (MPa)	Normalized Ultimate Deformation (Δ/d^*)
L100-1	Front	1470	1691	434	0.0910
L100-2	Back	1469	1711	429	0.0983
L100-3	Both	1780	3746	475	0.1229
L100-4	Back	1264	1498	422	0.1178
L100-5	Front	1208	1520	397	0.1421
L100-6	Back	1386	1560	444	0.2018
L150-4	Front	2263	2498	453	0.1264
L150-5	Both	2431	4864	500	0.1380
L150-6	Back	2473	2383	519	0.1522
TNY-1	Front	1005	687	732	0.0309
TNY-2	Front	1026	693	740	0.0285
TNY-3	Back	1088	703	774	0.0312

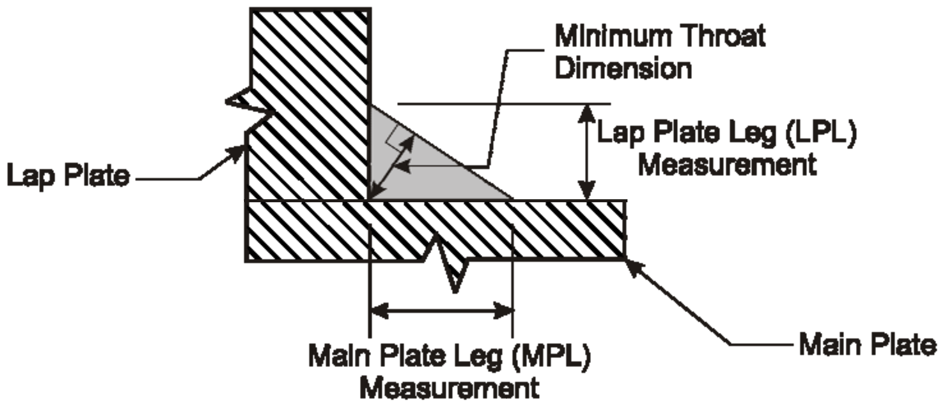

Figure 4.1 – Fillet Weld Dimensions

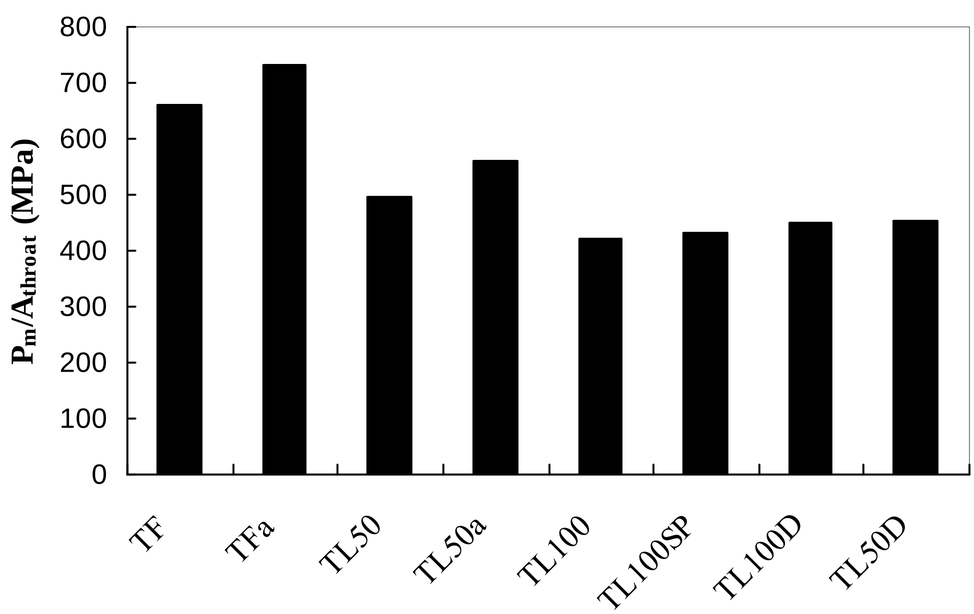

Figure 4.2 – Test Capacities

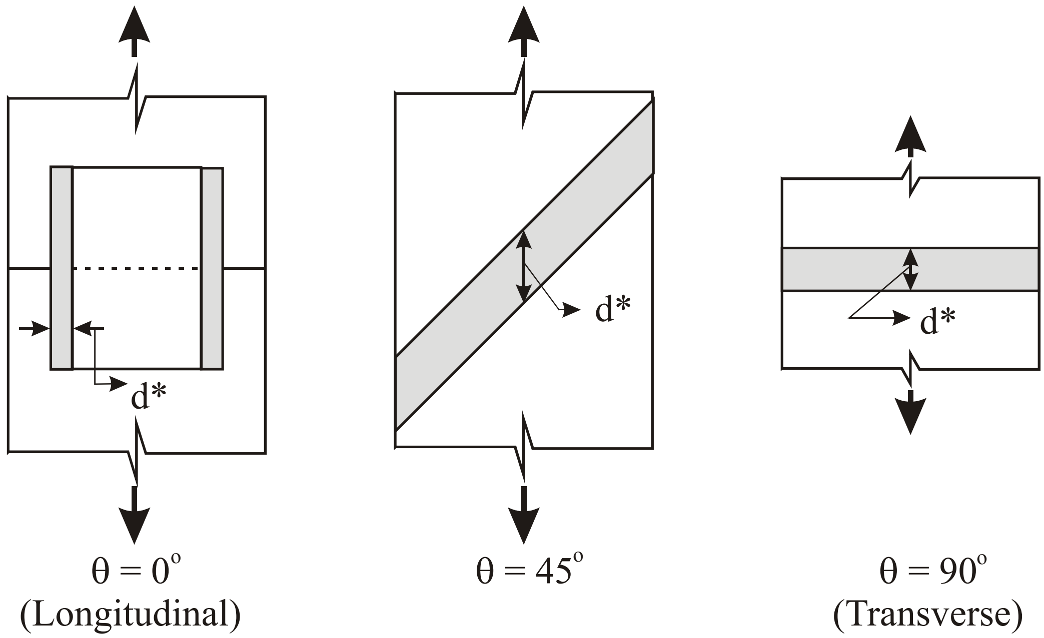

(a) Plan View of Lap Spliced Fillet Weld Connections

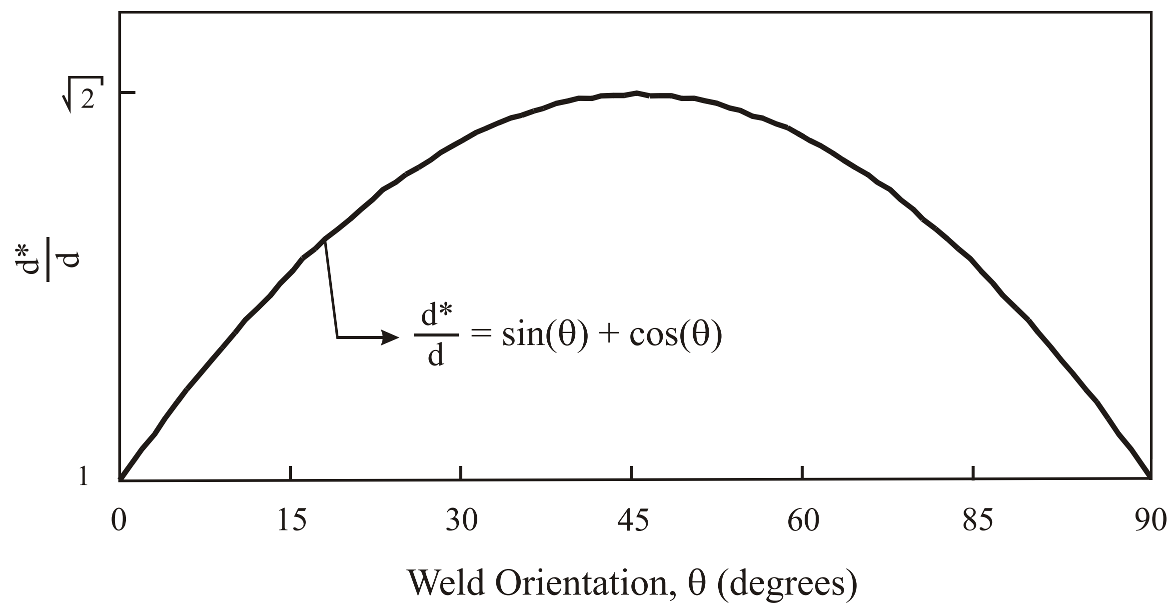

Note: d = MPL Weld Dimension

(b) Normalized Weld Deformation versus Weld Orientation

Figure 4.3 – Deformation Normalization Definition

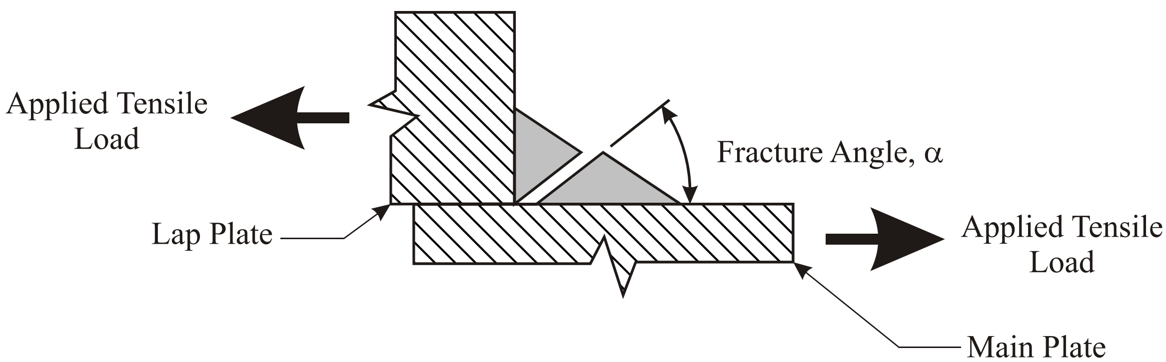

Figure 4.4 – Fracture Angle Definition

CHAPTER 5

ANALYSIS AND DISCUSSION

5.1 Introduction

In this chapter the strength and behaviour of MOFW (multi-orientation fillet weld) connections are investigated. The investigation of the interaction of the different ductility limits of different weld segments in a MOFW connection is the primary objective of this research program. A MOFW connection segment is defined as a section of fillet weld having a single orientation. This interaction is found to be manifested in a ductility incompatibility where the connection capacity is reached once one segment reaches its ductility limit but the other segments have not reached their individual capacities. A detailed method of dealing with the ductility incompatibility is presented. This method is then simplified into a modified version of the current fillet weld design equation. The safety index for the design of MOFW connections is evaluated for both the current design equation and the modified equation.

5.1.1 Ductility Incompatibility

One possible method of designing MOFW connections is to use the method of strength summation. This method predicts that the MOFW connection strength is equal to the summation of the ultimate capacities of the individual segments that make up the connection. If a ductility incompatibility exists in a MOFW connection then its effect would be to reduce the strength of the connection to a value below that predicted by the method of strength summation. This is because the ductility incompatibility causes the capacity of the MOFW connection to be reached before the capacity of the more ductile segments has been reached. Comparisons of weld group capacity predictions using the strength summation approach with experimental results indicate that such a ductility incompatibility exists and must be accounted for in design. To facilitate discussions in subsequent sections, the least ductile segment of the weld group is referred to as the critical segment, whereas all other segments are called non-critical.

5.1.2 Longitudinal Fillet Weld Length Effect

Before looking at the predicted capacities for the MOFW connections from this research program, it is necessary to discuss the test results from Miazga and Kennedy (1989), Deng *et al.* (2003), and the complementary tests from this research. Only the longitudinal test results from these three testing programs will be discussed here. Table 5.1 summarizes the pertinent test characteristics for each of the three testing programs. Test data from these three programs are reported in Table 5.2. The P_m/A_{throat} values are shown both in their raw form and also normalized by dividing by the measured value of the ultimate tensile strength of the respective weld metal, designated as σ_{UTS}, so that the actual performance of the welds can be compared directly. The relationship between the two quantities is as follows:

$$\text{Normalized } P_m / A_{throat} = \frac{P_m / A_{throat}}{\sigma_{UTS}} \quad (5.1)$$

A plot of the normalized P_m/A_{throat} values is presented in Figure 5.1. It can be seen that the means of the normalized P_m/A_{throat} values for the lengths plotted are different and that there is a relatively large scatter of the test data overall. If considering only the test results for longitudinal segment lengths of 50, 80, and 100 mm, then it would appear that there is significant drop in strength with length. However, the test data for the specimens with 150 mm long welds show a higher strength than the 80 and 100 mm specimens, which is inconsistent with the previous observation. Thus, whether or not the strength of longitudinal fillet welds decreases with increased length is inconclusive from these test results. Even though it is inconclusive as to whether or not length affects the strength of longitudinal welds for the lengths presented here, these data will be used to predict the capacity of the MOFW connections. The predicted ultimate capacity of the longitudinal segments in the MOFW connections is calculated using the following equation:

$$P_{m_{SEGMENT}} = \text{Normalized } P_m / A_{throat} \times \sigma_{UTS} \times A_{throat}(\text{segment}) \quad (5.2)$$

5.2 MOFW Connection Behaviour

The development of a method of MOFW capacity prediction will begin with the philosophy of strength summation, as described previously. The ultimate capacities of each of the individual weld segments are predicted based upon test results from Deng *et al.* (2003) and the complementary testing program. The test results from Miazga and Kennedy (1989) will not be used in the ultimate capacity prediction as the specimens from their research program were prepared using the shielded metal arc welding process rather than the flux cored arc welding process that was used in the preparation of the specimens for the current research and that of Deng *et al.* (2003). The specimens tested by Miazga and Kennedy (1989), Deng *et al.* (2003), and the complementary research program were all single orientation fillet weld (SOFW) connections. A simple example showing the difference between MOFW connections and SOFW connections is shown in Figure 5.2.

Tables 5.2 and 5.3 contain the data used in the strength prediction for each segment orientation. Using these normalized strengths, the capacity of each segment is predicted by multiplying the normalized capacity by the tensile strength of the weld metal used in the MOFW connection and the throat area, A_{throat}, of the segment (see Equation 5.2). Since the predicted connection capacity is based upon the strength summation method, each of the predicted segment capacities are summed. Figure 5.3 compares the predicted capacities of the MOFW connections with the test capacities. The mean test-to-predicted ratio is seen to be non-conservative, having a value of 0.79.

The implication of having a non-conservative test-to-predicted ratio for the strength summation method is that the individual segments are not contributing their full capacity to the strength of the connection. One possible reason why these segments would be inefficient (i.e., contribute less than their full strength) is a ductility incompatibility between the weld segments. The ductility incompatibility occurs when one (or more) of the weld segments in the connection fractures before the other segments reach their maximum capacity.

5.2.1 Accounting for the Ductility Incompatibility

A deformation compatibility approach is adopted in order to account for the apparent ductility incompatibility. The approach consists of two steps. First, the deformations at the ultimate capacity of the MOFW connection are measured. (These deformations are reported in Table 4.3.) Then, using a fillet weld response curve similar to that reported by Lesik and Kennedy (1990), the capacity of each weld segment at this deformation is obtained. The sum of these capacities is the load capacity of the MOFW connection obtained using the deformation compatibility approach.

5.2.2 Fillet Weld Response Curves

The general form for the response curve presented by Lesik and Kennedy (1990), and used here because of its ability to fit the experimental data well, is as follows:

$$\frac{P_\theta}{P_{u\theta}} = \sum_{i=1}^{6} a_i \rho^{\frac{1}{i}} \text{ when } \rho < \text{Proportional Limit} \tag{5.3}$$

$$\frac{P_\theta}{P_{u\theta}} = a_S \rho \text{ when } \rho \geq \text{Proportional Limit} \tag{5.4}$$

The term $P_\theta / P_{u\theta}$ is the fraction of the ultimate capacity that is mobilized for a particular value of ρ, where ρ is the weld deformation divided by the deformation at the ultimate capacity of the weld. The value of the "Proportional Limit" is the intersection point between modelling the weld behaviour as linear and non-linear. The normalized parameters permit the use of a single equation for any fillet weld orientation. The coefficients a_i and a_s, shown in Table 5.4, were obtained by fitting the response curve to the test data with a least-squares analysis and constraining $P_\theta / P_{u\theta}$ to 1.0 at ρ equal to 1.0. The first three column headings for the coefficients presented in Table 5.4 describe the fillet weld orientation. These three response curves are taken from the test data for the SOFW tests conducted in the complementary test program and in the test program by Deng *et al*. (2003). The second last column in Table 5.4 contains the coefficients presented by Lesik and Kennedy (1990) based on the test results of Miazga and Kennedy (1989). The last column represents the three response curves from the complementary test program and Deng *et al.* (2003). The average was obtained by specifying a value of ρ and then calculating the value of $P_\theta / P_{u\theta}$ for each of the three curves. A regression line was then fitted through the average of these three values for different values of ρ. This is illustrated in Figure 5.4. The average curve that is used for all deformations is seen to represent the three weld orientations reasonably well, with the major deviation being in the transition from the elastic part of the curve to the plastic part.

Figure 5.5 presents a comparison between the average curve of Figure 5.4 and the relationship proposed by Lesik and Kennedy. This shows more variation between the fillet weld response curve of Lesik and Kennedy and the average response curve in the post-peak region (i.e., $\rho > 1.0$). This is the result of Lesik and Kennedy's curve being based upon test data that frequently had fracture deformations that nearly coincide with the deformations at ultimate capacity, whereas the test data by Deng *et al.* (2003) and in the complementary test results generally showed a greater separation between the fracture deformations and the deformations at the ultimate capacity. The ultimate and fracture deformations are predicted by Lesik and Kennedy (1990) using the following equations:

$$\frac{\Delta_{ult}}{d} = 0.209(\theta + 2)^{-0.32} \tag{5.5}$$

$$\frac{\Delta_{f}}{d} = 1.087(\theta + 6)^{-0.65} \tag{5.6}$$

where θ is the weld orientation in degrees. By combining these two equations, the value of ρ at fracture can be predicted for any orientation. As seen in Figure 5.6, the maximum predicted value of ρ for a transverse weld is approximately 1.14, which is significantly less than that calculated using the transverse test results of the complementary testing program. In fact, most of the tests reported by Lesik and Kennedy show significantly smaller values of ρ at fracture than the tests reported by Deng *et al.* (2003) and the complementary testing program. This means that response curve used by Lesik and Kennedy cannot be used to predict the response of the test data reported that have values of ρ greater than those reported in Figure 5.6 because the values would be predicted by extrapolation. This extrapolation could be the cause of the deviation of the two curves shown in Figure 5.5 for $\rho > 1.0$.

5.2.3 Deformation Compatibility Predictions

Using the average fillet weld response curve described above, the predicted capacities of the tested MOFW connections are calculated. The first step in the prediction is to calculate the value of ρ for each segment of the MOFW connection at the ultimate capacity of the connection from the MOFW test, designated as $\rho_{segment\ ult.}$. To compute $\rho_{segment\ ult.}$, the ultimate normalized deformations of the MOFW connections, reported in Table 4.3, are divided by the predicted value of the segment's SOFW ultimate normalized deformation. The predicted normalized ultimate deformation for a segment is taken as the average normalized deformation from the complementary testing program and Deng *et al.* (2003) for the E70T-7 electrode. There are only three different segment orientations in all of the MOFW connections tested: transverse, longitudinal and 45°. The values used as the prediction of the normalized ultimate deformation for the three orientations are reported in Table 5.5. Once the values of $\rho_{segment\ ult.}$ are calculated, the next step is to calculate the value of $P_{\theta}/P_{u\theta}$ that corresponds to the value of $\rho_{segment\ ult.}$. This value of $P_{\theta}/P_{u\theta}$ is the predicted fraction of the ultimate capacity of the segment that is contributed to the total MOFW connection strength. The following list provides more details and summarizes how the deformation compatibility predictions are calculated.

1. Divide the measured MOFW normalized deformation by the predicted normalized ultimate deformation for the segment in a SOFW connection (see Table 5.5) to obtain $\rho_{\text{segment ult}}$.
2. Using the value of $\rho_{\text{segment ult}}$, calculate the respective values of $P_{\theta}/P_{u\theta}$ for each segment using the "average" response curve described in Table 5.4.
3. Multiply the normalized SOFW strengths of each segment by their respective value of $P_{\theta}/P_{u\theta}$. The values for the normalized strengths (normalized P_m/A_{throat}) are obtained from Tables 5.2 and 5.3. The average normalized strength of only the E70T-7 electrodes was used since the test specimens were prepared with this weld metal. The normalized strengths of the longitudinal weld segments were predicted using test results from welds that had the same nominal length. The predicted normalized strengths of the segments with single pass 8 mm welds were calculated by multiplying the normalized capacity of a corresponding three pass 12 mm weld by 1.24. This increase in strength was observed by Ng *et al.* (2004b) for the single pass 6 mm (1/4") and three pass 12 mm (1/2") welds fabricated with E70T-7 electrodes (refer to Table 5.6). Because the weld size adjustment is based on the 6 mm values of Ng *et al.* (2004b), application of this factor to the 8 mm (5/16") MOFW specimens will lower the test-to-predicted ratio, which will lead to a reduction of the resistance factor for a given safety index. Although weld size affects the P_m/A_{throat} value (refer to Section 5.6), this size effect is known only qualitatively. For this reason, and because tests have not been conducted on 8 mm single pass SOFW, the factor 1.24 will be used. The 1.24 multiplier was also used in the prediction of the capacity by the summation of strength method.
4. Depending on which side of the specimen fails, either front or back or both, the value of A_{throat} is found using Table 5.7. This value of A_{throat} is multiplied by the value of the normalized strength calculated in Step 3 and then multiplied by the tensile strength of the weld metal used in the MOFW connection.
5. The predicted MOFW connection capacity is equal to the sum of the adjusted segment capacities, which take into account the ductility incompatibility effect. If the MOFW connection failed on either the front or back face alone, the predicted capacity is equal to twice the value computed using just the front or back throat areas from Table 5.7.

It should be noted that the value of $P_{\theta}/P_{u\theta}$ obtained in Step 3 from the average fillet weld response curve described in Table 5.4 takes into account the decrease in capacity of a fillet weld after the ultimate capacity has been reached. This is significant because the connection behaviour is being modelled using response curves that are developed from SOFW tests. Therefore, once the transverse weld segments reach a deformation greater than the deformation required to mobilize the ultimate strength of a transverse weld in a

SOFW connection, these segments are expected to contribute less than their full capacity to the connection strength. To illustrate this concept, Figure 5.7 was produced by considering a nominal TL100 specimen, using the transverse and longitudinal response curves described in Table 5.4, and using Equation 5.9, presented in section 5.5.1, for the prediction of the weld deformations at their respective ultimate SOFW capacities. It can be seen in this figure that the descending branch of the transverse segment is offset by the increasing contribution of the longitudinal segment beyond the point where the ultimate capacity of the transverse weld had been reached. This interaction between the different response curves of a weld segment is dependent upon the relative proportions of the segments in the connection and the individual response curves.

The result of this deformation compatibility approach is shown in Figure 5.8 and is seen to be an improvement over the strength summation method. However the mean test-to-predicted ratio for the deformation compatibility is still non-conservative. Based upon the measured deformations and the selected response curve, the average percentage of ultimate capacity for the longitudinal and 45° segments are 92% and 87%, respectively. This suggests that there is a ductility incompatibility effect, but as the test-to-predicted ratios show, it does not fully account for the capacity of MOFW connections.

Another way to look at the test results is to introduce an efficiency factor. The efficiency factor is applied to the non-transverse weld segments of a MOFW joint, and is used to reduce the contribution of the segment to the connection capacity. Thus, the assumed contribution of the non-transverse weld segment to the MOFW connection capacity is equal to the predicted ultimate capacity of the segment (from SOFW test results) multiplied by the efficiency factor. This method is similar to Step 3 above, but it uses an efficiency factor selected empirically to optimize the connection capacity predictions instead of $P_\theta / P_{u\theta}$. The efficiency factors that minimize the scatter of the test-to-predicted ratios and result in a mean test-to-predicted ratio equal to 1.0 are 0.61 and 0.71 for longitudinal and 45° segments, respectively. The plot of the test and predicted capacities using these efficiency factors is shown in Figure 5.9. This analysis reveals that in order to provide a good prediction of the MOFW connection capacity, the non-transverse weld segment capacities need to be reduced from what is predicted by the deformation compatibility approach. This suggests that there is another mechanism at work in MOFW connections that affects the capacity besides ductility incompatibility.

5.2.4 Other Mechanisms Affecting Connection Capacity

The overall MOFW connection capacity is ultimately a function of the interaction between the individual segments that make up the connection. Thus far, one type of segment interaction has been studied in the deformation compatibility prediction, where the assumed interaction between the segments is a ductility limit. One segment's limit results in the remaining segments not having sufficient ductility to mobilize their full capacity.

It is important to note that the analysis presented here has taken the response of the individual weld segments of a MOFW connection as equivalent to the response of a corresponding segment from a SOFW connection. In light of the claim stated in the previous section that another mechanism must be at work that affects the weld segment capacity, the weld segment response is brought into question. The segment response could be different than that predicted by SOFW tests for the following two reasons.

1. The force that develops between weld segments may influence the individual segment response and therefore the connection behaviour. Figure 5.10(a) shows a picture of a fractured specimen containing transverse and longitudinal weld segments. A schematic of part of the lap plate and the adjacent welds is shown in Figure 5.10(b). A free body diagram (FBD) of the transverse weld segment, shaded in Figure 5.10(b), is shown in Figure 5.10(c). A similar FBD could be drawn for a transverse weld segment in a SOFW connection (see Miazga and Kennedy, 1989). The difference between that FBD and the FBD in Figure 5.10(c) is the shear forces, S, on the ends of the transverse weld segment. These shear forces arise as a result of the continuity of the weld between the transverse and longitudinal segments. The shear forces make the state of stress on the failure plane of weld segments in a MOFW connection different than that of weld segments in a SOFW connection. In an attempt to determine the effect of the continuous weld between two segments on the MOFW connection capacity, some specimens were fabricated with discontinuous corners, as described in Chapter 3. Unfortunately, the test results were inconclusive as there was a large amount of porosity in these welds, which would have decreased the connection capacity. It was expected that these discontinuous corner specimens would have had larger P_m/A_{throat} values than connections with continuous corners and identical geometry.
2. The second possible reason for the observed reduction in strength of MOFW connections as compared to SOFW connections is the influence of the geometry on the stress flow through the connection. In a SOFW connection of any geometry, all of the stress flow must pass through the fillet weld. However, in a MOFW connection, the amount of stress that passes through each weld segment is a function of the connection geometry. A cross section through one of the specimens containing transverse and longitudinal segments is shown in Figure 5.11, where the possible stress flow trajectories through the connection are depicted. The trajectories shown indicate that the stress flow to the longitudinal weld segments is different than if the connection were a SOFW connection containing longitudinal weld segments alone. In Figure 5.11, the majority of the stress trajectories run through the transverse welds. Thus, the transverse welds resist the majority of the load in the connection. If this is the case, then when failure of the transverse weld occurs (which triggers failure of the entire connection), the longitudinal weld would not be loaded to its full SOFW connection capacity, or even the capacity reduced to account for ductility incompatibility alone.

Although it appears that ductility incompatibility accounts for a significant part of the reduction in the effective capacity of non-transverse welds in MOFW connections, analysis of the experimental data has revealed that other mechanisms may also be influential. The two theories above provide possible explanations that require further investigation. However, in the interim these can be represented reasonably well through the use of semi-empirical efficiency factors.

5.3 Fracture Angle

The fracture angles from several research programs are presented in Table 5.8, which is reproduced from Deng *et al.* (2003). A comparison of these fracture angles with the fracture angles reported in Table 4.5 shows that the mean fracture angle of the transverse segment in MOFW connections containing transverse and longitudinal segments is at least twice as large as those reported from SOFW tests. The longitudinal segments as well as the 45° segments, and the transverse segments from the TF MOFW connections, all have mean fracture angles that show reasonable agreement (within 25% of the mean) with those presented in Table 5.8. The mean transverse fracture angle from the TL MOFW connections is actually close to the mean longitudinal fracture angle from the SOFW specimens in Table 5.8. This suggests that the longitudinal segments affected the fracture angle of the transverse segments in the MOFW connections. Since the mean transverse segment fracture angle for the TL MOFW connections is different from the mean fracture angle reported in Table 5.8, the ultimate strength prediction for these weld segments is very likely affected. Thus, the comparison of the fracture angles gives another indication that the weld segment response in MOFW connections is not exactly the same as the weld response in SOFW connections.

5.4 Effect of Connection Plate Yielding on Fillet Weld Strength and Ductility

In the analysis of fillet weld strength by Miazga and Kennedy (1989), it is suggested that fillet welded connections whose plates yield could have a strength less than connections with plates that remain elastic. Plate yielding was observed to affect the ductility of the transverse fillet welds tested by Ng *et al.* (2004b). The test results of the three transverse fillet weld connections tested as part of the complementary testing program are compared with the transverse weld test results from Miazga and Kennedy (1989) and Ng *et al.* (2004a) in Table 5.9. These tests are important because it was necessary to develop a response curve for the fillet welds that formed the MOFW connections, all of which had connection plates that remain elastic, and to investigate the effect of plate yielding on fillet weld behaviour. The test results from Miazga and Kennedy (1989) are from connections that had plates that remained elastic while the test specimens from Ng *et al.* (2004a) had connection plates that yielded.

When comparing the weld strengths (normalized P_m/A_{throat} values) from Table 5.9 it is important to compare fillet welds of the same leg size because of the influence of leg size on fillet weld strength; refer to Section 5.6 for a discussion on this. Therefore, it is only possible to compare directly the 12 mm fillet welds from Ng *et al.* (2004a) and the current research. Upon comparing these two sets of test results it is seen that the 12 mm fillet welds differ in strength by only 3%.

The normalized P_m/A_{throat} values for the transverse 5 mm weld from Miazga and Kennedy (1989) and the values for the transverse 6 mm welds from Ng *et al.* (2004a), shown in Table 5.9, differ by more than 40%. The larger weld size has the higher unit strength, which is opposite to the usual observation. However, there is a significant difference between the two testing programs that could explain this apparent discrepancy. The welding process and procedure used in the two research programs were different. Several different electrode classifications were used by Ng *et al.* (2004a) (see Section 2.2.2), while only a single electrode classification was used by Miazga and Kennedy (1989). As the specimens prepared by Ng *et al.* (2004a) were prepared with the FCAW process they are expected to show larger weld penetration (Miller 1994) than the specimens prepared by Miazga and Kennedy (1989), which used the SMAW process. In addition to this, the test specimens of Ng *et al.* (2004a) were fabricated by commercial steel fabricators, while the test specimens of Miazga and Kennedy (1989) were prepared in the laboratory by a research welding technician. This difference in fabrication conditions allowed a better control over the fillet weld geometry; specifically, their cross-section was close to triangular. Conversely, Ng *et al.* (2004a) reported fillet weld cross sections that showed significant weld face reinforcement, which is not accounted for in the quantity A_{throat}. This basic difference between the two test programs tend to increase the strength of the fillet welds prepared by Ng *et al.* (2004a).

Because of the influences of weld size and welding procedures used in specimen fabrication, it is reasonable to compare only the test results of Ng *et al.* (2004a) and the complementary program for the purposes of investigating the effect of connection plate yielding on fillet weld response. As mentioned above, the strengths of these two sets of specimens differ by only 3%, however, the average weld deformation at P_m of the specimens having plates that yielded is more than 400% greater than that of the specimens with elastic plates.

The test data reported in Table 5.9 imply that there is a greater effect of connection plate yielding on weld deformation than there is on weld strength. However, as there is a limitation on the weld strengths that can be compared, only limited data are available to make this comparison at present.

5.5 General Treatment of the Ductility Incompatibility

In order to assess the safety of MOFW connections, a way of dealing with the ductility incompatibility for a general case is required. The objective of this method is to apply a deformation compatibility approach to any type of MOFW connection.

In order to apply this method, it is assumed that the MOFW connection reaches its ultimate capacity when the critical (least ductile) weld segment in the connection reaches its capacity. If this assumption is made and the deformation at ultimate capacity for a segment of any orientation and the fillet weld response curve are both known, then the ultimate capacity of any MOFW connection can be estimated.

Test data from Miazga and Kennedy (1989), Deng *et al.* (2003), and the complementary testing program are used in the analysis of a general MOFW connection. In order to use the deformation test data from all three test programs, a method different from that presented by Lesik and Kennedy (1990) for normalizing the deformations is required. Using the measured weld deformations from Miazga and Kennedy (1989), Lesik and Kennedy (1990) proposed Equations 5.5 and 5.6. It can be seen from these equations that the weld deformation, Δ, is normalized by dividing by the fillet weld leg size, d. This method of normalization is identical to that used for the deformation results from Deng *et al.* (2003) and the complementary testing program for transverse and longitudinal fillet welds, but it gives values that are $\sqrt{2}$ larger than those reported by Deng *et al.* (2003) for 45° fillet welds. To achieve a common comparison of the deformation data between the testing programs, the deformations are normalized by d*, as defined in Equation 4.2. This method of normalization is equivalent to the method used by Deng *et al.* (2003) for orientations of 0°, 45°, and 90°, while providing a smooth transition between these orientations.

The general procedure for estimating the capacity of a MOFW connection can be summarized as follows. The ultimate deformation of the critical segment, which is taken to represent the ultimate capacity of the MOFW connection, is estimated. Assuming rigid body translation of the connection plates, a value of ρ is calculated for each segment. The contribution from each segment to the joint capacity is estimated using the average response curve described in Section 5.2.2.

The assumption that each weld segment undergoes the same deformation measured in the direction of the load follows from assuming rigid body motion of the plates. Figure 5.12(a) shows a MOFW connection with two segments at two arbitrary orientations. In Figure 5.12(b), the rigid body motion assumption is explained in more detail. By assuming that the two segments undergo the same deformation, the following expression for the deformation of the non-critical segment (Segment 2) in terms of that of the critical segment (Segment 1) is derived as follows:

$$\left(\frac{\Delta}{d^*}\right)_2 = \frac{\Delta_2}{d^*_2} = \frac{\left(\frac{\Delta}{d^*}\right)_1 \times d^*_1}{d^*_2} \qquad (5.7)$$

where the ratio d^*_1/d^*_2 can be expanded by applying the definition of d*, as defined in Equation 4.2, and assuming that each segment has the same fillet leg size, d. This results in the following equation:

$$\left(\frac{\Delta}{d^*}\right)_2 = \frac{\Delta_2}{d^*_2} = \left(\frac{\Delta}{d^*}\right)_1 \times \frac{\sin(\theta_1)+\cos(\theta_1)}{\sin(\theta_2)+\cos(\theta_2)} \qquad (5.8)$$

Once Equation 5.8 is evaluated, it is divided by the estimate of the normalized ultimate deformation for Segment 2 to obtain the value of ρ for Segment 2. With this value of ρ, the fraction of the ultimate capacity of Segment 2 can be evaluated using the SOFW response curve. The MOFW connection capacity is then estimated by summing the full capacity of the least ductile segments with the reduced capacities of the other segments.

5.5.1 Ultimate Deformation of Fillet Welds

In order to carry out the procedure described in the previous section, it is necessary to determine the deformation of fillet welds at their ultimate capacity. Besides the test data reported in Table 4.7 from the complementary tests of this research program, test data from Miazga and Kennedy (1989) and Deng *et al.* (2003) were used to assess the ultimate deformation of fillet welds. Miazga and Kennedy (1989) used the main plate leg dimension (MPL), as defined in Figure 4.1, to normalize the weld deformations for all weld orientations. On the other hand, Deng *et al.* (2003) used the MPL for normalizing weld deformations for transverse and longitudinal orientations, and $\mathrm{MPL}/\sin(45°)$ for the 45° orientation. In order to have a means of comparing the data in a consistent manner, the definition of d* from Equation 4.2 is required.

The test data reported by Miazga and Kennedy (1989) are converted into the form of Equation 4.2 and are reported Figure 5.13, along with deformation data from Deng *et al.* (2003) and the complementary testing program. Note that there is significant scatter in the longitudinal and 45° values of Δ_{ult}/d^* and the 45° values from Deng *et al.* (2003) are significantly different than those reported by Miazga and Kennedy (1989). Because of the significant difference between the two groups of data reported for the 45° orientation, two possible equations are proposed for the prediction of Δ_{ult}/d^* as follows:

$$\frac{\Delta_{ult}}{d^*} = 0.19(\theta + 2)^{-0.36} \tag{5.9}$$

$$\frac{\Delta_{ult}}{d^*} = 0.148 - 0.00130\theta \tag{5.10}$$

where θ is the weld orientation in degrees. Equation 5.9 is evaluated by conducting a least squares analysis on all the test data, except the 45° data from Deng *et al.* (2003). Equation 5.10 is a linear equation that connects the means weld deformations from orientations 0° and 90° for the test data from Deng *et al.* (2003) and the complementary test program. These equations are plotted along with the test data in Figure 5.14. Equation 5.10 predicts the value of Δ_{ult}/d^* for the 45° test data of Deng *et al.* (2003) better than Equation 5.9, and yet it still provides good predictions of the values of Δ_{ult}/d^* for both transverse and longitudinal welds.

Even though Equations 5.9 and 5.10 provide estimates of the ultimate deformation that are not significantly different for transverse and longitudinal orientations, they show a significant departure for the intermediate orientations. The test data from

Deng *et al.* (2003) indicate a linear trend between the two extreme orientations, whereas the test data from Miazga and Kennedy (1989) indicate a non-linear trend. Miazga and Kennedy are not the only researchers to discover a non-linear relationship between Δ_{ult}/d^* and weld orientation. Research by Butler and Kulak (1971) also indicates a non-linear relationship, as shown in Figure 5.15. Thus, there is further support for the non-linear model of the ultimate capacities. Nevertheless, the fact that there is significant scatter in the experimental results must be kept in mind. It should be noted that the specimens tested by Deng *et al.* (2003) had fillet welds fabricated with three different electrode classifications, whereas the specimens from Miazga and Kennedy (1989) were fabricated with only E7014 electrodes. This may explain some of the scatter in the test results shown in Figure 5.13. Moreover, the data reported by Butler and Kulak (1971) is significantly different from the results of either Deng *et al.* (2003) or Miazga and Kennedy (1989), however the test specimens of Butler and Kulak (1971) were fabricated with E60XX electrodes and the SMAW process. Thus, the true response of fillet weld ultimate deformations is difficult to assess because of the scatter in the test results. Therefore, both Equations 5.9 and 5.10 will be used in the following analysis.

5.5.2 Selection of a Combination Reduction Factor

In order to assess the capacity of a MOFW connection, a Combination Reduction Factor (CRF) is used to account for the ductility incompatibility between the segments. This provides a simple means of accounting for the contribution from each segment of a MOFW.

The value of the combination reduction factor is calculated using the following steps. First, the ultimate deformation of the critical segment is estimated using either Equation 5.9 or 5.10. The normalized deformations of the non-critical segments are then calculated using the procedure outlined in Figure 5.12 and Equation 5.8. At this point, the normalized deformations of all the segments at the ultimate capacity of the MOFW connection are known since it is assumed that the connection will reach its ultimate capacity when the critical segment reaches its capacity. The value of ρ for each segment is then determined using the calculated failure deformation and the predicted ultimate deformation of the segment had it been in a SOFW connection. It is assumed that each weld segment in the MOFW connection has the same leg size. Using the average response curve described in Table 5.4 and the calculated values of ρ, a value of $P_\theta / P_{u\theta}$, equivalent to a combination reduction factor, can be calculated for each segment.

The ultimate capacity of the segment is modified by multiplying its predicted ultimate capacity by the combination reduction factor. The predicted capacity of a MOFW connection is equal to the summation of each segment’s reduced capacity.

Values for the combination reduction factor for various critical segment orientations are presented in Figures 5.16 and 5.17. The values reported in Figure 5.16 are calculated by using Equation 5.9 to predict the ultimate deformation of a weld segment, whereas Figure 5.17 uses Equation 5.10 to predict the ultimate deformation. Note that the predictions of the combination reduction factor, shown in Figures 5.16 and 5.17, show the closest agreement for a critical segment orientation of 90° with a non-critical segment orientation of 0°. The difference between the data reported in Figures 5.16 and 5.17 is a result of the ultimate deformation predictions. Values of the combination reduction factor for critical orientations of 30° and 15° are not given in Figure 5.17 as the combination reduction factors for these two critical orientations all differ from 1.0 by less than 0.01%.

In order to apply this method to a design situation the method must be simplified. Thus, the goal is to provide the designer with an equation that predicts the contribution of the non-critical segment to the MOFW connection capacity. The value of the combination reduction factor is the fraction of the segment single orientation connection capacity prediction that is contributed to the MOFW connection capacity. The first step is to predict the value of the combination reduction factor for all critical orientations using only the values of the combination reduction factor for the case where a transverse segment is the critical segment (this is the most common case). In order to use only combination reduction factor values from transversely oriented segments, the following approximate equation is proposed:

$$\mathrm{CRF}_{\mathrm{X}}^{\mathrm{Y}} = \frac{\mathrm{CRF}_{\mathrm{X}}^{90}}{\mathrm{CRF}_{\mathrm{Y}}^{90}} \tag{5.11}$$

where the value of “Y” is the critical segment orientation and the value of “X” is the non-critical segment orientation. Thus, the term $\mathrm{CRF}_{\mathrm{X}}^{90}$ is the value of the combination reduction factor evaluated with a critical segment orientation of 90° and a non-critical orientation of “X”. Once Equation 5.11 is evaluated, the value of $\mathrm{CRF}_{\mathrm{X}}^{\mathrm{Y}}$ is multiplied by the non-critical segment’s ultimate capacity. The non-critical segment is assumed to contribute the modified capacity to the total connection capacity. The results of this procedure are shown in Figures 5.18 and 5.19. A comparison of Figure 5.18 with 5.16 and Figure 5.19 with 5.17 shows that the estimate of the combination reduction factor using Equation 5.11 is always conservative (i.e., lower), thus it is only necessary to predict the value of the combination reduction factor for critical segment orientations of 90°.

With a critical orientation of 90°, the two predictions (based on Equations 5.9 and 5.10) of the combination reduction factor for any non-critical orientation are shown in Figure 5.20. A simplified equation is proposed, also shown in Figure 5.20, that is a linear interpolation between the value of the combination reduction factor for a non-critical orientation of 0° equal to 0.85 and the value of the combination reduction factor at 90°, which is 1.0:

$$\mathrm{CRF}(\theta) = 0.85 + 0.0017 \times \theta \tag{5.12}$$

Equation 5.12 is chosen to predict the value of combination reduction factors with a critical segment orientation of 90° because of its simplicity and the wide scatter of the measured ultimate weld deformations. Recall that for this method the difference between the ultimate deformations of the critical and non-critical segments affects the value of the combination reduction factor. The closer that the ultimate deformation of the non-critical segment is to the deformation of the critical segment, the closer the value of the combination reduction factor is to 1.0. The sensitivity of the combination reduction factor to the scatter in the ultimate deformation data also explains the difference in the value of the combination reduction factor for a non-critical segment orientation of 0°, as shown in Figures 5.16 and 5.17. Figure 5.21 shows the results of using Equation 5.12 to predict the efficiency factors. The values show good agreement with Figure 5.8, which used the measured weld deformations and the average response curve of Table 5.4 to predict the MOFW capacities. The combination reduction factors calculated with Equation 5.12 are used in the reliability analysis in Section 5.7.

5.6 Effect of Weld Size and Number of Passes on Weld Strength

Ng *et al*. (2004b) and Miazga and Kennedy (1989) have observed that leg size affects the strength of fillet welds. Typically, fillet welds that have been prepared with a single pass (most often with a nominal leg size of 6 mm) have shown greater unit strength than fillet welds prepared with three passes (usually with a nominal leg size of 12 mm). From past research it is unclear whether or not the higher unit strength that has been observed for smaller single pass fillet welds is the result of the fillet weld leg size, the number of passes, or both. It is believed that the effect of tempering by subsequent passes and the interface between passes represents a plane of weakness that contributes to the difference in unit strength between single pass and multi-pass welds (Ng *et al*. 2002).

In order to assess the effect of weld size and number of passes, the test results from Miazga and Kennedy (1989), Ng *et al*. (2004a), and the current research program are examined. The test results from Miazga and Kennedy (1989) and Ng *et al*. (2004a) that are used here are presented in Tables 5.10 and 5.11. Fillet welds of two different leg sizes are reported in each table; Miazga and Kennedy (1989) tested 5 mm (1 pass) and 9 mm (3 pass) fillet welds, while Ng *et al*. (2004a) tested 6 mm (1 pass) and 12 mm (3 pass) fillet welds. The strength of the weld specimens from Miazga and Kennedy (1989) have been reported as P_m/A_{throat} values because only E7014 electrodes from a single heat were used to fabricate the specimens. However, the P_m/A_{throat} values are normalized by the measured tensile strength of the fillet weld for the Ng *et al*. (2004a) test results, as several different electrodes, both classifications and heats, were used. It is seen from these tables that there is a definite effect of weld size and/or number of passes on the strength of fillet welds. The average ratio of the smaller single pass fillet weld strength to the larger three pass fillet weld strength is 1.09 and 1.28 for the test results from Miazga and Kennedy(1989) and Ng *et al*. (2004a), respectively. Analogous ratios can be computed for the MOFW specimens of the following designations for which different weld sizes were tested: TF, TFa, TL50, and TL50a. From these test results, the average ratio of the smaller single pass weld strength to the larger three pass weld strength is 1.12.

From the three ratios reported above it is seen that the strength of fillet welds is affect by weld size and/or number of passes. In order to determine whether or not the two factors' (weld size and number of passes) individual contributions to fillet weld strength can be assessed, the average values of P_m/A_{throat} will be compared for the TL100 and TL100SP specimens (refer to Table 4.2 for these values). These specimen types are nominally identical (including leg size) except that the TL100 specimens were fabricated with three weld passes and the TL100SP specimens were fabricated with only one pass. It is seen that the TL100SP specimen P_m/A_{throat} values are only marginally greater (2%) than the TL100 specimens. This implies that the effect of the number of weld passes on fillet weld strength is not significant.

It should be noted that the weld strength ratios for small single pass fillet welds and large three pass fillet welds reported above are averages. There is significant scatter between the actual ratios, which are either reported or can be calculated from the values reported in Tables 5.10 and 5.11. In fact, based on the transverse test data of Miazga and Kennedy (1989), the three pass 9 mm welds show a higher strength than the single pass 5 mm welds. In general, however, the smaller weld sizes exhibit higher strength.

5.7 Reliability Analysis

This section presents the procedure used to assess the level of safety of MOFW connections as designed in North America. The fillet weld design equation used in the Canadian design standard, CSA–S16–01 (CSA 2001), is given as:

$$V_R = 0.67\, \phi_w A_w\, X_U\, (1.00 + 0.50 \sin^{1.5} \theta) \tag{5.13}$$

The factored ultimate strength of a fillet weld, V_R, is a function of the fillet weld throat area and the corresponding stress. These two parts are represented in Equation 5.13 as A_w and $0.67\, X_U\, (1.00 + 0.50 \sin^{1.5} \theta)$, respectively. The term $(1.00 + 0.50 \sin^{1.5} \theta)$ is an empirical modification factor that reflects the effect of loading orientation, θ, on the capacity of fillet welds, where θ is the angle between the line of action of the applied load and the longitudinal axis of the fillet weld. The empirical modification factor comes from the work by Lesik and Kennedy (1990).

The throat area, A_w, in Equation 5.13 is calculated by assuming that the fillet welds have a cross section as shown in Figure 5.22. The throat dimension for the assumed cross section is therefore equal to the specified leg size multiplied by sin(45°). The throat area, is calculated by multiplying the throat dimension for the assumed fillet weld cross section by the length of the fillet weld.

In reality, when a fillet weld fails the leg sizes may not be equal and the fracture surface may be at an angle, α, other than 45°, as shown in Figure 5.23. Work by Miazga and Kennedy (1989) led to an equation that predicts the failure angle, α, based on the angle of loading for equal legged fillet welds. However, when welds are deposited in the horizontal position, as was the case for the preparation of the test specimens, the main plate leg size is usually greater than the lap plate leg size (see Figure 4.1). The unequal leg sizes affect the fracture surface angle and thus the fracture surface area.

The term X_U in Equation 5.13 represents the nominal ultimate tensile strength of the filler metal. The constant 0.67 modifies this tensile strength to a shear strength which is applied on the throat area of the fillet weld. The throat area of a longitudinal fillet weld is generally under a state of pure shear, but welds of other orientations have a combination of tension and shear on the throat area. Because of the difference in the stress state of the throat area of fillet welds of different orientations, fillet weld strength is affected by orientation. Work by Lesik and Kennedy (1990) led to the term $(1.00 + 0.50\sin^{1.5}\theta)$, which is a simplified way of accounting for the variation in the fillet weld throat stress state with orientation as developed by Miazga and Kennedy (1989).

The level of safety for fillet welds will be investigated by starting with the following two equations, which are based on Galambos and Ravindra (1978):

$$\phi R \geq \alpha D \tag{5.14}$$

$$\phi = \Phi_\beta \rho_R \exp(-\beta \alpha_R V_R) \tag{5.15}$$

Equation 5.14 is the basic limit states design equation which indicates that the factored resistance, ϕR, of all members in a structure must be equal to or greater than the factored load effects, αD, on those members. In the case of connections fabricated using fillet welds, the factored resistance is calculated using Equation 5.13.

Equation 5.15 expresses the resistance factor, ϕ, as a function of the safety index , β, and other factors which will be defined subsequently. It is the safety index that indicates the level of safety inherent in the limit states design equation. The factor Φ_β is a function of β and its purpose is to modify the resistance factor if β is different than 3.0. A β value of 3.0 is used to calculate the term αD in Equation 5.14 and if the ϕ factor is based upon a β value other than 3.0, Equation 5.15 must be modified so that both sides of the inequality in Equation 5.14 use a consistent β value (Fisher *et al.* 1978). Franchuk *et al.* (2002) have proposed the following expression for Φ_β:

$$\Phi_\beta = 0.0062\beta^2 - 0.131\beta + 1.338 \tag{5.16}$$

A value of 0.55 has been suggested by Galambos and Ravindra (1978) for the separation factor for resistance, α_R. The remaining two terms, ρ_R and V_R, are the bias coefficient of the resistance and the coefficient of variation of the resistance, respectively. The factors are a measure of the mean and dispersion of the actual resistance compared to the nominal resistance of the structural member in question. In the case of Equation 5.13, ϕ_w is equal to 0.67 (CSA 2001). Using this value for the resistance factor, ϕ_w, β can be determined using different values of ρ_R and V_R, as shown graphically in Figure 5.24. The figure also indicates the traditional target safety index for connections of $\beta = 4.5$.

Galambos and Ravindra (1978) suggest that ρ_R and V_R take the following form:

$$\rho_R = \rho_G \rho_M \rho_P \tag{5.17}$$

$$V_R^2 = V_G^2 + V_M^2 + V_P^2 \tag{5.18}$$

The variation between the mean and nominal resistance of a structural element is assumed to be a function of the variations in the geometric and material properties of the element, as well as the assumptions of the design equation used to model of the structural element's behaviour. These three parameters are the geometric factor, ρ_G, the material factor, ρ_M, and the professional factor, ρ_P. The three terms in Equation 5.18, V_G, V_M, and V_P, are the coefficients of variation associated with the geometric, material, and professional factors, respectively.

The curves presented in Figure 5.24 show that the value of β can change considerably with small changes in either ρ_R or V_R. Both ρ_R and V_R vary depending on how the parameters ρ_G, ρ_M, and ρ_P are defined.

The safety indices for two different design approaches for MOFW connections are evaluated. The first method uses the strength summation approach with the segment capacity predicted by Equation 5.13. Although no explicit guidance is offered in S16-01 on the design of concentrically loaded MOFW connections, the strength summation approach is an intuitive one for connection design. The safety index resulting from this method will be seen to be unacceptably low. Thus, the safety index of a second method, which uses Equation 5.12 to account for the observed ductility incompatibility in a MOFW connection, is evaluated. The safety index for this method will be seen to be adequate.

The general approach used by both methods has been used by Lesik and Kennedy (1990), Ng *et al.* (2004b), and Deng *et al.* (2003). The important feature of this procedure is that it deals directly with the variability in fillet weld strength that occurs as a result of the conversion from tensile to shear strength. The Canadian fillet weld design equation uses a factor of 0.67 for this conversion.

5.7.1 Strength Summation (Method 1)

The capacities of MOFW connections are evaluated using Equation 5.13 and the strength summation approach. This intuitive method of MOFW connection design is implicitly supported by clause 11.4.2 of W59–98, Welded Steel Construction (CSA 1998).

5.7.1.1 Geometric Factor, ρ_G

As discussed previously, a cross section of a fillet weld is rarely equal legged. With reference to Figure 4.1, both the Main Plate Leg (MPL) and the Lap Plate Leg (LPL) measurements were taken prior to testing. The Minimum Throat Dimension (MTD), neglecting face reinforcement, can then be calculated using Equation 4.1.

The calculated minimum throat dimension (Equation 4.1) is different than the nominal minimum throat dimension, which is assumed to be the 45° throat for an equal legged fillet weld (see Figure 5.22). Using these definitions the following ratio is defined:

$$\text{Ratio G} = \frac{\text{Calculated MTD}}{\text{Nominal MTD}} \tag{5.19}$$

Data only from the current testing program was used in the calculation of ρ_G. A maximum fillet weld leg size tolerance equal to the nominal leg size was specified for the test specimens used in the research by Ng *et al.* (2002) and Deng *et al.* (2003). That is, in both research programs the fillet weld leg size was required to be no larger than the specified leg size. It is felt that this requirement does not represent actual practice; rather, it is suspected that the actual leg size of the fillet welds fabricated are generally significantly greater than the specified leg size. Because the weld tolerances of Ng *et al.* (2002) and Deng *et al.* (2003) did not allow the actual leg size to be greater than the specified leg size, these specimens will not be used in the evaluation of ρ_G and V_G.

Ratio G is then calculated for each weld segment of every specimen using the measurements reported in Tables 3.4, 3.5, and 3.6 with the mean of Ratio G being ρ_G and the coefficient of variation (COV) of Ratio G being V_G.

The TL100SP specimens from the current research were not used in the calculation of ρ_G as the fillet weld, which had a 12 mm specified leg size, was deposited in a single pass. Normally a 12 mm weld would be deposited in three passes so these specimens were not considered to give an accurate representation of the population of fillet weld cross sections.

5.7.1.2 Material Factor, ρ_M

The material factor includes two parameters, ρ_{M1} and ρ_{M2}. The factor ρ_{M1} addresses the variation in the weld metal tensile strength, while ρ_{M2} addresses the variation in the conversion from the tensile strength to shear strength. Thus, the material factor takes the following form:

$$\rho_M = \rho_{M1}\rho_{M2} \tag{5.20}$$

$$V_M^{\ 2} = V_{M1}^{\ 2} + V_{M2}^{\ 2} \tag{5.21}$$

The material factor, ρ_{M1}, relates the actual strength of the filler metal to its nominal strength. The results of several all-weld-metal coupon tests, conducted in accordance with Clause 8 of ANSI/AWS A5.20 (AWS 1995), were used to determine ρ_{M1}. Both SMAW and FCAW, as well as several different electrode classifications, were used in the calculation of ρ_{M1}. The test results used to determine ρ_{M1} are shown in Table 5.12. The test results come from the testing programs of Miazga and Kennedy (1989), Ng *et al.* (2004a), and the current research program.

In order to define the bias coefficient ρ_{M2}, the following equation is defined:

$$\text{Ratio M}_2 = \frac{\tau_u}{0.67 \times \sigma_{UTS}} \tag{5.22}$$

The ratio is determined from longitudinal weld tests, which are assumed to fail in pure shear. The term σ_{UTS} in Equation 5.22 is the measured tensile strength of the weld metal for the tested longitudinal weld. The value of τ_u in Equation 5.22 is equal to P_m/A_{throat} for the longitudinal SOFW connection. Thus, Ratio M_2 is equal to the value of the normalized P_m/A_{throat} described in Equation 5.1 divided by 0.67. Ratio M_2 is evaluated for all the test results reported in Table 5.2, and the mean and coefficient of variation of Ratio M_2 for these results are equal to ρ_{M2} and V_{M2}, respectively.

5.7.1.3 Professional Factor, ρ_P

The professional factor, ρ_P, is equal to the mean ratio of the test capacity to predicted capacity for all of the MOFW connection test results used in the calculation of ρ_P. The TL100D and TL50D specimens were not used because of the unusual welding geometry and the significant porosity observed at the weld root for these specimens. The predicted capacity of each MOFW connection was calculated by summing the individual capacities of each weld segment in the connection. Each weld segment's individual capacity is calculated using the following equation:

$$\text{Segment Capacity} = \tau_u \times A_{\text{throat}} \times (1.0 + 0.5\sin^{1.5}\theta) \tag{5.23}$$

Except for the results from Miazga and Kennedy (1989), all of the test results presented in Table 5.2 are from test specimens with 12 mm specified fillet welds prepared using the FCAW process. Since all of the MOFW specimens were prepared using the FCAW process the values of τ_u used for 12 mm specimens is taken equal to the mean value of the normalized P_m/A_{throat} for all FCAW longitudinal welds reported in Table 5.2, multiplied by the tensile strength of the weld metal used in the MOFW specimen. However, the value of τ_u is modified for the specimens that have single pass 8 mm specified leg size welds because of the observed effect that leg size and number of passes have on fillet weld strength, as discussed in Section 5.6. The value used for τ_u is multiplied by 1.28 for specimens TL50a and TFa which were prepared with a single pass and 8 mm specified leg size. The number 1.28 is a weld leg size modifier and is equal to the mean normalized P_m/A_{throat} of all the 6 mm specified leg size specimens reported by Ng *et al.* (2004a) divided by the mean normalized P_m/A_{throat} of all the 12 mm specified leg size specimens reported by the same author; Section 5.6 gives more details on the calculation of the size modification factor. As discussed in Section 5.2.3, this weld size modifier, derived from 6 mm welds, provides a conservative estimate of the safety index for other weld sizes.

The values for A_{throat} are obtained from Table 5.7. In the table, the specimen failure side is listed; "Front" stands for the front side, "Back" for the back side, "Both" for both sides, and "Combo" stands for a combination of segments from both the front and back sides of the specimen. Specimen TF-1 is the only specimen to be listed as "Combo" in Table 5.7, and it has this designation as its front side transverse weld segment failed along with all of the segments on the back side. However, as it is still necessary to account for the load that is carried by the front two 45° segments they were assumed to carry the same amount of load as the back face 45° segments, as predicted using Equation 5.23. For the rest of the specimens, if the fillet weld fractured on both sides, then the specimen capacity was estimated by summing each segment's predicted capacity, again using Equation 5.23 for each segment. However, if the fillet weld segments that fractured were located only on the front or the back side, then the connection capacity was estimated as the sum of the predicted segment capacities on the failure side multiplied by two.

5.7.1.4 Safety Index

The values for all of the parameters used in this reliability analysis are presented in Table 5.13. Equation 5.15 is used to solve for the value of β that corresponds to the values given in Table 5.13, with $\phi = 0.67$ and $\alpha_R = 0.55$. This is done by rearranging Equation 5.15 into a function of β and finding the root of this function:

$$f(\beta) = \ln\left(\frac{\Phi_\beta \times \rho_R}{\phi}\right) - \beta \times \alpha_R \times V_R \tag{5.24}$$

The value of β is determined to be 4.1 for this method of estimating the capacities of MOFW connections, which does not account for the observed ductility incompatibility effect. This value of β is less than the value of 4.5 suggested by Galambos and Ravindra (1978).

As stated in Section 5.7.1.3, the value of τ_u used for evaluating Equation 5.23 is based upon only the FCAW normalized P_m/A_{throat} values from Table 5.2 since the MOFW joints were prepared with the FCAW process. The mean P_m/A_{throat} value for the FCAW specimens is 0.848, which is approximately 3% greater than the mean value of all the specimens reported in the table, 0.827. This latter value, however, was used in evaluating the bias coefficient ρ_{M2} (refer to Section 5.7.1.2).

5.7.2 Accounting for Fillet Weld Response (Method 2)

This method assesses the safety index if both Equations 5.12 and 5.13 are used to predict the capacity of a MOFW connection. As in the previous method, the capacity of each segment is predicted using Equation 5.13. However, the predicted capacity of the non-critical segments is modified with Equation 5.12. The total capacity of the MOFW connection is assumed to be the sum of these modified capacities of the non-critical segments along with the capacities of the critical segments, which are predicted using Equation 5.13.

5.7.2.1 Safety Index

The reliability analysis is carried out in exactly the same way as in Method 1 with the only difference being the calculation of the professional factor. In this method, the individual segment capacities are computed using the following equation:

$$\text{Segment Capacity} = \tau_u \times A_{throat} \times (1.0 + 0.5\sin^{1.5}\theta) \times CRF(\theta) \tag{5.25}$$

It is seen that Equation 5.25 is the same as Equation 5.23 with the exception of the CRF(θ) term. The value of CRF(θ) is calculated using Equation 5.12.

When the ductility incompatibility is accounted for in this way, the value of β is found to be 4.5. Because this method yields an acceptable safety index, it is recommended that the fillet weld design equation be modified in the following way:

$$\begin{aligned} &V_R = 0.67\,\phi_w A_w\, X_U\,(1.00 + 0.50\sin^{1.5}\theta) \times CRF(\theta) \\ &\text{with } CRF(\theta) = 0.85 + 0.0017 \times \theta \text{ for MOFW segments} \\ &\text{and } CRF(\theta) = 1.0 \text{ for SOFW segments} \end{aligned} \tag{5.26}$$

Equation 5.26 assumes that the critical segment in the MOFW connection is a transverse segment. While this is the most common case, a method of extending the method of combination reduction factors to any MOFW connection configuration has been presented in Section 5.5.2. Thus, the equation for the combination reduction factor that is presented in Equation 5.26 can be used with the following equation to account for any MOFW connection configuration with a critical segment orientation, Y, and a non-critical segment orientation, X.

$$CRF_X^Y = \frac{CRF_X}{CRF_Y} \tag{5.27}$$

The values of CRF_X and CRF_Y are both calculated using the equation for the combination reduction factor presented in Equation 5.26.

5.7.3 Base Metal Failure and the Current North American Design Standards

It is important to note that in both Methods 1 and 2 there is no check of the base metal failure. It has been observed that transverse fillet welds may not fracture through the fillet weld, but rather through the base metal to which the fillet weld is fused. In the Canadian structural steel design standard, S16–01 (CSA 2001), the potential of base metal failure is accounted for. However, the present reliability analysis, as well as the reliability analyses carried out by Ng *et al*. (2004b), Deng *et al.* (2003), and Lesik and Kennedy (1990), do not take into account the base metal failure. It is proposed that since the reliability analyses to date reveal an adequate safety index without taking into account the base metal failure, the base metal failure criteria need not be accounted for in fillet weld connection design.

The current practice of accounting for the possibility of rupture through the base metal is conservative. The tensile strength of the base metal used in the design equation does not reflect the actual tensile strength of the metal at the fusion interface, which is affected by both tempering, as a result of the welding process, and intermixing of the weld and base metal. Considering that the tensile strength of the weld metal is typically greater than that of the base metal, the tensile strength of the metal at the fusion interface can be greater than the tensile strength of the base material.

Accounting for base metal rupture is therefore believed to be too conservative. It does not allow for the 50% increase in transverse fillet weld strength over longitudinal fillet weld strength since the base metal strength is predicted to be lower than the weld metal strength. In fact, by accounting for the base metal failure of a transverse weld fabricated with E480XX electrodes and 350W plate, its capacity is limited to only 33% higher than the capacity of an equivalent longitudinal weld. However, Deng *et al.* (2003) and Lesik and Kennedy (1990) show that accounting for a 50% increase in strength of a transverse weld over a longitudinal weld provides an adequate safety index.

Table 5.1 –Description of the Test Specimens Used in Assessing the Longitudinal Weld Length Effect

<table>
<tr><th>Specimen</th><th>AWS Classification</th><th>Number of Passes</th><th>Specified Leg Size (mm)</th><th>Nominal Length of Longitudinal Segment (mm)</th><th>Research Program</th></tr>
<tr><td>L1-1
L1-2
L1-3</td><td>E70T-4</td><td rowspan="3">3</td><td rowspan="3">12.5</td><td rowspan="3">50</td><td rowspan="3">Deng et al.</td></tr>
<tr><td>L2-1
L2-2
L2-3</td><td>E70T-7</td></tr>
<tr><td>L3-1
L3-2
L3-3</td><td>E71T8-K6</td></tr>
<tr><td>0.1
0.2
0.3</td><td>E7014</td><td>1</td><td>6.4</td><td rowspan="2">80</td><td rowspan="2">Miazga and Kennedy</td></tr>
<tr><td>0.11
0.12
0.13</td><td>E7014</td><td>3</td><td>12.5</td></tr>
<tr><td>L100-1
L100-2
L100-3</td><td>E70T-7</td><td>3</td><td rowspan="2">12.5</td><td rowspan="2">100</td><td rowspan="3">Current Research</td></tr>
<tr><td>L100-4
L100-5
L100-6</td><td>E70T-7</td><td>1</td></tr>
<tr><td>L150-4
L150-5
L150-6</td><td>E70T-7</td><td>3</td><td>12.5</td><td>150</td></tr>
</table>

Table 5.2 – Normalized Longitudinal Weld Strengths

Specimen	P_m/A_{throat} * (MPa)	Weld Metal UTS (MPa)	Normalized P_m/A_{throat}		
			Individual Tests	Length Averages	Average for all Specimens
L1-1	505	631	0.801	0.901	0.827
L1-2	482	631	0.763		
L1-3	502	631	0.795		
L2-1	536	605	0.887		
L2-2	551	605	0.911		
L2-3	548	605	0.905		
L3-1	512	493	1.039		
L3-2	477	493	0.968		
L3-3	511	493	1.037		
0.1	464	538	0.864	0.764	
0.2	427	538	0.794		
0.3	420	538	0.781		
0.11	373	538	0.694		
0.12	399	538	0.743		
0.13	383	538	0.712		
L100-1	434	569	0.763	0.762	
L100-2	429	569	0.754		
L100-3	475	569	0.834		
L100-4	422	569	0.741		
L100-5	397	569	0.698		
L100-6	444	569	0.780		
L150-4	453	569	0.795	0.861	
L150-5	500	569	0.878		
L150-6	519	569	0.911		

* See Table 4.6 and Appendix F for the P_m and A_{throat} values.

Table 5.3 – Data From Deng *et al.* (2003) and Complementary Testing Program

Specimen	Electrode	P/Athroat (MPa)	UTS (MPa)	Normalized P/Athroat	Electrode Average
TNY-1	E70T-7	732	569	1.285	1.315
TNY-2	E70T-7	740		1.300	
TNY-3	E70T-7	774		1.359	
F1-1	E70T-4	675	631	1.070	1.170
F1-2	E70T-4	783		1.242	
F1-3	E70T-4	755		1.198	
F2-1	E70T-7	816	605	1.350	1.336
F2-2	E70T-7	787		1.301	
F2-3	E70T-7	820		1.356	
F3-1	E71T8-K6	691	493	1.402	1.196
F3-2	E71T8-K6	683		1.384	

Table 5.4 – Coefficients for Response Curves for Various Weld Orientations

Coefficients	Longitudinal	45°	Transverse	Lesik and Kennedy	Average*
a_1	-2.6	-17.5	-2.6	1.5	1.47
a_2	131.2	577.2	181.9	-95.5	-95.42
a_3	-1075.7	-4139.2	-1697.9	887.6	887.57
a_4	2974.4	10848.2	5063.0	-2724.7	-2724.66
a_5	-3309.7	-11764.7	-5926.9	3286.4	3286.37
a_6	1283.4	4497	2383.5	-1354.3	-1354.33
a_s	8.97	9.67	7.05	8.48	8.476
Proportional Limit	0.05	0.05	0.05	0.035	0.05

* based upon the longitudinal, 45°, and transverse fillet weld response curves, see Section 5.2.2.

Table 5.5 – Deformations Used In Deformation Compatibility Analysis

Fillet Weld Orientation	Values Used for the Normalized Ultimate Deformation
Longitudinal	0.1351
45°	0.1141
Transverse	0.0302

Table 5.6 – Weld Size Effect for E70T-7 Electrodes (based on Ng *et al.*, 2004a)

Specimen	Specified Leg Size (mm)	P_m/A_{throat} (MPa)	UTS (MPa)	Normalized P_m/A_{throat}		Size Ratio*
				Individual Assemblies	Averages	
T11	6	930	605	1.538	1.558	1.241
T12	6	1021	631	1.619		
T13	6	964	584	1.650		
T14	6	930	652	1.426		
T15	6	1015	652	1.557		
T25	12	783	605	1.295	1.256	
T26	12	822	631	1.304		
T27	12	710	584	1.215		
T28	12	788	652	1.209		

***** The ratio between the average normalized P_m/A_{throat} value for the 6 mm leg size over the average P_m/A_{throat} value for the 12 mm leg size.

Table 5.7 – Breakdown of the Values of A_{throat}

Specimen	Weld Failure Side	Throat Areas (mm^2)			
		Front Side		Back Side	
		Transverse	Non–Transverse	Transverse	Non–Transverse
TF-1	Combo*	564	1086	557	1269
TF-2	Both	616	1208	613	1117
TF-3	Both	579	1113	539	1089
TF-4	Back	635	1068	663	1182
TFa-1	Both	422	792	380	768
TFa-2	Both	383	794	355	714
TFa-3	Both	408	756	361	792
TFa-4	Both	445	801	416	720
TL50-1	Both	748	945	688	858
TL50-2	Both	717	952	688	872
TL50-3	Both	748	898	717	837
TL50-4	Both	737	926	701	920
TL50a-1	Both	497	626	496	596
TL50a-2	Both	500	631	509	649
TL50a-3	Both	497	600	507	639
TL50a-4	Both	564	681	521	692
TL100-1	Back	768	1929	801	2004
TL100-2	Back	686	1668	731	1890
TL100-3	Front	776	1853	678	1705
TL100SP-1	Back	569	1550	591	1646
TL100SP-2	Both	585	1641	592	1584
TL100SP-3	Back	664	1632	604	1588
TL100D-1	Front	626	1601	720	1656
TL100D-2	Front	615	1516	682	1649
TL100D-3	Front	721	2006	667	1963
TL50D-1	Both	675	909	723	907
TL50D-2	Back	653	874	727	939
TL50D-3	Both	688	890	641	988

* All segments on back face plus the front face transverse segment failed.

Table 5.8 – Mean Fracture Angle Reported By Other Researchers for SOFW Tests

Loading Angle (°)	Miazga & Kennedy (1989) (°)	McClellan (1989) (°)	Bowman & Quinn (1994) (°)	Deng *et al.* (2003) (°)	Predicted Fracture Angle (M&K Equation) (°)
90	19	20 - 25	16	14	15
45	21	—	—	28	24
0	49	42 - 48	56	30	45

Note: Reproduced from Deng *et al.* (2003)

Table 5.9 – Effect of Plate Yielding on Strength and Ductility

Leg Size (mm)	Research Program	Plate Yielded?	Average (Δ/d) at P_m	COV	Average Normalized P_m/A_{throat}	COV	Sample Size
5	Miazga and Kennedy (1989)	No	0.05	0.27	1.04	0.03	3
6	Ng *et al.* (2004a)	Yes	0.13	0.59	1.74	0.17	51
9	Miazga and Kennedy (1989)	No	0.05	0.09	1.15	0.01	3
12	Ng *et al.* (2004a)	Yes	0.17	0.34	1.36	0.13	34
12	Current Research	No	0.03	0.05	1.32	0.03	3

Table 5.10 – Fillet Weld Leg Size Effect (based on Ng *et al.*, 2002)

Specimen	Number of Passes	Normalized P_m/A_{throat} (MPa)	Specimen	Number of Passes	Normalized P_m/A_{throat} (MPa)
T1-1	1	1.397	T17-1	1	1.956
T1-2	1	1.409	T17-2	1	2.063
T1-3	1	1.459	T17-3	1	1.994
T2-1	1	1.414	T18-1	1	2.264
T2-2	1	1.402	T18-2	1	2.355
T2-3	1	1.345	T18-3	1	2.342
T3-1	1	1.336	T19-1	1	2.036
T3-2	1	1.257	T19-2	1	2.173
T3-3	1	1.250	T19-3	1	2.020
T4-1	1	1.836	T20-1	3	1.015
T4-2	1	1.820	T20-2	3	1.310
T4-3	1	1.817	T20-3	3	1.147
T5-1	1	1.865	T21-1	3	1.387
T5-2	1	1.764	T21-2	3	1.331
T5-3	1	1.857	T21-3	3	1.252
T6-1	1	2.198	T22-1	3	1.343
T6-2	1	2.007	T22-2	3	1.305
T6-3	1	2.191	T22-3	3	1.386
T8-2	1	1.655	T23-1	3	1.259
T8-3	1	1.662	T23-2	3	1.209
T9-1	1	1.952	T23-3	3	1.173
T9-2	1	1.930	T24-1	3	1.422
T9-3	1	1.977	T24-2	3	1.442
T10-1	1	1.726	T24-3	3	1.397
T10-2	1	1.866	T25-2	3	1.275
T10-3	1	1.694	T25-3	3	1.315
T11-1	1	1.631	T26-1	3	1.359
T11-2	1	1.507	T26-2	3	1.382
T11-3	1	1.473	T26-3	3	1.333
T12-1	1	1.828	T27-1	3	1.107
T12-2	1	1.964	T27-2	3	1.260
T12-3	1	1.781	T27-3	3	1.282
T13-1	1	1.661	T28-1	3	1.188
T13-3	1	1.638	T28-2	3	1.242
T14-1	1	1.435	T28-3	3	1.198
T14-2	1	1.470	T30-2	3	1.514
T14-3	1	1.373	T30-3	3	1.478
T15-1	1	1.647	T31-1	3	1.729
T15-2	1	1.476	T31-2	3	1.677
T15-3	1	1.544	T31-3	3	1.775
T16-1	1	1.581	T32-1	3	1.581
T16-3	1	1.609	T32-2	3	1.601
			T32-3	3	1.681

Note: Specimens T1 to T19 were prepared with 6 mm single pass fillet welds, and specimens T20 to T32 were prepared with 12 mm three pass fillet welds.

Table 5.11 – Miazga and Kennedy (1989) Results Indicating Weld Size Effect

Orientation	Number of Passes	Specimen	P_m/A_{throat} (MPa)		Size Comparison*	
			Individual	Average	Individual Orientation	All Orientations
90°	1	90.1	567	560	0.91	1.09
		90.2	572			
		90.3	542			
	3	90.11	623	616		
		90.12	617			
		90.13	610			
75°	1	75.1	596	607	1.01	
		75.2	604			
		75.3	620			
	3	75.11	600	600		
		75.12	610			
		75.13	589			
60°	1	60.1	682	687	1.19	
		60.2	685			
		60.3	695			
	3	60.11	595	576		
		60.12	571			
		60.13	561			
45°	1	45.1	577	589	1.26	
		45.2	600			
		45.3	590			
	3	45.11	464	466		
		45.12	460			
		45.13	475			
30°	1	30.1	556	547	1.10	
		30.2	533			
		30.3	553			
	3	30.11	498	497		
		30.12	505			
		30.13	488			
15°	1	15.1	431	427	1.05	
		15.2	419			
		15.3	431			
	3	15.11	415	408		
		15.12	377			
		15.13	432			

Table 5.11 continued – Miazga and Kennedy (1989) Results Indicating Weld Size Effect

Orientation	Number of Passes	Specimen	P_m/A_{throat} (MPa)		Size Comparison*	
			Individual	Average	Individual Orientation	All Orientations
0°	1	0.1	464	437	1.13	1.09
		0.2	427			
		0.3	420			
	3	0.11	373	385		
		0.12	399			
		0.13	383			

* Mean of single pass weld strength/ three pass weld strength

Table 5.12 – Weld Metal Tensile Strength Results Used in Calculating ρ_{M1}

AWS Designation	Measured Tensile Strength (MPa)	Nominal Tensile Strength (MPa)	Ratio of Measured to Nominal Strength
E70T-7	571	480	1.19
	576	480	1.20
	578	480	1.20
	568	480	1.18
	566	480	1.18
	574	480	1.20
	609	480	1.27
	600	480	1.25
	584	480	1.22
	652	480	1.36
E70T-4	513	480	1.07
	513	480	1.07
	557	480	1.16
	557	480	1.16
	562	480	1.17
	563	480	1.17
	630	480	1.31
	631	480	1.31
E70T7-K2	592	480	1.23
	591	480	1.23
E71T8-K6	495	480	1.03
	484	480	1.01
	488	480	1.02
	485	480	1.01
	494	480	1.03
	495	480	1.03
	491	480	1.02
E7014	517	480	1.08
	523	480	1.09
	543	480	1.13
	529	480	1.10
	541	480	1.13

Table 5.13 – Summary of Reliability Parameters

	Method 1	Method 2
ρ_G	1.03	1.03
V_G	0.10	0.10
ρ_{M1}	1.15	1.15
V_{M1}	0.08	0.08
ρ_{M2}	1.23	1.23
V_{M2}	0.12	0.12
ρ_P	0.83	0.89
V_P	0.12	0.11
ρ_R	1.21	1.30
V_R	0.22	0.21
$\Phi(\beta)$	0.90	0.87
β	4.1	4.5

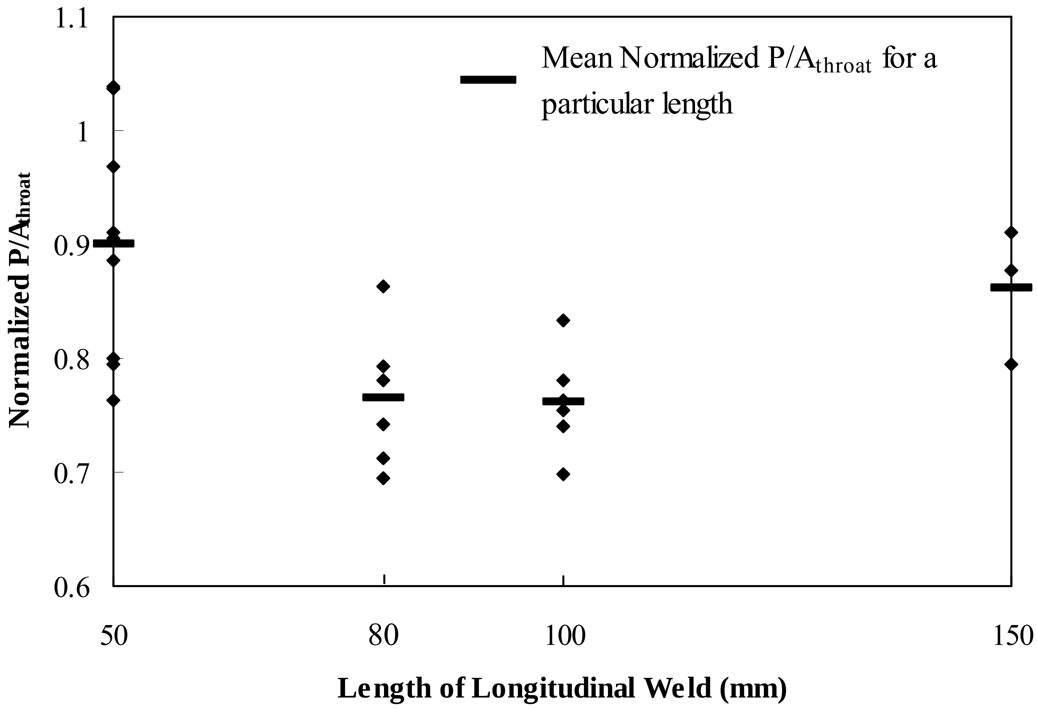

Figure 5.1 – Longitudinal Strength Variation with Length

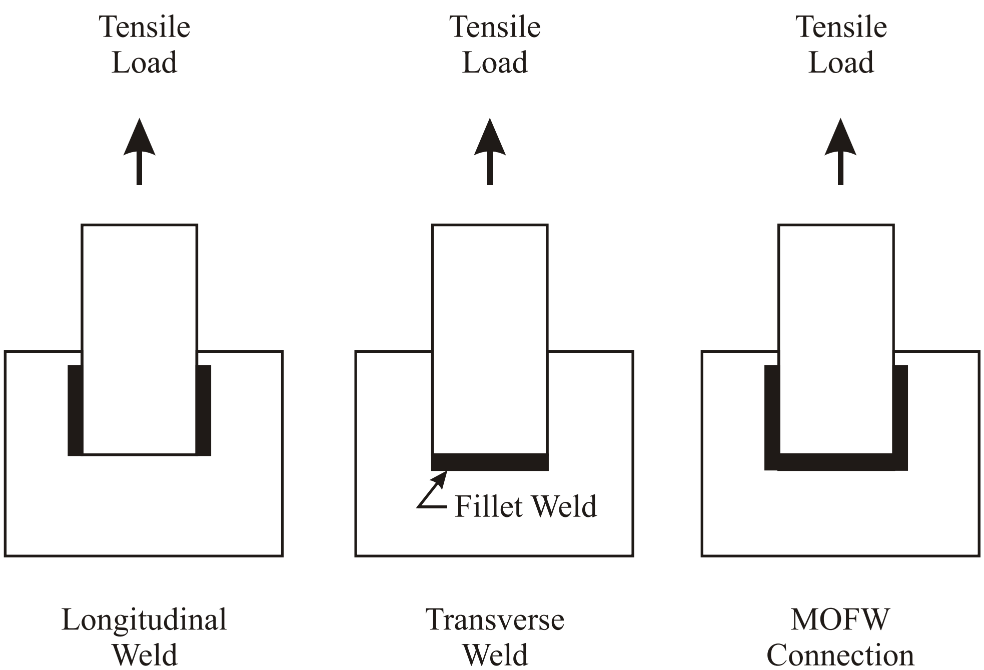

Figure 5.2 – Plan View of Different Simple Fillet Configurations

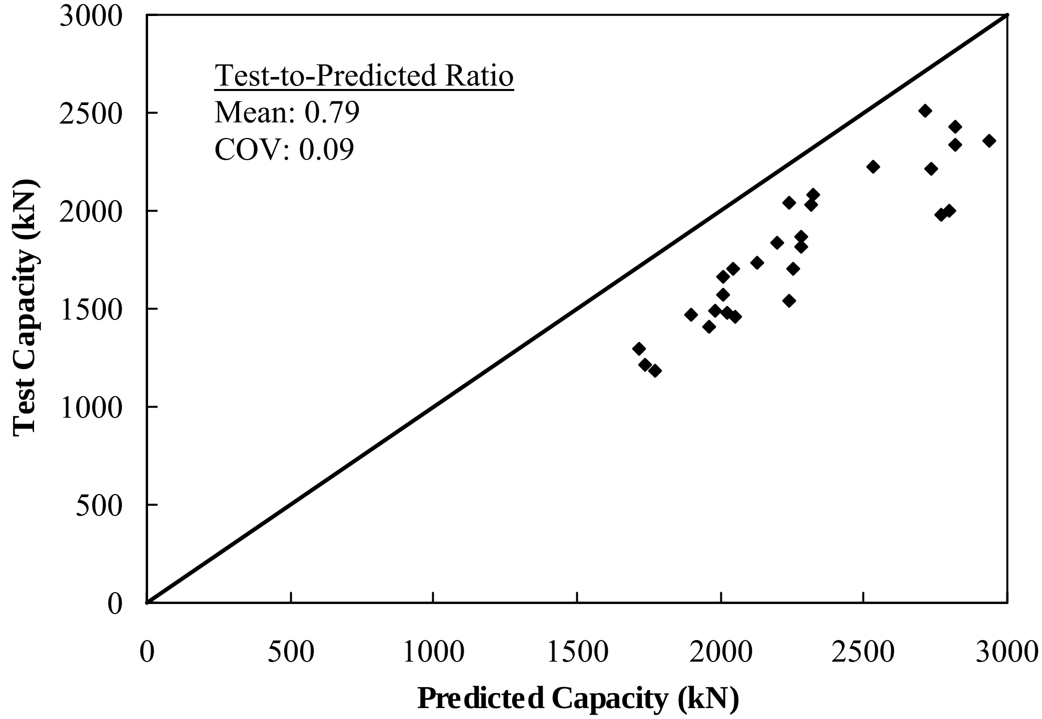

Figure 5.3 – Strength Summation Prediction

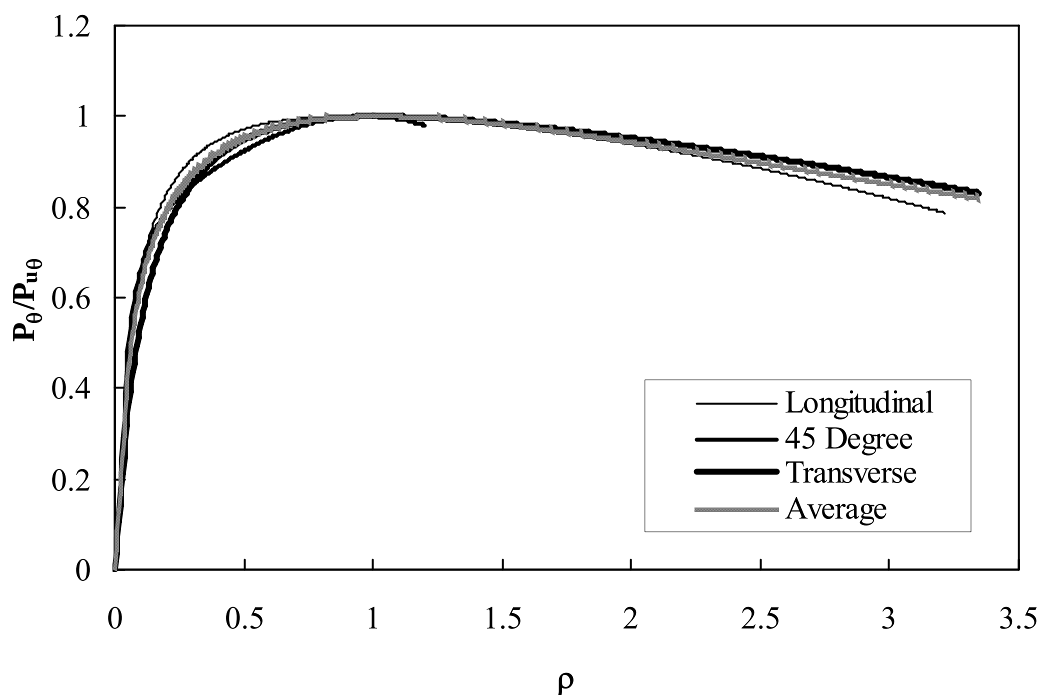

Figure 5.4 – Response Curves from Deng *et al.* (2002) and the Complementary Testing Program

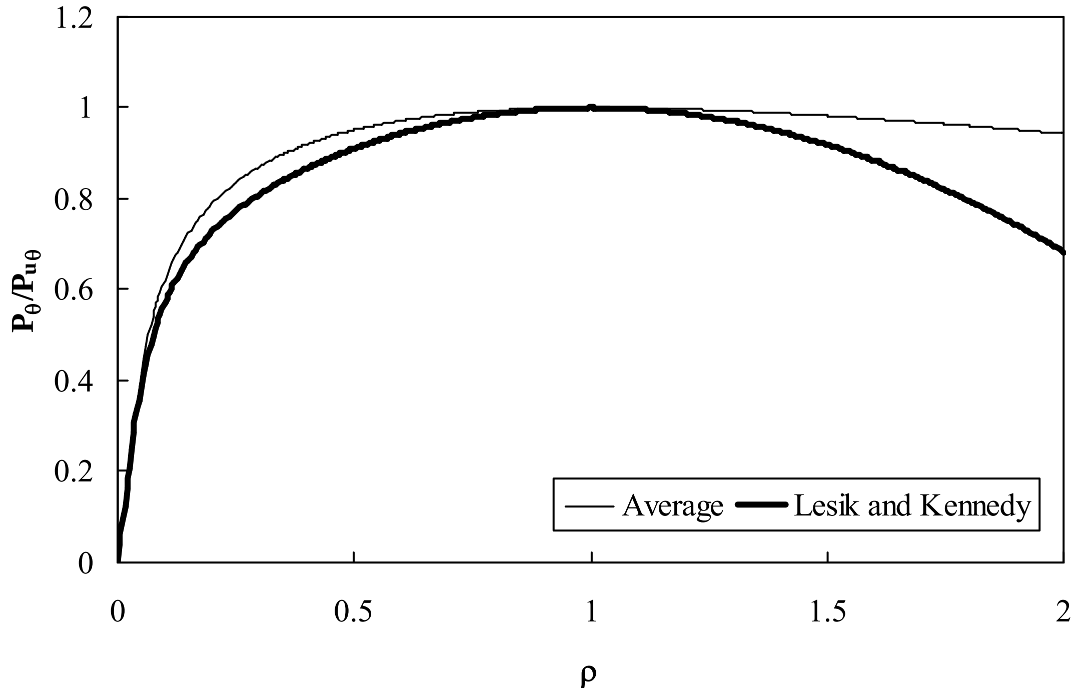

Figure 5.5 – Response Curve Comparison

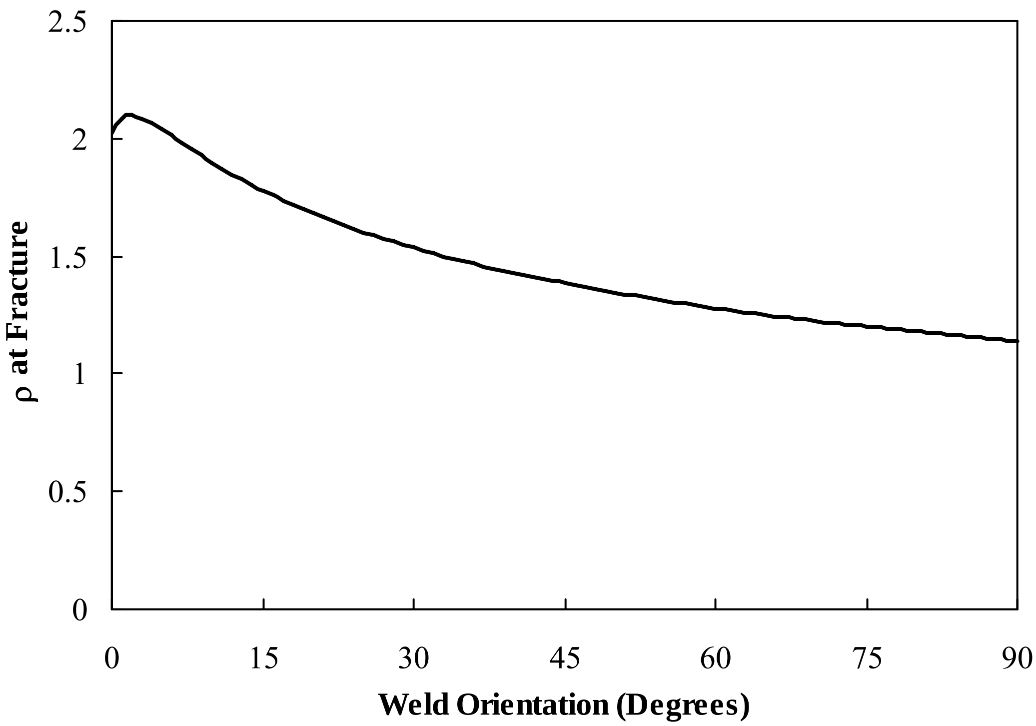

Figure 5.6 – Maximum Predicted Value of ρ (based on Lesik and Kennedy, 1990)

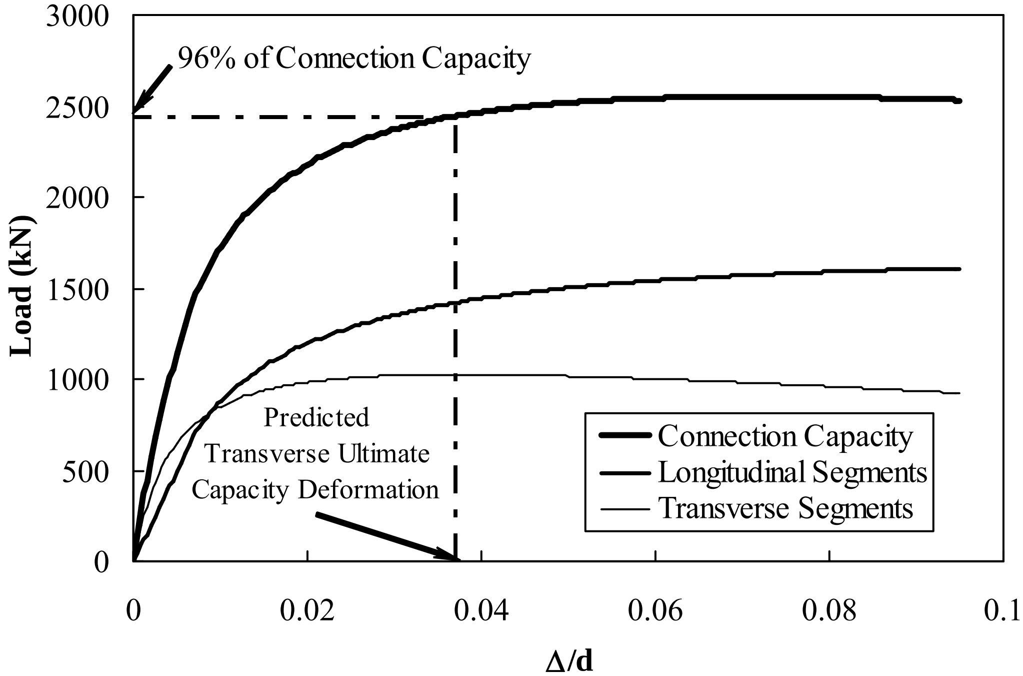

Figure 5.7 – Connection Behaviour of TL100 Specimen as Modelled by Response Curves

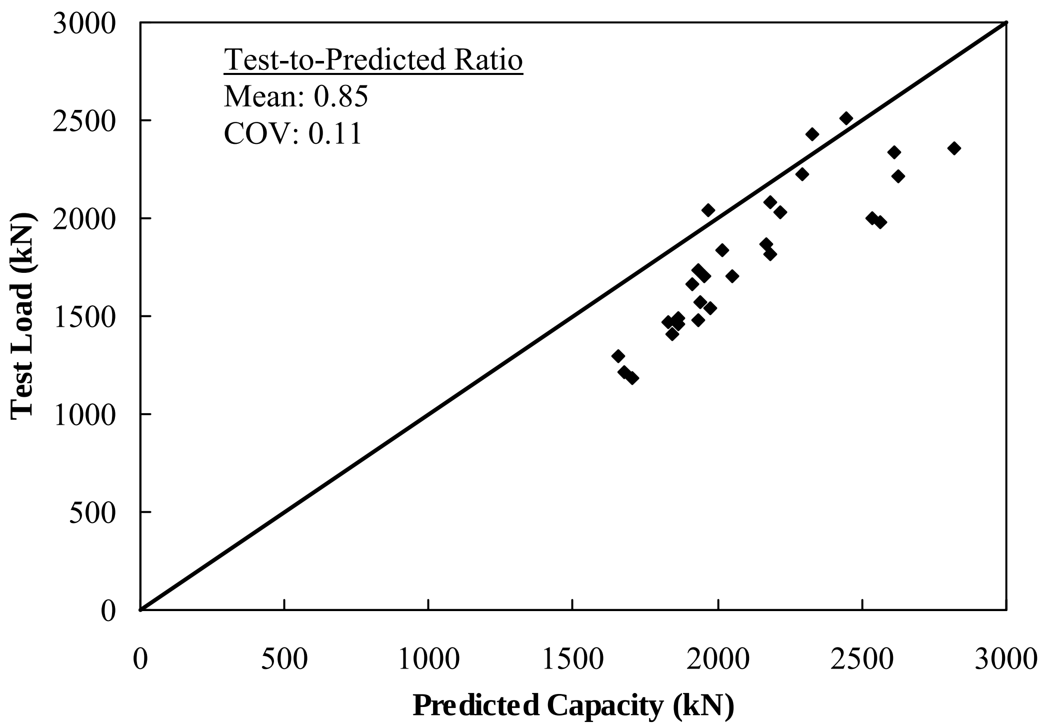

Figure 5.8 – Ductility Compatibility Approach with Average Response Curve

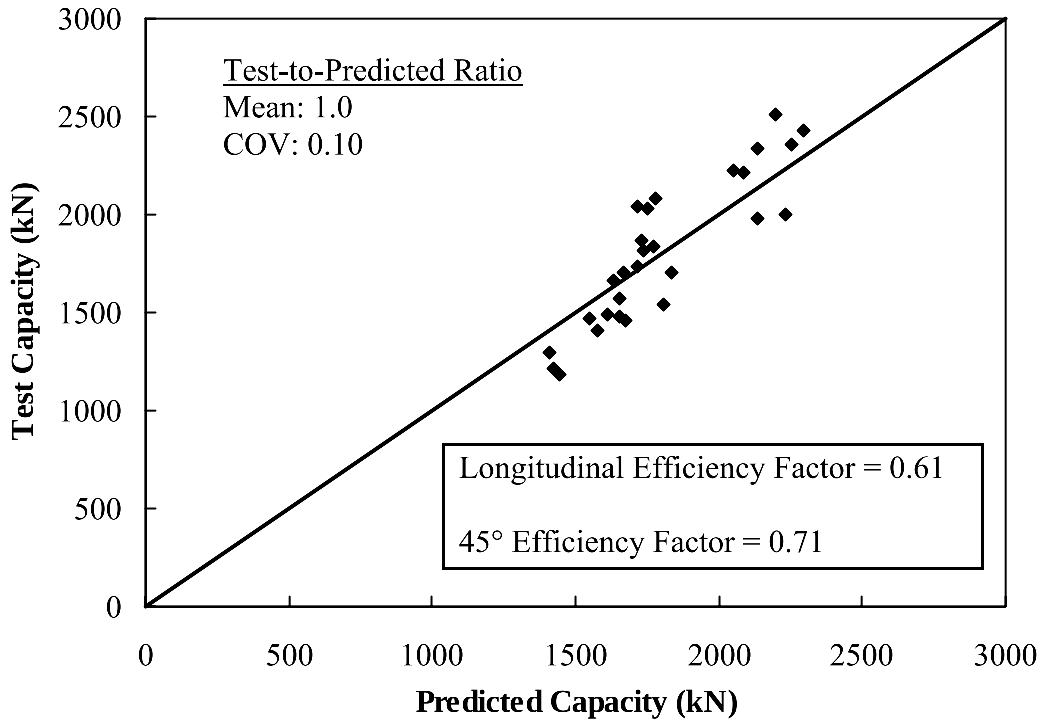

Figure 5.9 – Capacity Prediction with Efficiency Factors

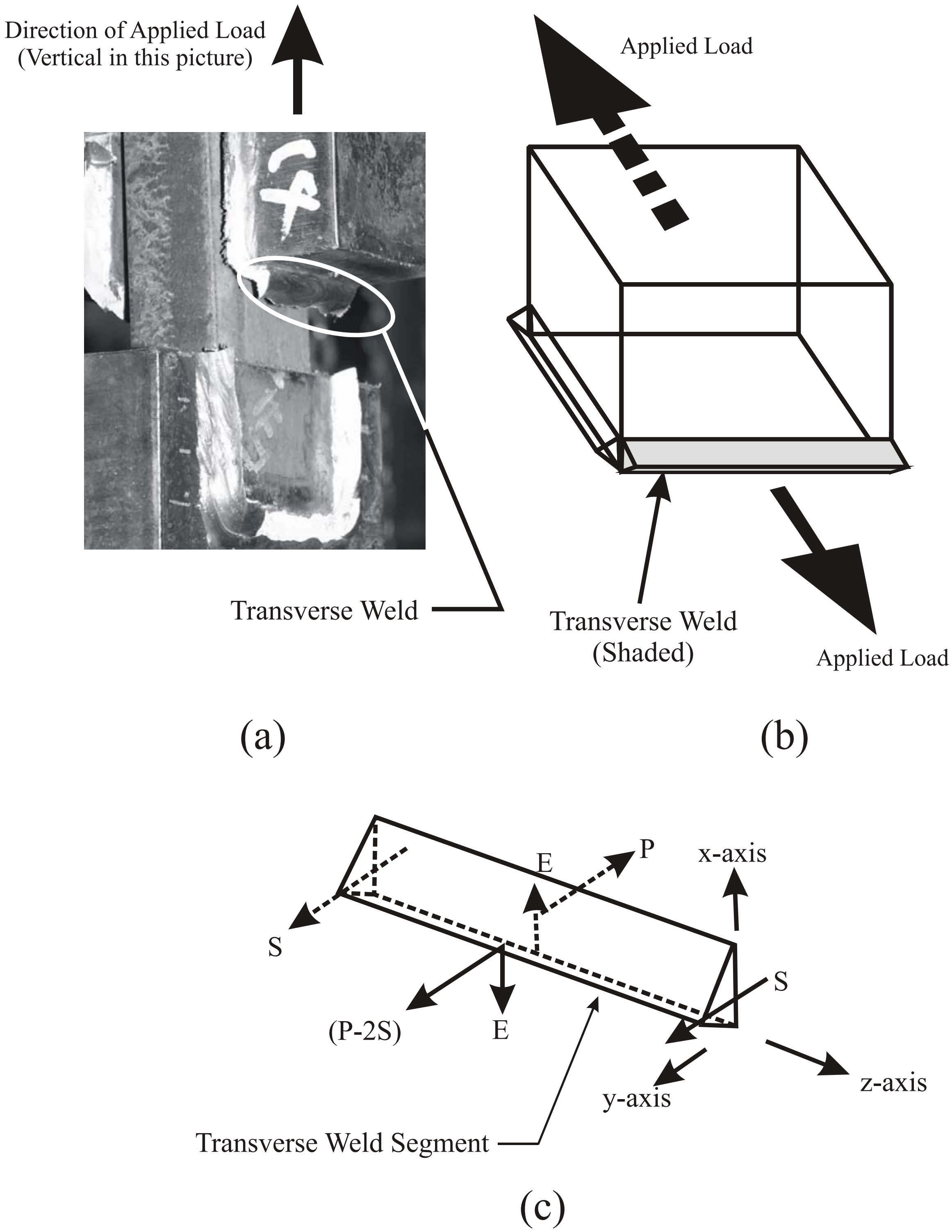

Figure 5.10 – Weld Segment Influence

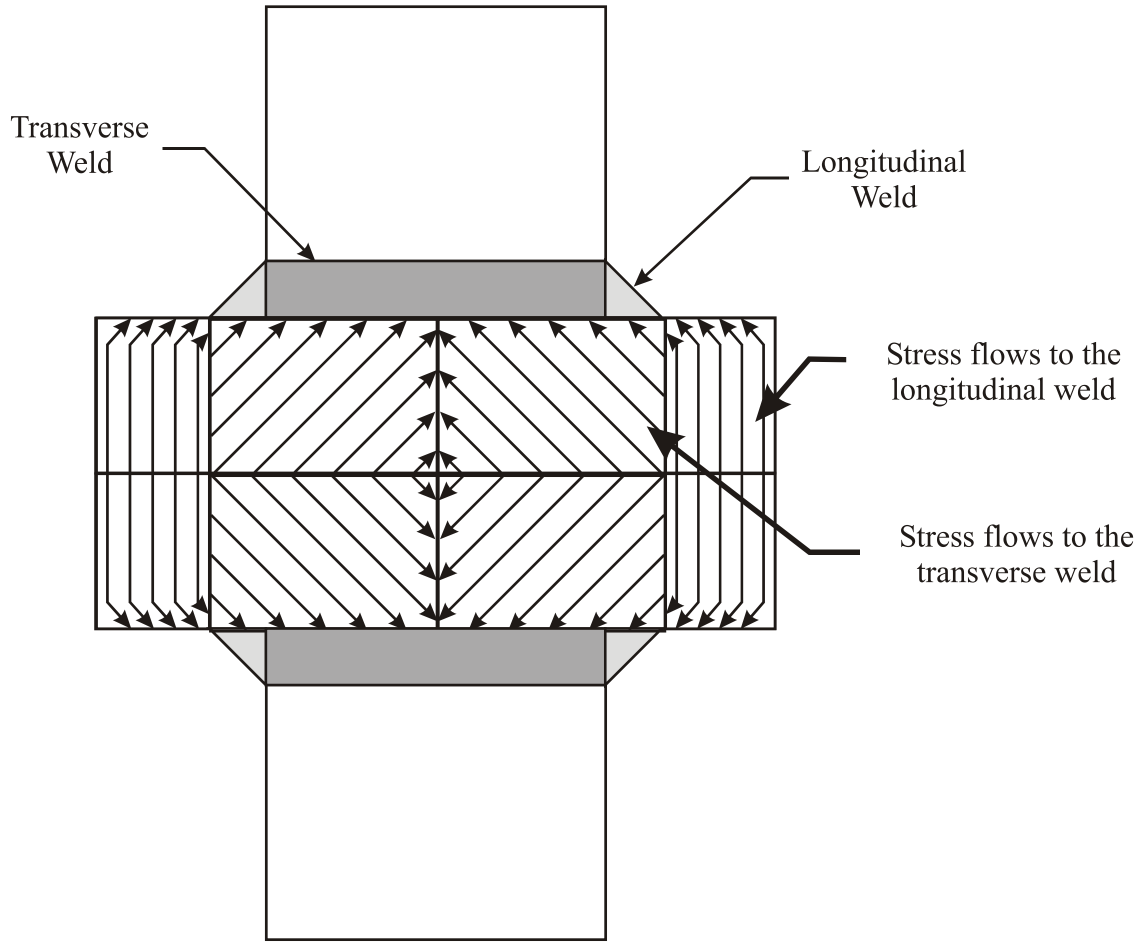

Figure 5.11 – Cross-section through Specimen Showing the Possible Stress Trajectories

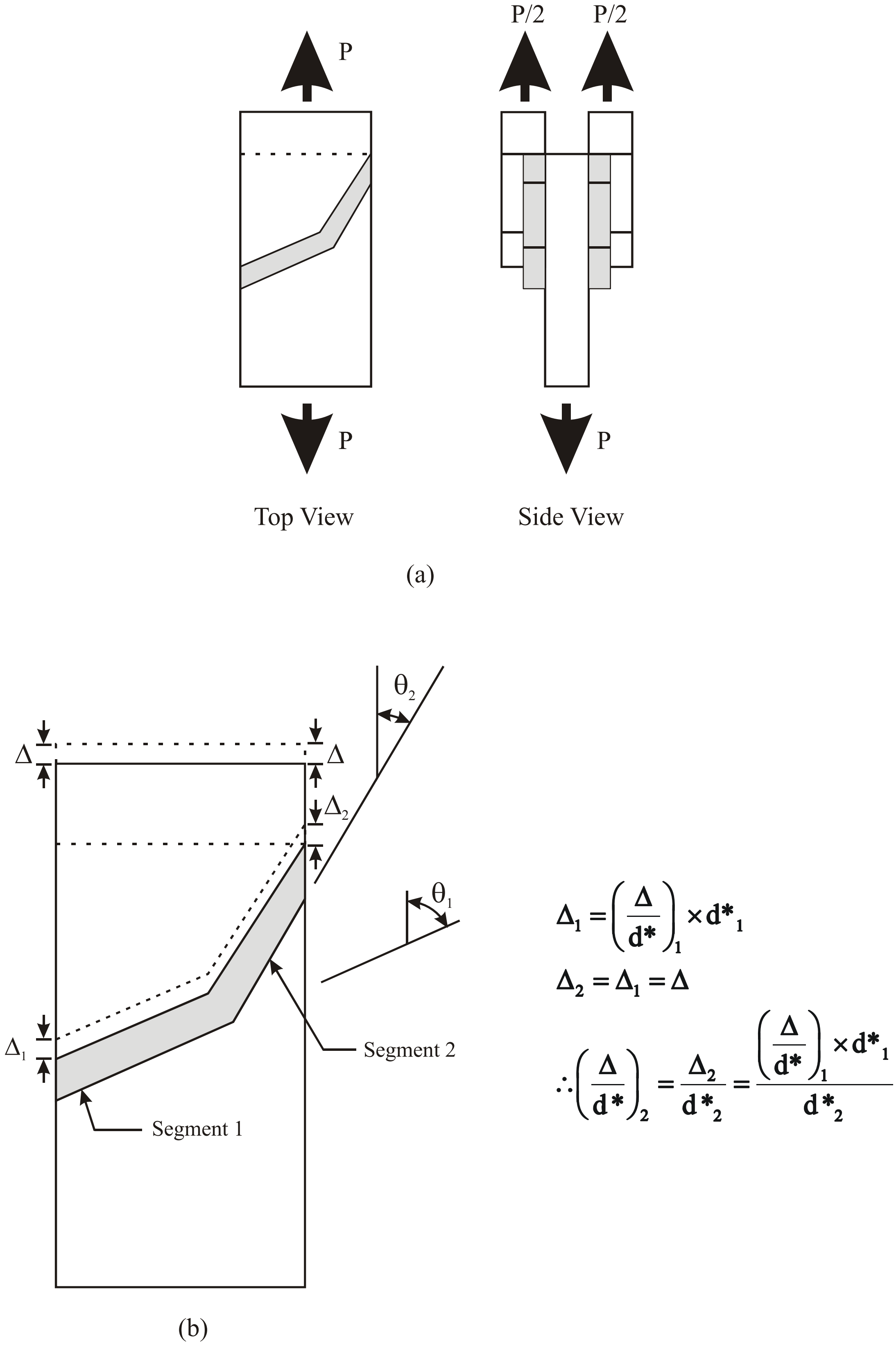

$$\Delta_1 = \left(\frac{\Delta}{d^*}\right)_1 \times d^*_1$$

$$\Delta_2 = \Delta_1 = \Delta$$

$$\therefore \left(\frac{\Delta}{d^*}\right)_2 = \frac{\Delta_2}{d^*_2} = \frac{\left(\frac{\Delta}{d^*}\right)_1 \times d^*_1}{d^*_2}$$

Figure 5.12 – Assumed Rigid Body Movement of the Connection

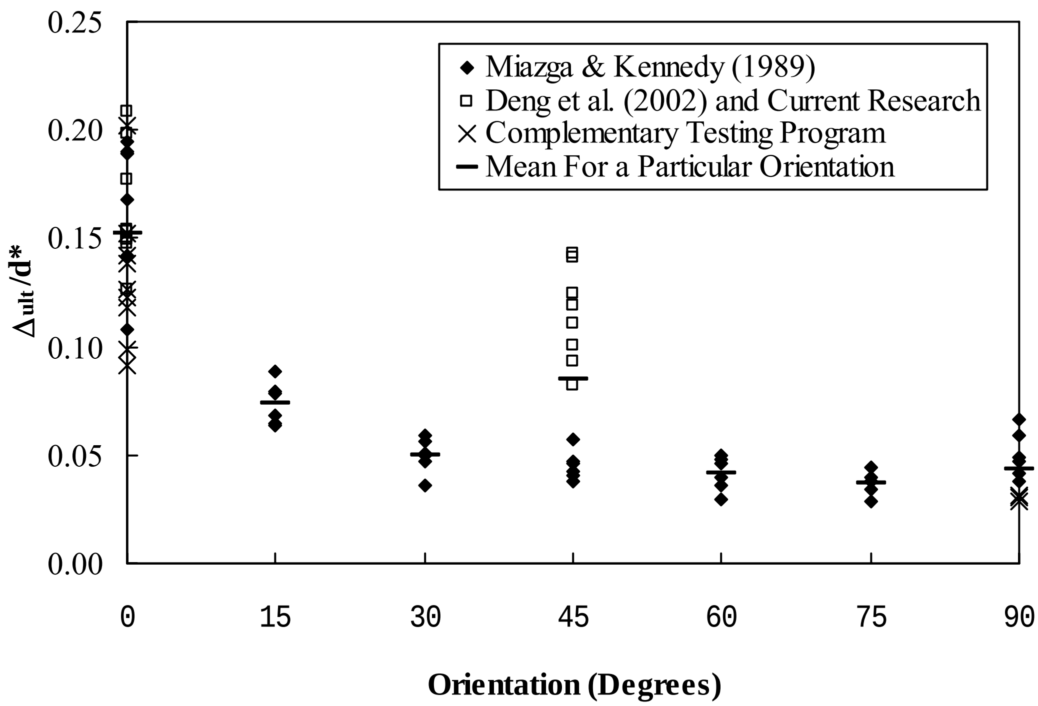

Figure 5.13 – Normalized Ultimate Deformations

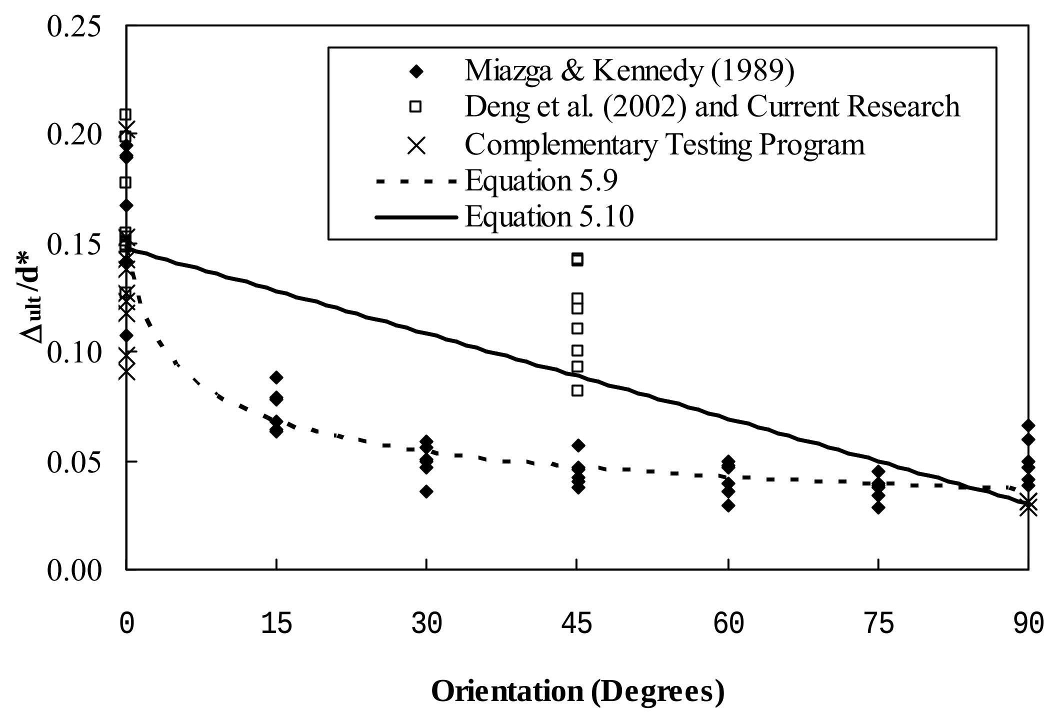

Figure 5.14 – Prediction of Weld Deformation at Ultimate Capacity

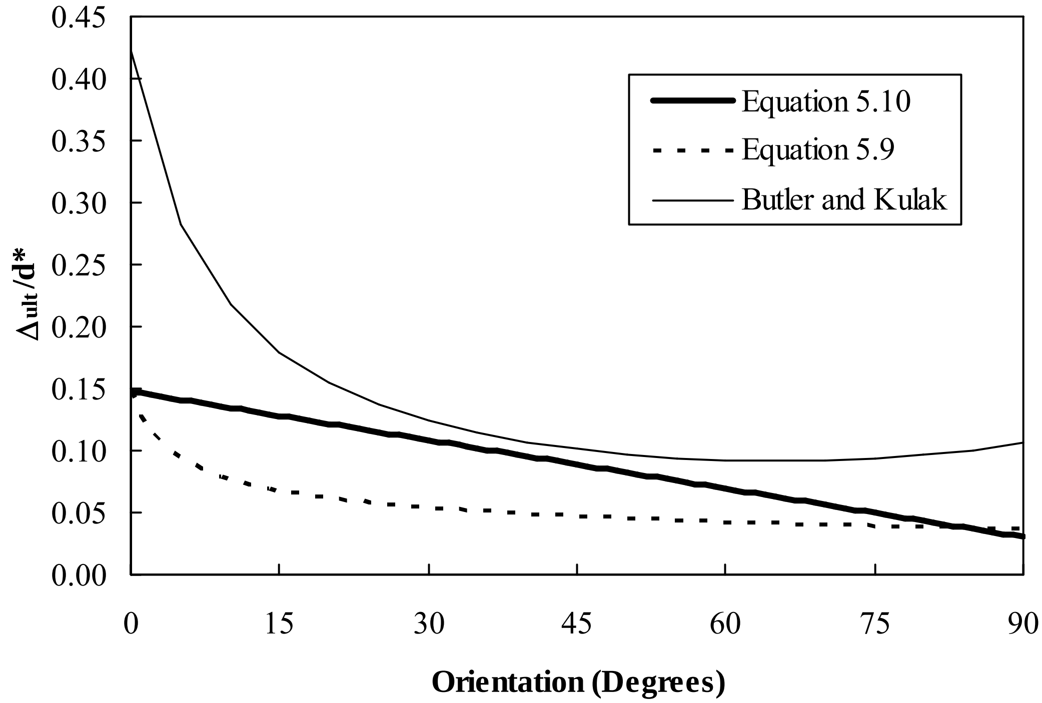

Figure 5.15 – Fillet Weld Ultimate Deformation Response

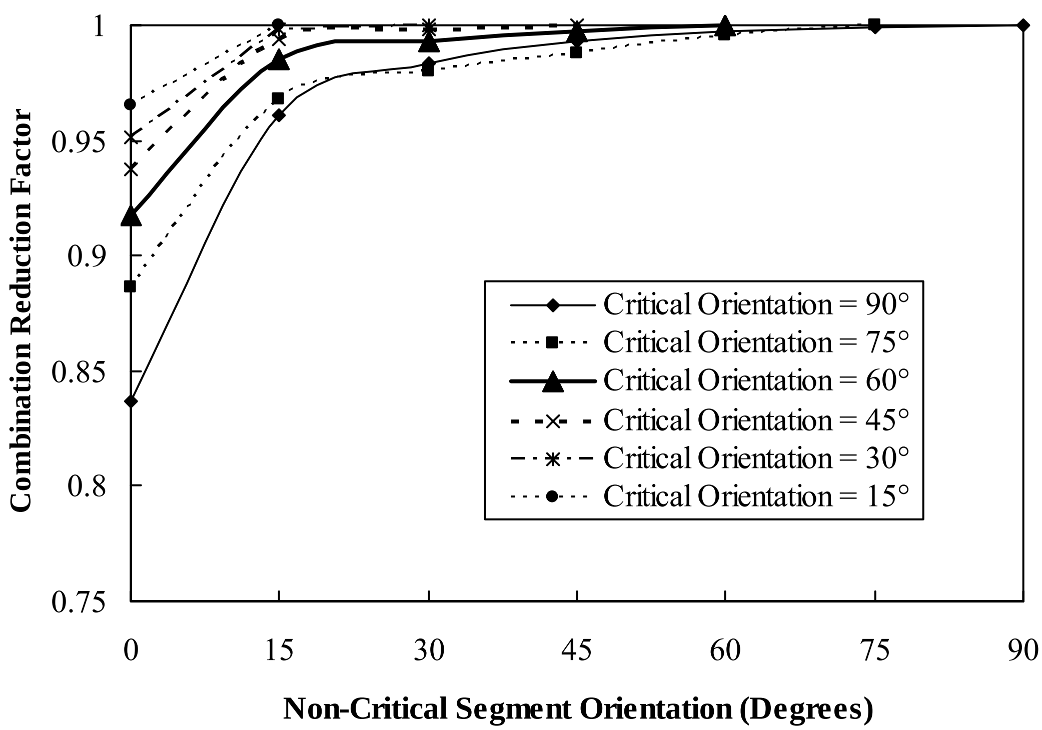

Figure 5.16 – Combination Reduction Factor Based on Equation 5.9

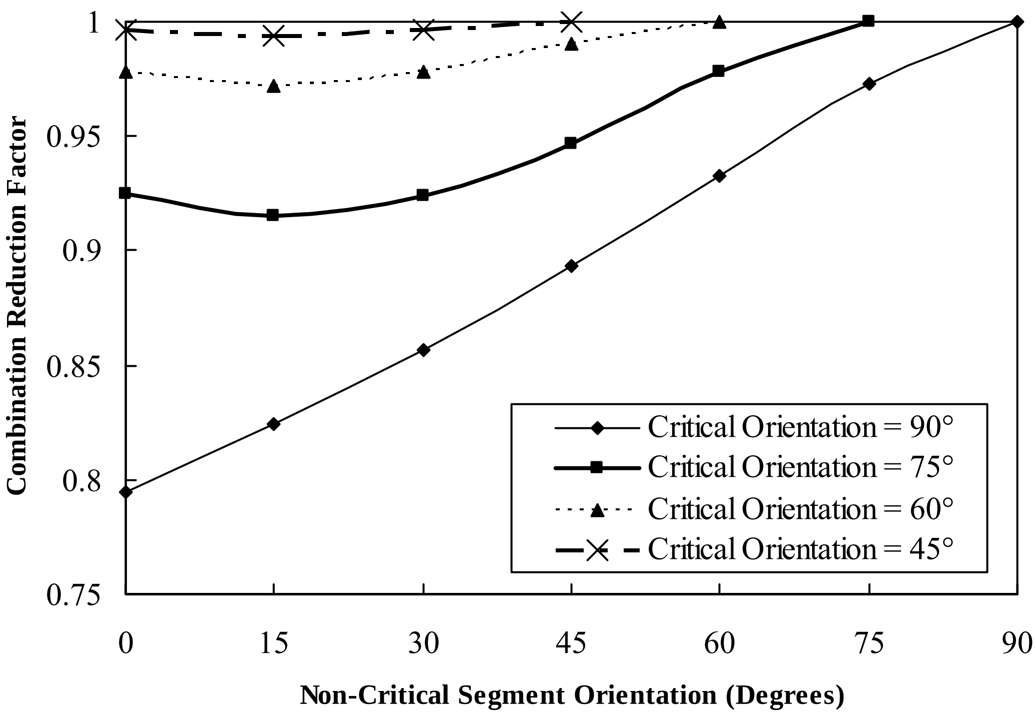

Figure 5.17 – Combination Reduction Factor Based on Equation 5.10

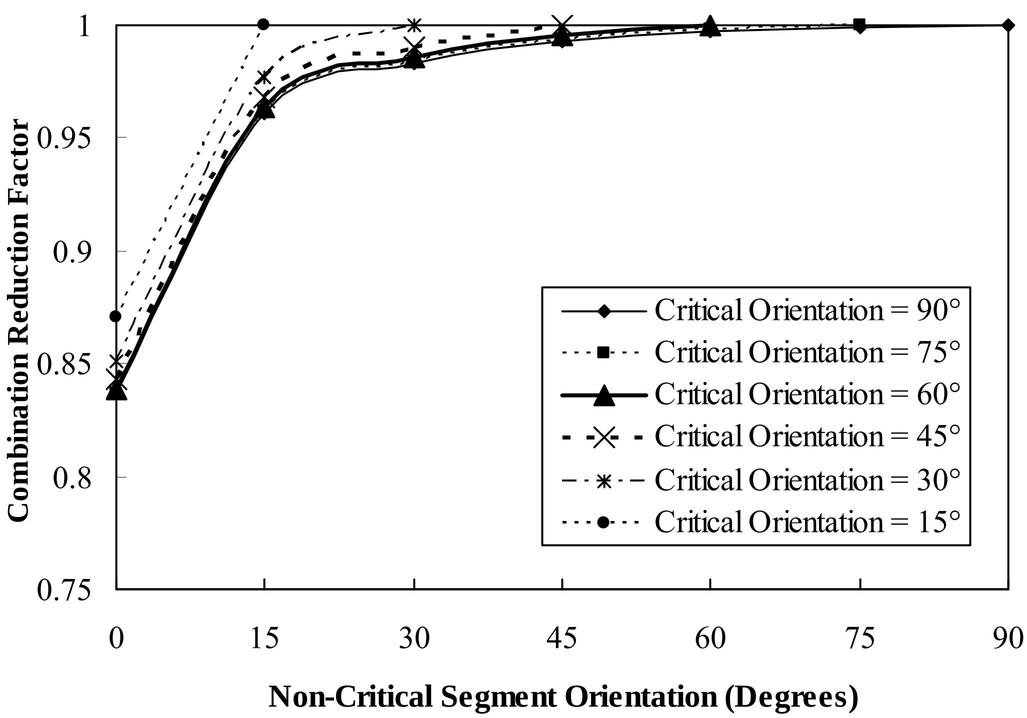

Figure 5.18 – Combination Reduction Factor Calculated Using Equations 5.9 and 5.11

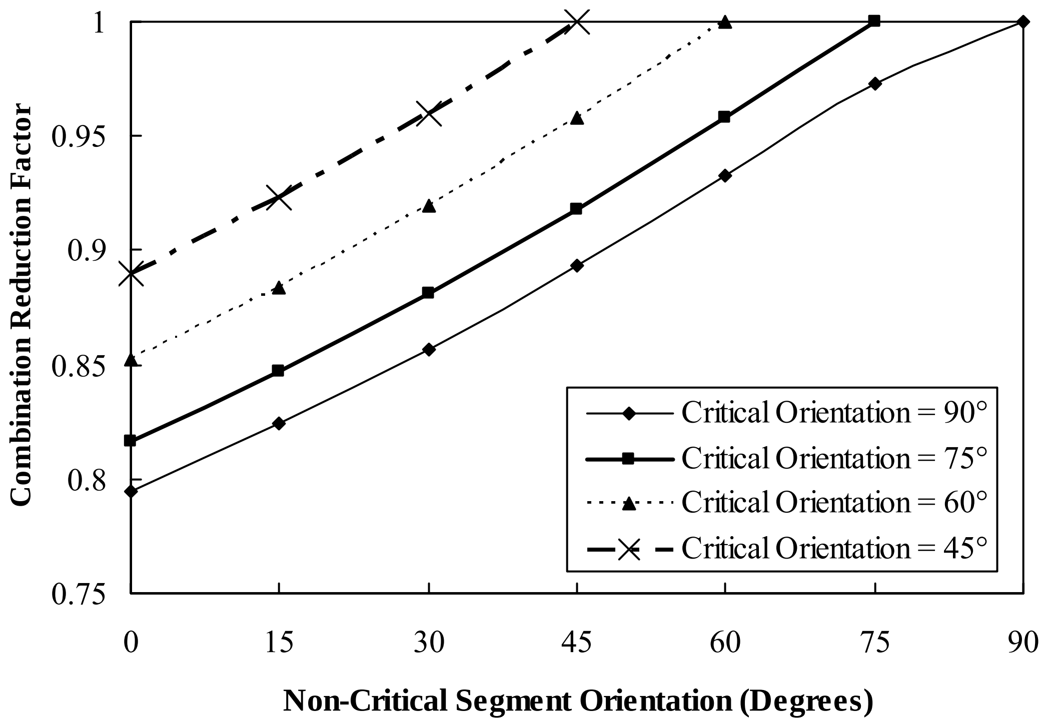

Figure 5.19 – Combination Reduction Factor Calculated Using Equation 5.10 and 5.11

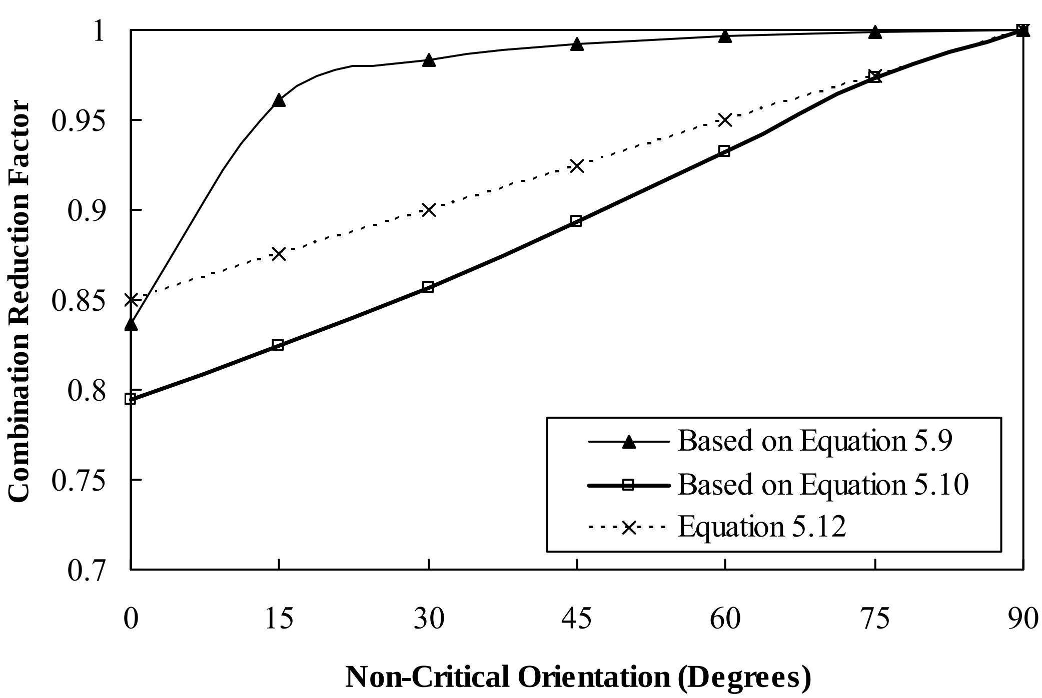

Figure 5.20 – Choosing an Equation to Describe the Combination Reduction Factor

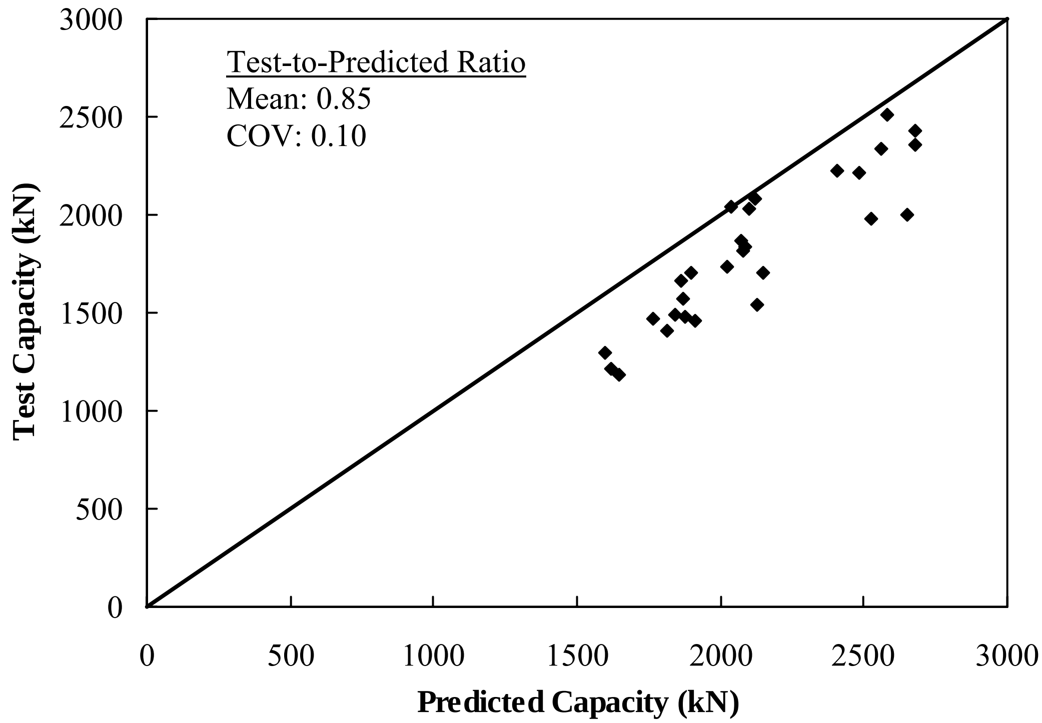

Figure 5.21 – Capacity Predictions with the Efficiency Factors Based on Equation 5.12

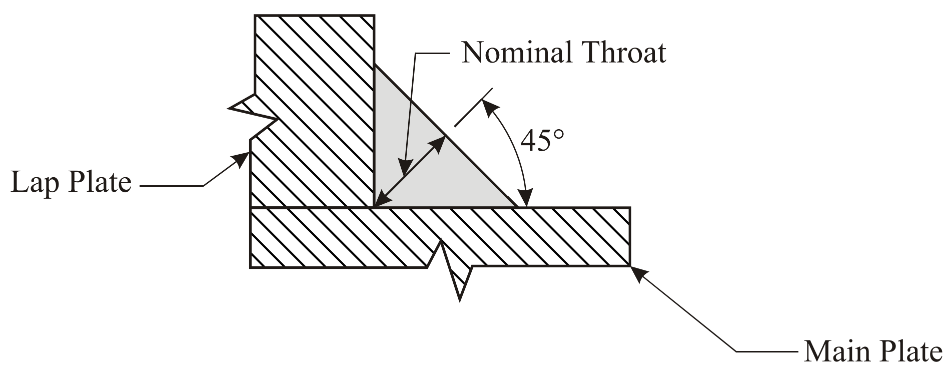

Figure 5.22 – Equal Legged Fillet Weld Cross-Section as Assumed in Design

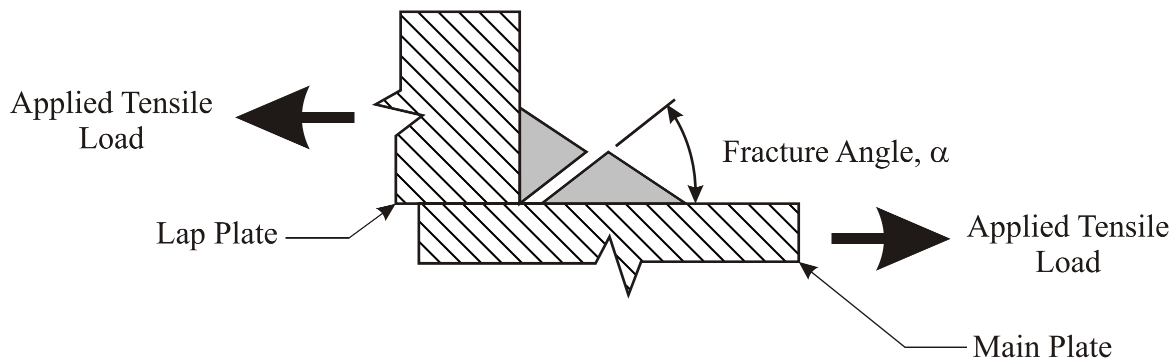

Figure 5.23 – Fillet Weld With Fracture Angle, α

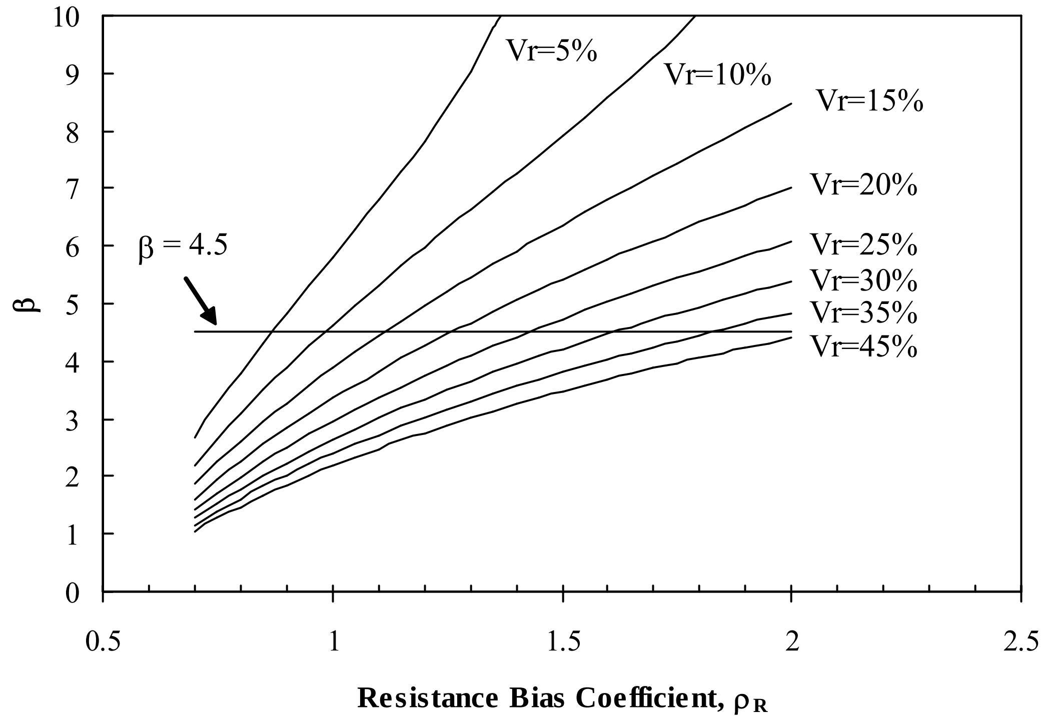

Figure 5.24 – β Sensitivity with ϕ=0.67

CHAPTER 6

SUMMARY AND CONCLUSIONS

6.1 Summary

A series of 31 welded joints that combine welds in two orientations (multiple orientation fillet welds (MOFW)) were tested as the third phase of an ongoing research program at the University of Alberta. This phase of the research has investigated the strength and behaviour of MOFW connections. The first phase of the project investigated several factors including: the effect of electrode classification, weld toughness, fabricator, electrode manufacturer, testing temperature, and weld size on transverse weld strength and ductility (Ng *et al.*, 2004a). The second phase of the project expanded on this work to look at the effect of loading angle on fillet weld strength and ductility (Deng *et al.*, 2003) and confirmed that the fillet weld design equation used in North America provides an acceptable level of safety. The third phase of the research program, presented in the current report, was designed to investigate the influence of ductility on the strength of welded connections that combine fillet welds of multiple orientations. All three research phases have used the flux cored arc welding (FCAW) process for specimen fabrication as this is commonly used in practice.

Two different configurations of MOFW connections were tested: connections with combined transverse and longitudinal fillet welds and connections with combined transverse and 45° fillet welds. Eight specimens were prepared with single pass 8 mm fillet welds, while the remaining specimens were prepared with a 12 mm specified leg size. Of the specimens that were prepared with a 12 mm specified leg size, three were prepared with a single pass while the rest were prepared with three passes. All of the connection plates of the MOFW test specimens remained elastic.

A complementary test program of single orientation fillet welded (SOFW) connections was also designed as it was necessary to test fillet welds different than what was available in the literature in order to complete the analysis of the MOFW connections. Nine longitudinal fillet weld specimens and three transverse fillet weld specimens were prepared. The longitudinal welded specimens were prepared with either one or three passes, and had two different lengths: 100 mm and 150 mm. Three transverse fillet weld specimens were prepared with connection plates that were designed to remain elastic. All of the twelve complementary test specimens were prepared with a specified leg size of 12 mm.

Once the specimens were prepared, the fillet welds to be tested were measured. Three different measurements were taken, as defined in Chapter 3, in order to characterize the fillet weld geometry.

All of the specimens were tested until rupture of either the fillet welds or the main plates. The specimens were tested in displacement control, and both connection load and fillet weld deformation was recorded throughout the test. Once testing was complete, measurements were taken to characterize the both the fracture surface size and angle.

6.2 Conclusions

The following conclusions are drawn from the present research.

1. Connections that combine fillet welds of multiple orientations are subject to a ductility incompatibility effect. It has been shown that because of the limited ductility of the least ductile fillet weld segment (critical segment) in the connection, the less critical segments cannot reach their full capacity. Because of the ductility incompatibility it is not conservative to estimate the strength of a MOFW connection as the sum of the full strength of all weld segments in a connection. A reliability analysis conducted on the MOFW test specimens indicates that the safety index is 4.1 for this strength summation method.
2. A method of estimating the capacity of MOFW connections that accounts for the ductility incompatibility was developed. This method provides a combination reduction factor for any non-critical segment orientation of a MOFW joint. The combination reduction factor reduces the capacity of the non-critical segments from their predicted capacity based on tests of joints with a single weld orientation. The reduction accounts for the ductility incompatibility between the critical and non-critical segments. A reliability analysis indicated that this method provides a safety index of 4.5.
3. An examination of test results has indicated that yielding of the connection plates in a fillet weld connection primarily affects the ductility of the fillet weld and not the strength. A comparison between transverse fillet weld connections fabricated with a 12 mm leg size and the FCAW process has shown that strength varies by only 3%, while weld deformations when plates yield can be 400% greater than when they remain elastic.
4. The transverse segments from the MOFW connection composed of transverse and longitudinal fillet welds were found to have a fracture angle significantly larger than the fracture angles observed by other researchers on transverse SOFW connections.
5. A comparison between 12 mm fillet welds prepared with a single pass and the same size of fillet welds prepared with three passes shows that the P_m/A_{throat} values differ by only 2%.
6. A comparison between 12 mm and 8 mm MOFW connections revealed that the 8 mm welds have 12% greater capacity based on P_m/A_{throat}. A similar weld size effect has been observed in other test programs.
7. An examination of the longitudinal fillet weld test data from the complementary testing program, Deng *et al.* (2003), and Miazga and Kennedy (1989) has

indicated that the strength of a longitudinal fillet weld is affected by its length. Because of the large scatter in the test results, the exact relationship between longitudinal weld strength and length has not been determined. However, the longitudinal welds that were nominally 50 mm long showed a significantly higher strength than those that were 100 mm long. This trend, showing a decrease in weld strength with increase in length, did not extend to the 150 mm long longitudinal welds, however.

8. The combination reduction factors proposed to account for the ductility incompatibility are seen to give consistent results with the method proposed in the 2005 draft AISC specification for the design of a MOFW connection that combines transverse and longitudinal fillet welds. The AISC document suggests that the longitudinal weld contributes only 85% of its strength to the total connection capacity. In contrast to the equation proposed in the AISC document, the combination reduction factor method proposed in this work has the advantage of being applicable to any configuration of a concentrically loaded MOFW connection.

9. The base metal failure check, which is present in both the Canadian and American design standards, S16–01 and LRFD 1999, is believed to be too conservative. This check limits the increase in strength of a transverse weld over a longitudinal weld to less than 50%, which has been shown to provide an acceptable safety index by several past research programs. It is suggested that the base metal failure check be removed from the design standards.

6.3 Recommendations for Future Research

Although the test results from the current research have contributed significantly to the knowledge base of fillet weld connections, areas where further research is required were identified as follows:

1. The fillet weld research program at the University of Alberta has included six different electrode classifications, which represents only a small portion of the electrodes available in industry. Future research is necessary to collect existing fillet weld test results from multiple sources and to conduct additional tests to broaden the range of tested electrode classifications. This is particularly important because electrode classification appears to affect the fillet weld response.

2. This research has shown that the interaction of fillet weld ductilities can play a significant role in the determination of the capacity of simple lap spliced connections. Because of this, other types of fillet weld connections need to be tested as different connection types can result in the fillet weld being loaded differently than in a simple lap splice connection. One example of this is a connection where the fillet weld group is loaded eccentrically. These types of connections have been investigated in the past but, as weld ductility has been

observed to be affected by electrode classification, further research on these type of connections should be considered.

3. A common longitudinal welded connection often involves a weld return to terminate the weld. This return is typically a very short transverse weld, which introduces a ductility incompatibility effect between the longitudinal weld and the return. It is questionable whether the fracture of the weld return will prevent the longitudinal welds from reaching their full capacity. Further testing is recommended to investigate longitudinal welds with weld returns to confirm the ability of the longitudinal welds to develop their full capacity.

4. Results of tests on longitudinal fillet welds seem to indicate that there is a relationship between weld length and strength that is more pronounced than the one suggested in section J2.2b of the AISC LRFD Specification (AISC, 1999). However, tests in this program were conducted on weld lengths that varied over a short range only (50 mm to 150 mm). Further investigation on weld length effect is therefore recommended.

5. An analysis of the results presented in this test program indicates that the reduction in MOFW connection strength as compared to the strength summation method is not strictly due to the effect weld orientation on ductility. In fact, the average test-to-predicted ratio for the deformation compatibility analysis is 0.85. Thus, there must be another factor that limits the capacity of the MOFW connections. One of the possible mechanisms that was investigated was the corner effect. Unfortunately, the specimens prepared to investigate this effect showed excessive weld porosity and the results of this comparison are therefore inconclusive. It is therefore suggested that further tests be completed to investigate whether or not the continuity of the weld segments in the connection has an effect on the connection strength.

REFERENCES

AISC, 2004. “Specification for Structural Steel Buildings – Draft dated November 22, 2004.” American Institute of Steel Construction, Chicago, IL.

AISC, 1999. “Load and Resistance Factor Design Specification for Structural Steel Buildings.” American Institute of Steel Construction, Chicago, IL.

AWS, 1995. “Specification for Carbon Steel Electrodes for Flux Cored Arc Welding,” ANSI/AWS A5.20-95, American Welding Society, Miami, FL.

Butler, L. J., and G. L. Kulak, 1971. “Strength of Fillet Welds as a Function of Direction of Load.” Welding Journal, Welding Research Council, Vol. 36, No. 5, pp. 231s-234s.

Butler, L. J., S. Pal, and G. L. Kulak, 1972. “Eccentrically Loaded Welded Connections” Journal of the Structural Division, ASCE, Vol. 98, No. ST5, May, pp. 989-1005

Canadian Institute of Steel Construction (2004). “Handbook of Steel Construction,” Eighth Edition, CISC, Toronto, Ontario.

CSA, 2001. “Limit States Design of Steel Structures.” CSA S16-01, Canadian Standards Association, Toronto, ON.

CSA 1998. “Welded Steel Construction (Metal Arc Welding).” CSA W59, Canadian Standards Association, Toronto, ON.

Deng, K., R. G. Driver, and G. Y. Grondin, 2003. “Effect of Loading Angle on the Behaviour of Fillet Welds” Structural Engineering Report 251, Department of Civil and Environmental Engineering, University of Alberta, Edmonton.

Duncan, C., 2004 “Connection Design in the 2005 AISC Specification,” Connections in Steel Structures V: Innovative Steel Connections, ECCS – AISC Workshop Amsterdam, June 3-4.

Fisher, J.W., Galambos, T.V., Kulak, G.L., and M.K. Ravindra, 1978. “Load and Resistance Factor Design Criteria for Connectors,” Journal of the Structural Division, ASCE, Vol. 104, No. ST9, Sept., pp. 1427-1441.

Franchuk, C. R., R. G. Driver, and G. Y. Grondin, 2002. “Block Shear Behaviour of Coped Steel Beams,” Structural Engineering Report 244, Department of Civil and Environmental Engineering, University of Alberta, Edmonton.

Galambos, T.V., and M. K. Ravindra, 1978. “Load and Resistance Factor Design for Steel,” Journal of the Structural Division, ASCE, Vol. 104, No. ST9, Sept., pp. 1337-1353.

Lesik, D. F. and D. J. L. Kennedy, 1990. “Ultimate Strength of Fillet Welded Connections Loaded in Plane.” Canadian Journal of Civil Engineering, Vol. 17, No. 1, pp. 55-67.

Lesik, D. F., and D. J. L. Kennedy, 1988. “Ultimate Strength of Eccentrically Loaded Fillet Welded Connections,” Structural Engineering Report 159, Department of Civil Engineering, University of Alberta, Edmonton, AB.

Manuel, T.J., and G.L. Kulak, 2000. “Strength of Joints that Combine Bolts and Welds.” Journal of Structural Engineering, ASCE, Vol. 126, No. 3, March, pp. 279-287.

Miazga, G. S. and D. J. L. Kennedy, 1989. “Behaviour of Fillet Welds as a Function of the Angle of Loading.” Canadian Journal of Civil Engineering, Vol. 16, No. 4, pp. 583-599.

Miazga, G. S., and D. J. L. Kennedy, 1986. “Behaviour of Fillet Welds as a Function of the Angle of Loading.” Structural Engineering Report 133, Department of Civil Engineering, University of Alberta, Edmonton, AB.

Miller, D.K., 1994. “Welding of Steel Bridges.” The Lincoln Electric Company, Cleveland, Ohio.

Ng, A. K. F., K. Deng, G.Y. Grondin, and R.G. Driver, 2004a. “Behavior of Transverse Fillet Welds: Experimental Program.” Engineering Journal, AISC, 2nd Quarter, pp. 39-54.

Ng, A. K. F., R.G. Driver, and G.Y. Grondin, 2004b. “Behavior of Transverse Fillet Welds: Parametric and Reliability Analyses.” Engineering Journal, AISC, 2nd Quarter, pp. 55-67.

Ng, A. K. F., R. G. Driver, and G. Y. Grondin, 2002. “Behaviour of Transverse Fillet Welds.” Structural Engineering Report 245, Department of Civil and Environmental Engineering, University of Alberta, Edmonton.

Tide, R. H. R., 1980, “Eccentrically Loaded Weld Groups – AISC Design Tables.” Engineering Journal, AISC, 4th Quarter, pp. 90-95.

APPENDIX A

Welding Procedures Specifications

Appendix A – Welding Procedure Specifications

The specimens in this research program were all fabricated by Empire Iron Works Ltd. over a two year period. Specimens TL50-1,2,3; TL50a-1,2,3; TF-1,2,3; and TFa-1,2,3 were prepared in August 2002. The remainder of the specimens were fabricated during August 2003. All of the specimens were welded with the flux core arc welding technique and the E70T-7 electrode. The welding procedure specifications are given in the following tables. Two specifications are reported for the specimens fabricated in 2003, one for the specimens prepared using three passes and one for the specimens prepared using a single pass.

Table A1 – Welding Procedure Specification for the Summer of 2002

Date: August 1, 2002
Job: University of Alberta Fillet Weld Project
Welder: Robbin Lewis
Conditions: Standard Shop Conditions

Wire: Lincoln Electric
3/32 Innershield NR311
Stock # ED012629
Batch # 5A5XP

Fillet Weld Leg Size	Mark	Producer	Filler Metal	Class	Polarity	Stick Out	Wire Speed	Travel Speed	Amps	Volts
5/16″	T7-L-S	Lincoln	Innershield NR311	E70T-7	DC-	1 1/4″	190	10-12	350	27
1/2″	T7-L-S	Lincoln	Innershield NR311	E70T-7	DC-	1 1/4″	190	10-12	350	27

Note: – All speeds are reported with units of inches per minute.

Table A2 – Welding Procedure Specification for the Summer of 2003

Date: August 1, 2003

Job: University of Alberta Fillet Weld Project
Welder: Rhys Halyk
Conditions: Standard Shop Conditions

Wire: Lincoln Electric
5/64 Innershield NR311
Stock # ED014464
Batch # 8R13RB

Welding Machine: Lincoln Electric
Model – DC-600
Code – KE5777
Type – K1288
Serial No. – 215385

Wire Feeder: Lincoln Electric
LN – 7 Wire Feeder
Code – 9220
Serial No. – 189605
Input Voltage 115 50/60 Hz current 2.0 Amps

Number of Passes	Producer	Filler Metal	Class	Polarity	Stick Out	Wire Speed	Travel Speed	Amps	Volts
3	Lincoln	Innershield NR311	E70T-7	DC-	$1\frac{1}{4}''$	240	12	350	26
1	Lincoln	Innershield NR311	E70T-7	DC-	$1\frac{1}{4}''$	240	7	350	26

Note: – A $\frac{1}{2}''$ fillet weld leg size is specified for both 1 and 3 passes.
– All speeds are reported with units of inches per minute.

APPENDIX B

Fillet Weld Specimen Measurements

Appendix B – Fillet Weld Specimen Measurements

All of the weld measurements taken, both before and after weld fracture, are presented in this appendix. The pre-test measurements that were taken to characterize the welds are the same as described in Chapter 3: (1) Shear Leg (MPL or Main Plate Leg), (2) Tension Leg (LPL or Lap Plate Leg), (3) throat, and (4) weld segment length. The first three measurement definitions are illustrated in Figure B1. In each case, the measurement locations were equally spaced along the segment length. The various segment lengths are defined in Figures B2, B3, and B4.

In some cases, weld measurements were not taken near the corners of the lap plate of the “discontinuous corner” (TL50D and TL100D) specimens. The detail used to prepare a discontinuous corner had the tendency to increase the Main Plate Leg size near the corner of the lap plate, within approximately 10 mm of the corner. Near the corner of the lap plate, the main plate leg size was generally increased by approximately 30%. Because of this deviation from the normal weld geometry, measurements were not taken at the corners of the lap plates. In the case where a measurement was not taken, a N/A will appear in the tables.

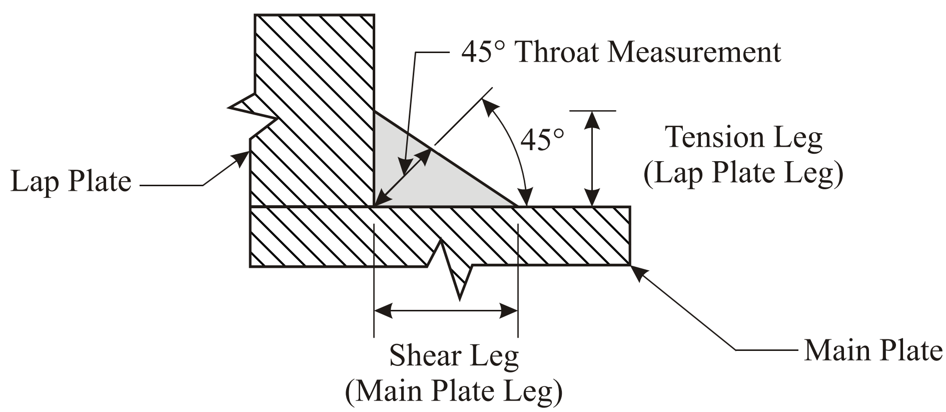

Figure B1 – Pre-Test Fillet Weld Measurements

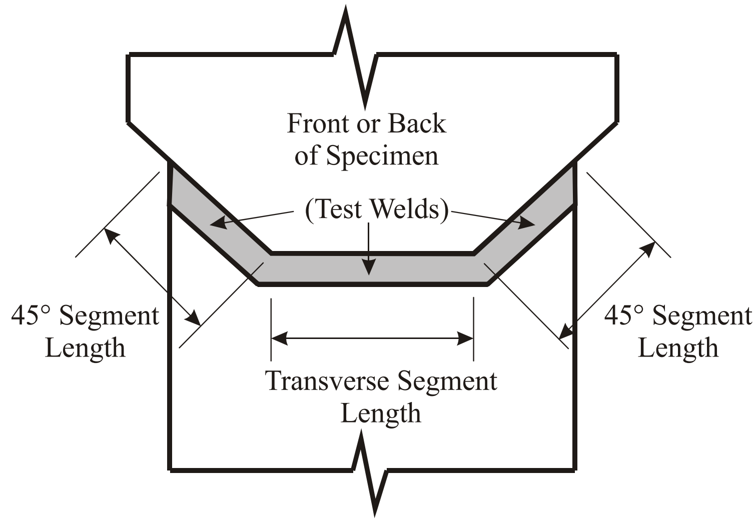

Figure B2 – TF Specimen Segment Lengths

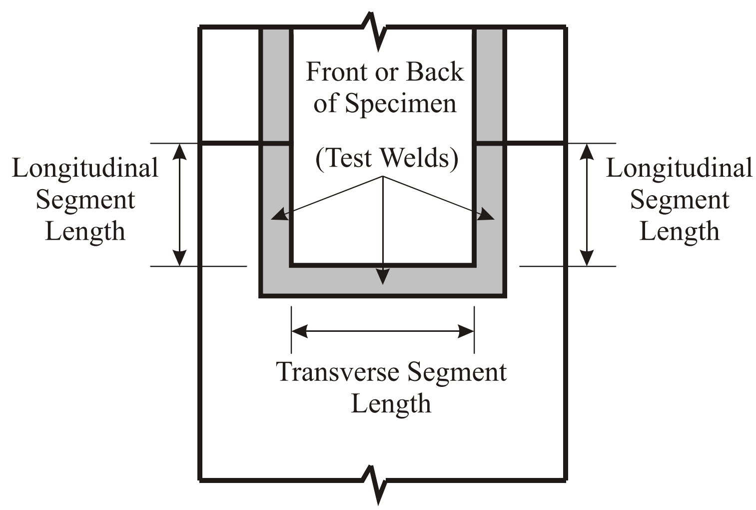

Figure B3 – TL Specimen Segment Lengths

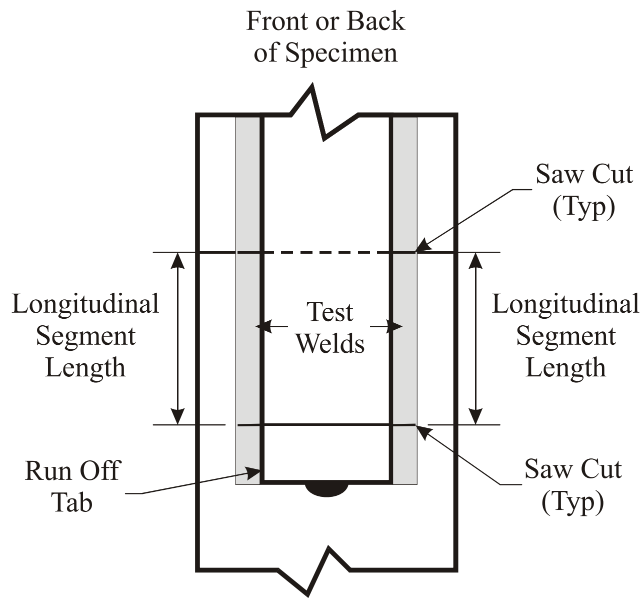

Figure B4 – Longitudinal Specimen Segment Lengths

Three post-fracture measurements were taken in order to characterize the failure surface and root penetration of the fillet weld. These three measurements are described in Figure B5. As discussed in Chapter 3, at some locations along a segment fracture surface, abrasion, which occurred as a result of pulling the specimens apart, did not allow for failure surface measurements to be taken.

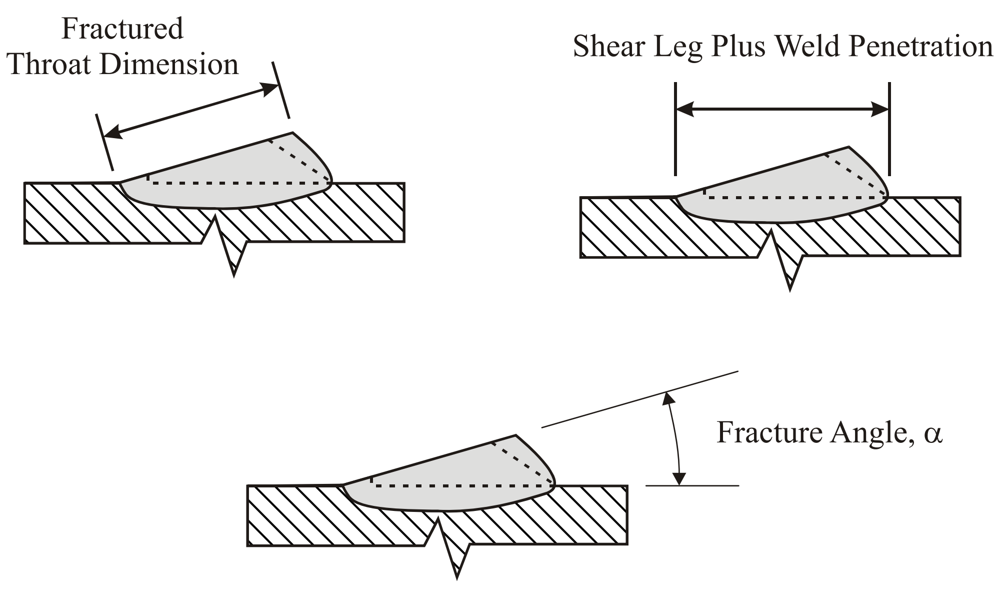

Figure B5 – Post- Fracture Measurements

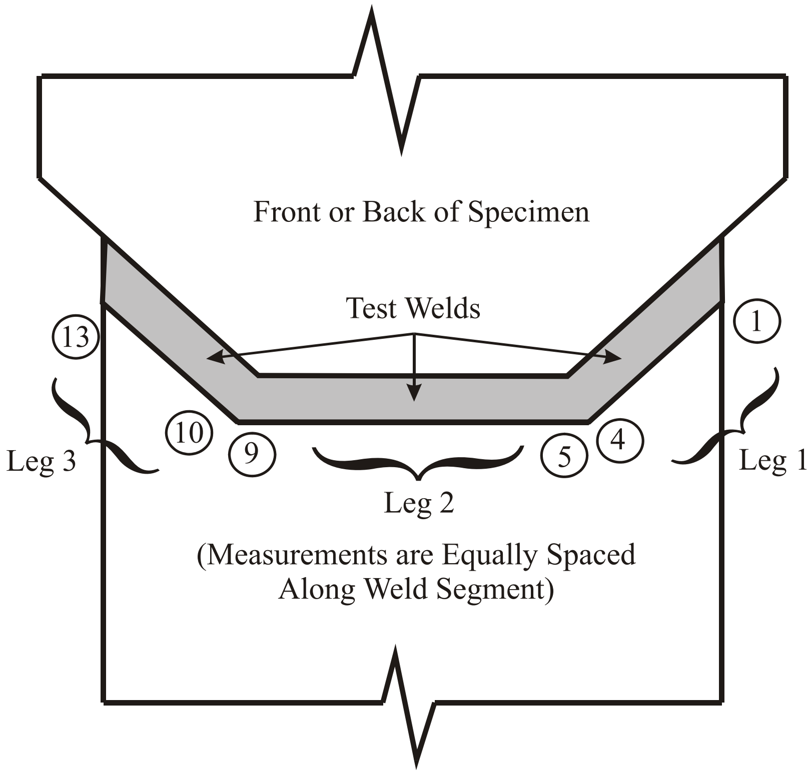

Figure B6 – Measurement Locations for the TF Specimens

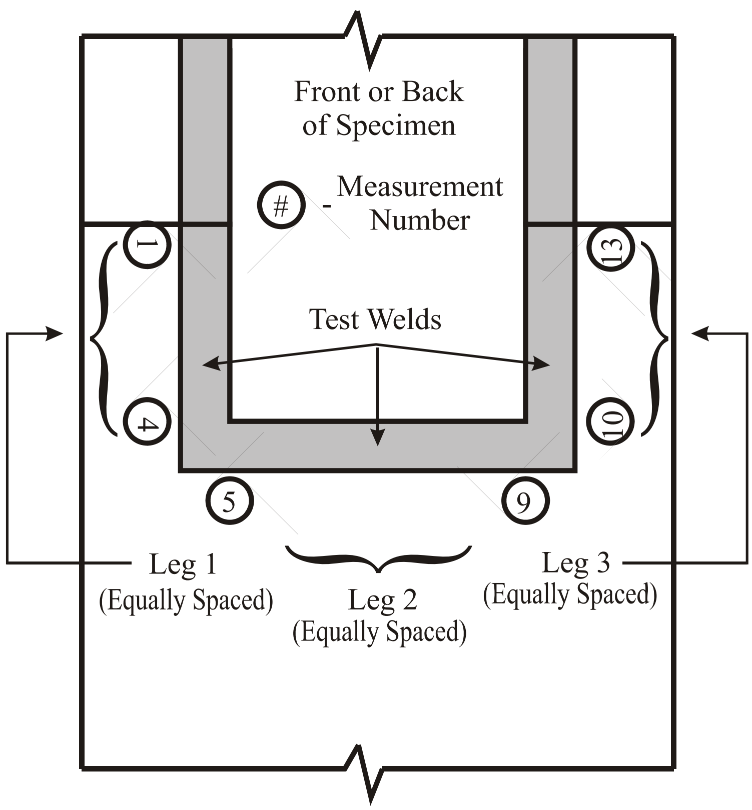

Figure B7 – Measurement Locations for the TL50 Specimens

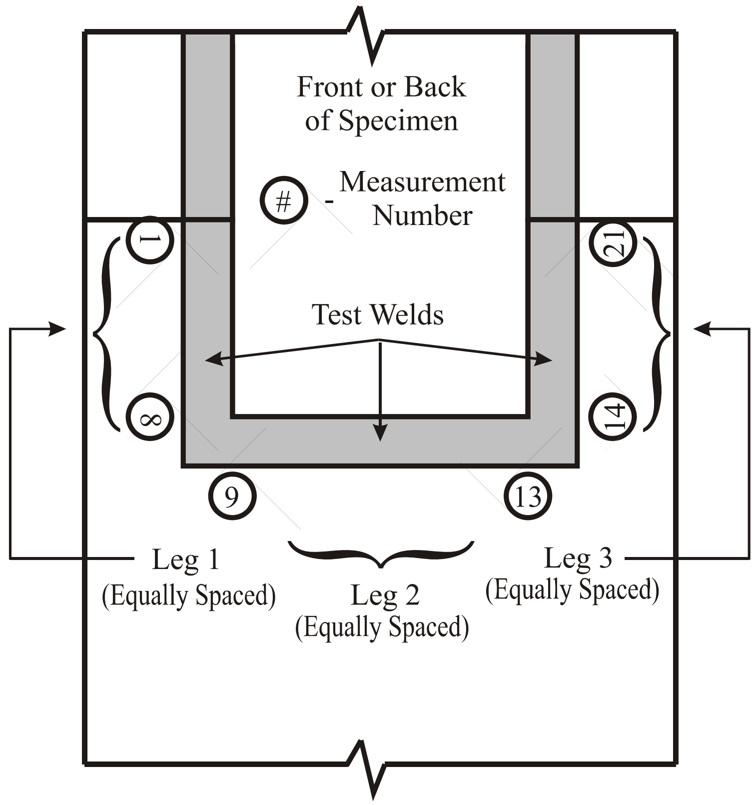

Figure B8 – Measurement Locations for the TL100 Specimens

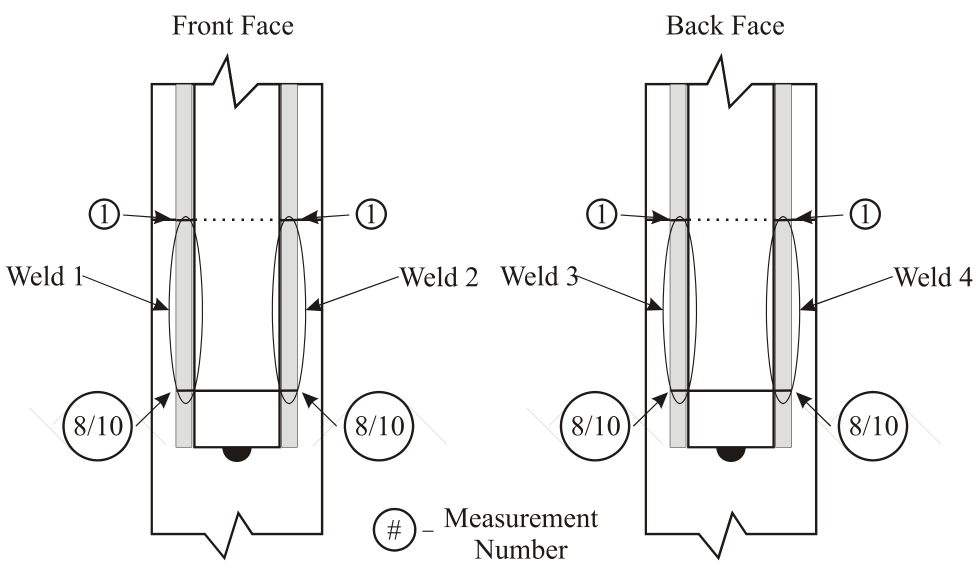

Figure B9 – Measurement Locations for the Longitudinal Specimens

Table B1 – Weld Measurements for Specimen TF-1

Leg Number†	Measurement Number	Front Face					Back Face				
		Shear Leg (mm)	Tension Leg (mm)	45° Meas. (mm)	Leg Length (mm)	Gauge Length (mm)	Shear Leg (mm)	Tension Leg (mm)	45° Meas. (mm)	Leg Length (mm)	Gauge Length (mm)
1	1	13.9	8.2	8.4	66.1	22.7	14.7	10.5	9.4	64.6	27.2
	2	14.3	11.3	9.5			15.7	11.6	9.7		
	3	12.0	11.5	8.3			13.2	12.4	9.8		
	4	11.3	11.1	7.3			13.8	11.9	9.5		
2	5	12.8	11.4	7.9	62.8	16.0	13.9	10.7	9.7	60.9	16.7
	6	15.5	12.2	9.4			15.3	12.2	9.7		
	7	15.2	11.2	9.0			14.0	11.8	9.8		
	8	13.6	11.5	9.0			12.6	14.0	9.8		
	9	13.6	11.8	8.7			12.8	12.9	8.4		
3	10	13.4	12.3	8.3	62.9	21.7	14.1	13.0	10.2	69.6	24.1
	11	15.6	10.3	8.4			16.5	13.3	11.1		
	12	14.6	11.5	8.4			14.6	13.0	10.0		
	13	13.9	9.8	8.6			14.2	13.5	10.2		

† See Figure B6 for the definition of the leg numbers.

Table B2 – Weld Measurements for Specimen TF-2

Leg Number[†]	Measurement Number	Front Face Shear Leg (mm)	Front Face Tension Leg (mm)	Front Face 45° Meas. (mm)	Front Face Leg Length (mm)	Front Face Gauge Length (mm)	Back Face Shear Leg (mm)	Back Face Tension Leg (mm)	Back Face 45° Meas. (mm)	Back Face Leg Length (mm)	Back Face Gauge Length (mm)
1	1	12.5	13.8	9.4	66.2	19.3	13.4	12.1	10.2	60.8	22.6
	2	12.6	13.3	9.5			13.4	12.1	9.4		
	3	11.6	13.1	9.7			12.1	13.2	9.4		
	4	13.1	14.3	9.8			11.2	13.1	9.7		
2	5	14.8	14.0	10.3	61.2	16.9	14.1	13.1	9.7	66.0	16.3
	6	13.0	13.9	10.6			14.0	13.8	10.2		
	7	14.8	13.5	10.0			13.2	13.9	9.5		
	8	16.5	13.9	10.3			14.8	11.6	10.2		
	9	15.7	12.6	10.2			11.9	11.3	9.7		
3	10	13.7	12.8	9.5	63.2	21.8	12.8	11.7	9.4	62.7	20.8
	11	13.7	13.3	9.5			13.7	12.3	9.4		
	12	12.6	14.4	9.5			13.9	12.7	9.4		
	13	12.6	14.4	9.5			13.5	13.3	9.4		

[†] See Figure B6 for the definition of the leg numbers.

Table B3 – Weld Measurements for Specimen TF-3

Leg Number†	Measurement Number	Front Face					Back Face				
		Shear Leg (mm)	Tension Leg (mm)	45° Meas. (mm)	Leg Length (mm)	Gauge Length (mm)	Shear Leg (mm)	Tension Leg (mm)	45° Meas. (mm)	Leg Length (mm)	Gauge Length (mm)
1	1	14.1	12.1	9.5	64.7	22.4	12.6	12.5	9.5	68.0	22.7
	2	13.5	12.3	8.1			12.0	12.7	9.2		
	3	15.2	11.9	9.5			12.6	12.1	9.5		
	4	12.7	12.1	7.9			11.9	10.5	7.9		
2	5	12.4	12.4	8.1	65.0	14.9	12.0	11.2	7.9	62.1	15.9
	6	13.7	13.1	9.5			12.1	11.7	8.7		
	7	13.0	12.3	9.2			13.1	11.8	8.7		
	8	14.4	11.6	9.0			13.9	11.6	9.4		
	9	14.1	9.7	7.8			14.4	11.8	9.2		
3	10	12.7	10.2	8.1	61.5	21.0	10.5	11.5	7.9	60.7	21.2
	11	12.5	11.3	8.7			12.2	11.6	8.3		
	12	13.6	11.6	8.6			14.0	10.5	8.4		
	13	13.9	11.7	9.2			13.0	11.5	8.4		

† See Figure B6 for the definition of the leg numbers.

Table B4 – Weld Measurements for Specimen TF-4

Leg Number[†]	Measurement Number	Front Face					Back Face				
		Shear Leg (mm)	Tension Leg (mm)	45° Meas. (mm)	Leg Length (mm)	Gauge Length (mm)	Shear Leg (mm)	Tension Leg (mm)	45° Meas. (mm)	Leg Length (mm)	Gauge Length (mm)
1	1	14.0	12.1	9.4	63.6	21.9	14.4	11.4	9.4	62.0	23.5
	2	14.9	12.1	9.4			14.4	12.6	9.5		
	3	14.1	11.8	9.5			15.5	13.4	10.0		
	4	14.2	10.7	8.6			14.9	12.4	9.8		
2	5	14.1	11.9	7.5	65.9	20.6	14.6	12.1	8.3	65.7	17.9
	6	18.2	12.7	8.6			18.7	12.9	9.7		
	7	18.6	12.0	9.2			16.8	11.7	9.8		
	8	19.2	10.8	9.4			17.8	13.4	11.0		
	9	15.6	10.8	8.4			16.0	13.1	10.2		
3	10	12.8	10.5	8.9	58.2	22.3	15.7	12.0	9.5	60.9	23.2
	11	15.0	12.4	9.4			15.0	13.2	9.7		
	12	15.4	11.2	8.6			15.9	12.4	9.7		
	13	11.8	9.1	8.4			14.8	12.5	9.2		

[†] See Figure B6 for the definition of the leg numbers.

Table B5 – Weld Measurements for Specimen TFa-1

Leg Number[†]	Measurement Number	Front Face					Back Face				
		Shear Leg (mm)	Tension Leg (mm)	45° Meas. (mm)	Leg Length (mm)	Gauge Length (mm)	Shear Leg (mm)	Tension Leg (mm)	45° Meas. (mm)	Leg Length (mm)	Gauge Length (mm)
1	1	9.6	7.9	7.5	56.8	15.9	8.0	6.8	5.6	66.8	15.1
	2	9.0	8.4	7.9			8.3	8.1	6.2		
	3	9.6	9.3	7.5			9.2	7.7	6.2		
	4	9.5	9.2	7.5			8.0	7.4	5.2		
2	5	8.9	9.4	7.5	64.9	12.1	8.2	7.2	5.4	60.8	11.4
	6	8.2	9.4	7.8			9.6	8.8	6.5		
	7	9.4	10.1	8.4			9.9	8.6	6.5		
	8	9.2	9.1	7.9			9.6	8.4	6.5		
	9	10.1	8.2	7.1			10.6	8.1	6.2		
3	10	9.7	8.5	7.6	68.2	15.3	10.2	7.5	6.0	64.2	15.2
	11	8.9	8.8	7.8			9.3	8.1	6.7		
	12	8.9	9.0	8.3			9.0	8.9	7.3		
	13	8.7	8.9	7.8			8.0	8.9	7.0		

[†] See Figure B6 for the definition of the leg numbers.

Table B6 – Weld Measurements for Specimen TFa-2

Leg Number[†]	Measurement Number	Front Face					Back Face				
		Shear Leg (mm)	Tension Leg (mm)	45° Meas. (mm)	Leg Length (mm)	Gauge Length (mm)	Shear Leg (mm)	Tension Leg (mm)	45° Meas. (mm)	Leg Length (mm)	Gauge Length (mm)
1	1	9.3	8.4	7.1	61.4	16.6	7.6	7.8	6.5	60.6	15.1
	2	9.0	8.0	6.8			8.3	7.7	6.7		
	3	8.9	8.5	7.8			8.3	6.7	6.0		
	4	10.4	8.1	6.7			9.4	7.9	6.8		
2	5	9.4	7.9	6.4	62.5	11.2	9.1	8.0	6.4	61.1	12.1
	6	9.2	8.2	6.8			8.6	7.8	6.5		
	7	9.3	8.4	6.4			8.9	8.2	6.7		
	8	10.0	7.8	6.5			9.0	7.8	6.2		
	9	9.8	7.5	5.6			8.8	6.5	4.8		
3	10	9.7	7.2	5.6	64.0	17.5	8.9	6.4	4.8	67.1	15.7
	11	9.5	8.8	7.5			8.9	7.5	6.2		
	12	9.9	9.6	7.9			9.5	7.3	6.2		
	13	9.3	9.4	7.1			8.9	7.3	6.0		

[†] See Figure B6 for the definition of the leg numbers.

Table B7 – Weld Measurements for Specimen TFa-3

Leg Number†	Measurement Number	Front Face					Back Face				
		Shear Leg (mm)	Tension Leg (mm)	45° Meas. (mm)	Leg Length (mm)	Gauge Length (mm)	Shear Leg (mm)	Tension Leg (mm)	45° Meas. (mm)	Leg Length (mm)	Gauge Length (mm)
1	1	9.0	8.7	7.5	57.9	13.2	8.5	6.9	4.9	65.5	15.3
	2	8.3	8.4	7.5			8.7	7.1	6.4		
	3	9.0	8.4	6.8			8.6	9.6	7.3		
	4	9.7	7.9	6.4			9.7	8.7	6.4		
2	5	8.3	8.1	6.4	65.8	11.1	9.4	7.4	5.9	61.0	11.7
	6	8.4	9.4	7.6			9.1	8.0	6.7		
	7	9.3	9.0	7.5			8.8	8.2	7.0		
	8	9.6	8.7	7.1			9.4	7.7	7.0		
	9	9.7	7.3	6.4			9.3	7.4	6.4		
3	10	8.2	8.3	6.4	67.4	15.8	10.0	8.3	6.4	65.9	14.2
	11	8.2	7.7	10.8			9.3	7.8	6.0		
	12	8.8	8.2	6.4			8.2	8.4	6.4		
	13	9.9	8.4	7.1			8.7	8.4	6.8		

† See Figure B6 for the definition of the leg numbers.

Table B8 – Weld Measurements for Specimen TFa-4

Leg Number†	Measurement Number	Front Face					Back Face				
		Shear Leg (mm)	Tension Leg (mm)	45° Meas. (mm)	Leg Length (mm)	Gauge Length (mm)	Shear Leg (mm)	Tension Leg (mm)	45° Meas. (mm)	Leg Length (mm)	Gauge Length (mm)
1	1	9.7	9.9	8.1	62.4	16.7	7.1	10.2	6.8	61.5	15.2
	2	8.6	10.0	7.9			8.3	9.0	7.0		
	3	9.1	10.6	8.3			8.7	10.3	7.9		
	4	9.7	7.9	7.3			10.0	8.0	7.8		
2	5	9.5	8.2	6.8	64.8	12.2	8.3	9.0	6.4	65.5	12.5
	6	9.7	10.0	8.1			8.3	9.6	7.5		
	7	9.1	10.4	8.1			8.4	9.6	7.8		
	8	10.1	11.4	9.2			9.5	9.7	8.3		
	9	9.4	9.5	8.4			9.5	8.1	7.5		
3	10	10.0	8.9	7.3	61.3	16.6	7.3	7.4	5.6	60.0	15.4
	11	8.6	10.1	7.9			7.5	7.9	6.0		
	12	7.6	9.7	7.5			9.6	7.5	6.8		
	13	7.7	8.6	6.4			9.2	6.6	6.5		

† See Figure B6 for the definition of the leg numbers.

Table B9 – Weld Measurements for Specimen TL50-1

Leg Number†	Measurement Number	Front Face					Back Face				
		Main Plate Leg (mm)	Lap Plate Leg (mm)	45° Meas. (mm)	Leg Length (mm)	Gauge Length (mm)	Main Plate Leg (mm)	Lap Plate Leg (mm)	45° Meas. (mm)	Leg Length (mm)	Gauge Length (mm)
1	1	14.3	11.5	7.9	51.4	52.6	14.1	9.6	7.3	51.3	51.1
	2	15.3	11.4	7.9			12.5	10.0	7.8		
	3	17.2	11.4	8.3			13.5	9.9	7.9		
	4	15.8	11.8	7.9			16.1	10.7	7.9		
2	5	16.2	10.9	10.3	76.2	N/A	17.5	11.2	8.3	76.1	N/A
	6	17.4	11.8	16.7			14.5	10.9	8.7		
	7	16.2	12.8	11.3			16.7	10.9	8.6		
	8	15.9	13.1	11.1			16.3	11.0	8.9		
	9	16.2	12.7	10.0			14.9	10.9	8.1		
3	10	14.6	12.0	11.9	51.2	51.7	12.2	10.7	8.6	51.2	52.0
	11	13.5	13.2	9.2			13.6	11.3	8.9		
	12	11.9	13.3	9.5			12.4	12.0	9.4		
	13	11.6	13.4	9.0			12.8	12.4	9.7		

† See Figure B7 for the definition of the leg numbers.

Table B10 – Weld Measurements for Specimen TL50-2

Leg Number†	Measurement Number	Front Face					Back Face				
		Main Plate Leg (mm)	Lap Plate Leg (mm)	45° Meas. (mm)	Leg Length (mm)	Gauge Length (mm)	Main Plate Leg (mm)	Lap Plate Leg (mm)	45° Meas. (mm)	Leg Length (mm)	Gauge Length (mm)
1	1	14.8	11.5	8.1	51.4	53.0	13.4	10.4	8.6	50.2	52.4
	2	14.9	11.8	9.4			12.8	10.6	8.9		
	3	14.0	12.9	9.0			14.3	10.0	9.2		
	4	11.2	12.7	9.4			13.4	10.1	8.7		
2	5	15.0	11.6	9.8	76.4	N/A	12.8	10.7	7.9	77.0	N/A
	6	14.6	12.2	9.8			14.2	12.8	10.2		
	7	15.7	12.3	9.2			12.9	11.4	9.2		
	8	14.9	12.1	8.9			14.7	11.6	9.4		
	9	15.8	11.5	9.5			12.9	13.0	9.5		
3	10	16.1	11.6	11.1	51.2	53.4	14.4	12.4	10.5	52.5	53.1
	11	15.6	13.3	12.4			12.2	12.7	10.0		
	12	13.9	11.7	9.7			13.8	11.1	8.3		
	13	14.0	12.2	9.5			11.9	11.4	8.1		

† See Figure B7 for the definition of the leg numbers.

Table B11 – Weld Measurements for Specimen TL50-3

Leg Number[†]	Measurement Number	Front Face					Back Face				
		Main Plate Leg (mm)	Lap Plate Leg (mm)	45° Meas. (mm)	Leg Length (mm)	Gauge Length (mm)	Main Plate Leg (mm)	Lap Plate Leg (mm)	45° Meas. (mm)	Leg Length (mm)	Gauge Length (mm)
1	1	16.9	10.9	8.1	52.1	52.7	13.2	10.9	8.7	50.6	50.7
	2	14.9	10.0	8.6			14.9	11.0	9.4		
	3	14.3	10.6	8.3			14.5	10.9	8.6		
	4	10.7	11.2	8.3			13.6	11.7	8.7		
2	5	15.5	11.2	10.5	76.3	N/A	15.1	11.1	8.7	76.7	N/A
	6	15.0	13.6	11.0			14.2	12.4	10.0		
	7	15.5	12.9	9.8			15.6	12.6	10.2		
	8	16.0	12.9	10.0			16.1	11.5	9.7		
	9	14.7	13.2	10.2			15.4	11.4	9.5		
3	10	11.1	12.7	9.4	51.7	51.5	13.1	11.4	9.7	50.8	51.7
	11	12.3	13.5	7.6			12.8	9.5	7.8		
	12	12.7	12.8	9.4			12.9	9.1	7.3		
	13	11.8	12.7	9.8			12.3	9.3	7.1		

[†] See Figure B7 for the definition of the leg numbers.

Table B12 – Weld Measurements for Specimen TL50-4

Leg Number[†]	Measurement Number	Front Face					Back Face				
		Main Plate Leg (mm)	Lap Plate Leg (mm)	45° Meas. (mm)	Leg Length (mm)	Gauge Length (mm)	Main Plate Leg (mm)	Lap Plate Leg (mm)	45° Meas. (mm)	Leg Length (mm)	Gauge Length (mm)
1	1	17.7	10.4	8.9	(mm)	(mm)	12.4	12.1	10.5	(mm)	(mm)
	2	17.3	10.0	9.4			13.7	11.5	9.0		
	3	17.7	11.4	9.5			13.5	10.7	9.2		
	4	15.7	9.1	9.0			12.8	10.9	8.6		
2	5	18.8	10.2	9.7	53.0	57.2	15.6	10.8	9.8	52.4	54.8
	6	16.3	10.8	9.8			16.9	10.6	10.8		
	7	20.6	11.2	9.8			16.7	11.1	10.6		
	8	18.6	11.7	10.5			17.0	12.5	11.1		
	9	16.9	10.9	9.2			12.6	11.1	10.5		
3	10	14.7	10.3	9.7	78.4	23.3	13.5	10.7	11.0	76.6	19.6
	11	13.2	11.7	10.3			14.5	11.6	11.0		
	12	14.2	12.5	10.2			15.5	11.9	10.8		
	13	12.8	12.6	9.4			14.7	12.8	11.6		

[†] See Figure B7 for the definition of the leg numbers.

Table B13 – Weld Measurements for Specimen TL50a-1

Leg Number†	Measurement Number	Front Face					Back Face				
		Main Plate Leg (mm)	Lap Plate Leg (mm)	45° Meas. (mm)	Leg Length (mm)	Gauge Length (mm)	Main Plate Leg (mm)	Lap Plate Leg (mm)	45° Meas. (mm)	Leg Length (mm)	Gauge Length (mm)
1	1	9.0	8.0	6.2	51.0	52.5	9.0	7.3	6.4	50.9	52.2
	2	8.8	7.6	6.2			9.2	7.4	6.5		
	3	9.2	8.0	6.2			8.0	7.6	5.4		
	4	11.5	7.7	6.0			7.2	7.3	5.4		
2	5	10.7	7.4	6.5	75.8	N/A	12.2	8.3	6.4	76.2	N/A
	6	10.1	8.0	6.4			12.0	8.4	7.6		
	7	10.3	8.1	6.5			10.7	9.1	8.1		
	8	11.8	9.2	7.8			9.9	7.5	7.9		
	9	10.7	8.7	8.1			8.8	7.6	5.7		
3	10	11.2	8.0	7.5	51.2	53.5	9.2	8.3	7.1	52.1	53.0
	11	9.0	8.7	6.2			9.0	8.6	6.5		
	12	8.3	8.4	6.5			8.3	8.9	7.0		
	13	8.3	8.4	6.0			7.7	8.3	6.4		

† See Figure B7 for the definition of the leg numbers.

Table B14 – Weld Measurements for Specimen TL50a-2

Leg Number[†]	Measurement Number	Front Face					Back Face				
		Main Plate Leg (mm)	Lap Plate Leg (mm)	45° Meas. (mm)	Leg Length (mm)	Gauge Length (mm)	Main Plate Leg (mm)	Lap Plate Leg (mm)	45° Meas. (mm)	Leg Length (mm)	Gauge Length (mm)
1	1	8.8	7.0	6.4	51.2	52.5	8.8	8.5	6.7	50.8	53.2
	2	10.1	7.9	6.4			9.5	8.2	7.6		
	3	9.4	8.4	6.2			9.8	8.5	6.8		
	4	10.1	7.9	5.4			8.9	8.8	6.4		
2	5	12.0	8.5	6.7	76.2	N/A	12.6	8.7	7.6	76.8	N/A
	6	10.3	7.5	7.8			11.7	8.0	7.9		
	7	10.2	7.6	6.5			10.2	7.6	6.8		
	8	10.4	8.8	7.1			11.0	8.0	6.5		
	9	10.4	9.3	7.0			11.2	8.6	7.3		
3	10	9.6	9.0	7.0	51.0	51.4	11.0	7.4	7.1	51.4	51.2
	11	9.1	7.1	5.6			9.4	9.1	6.8		
	12	11.4	8.5	6.0			10.7	8.7	7.1		
	13	9.0	8.4	6.4			8.8	8.5	6.8		

[†] See Figure B7 for the definition of the leg numbers.

Table B15 – Weld Measurements for Specimen TL50a-3

Leg Number†	Measurement Number	Front Face					Back Face				
		Main Plate Leg (mm)	Lap Plate Leg (mm)	45° Meas. (mm)	Leg Length (mm)	Gauge Length (mm)	Main Plate Leg (mm)	Lap Plate Leg (mm)	45° Meas. (mm)	Leg Length (mm)	Gauge Length (mm)
1	1	8.2	7.4	6.5	50.1	51.2	7.3	8.9	5.9	50.2	51.0
	2	8.7	8.4	7.0			12.1	10.2	7.6		
	3	8.2	7.5	6.4			8.5	9.5	6.4		
	4	8.4	6.9	5.4			8.0	8.1	4.8		
2	5	11.6	6.5	6.0	76.5	N/A	11.3	8.4	6.7	75.6	N/A
	6	9.5	8.6	7.6			10.1	8.1	8.6		
	7	10.0	9.2	7.1			10.3	8.0	6.5		
	8	10.5	8.1	7.1			9.4	10.0	7.9		
	9	12.0	8.5	7.8			9.6	10.5	7.0		
3	10	11.3	7.9	7.6	51.8	53.0	11.2	8.7	7.3	50.3	52.4
	11	8.5	8.2	6.4			9.6	8.6	7.0		
	12	9.3	7.3	6.8			9.6	8.2	6.4		
	13	9.8	8.5	7.0			8.3	7.8	6.0		

† See Figure B7 for the definition of the leg numbers.

Table B16 – Weld Measurements for Specimen TL50a-4

Leg Number†	Measurement Number	Front Face					Back Face				
		Main Plate Leg (mm)	Lap Plate Leg (mm)	45° Meas. (mm)	Leg Length (mm)	Gauge Length (mm)	Main Plate Leg (mm)	Lap Plate Leg (mm)	45° Meas. (mm)	Leg Length (mm)	Gauge Length (mm)
1	1	8.0	8.7	6.7	52.7	53.9	10.3	8.5	6.8	50.3	52.6
	2	9.1	8.4	7.0			11.0	8.6	7.3		
	3	12.2	9.0	7.1			11.0	9.4	8.1		
	4	10.6	7.7	6.5			10.8	8.1	7.0		
2	5	12.3	8.7	7.0	78.3	13.0	14.4	8.1	6.7	78.2	15.1
	6	13.1	8.6	7.9			13.8	6.8	7.8		
	7	11.5	9.6	7.6			11.4	7.7	7.9		
	8	10.6	9.9	7.8			11.4	8.4	7.5		
	9	11.5	8.5	7.6			10.8	8.5	7.3		
3	10	9.5	7.2	6.5	51.7	55.6	10.2	7.8	7.6	51.4	52.3
	11	9.8	9.4	6.4			9.5	9.4	7.8		
	12	9.2	10.5	7.6			10.1	10.0	8.1		
	13	8.0	11.2	8.3			10.2	10.5	9.0		

† See Figure B7 for the definition of the leg numbers.

Table B17 – Weld Measurements for Specimen TL100-1

Leg Number†	Measurement Number	Front Face Main Plate Leg (mm)	Front Face Lap Plate Leg (mm)	Front Face 45° Meas. (mm)	Front Face Leg Length (mm)	Front Face Gauge Length (mm)	Back Face Main Plate Leg (mm)	Back Face Lap Plate Leg (mm)	Back Face 45° Meas. (mm)	Back Face Leg Length (mm)	Back Face Gauge Length (mm)
1	1	15.0	13.1	10.0	97.9	99.1	14.6	12.4	10.5	96.9	98.6
	2	13.7	13.8	9.8			15.1	13.0	10.2		
	3	12.9	13.0	10.6			14.5	12.4	11.1		
	4	13.7	12.4	10.3			14.6	12.6	11.0		
	5	13.4	13.3	10.8			15.7	12.6	10.6		
	6	14.1	12.8	11.1			13.6	13.9	10.8		
	7	14.4	13.0	11.0			13.4	13.7	11.0		
	8	14.1	11.9	10.6			14.8	12.8	10.3		
2	9	16.1	11.5	10.5	76.6	19.9	17.3	12.2	11.6	77.0	20.5
	10	17.5	13.9	12.2			19.6	13.4	12.1		
	11	18.5	13.1	11.0			17.3	13.9	11.9		
	12	17.5	13.0	11.7			15.8	13.3	11.9		
	13	15.9	10.4	11.1			17.1	12.0	9.8		
3	14	16.7	11.2	11.4	98.1	99.0	19.7	10.9	11.0	100.9	100.9
	15	14.2	14.0	12.1			20.2	11.9	12.2		
	16	14.3	13.7	10.8			16.2	13.6	11.7		
	17	15.0	13.6	11.0			15.0	15.5	11.9		
	18	16.3	14.0	11.4			15.9	14.4	12.2		
	19	15.4	15.3	11.6			16.0	15.4	12.1		
	20	15.2	14.7	11.1			14.1	14.4	12.1		
	21	14.2	14.4	10.8			14.1	15.0	11.7		

† See Figure B8 for the definition of the leg numbers.

Table B18 – Weld Measurements for Specimen TL100-2

Leg Number†	Measurement Number	Front Face					Back Face				
		Main Plate Leg (mm)	Lap Plate Leg (mm)	45° Meas. (mm)	Leg Length (mm)	Gauge Length (mm)	Main Plate Leg (mm)	Lap Plate Leg (mm)	45° Meas. (mm)	Leg Length (mm)	Gauge Length (mm)
1	1	13.6	11.0	8.4	98.8	98.8	13.0	12.7	10.6	98.7	101.9
	2	14.7	11.0	8.6			13.7	12.9	10.5		
	3	13.6	11.2	9.4			15.9	12.7	11.0		
	4	13.9	10.9	9.5			15.6	13.0	11.1		
	5	14.0	10.5	9.5			14.8	12.4	11.7		
	6	14.4	9.8	9.5			16.4	12.4	11.4		
	7	14.7	10.0	9.8			16.6	12.5	11.0		
	8	14.2	10.3	8.7			17.4	12.1	9.8		
2	9	14.9	10.2	8.4	78.0	16.7	17.8	12.0	11.1	75.6	18.3
	10	16.0	11.8	9.4			17.7	11.9	11.3		
	11	16.2	11.1	9.7			16.7	12.2	10.6		
	12	12.9	11.1	9.2			15.4	12.6	10.5		
	13	12.7	11.0	9.2			16.1	10.6	9.7		
3	14	13.5	11.0	9.7	99.4	109.4	19.2	9.3	11.0	100.8	103.0
	15	15.0	9.4	11.1			15.0	9.1	11.3		
	16	14.8	10.9	10.2			15.2	11.2	10.5		
	17	13.6	9.7	9.7			15.4	11.5	10.3		
	18	13.8	11.8	10.3			13.3	12.8	10.3		
	19	12.7	10.6	10.5			14.6	12.8	11.0		
	20	13.0	10.9	9.5			15.3	12.8	10.8		
	21	11.8	10.7	9.5			14.7	12.7	11.0		

† See Figure B8 for the definition of the leg numbers.

Table B19 – Weld Measurements for Specimen TL100-3

Leg Number†	Measurement Number	Front Face					Back Face				
		Main Plate Leg (mm)	Lap Plate Leg (mm)	45° Meas. (mm)	Leg Length (mm)	Gauge Length (mm)	Main Plate Leg (mm)	Lap Plate Leg (mm)	45° Meas. (mm)	Leg Length (mm)	Gauge Length (mm)
1	1	14.1	12.1	10.2	98.9	101.3	11.6	12.8	7.9	102.0	105.9
	2	14.7	12.3	10.2			11.6	11.7	8.4		
	3	14.7	12.4	10.3			13.6	11.6	8.3		
	4	13.1	12.2	10.5			13.4	11.5	8.6		
	5	13.6	12.8	10.8			12.5	12.2	8.7		
	6	14.2	13.3	10.6			13.6	11.4	8.1		
	7	13.2	13.1	10.2			11.9	10.7	7.9		
	8	12.8	12.1	9.4			11.9	9.7	8.1		
2	9	16.5	12.2	12.1	77.2	17.0	15.1	9.7	8.9	76.0	19.2
	10	16.9	13.1	11.1			16.2	10.4	8.4		
	11	17.0	10.3	10.2			16.8	11.7	8.7		
	12	16.2	13.9	10.3			14.9	11.6	9.0		
	13	17.2	13.2	9.4			15.4	10.8	7.8		
3	14	13.2	11.2	10.0	99.3	100.7	14.6	10.1	7.9	101.9	103.9
	15	12.8	10.8	10.8			14.4	10.7	7.8		
	16	14.4	13.3	11.0			14.0	9.1	7.9		
	17	14.6	12.2	10.8			13.4	10.9	7.9		
	18	15.4	12.4	11.0			14.4	10.8	8.1		
	19	13.1	14.2	11.1			14.5	10.7	8.3		
	20	12.4	14.8	10.6			13.9	9.6	7.6		
	21	13.6	15.0	10.5			12.7	10.2	6.7		

† See Figure B8 for the definition of the leg numbers.

Table B20 – Weld Measurements for Specimen TL100D-1

Leg Number[†]	Measurement Number	Front Face					Back Face				
		Main Plate Leg (mm)	Lap Plate Leg (mm)	45° Meas. (mm)	Leg Length (mm)	Gauge Length (mm)	Shear Leg (mm)	Main Plate Leg (mm)	Lap Plate Leg (mm)	Leg Length (mm)	Gauge Length (mm)
	1	11.6	11.1	8.6			14.5	11.1	11.1		
	2	12.2	11.1	9.0			14.0	11.1	10.5		
	3	13.0	11.3	9.8			14.9	11.0	10.6		
1	4	12.8	11.8	10.0	95.8	98.4	15.0	11.4	10.5	94.2	99.0
	5	12.8	12.7	10.5			14.4	11.8	10.3		
	6	12.1	13.3	10.6			13.2	10.8	10.6		
	7	12.5	13.5	10.3			12.6	12.2	11.0		
	8	N/A	N/A	N/A			N/A	N/A	N/A		
	9	12.6	11.2	9.5			13.7	14.2	11.9		
	10	11.8	10.8	9.2			14.3	12.4	9.4		
2	11	13.0	10.6	9.5	75.2	14.6	13.8	11.5	9.8	75.9	16.8
	12	14.5	10.8	9.8			16.4	12.1	10.0		
	13	N/A	N/A	N/A			N/A	N/A	N/A		
	14	13.4	11.2	9.5			12.9	11.7	10.0		
	15	13.9	10.7	8.7			13.8	11.0	9.5		
	16	13.5	9.6	8.9			14.1	11.5	10.6		
3	17	12.9	9.6	9.0	94.9	99.4	14.4	12.6	10.6	93.3	97.1
	18	12.8	10.2	8.6			13.6	11.7	9.7		
	19	12.2	10.3	9.0			12.6	11.6	9.4		
	20	12.3	11.2	8.9			12.9	11.5	8.1		
	21	N/A	N/A	N/A			N/A	N/A	N/A		

[†] See Figure B8 for the definition of the leg numbers.

Table B21 – Weld Measurements for Specimen TL100D-2

Leg Number†	Measurement Number	Front Face					Back Face				
		Main Plate Leg (mm)	Lap Plate Leg (mm)	45° Meas. (mm)	Leg Length (mm)	Gauge Length (mm)	Main Plate Leg (mm)	Lap Plate Leg (mm)	45° Meas. (mm)	Leg Length (mm)	Gauge Length (mm)
1	1	13.4	10.9	8.3	94.7	99.6	13.2	11.2	7.9	93.7	96.6
	2	13.2	11.2	9.2			13.7	11.3	9.0		
	3	13.3	11.9	9.5			12.0	11.1	9.2		
	4	12.9	10.7	9.4			13.2	12.0	10.0		
	5	11.2	9.8	9.5			13.8	12.0	10.3		
	6	12.5	11.9	9.5			13.8	12.0	10.2		
	7	13.4	13.5	8.7			13.8	12.5	10.8		
	8	N/A	N/A	N/A			N/A	N/A	N/A		
2	9	12.5	11.7	8.7	73.8	15.1	13.9	12.6	11.3	76.3	16.0
	10	11.5	10.4	8.4			13.8	11.9	9.8		
	11	12.7	11.1	9.0			13.1	10.6	9.2		
	12	12.5	12.1	9.2			14.9	11.5	9.7		
	13	N/A	N/A	N/A			N/A	N/A	N/A		
3	14	0.0	0.0	0.0	91.8	97.6	0.0	0.0	0.0	95.4	101.2
	15	13.5	9.6	9.8			12.3	12.5	9.7		
	16	13.3	9.9	9.4			13.0	11.8	9.7		
	17	13.9	9.8	9.4			13.7	12.0	9.7		
	18	13.6	8.9	9.5			12.3	12.3	9.7		
	19	12.8	9.4	9.2			12.0	12.0	9.7		
	20	12.8	9.6	9.0			11.4	11.3	9.2		
	21	13.0	9.2	8.3			14.0	11.0	8.4		

† See Figure B8 for the definition of the leg numbers.

Table B22 – Weld Measurements for Specimen TL100D-3

Leg Number†	Measurement Number	Front Face					Back Face				
		Main Plate Leg (mm)	Lap Plate Leg (mm)	45° Meas. (mm)	Leg Length (mm)	Gauge Length (mm)	Main Plate Leg (mm)	Lap Plate Leg (mm)	45° Meas. (mm)	Leg Length (mm)	Gauge Length (mm)
1	1	13.4	13.0	9.5	99.9	102.7	14.5	13.8	10.0	97.5	103.3
	2	13.0	13.6	9.8			14.7	13.7	10.5		
	3	14.3	13.9	10.2			16.2	14.0	10.6		
	4	15.0	13.5	10.8			16.8	14.1	10.8		
	5	16.0	13.8	10.3			15.3	13.6	10.8		
	6	14.6	13.7	10.2			15.3	13.9	11.9		
	7	14.5	13.3	11.3			16.5	13.4	12.5		
	8	N/A	N/A	N/A			N/A	N/A	N/A		
2	9	15.9	13.8	10.3	75.2	15.6	14.5	13.1	11.3	73.5	15.8
	10	13.8	12.2	8.9			13.6	10.6	9.5		
	11	12.2	13.1	9.0			13.4	11.3	9.5		
	12	14.3	13.4	10.6			15.7	12.1	10.8		
	13	N/A	N/A	N/A			N/A	N/A	N/A		
3	14	0.0	0.0	0.0	100.1	105.9	0.0	0.0	0.0	97.9	101.6
	15	17.5	14.7	12.9			16.6	13.9	11.7		
	16	14.9	13.7	10.8			15.9	12.9	11.1		
	17	14.8	14.0	11.0			16.0	11.6	11.0		
	18	15.4	13.7	11.1			16.0	12.3	11.3		
	19	14.9	13.7	10.6			14.7	12.7	11.3		
	20	13.9	13.4	10.3			15.4	12.0	11.1		
	21	15.8	12.6	9.8			14.8	12.1	10.8		

† See Figure B8 for the definition of the leg numbers.

Table B23 – Weld Measurements for Specimen TL100SP-1

Leg Number†	Measurement Number	Front Face					Back Face				
		Main Plate Leg (mm)	Lap Plate Leg (mm)	45° Meas. (mm)	Leg Length (mm)	Gauge Length (mm)	Main Plate Leg (mm)	Lap Plate Leg (mm)	45° Meas. (mm)	Leg Length (mm)	Gauge Length (mm)
	1	13.4	10.6	10.0			11.3	8.6	9.2		
	2	12.0	11.3	9.7			13.4	8.9	9.4		
	3	12.6	11.1	11.0			11.5	8.8	8.9		
1	4	13.9	11.4	9.7	98.7	98.3	11.5	9.8	8.7	101.3	104.6
	5	12.8	11.0	9.7			11.4	9.8	9.4		
	6	13.4	10.6	10.0			12.7	10.1	9.5		
	7	13.4	10.1	9.8			11.5	9.2	8.4		
	8	12.1	8.9	8.7			10.6	8.8	8.1		
	9	12.8	8.5	8.6			13.3	9.8	9.4		
	10	10.3	10.0	9.0			12.9	10.4	10.0		
2	11	12.1	9.5	9.8	76.8	16.7	12.2	9.6	9.5	76.7	15.0
	12	13.3	10.3	9.4			12.5	9.3	8.3		
	13	12.6	8.2	8.1			13.3	9.2	8.1		
	14	12.5	8.6	6.8			14.5	10.7	8.9		
	15	10.8	9.3	8.4			13.7	11.0	10.6		
	16	11.7	10.1	9.4			14.1	11.1	11.0		
3	17	12.4	10.0	9.0	98.5	97.4	13.9	12.2	11.0	101.9	102.3
	18	12.0	9.9	9.0			14.4	12.2	11.7		
	19	11.6	10.2	8.9			13.0	12.0	10.6		
	20	11.4	9.7	7.9			13.4	12.2	11.6		
	21	13.0	9.5	8.3			14.0	12.1	11.4		

† See Figure B8 for the definition of the leg numbers.

Table B24 – Weld Measurements for Specimen TL100SP-2

Leg Number[†]	Measurement Number	Front Face					Back Face				
		Main Plate Leg (mm)	Lap Plate Leg (mm)	45° Meas. (mm)	Leg Length (mm)	Gauge Length (mm)	Main Plate Leg (mm)	Lap Plate Leg (mm)	45° Meas. (mm)	Leg Length (mm)	Gauge Length (mm)
1	1	12.3	10.1	7.8	100.3	103.2	12.4	12.8	9.0	97.1	100.3
	2	11.7	9.3	7.6			10.8	12.2	8.3		
	3	11.9	9.8	7.3			11.6	11.2	8.6		
	4	12.1	10.7	8.6			11.2	11.3	9.0		
	5	12.5	10.6	9.5			11.6	11.1	9.2		
	6	10.6	10.3	9.0			11.1	11.4	8.7		
	7	11.3	9.5	8.4			13.4	8.5	7.9		
	8	12.8	8.9	7.9			13.1	7.8	7.8		
2	9	13.6	8.3	7.6	75.4	16.0	16.0	8.5	8.3	74.6	19.5
	10	13.9	12.0	8.3			14.8	10.7	9.4		
	11	10.5	10.6	8.9			14.9	11.2	10.0		
	12	11.6	11.8	9.5			12.7	9.5	9.4		
	13	11.3	7.7	7.8			11.1	8.3	7.6		
3	14	13.7	8.8	9.0	98.5	102.0	13.7	10.3	9.5	95.2	98.6
	15	14.7	11.6	9.5			14.0	10.9	9.5		
	16	15.7	12.2	9.5			13.9	11.2	9.4		
	17	14.3	11.8	10.3			13.6	10.6	10.0		
	18	14.6	12.1	9.5			14.5	8.5	8.7		
	19	14.4	12.5	10.5			14.9	10.7	9.7		
	20	12.0	11.5	9.8			13.5	11.4	9.5		
	21	12.6	12.1	10.5			14.4	11.5	9.0		

[†] See Figure B8 for the definition of the leg numbers.

Table B25 – Weld Measurements for Specimen TL100SP-3

Leg Number†	Measurement Number	Front Face					Back Face				
		Main Plate Leg (mm)	Lap Plate Leg (mm)	45° Meas. (mm)	Leg Length (mm)	Gauge Length (mm)	Main Plate Leg (mm)	Lap Plate Leg (mm)	45° Meas. (mm)	Leg Length (mm)	Gauge Length (mm)
	1	14.6	9.3	8.3			14.1	10.1	9.4		
	2	15.0	10.6	8.1			13.1	10.0	9.0		
	3	14.6	10.1	9.2			13.5	10.2	9.0		
1	4	14.6	10.3	9.4	99.2	99.9	13.0	10.1	9.4	98.8	97.6
	5	15.0	10.7	8.4			14.7	10.1	8.7		
	6	13.1	10.6	8.3			13.5	9.5	9.5		
	7	14.6	8.4	7.9			13.4	9.2	7.9		
	8	12.6	10.0	8.1			11.6	8.0	7.8		
	9	13.4	9.9	8.1			13.4	8.3	8.4		
	10	13.5	11.2	9.4			12.4	9.5	8.9		
2	11	13.3	11.2	8.7	78.3	15.7	12.8	9.2	8.1	77.9	16.7
	12	13.8	11.4	8.3			14.2	10.2	9.5		
	13	13.6	10.7	7.6			15.4	10.0	9.4		
	14	12.9	9.8	7.3			15.4	9.9	7.9		
	15	13.0	10.0	8.3			14.1	9.6	8.4		
	16	12.3	10.3	8.4			13.3	9.1	8.9		
3	17	11.8	10.6	9.2	100.3	101.7	13.6	9.5	8.3	98.7	99.8
	18	12.8	11.2	9.4			13.5	9.9	9.5		
	19	13.1	11.4	9.7			13.2	11.1	9.7		
	20	13.3	10.9	8.4			14.2	11.9	9.5		
	21	13.3	10.9	9.2			13.7	11.4	9.2		

† See Figure B8 for the definition of the leg numbers.

Table B26 – Weld Measurements for Specimen TL100LT-1

Leg Number[†]	Measurement Number	Front Face					Back Face				
		Main Plate Leg (mm)	Lap Plate Leg (mm)	45° Meas. (mm)	Leg Length (mm)	Gauge Length (mm)	Main Plate Leg (mm)	Lap Plate Leg (mm)	45° Meas. (mm)	Leg Length (mm)	Gauge Length (mm)
1	1	14.0	12.1	10.0	100.5	101.0	13.7	12.5	9.7	101.7	100.7
	2	14.8	11.6	10.0			14.7	13.1	10.6		
	3	14.3	12.2	10.5			14.2	11.9	10.5		
	4	13.7	12.6	10.0			14.4	11.6	10.0		
	5	16.3	12.4	9.8			15.1	13.2	9.8		
	6	14.4	12.4	10.6			13.8	12.0	10.3		
	7	13.9	12.5	10.0			15.0	12.5	10.0		
	8	11.8	11.2	9.4			14.0	11.4	9.4		
2	9	17.0	10.2	11.4	77.9	18.4	19.4	10.2	10.6	76.9	20.1
	10	18.7	12.2	11.7			17.7	12.5	11.6		
	11	16.2	11.6	11.1			17.8	12.4	11.7		
	12	16.7	12.4	10.6			17.8	12.6	11.6		
	13	17.5	11.6	10.8			17.7	12.1	9.7		
3	14	17.8	11.4	11.1	99.9	99.4	15.0	11.2	10.8	99.6	101.7
	15	18.1	11.4	11.3			14.8	12.8	11.1		
	16	15.5	12.3	11.1			15.0	12.1	10.0		
	17	15.2	11.4	11.0			14.9	12.6	10.6		
	18	14.9	12.0	10.6			14.7	12.6	9.7		
	19	16.0	13.1	10.5			14.4	12.5	10.6		
	20	15.8	13.0	11.0			12.6	12.3	10.3		
	21	14.4	12.4	10.8			13.2	11.5	10.0		

[†] See Figure B8 for the definition of the leg numbers.

Table B27 – Weld Measurements for Specimen TL100LT-2

Leg Number†	Measurement Number	Front Face					Back Face				
		Main Plate Leg (mm)	Lap Plate Leg (mm)	45° Meas. (mm)	Leg Length (mm)	Gauge Length (mm)	Main Plate Leg (mm)	Lap Plate Leg (mm)	45° Meas. (mm)	Leg Length (mm)	Gauge Length (mm)
1	1	14.0	11.6	10.8	99.8	103.5	13.9	12.4	9.4	98.2	102.9
	2	14.4	11.3	10.8			15.7	13.1	10.2		
	3	14.1	11.8	10.6			15.5	12.6	11.0		
	4	14.8	11.1	9.7			15.8	12.9	10.5		
	5	15.0	12.5	10.3			17.6	13.2	11.1		
	6	14.2	12.8	9.7			17.5	12.6	10.3		
	7	15.1	12.0	8.9			15.9	12.6	10.2		
	8	14.1	11.1	9.8			14.9	12.1	9.7		
2	9	15.6	11.9	10.3	77.2	18.2	19.1	12.5	11.0	76.0	20.2
	10	17.1	12.0	11.0			17.6	15.1	11.9		
	11	17.1	12.1	10.8			18.2	14.8	11.9		
	12	16.6	13.1	10.6			19.2	13.5	11.1		
	13	15.6	12.3	10.8			18.6	13.6	10.8		
3	14	16.7	11.3	11.0	97.8	98.0	16.4	12.1	10.0	99.6	102.2
	15	16.0	13.6	11.9			16.4	13.3	11.3		
	16	14.8	13.3	11.1			16.5	13.0	11.1		
	17	14.6	13.0	11.0			17.4	13.3	11.3		
	18	14.6	14.0	11.3			16.3	15.1	11.9		
	19	13.3	14.2	11.7			14.5	14.7	11.7		
	20	14.2	14.4	11.4			14.6	13.9	11.6		
	21	12.3	13.9	9.7			13.6	13.9	11.1		

† See Figure B8 for the definition of the leg numbers.

Table B28 – Weld Measurements for Specimen TL100LT-3

Leg Number†	Measurement Number	Front Face					Back Face				
		Main Plate Leg (mm)	Lap Plate Leg (mm)	45° Meas. (mm)	Leg Length (mm)	Gauge Length (mm)	Main Plate Leg (mm)	Lap Plate Leg (mm)	45° Meas. (mm)	Leg Length (mm)	Gauge Length (mm)
1	1	13.7	11.9	9.4	97.3	98.7	14.1	12.1	9.4	98.6	98.9
	2	13.7	11.3	9.4			14.9	12.2	9.8		
	3	13.4	11.1	9.2			13.8	12.9	10.5		
	4	14.0	11.1	9.4			15.1	12.3	10.8		
	5	14.8	12.3	9.5			14.5	12.5	10.8		
	6	12.7	12.4	9.8			14.5	13.2	10.2		
	7	12.2	12.3	10.0			14.7	12.5	9.5		
	8	12.3	11.5	9.4			14.6	12.7	9.5		
2	9	13.8	11.8	9.4	77.2	16.5	19.3	12.0	11.6	78.8	18.7
	10	15.0	12.2	10.5			17.8	11.8	11.7		
	11	14.7	12.7	10.8			17.1	13.0	11.1		
	12	15.8	12.7	9.8			17.3	12.2	11.3		
	13	15.3	11.6	10.3			15.9	11.8	10.8		
3	14	17.1	8.9	10.0	94.0	91.8	16.1	10.3	11.1	96.2	101.1
	15	16.2	11.0	10.2			16.3	11.2	11.3		
	16	15.2	10.5	10.0			16.0	11.3	11.1		
	17	13.7	12.7	10.3			16.0	10.0	11.0		
	18	14.5	12.2	10.2			17.0	12.3	11.3		
	19	16.7	12.6	10.6			15.2	9.9	11.1		
	20	14.3	11.6	10.3			16.7	12.1	10.8		
	21	13.8	11.4	10.8			13.9	11.8	10.0		

† See Figure B8 for the definition of the leg numbers.

Table B29 – Weld Measurements for Specimen TL50D-1

Leg Number†	Measurement Number	Front Face					Back Face				
		Main Plate Leg (mm)	Lap Plate Leg (mm)	45° Meas. (mm)	Leg Length (mm)	Gauge Length (mm)	Main Plate Leg (mm)	Lap Plate Leg (mm)	45° Meas. (mm)	Leg Length (mm)	Gauge Length (mm)
1	1	15.2	12.7	11.1	47.8	57.7	14.7	13.8	12.2	47.4	53.4
	2	14.7	11.7	10.2			14.6	13.2	10.8		
	3	15.9	12.5	10.6			15.2	13.6	10.6		
	4	16.2	12.9	11.0			16.3	13.5	11.0		
2	5	12.8	13.0	9.8	72.5	16.2	14.0	14.0	11.4	72.2	18.1
	6	11.3	12.1	10.0			13.7	14.3	11.3		
	7	13.4	12.1	10.5			14.0	14.4	10.5		
	8	14.1	12.2	11.1			15.4	13.3	11.0		
	9	17.6	13.7	11.6			14.4	14.1	12.7		
3	10	15.7	14.6	12.4	47.0	58.9	15.4	14.8	11.6	45.8	58.3
	11	12.5	13.5	11.4			13.5	13.2	10.0		
	12	12.6	12.2	9.7			12.2	12.0	9.5		
	13	13.2	12.8	9.4			12.4	12.4	9.4		

† See Figure B7 for the definition of the leg numbers.

Table B30 – Weld Measurements for Specimen TL50D-2

Leg Number†	Measurement Number	Front Face					Back Face				
		Shear Leg (mm)	Tension Leg (mm)	45° Meas. (mm)	Leg Length (mm)	Gauge Length (mm)	Shear Leg (mm)	Tension Leg (mm)	45° Meas. (mm)	Leg Length (mm)	Gauge Length (mm)
1	1	11.6	13.9	9.8	46.3	53.3	15.1	13.3	11.0	46.3	58.7
	2	11.9	13.2	10.3			14.2	13.3	11.0		
	3	12.8	14.0	11.0			14.5	13.3	11.4		
	4	13.3	12.8	12.2			16.1	13.9	12.7		
2	5	13.9	12.6	10.2	71.1	15.9	16.9	13.7	12.2	74.2	18.5
	6	13.9	11.4	9.8			15.7	12.3	11.3		
	7	14.0	11.3	9.4			15.4	12.0	10.8		
	8	13.5	12.6	10.2			13.7	12.7	10.8		
	9	14.6	13.1	10.5			15.1	12.9	10.8		
3	10	13.7	13.7	10.8	48.6	59.3	13.2	12.2	10.8	50.0	58.0
	11	12.8	13.6	10.6			14.2	12.9	9.8		
	12	12.6	12.7	10.0			14.4	12.8	10.3		
	13	13.0	12.9	10.0			14.9	13.6	10.3		

† See Figure B7 for the definition of the leg numbers.

Table B31 – Weld Measurements for Specimen TL50D-3

Leg Number†	Measurement Number	Front Face					Back Face				
		Main Plate Leg (mm)	Lap Plate Leg (mm)	45° Meas. (mm)	Leg Length (mm)	Gauge Length (mm)	Main Plate Leg (mm)	Lap Plate Leg (mm)	45° Meas. (mm)	Leg Length (mm)	Gauge Length (mm)
1	1	12.0	13.8	9.5	47.6	52.5	15.0	13.0	9.7	52.5	59.0
	2	11.1	12.6	9.4			17.3	12.4	10.6		
	3	12.4	14.1	10.2			18.0	13.0	10.6		
	4	13.1	15.6	11.4			17.2	12.4	10.8		
2	5	15.8	12.4	10.0	71.5	18.1	16.2	10.4	9.2	74.5	16.2
	6	15.9	11.3	9.4			14.2	11.2	8.7		
	7	16.1	11.4	9.8			13.2	9.8	8.1		
	8	15.8	11.9	10.2			13.4	11.3	9.2		
	9	19.9	12.0	10.6			17.4	10.0	9.5		
3	10	15.3	10.3	9.8	48.8	51.8	16.0	11.0	9.4	52.5	57.2
	11	15.4	11.1	9.7			14.3	10.4	8.4		
	12	16.2	12.5	9.5			14.1	10.7	8.9		
	13	14.8	12.5	9.2			13.3	11.3	9.0		

† See Figure B7 for the definition of the leg numbers.

Table B32 – Weld Measurements for Specimen L100-1

Measurement Number†	Front Face								Back Face							
	Weld 1				Weld 2				Weld 3				Weld 4			
	Main Plate Leg (mm)	Lap Plate Leg (mm)	45° Meas. (mm)	Leg Length†/ Gauge Length‡ (mm)	Main Plate Leg (mm)	Lap Plate Leg (mm)	45° Meas. (mm)	Leg Length†/ Gauge Length‡ (mm)	Main Plate Leg (mm)	Lap Plate Leg (mm)	45° Meas. (mm)	Leg Length†/ Gauge Length‡ (mm)	Main Plate Leg (mm)	Lap Plate Leg (mm)	45° Meas. (mm)	Leg Length†/ Gauge Length‡ (mm)
1	13.7	11.9	9.7	98.2†	12.0	10.5	9.7	98.9†	13.6	11.7	9.5	100.9†	12.9	11.5	9.2	99.7†
2	13.2	11.7	9.5		12.7	10.6	9.8		12.0	11.5	9.7		12.3	11.3	9.2	
3	12.8	12.0	10.0	98.2†	12.6	12.2	9.8	98.8†	12.9	11.2	10.0	100.7†	11.8	11.6	9.5	99.6†
4	12.4	12.1	10.3		12.8	11.8	9.8		12.7	11.4	10.2		13.5	12.0	10.0	
5	13.1	12.7	9.7	106‡	13.1	11.1	9.7	107‡	12.2	11.3	10.2	106‡	13.9	12.9	10.3	107‡
6	12.5	13.0	10.0		12.7	11.5	9.7		11.3	11.9	9.7		13.4	12.9	10.2	
7	12.6	12.2	9.7		11.2	11.8	9.5		11.8	11.8	9.8		12.8	12.5	10.0	
8	12.8	11.8	9.8		11.4	10.8	9.7		11.8	12.0	9.4		12.8	11.5	9.7	

† See Figure B9 for the definition of the leg numbers.

Table B33 – Weld Measurements for Specimen L100-2

Measurement Number†	Front Face								Back Face							
	Weld 1				Weld 2				Weld 3				Weld 4			
	Main Plate Leg (mm)	Lap Plate Leg (mm)	45° Meas. (mm)	Leg Length†/ Gauge Length‡ (mm)	Main Plate Leg (mm)	Lap Plate Leg (mm)	45° Meas. (mm)	Leg Length†/ Gauge Length‡ (mm)	Main Plate Leg (mm)	Lap Plate Leg (mm)	45° Meas. (mm)	Leg Length†/ Gauge Length‡ (mm)	Main Plate Leg (mm)	Lap Plate Leg (mm)	45° Meas. (mm)	Leg Length†/ Gauge Length‡ (mm)
1	15.8	11.6	10.0	99.2†	15.0	10.4	10.5	98.1†	12.2	12.3	9.8	99.6†	13.2	9.9	8.1	100.1†
2	15.7	12.2	11.0		14.1	10.9	10.8		13.3	12.6	10.8		14.7	10.3	8.6	
3	14.2	13.4	11.3	99.4†	14.8	11.1	11.4	98.2†	13.3	12.2	10.6	99.5†	14.3	10.4	9.2	99.9†
4	15.0	12.5	11.4		14.9	11.8	11.7		13.0	11.5	11.0		13.7	10.9	9.4	
5	14.8	13.0	11.1	112‡	14.9	11.3	11.3	110‡	14.6	11.9	11.3	115‡	14.0	11.1	9.5	117‡
6	14.8	12.8	11.1		14.1	10.8	11.0		13.9	11.9	10.3		12.8	11.1	9.5	
7	13.2	12.7	10.8		13.8	10.7	10.2		13.7	11.2	11.1		13.5	11.2	9.2	
8	14.4	12.6	11.0		12.4	10.2	10.5		10.9	10.2	9.8		13.9	10.1	9.2	

† See Figure B9 for the definition of the leg numbers.

Table B34 – Weld Measurements for Specimen L100-3

Measurement Number†	Front Face								Back Face							
	Weld 1				Weld 2				Weld 3				Weld 4			
	Main Plate Leg (mm)	Lap Plate Leg (mm)	45° Meas. (mm)	Leg Length†/ Gauge Length‡ (mm)	Main Plate Leg (mm)	Lap Plate Leg (mm)	45° Meas. (mm)	Leg Length†/ Gauge Length‡ (mm)	Main Plate Leg (mm)	Lap Plate Leg (mm)	45° Meas. (mm)	Leg Length†/ Gauge Length‡ (mm)	Main Plate Leg (mm)	Lap Plate Leg (mm)	45° Meas. (mm)	Leg Length†/ Gauge Length‡ (mm)
1	14.6	12.6	10.8	101.5†	14.1	12.8	11.3	103.1†	13.0	12.9	11.0	102.0†	13.3	12.7	10.8	101.2†
2	14.5	12.1	11.3		14.5	12.2	11.0		12.1	13.1	11.1		12.7	13.5	11.3	
3	13.7	13.3	11.6	101.7†	14.1	12.3	11.1	103.4†	13.2	12.6	11.0	102.1†	13.5	12.9	11.4	101.2†
4	12.9	12.7	11.0		13.3	12.5	11.0		12.9	13.5	11.0		13.7	13.0	11.3	
5	12.7	12.5	10.8	109‡	13.9	12.8	11.3	111‡	11.7	12.9	10.8	110‡	13.6	12.9	11.4	110‡
6	13.0	13.3	11.0		14.0	13.3	11.4		11.3	13.0	10.6		13.0	12.9	10.8	
7	13.0	12.8	9.7		12.8	12.7	11.3		12.1	12.9	10.8		12.9	12.8	10.8	
8	12.6	13.1	9.8		13.0	13.2	11.0		12.2	13.1	11.3		12.5	12.8	11.3	

† See Figure B9 for the definition of the leg numbers.

Table B35 – Weld Measurements for Specimen L100-4

Measurement Number†	Front Face								Back Face							
	Weld 1				Weld 2				Weld 3				Weld 4			
	Main Plate Leg (mm)	Lap Plate Leg (mm)	45° Meas. (mm)	Leg Length†/ Gauge Length‡ (mm)	Main Plate Leg (mm)	Lap Plate Leg (mm)	45° Meas. (mm)	Leg Length†/ Gauge Length‡ (mm)	Main Plate Leg (mm)	Lap Plate Leg (mm)	45° Meas. (mm)	Leg Length†/ Gauge Length‡ (mm)	Main Plate Leg (mm)	Lap Plate Leg (mm)	45° Meas. (mm)	Leg Length†/ Gauge Length‡ (mm)
1	12.7	8.3	9.2	99.8†	13.2	9.3	9.4	97.8†	11.6	9.5	8.3	99.1†	12.4	8.9	9.8	100.2†
2	12.1	9.1	9.0		12.4	9.5	9.2		11.9	8.9	8.4		12.6	9.6	10.0	
3	12.3	10.1	9.8	99.3†	12.6	9.9	9.7	97.7†	12.2	9.3	9.0	99.2†	12.6	10.2	10.3	100.2†
4	12.1	8.8	9.5		13.0	10.6	9.5		11.5	9.5	8.1		12.8	11.0	10.6	
5	12.5	8.9	8.9	107‡	12.0	10.7	9.8	106‡	12.1	8.6	8.4	107‡	12.8	10.1	10.2	107‡
6	12.3	8.9	9.5		13.7	9.7	9.4		12.6	9.5	8.3		12.2	10.2	10.0	
7	12.3	8.7	9.2		12.2	8.7	9.0		12.1	8.6	8.7		12.7	10.4	11.0	
8	11.9	8.7	9.4		12.0	9.4	9.7		11.9	8.7	8.1		12.4	9.3	9.8	

† See Figure B9 for the definition of the leg numbers.

Table B36 – Weld Measurements for Specimen L100-5

Measurement Number†	Front Face								Back Face							
	Weld 1				Weld 2				Weld 3				Weld 4			
	Main Plate Leg (mm)	Lap Plate Leg (mm)	45° Meas. (mm)	Leg Length†/ Gauge Length‡ (mm)	Main Plate Leg (mm)	Lap Plate Leg (mm)	45° Meas. (mm)	Leg Length†/ Gauge Length‡ (mm)	Main Plate Leg (mm)	Lap Plate Leg (mm)	45° Meas. (mm)	Leg Length†/ Gauge Length‡ (mm)	Main Plate Leg (mm)	Lap Plate Leg (mm)	45° Meas. (mm)	Leg Length†/ Gauge Length‡ (mm)
1	13.4	10.7	10.0	99.2†	12.2	7.5	9.4	98.9†	15.2	10.3	9.8	99.5†	13.2	9.3	11.0	99.2†
2	12.3	10.6	10.3		12.1	9.0	9.8		15.2	10.7	10.2		12.1	9.8	10.6	
3	11.6	10.4	9.8	99.3†	12.7	10.0	11.0	98.8†	13.6	10.7	10.8	99.5†	12.8	10.0	10.0	99.1†
4	11.4	10.4	10.3		12.5	9.6	10.8		13.5	10.8	10.6		12.8	10.7	10.6	
5	11.5	10.7	9.8	107‡	12.3	9.9	11.0	109‡	13.9	10.3	11.0	105‡	13.6	10.5	11.0	106‡
6	12.1	10.6	9.8		11.9	9.3	9.8		13.9	11.0	10.6		12.5	10.1	11.0	
7	11.8	9.8	9.7		12.4	9.3	9.7		13.2	9.0	10.6		12.2	9.6	10.5	
8	11.4	9.9	9.0		12.1	9.3	9.8		14.6	10.6	10.5		13.7	8.9	10.8	

† See Figure B9 for the definition of the leg numbers.

Table B37 – Weld Measurements for Specimen L100-6

Measurement Number†	Front Face								Back Face							
	Weld 1				Weld 2				Weld 3				Weld 4			
	Main Plate Leg (mm)	Lap Plate Leg (mm)	45° Meas. (mm)	Leg Length†/ Gauge Length‡ (mm)	Main Plate Leg (mm)	Lap Plate Leg (mm)	45° Meas. (mm)	Leg Length†/ Gauge Length‡ (mm)	Main Plate Leg (mm)	Lap Plate Leg (mm)	45° Meas. (mm)	Leg Length†/ Gauge Length‡ (mm)	Main Plate Leg (mm)	Lap Plate Leg (mm)	45° Meas. (mm)	Leg Length†/ Gauge Length‡ (mm)
1	11.2	10.5	9.8	100.8†	11.5	10.2	9.7	102.4†	11.8	10.1	10.6	101.0†	12.5	9.0	9.2	102.0†
2	10.7	11.3	10.2		10.3	10.8	9.7		10.6	10.1	10.2		12.4	10.1	9.4	
3	12.0	11.4	11.0	100.6†	11.8	11.0	10.0	102.3†	12.0	10.1	11.3	100.7†	12.4	11.0	10.8	101.9†
4	11.3	11.4	10.5		11.2	11.1	10.2		10.8	11.1	11.0		12.9	10.4	11.3	
5	12.3	10.2	10.6	109‡	11.1	11.0	10.6	110‡	10.1	10.9	11.0	109‡	11.9	10.0	10.5	110‡
6	11.1	10.3	10.0		11.1	11.1	10.6		12.2	11.0	11.0		12.2	9.9	9.4	
7	10.2	10.8	9.7		11.7	10.8	10.5		11.7	10.4	10.3		12.2	9.5	9.5	
8	10.2	10.7	9.7		11.3	10.5	10.0		10.6	10.3	9.8		12.4	9.2	9.4	

† See Figure B9 for the definition of the leg numbers.

Table B38 – Weld Measurements for Specimen L150-4

Measurement Number[†]	Front Face								Back Face							
	Weld 1				Weld 2				Weld 3				Weld 4			
	Main Plate Leg (mm)	Lap Plate Leg (mm)	45° Meas. (mm)	Leg Length[†]/ Gauge Length[‡] (mm)	Main Plate Leg (mm)	Lap Plate Leg (mm)	45° Meas. (mm)	Leg Length[†]/ Gauge Length[‡] (mm)	Main Plate Leg (mm)	Lap Plate Leg (mm)	45° Meas. (mm)	Leg Length[†]/ Gauge Length[‡] (mm)	Main Plate Leg (mm)	Lap Plate Leg (mm)	45° Meas. (mm)	Leg Length[†]/ Gauge Length[‡] (mm)
1	13.4	11.9	9.0	149.6[†]	11.3	10.4	9.0	151.1[†]	13.2	11.0	9.0	151.8[†]	12.5	9.7	8.1	150.7[†]
2	12.0	10.9	9.4		12.8	9.8	9.4		12.0	11.0	9.4		13.4	10.0	8.4	
3	12.1	11.2	9.2	149.7[†]	13.2	10.3	9.8	151.2[†]	11.5	10.8	9.4	151.5[†]	12.6	9.9	8.9	151.0[†]
4	12.4	10.7	9.2		14.9	10.8	10.5		12.9	10.7	9.4		13.6	11.0	9.2	
5	13.8	10.6	9.5	159[‡]	14.2	9.9	11.0	159[‡]	14.2	10.1	9.7	159[‡]	14.6	10.4	9.7	161[‡]
6	14.3	10.8	9.8		15.5	10.4	11.0		14.5	11.0	9.8		13.8	10.2	9.5	
7	13.8	11.6	9.8		14.4	10.4	9.8		13.8	11.3	9.7		13.7	10.6	9.0	
8	14.6	11.2	9.5		12.9	9.3	9.4		12.7	11.0	8.9		12.2	11.1	9.2	
9	13.6	10.6	9.5		13.5	9.4	9.4		12.5	10.8	9.4		11.5	11.0	8.3	
10	13.8	10.1	9.5		12.6	9.4	9.0		12.9	10.3	9.2		12.5	11.0	8.3	

[†] See Figure B9 for the definition of the leg numbers.

Table B39 – Weld Measurements for Specimen L150-5

Measurement Number†	Front Face								Back Face							
	Weld 1				Weld 2				Weld 3				Weld 4			
	Main Plate Leg (mm)	Lap Plate Leg (mm)	45° Meas. (mm)	Leg Length†/ Gauge Length‡ (mm)	Main Plate Leg (mm)	Lap Plate Leg (mm)	45° Meas. (mm)	Leg Length†/ Gauge Length‡ (mm)	Main Plate Leg (mm)	Lap Plate Leg (mm)	45° Meas. (mm)	Leg Length†/ Gauge Length‡ (mm)	Main Plate Leg (mm)	Lap Plate Leg (mm)	45° Meas. (mm)	Leg Length†/ Gauge Length‡ (mm)
1	13.0	9.4	9.2	151.3†	11.8	9.6	8.3	152.0†	10.9	10.2	8.1	151.6†	9.7	11.0	8.1	151.3†
2	12.2	10.6	9.0		12.3	10.4	8.7		11.8	9.5	8.3		10.9	10.7	8.1	
3	12.4	11.4	8.9	150.3†	13.0	11.2	9.0	152.4†	11.4	9.6	8.6	151.5†	12.2	10.8	8.1	151.6†
4	13.8	11.2	9.5		12.8	10.7	9.4		11.8	9.3	9.4		11.7	10.4	8.3	
5	13.0	9.8	9.5	158‡	12.8	11.2	9.7	160‡	12.5	10.8	9.2	158‡	12.6	10.2	8.9	159‡
6	13.3	10.5	9.2		13.7	10.7	9.5		12.7	11.9	8.6		14.6	9.7	9.4	
7	13.3	10.5	9.4		12.8	10.9	9.4		12.2	10.8	8.3		13.3	10.2	9.2	
8	13.3	10.5	9.2		12.1	11.2	9.4		12.4	10.7	8.6		12.3	10.7	9.0	
9	12.1	10.2	8.9		12.1	10.6	9.4		13.2	10.7	8.3		12.8	11.1	9.0	
10	12.5	10.0	9.2		12.3	10.8	9.7		12.5	10.0	8.7		12.4	10.8	9.0	

† See Figure B9 for the definition of the leg numbers.

Table B40 – Weld Measurements for Specimen L150-6

Measurement Number†	Front Face								Back Face							
	Weld 1				Weld 2				Weld 3				Weld 4			
	Main Plate Leg (mm)	Lap Plate Leg (mm)	45° Meas. (mm)	Leg Length†/ Gauge Length‡ (mm)	Main Plate Leg (mm)	Lap Plate Leg (mm)	45° Meas. (mm)	Leg Length†/ Gauge Length‡ (mm)	Main Plate Leg (mm)	Lap Plate Leg (mm)	45° Meas. (mm)	Leg Length†/ Gauge Length‡ (mm)	Main Plate Leg (mm)	Lap Plate Leg (mm)	45° Meas. (mm)	Leg Length†/ Gauge Length‡ (mm)
1	12.4	9.8	7.8	152.5†	12.2	11.0	8.4	150.6†	12.2	10.3	10.2	151.3†	13.1	11.2	8.3	151.2†
2	11.4	9.1	7.8		12.0	10.7	8.1		11.4	10.0	9.7		12.3	11.8	9.2	
3	10.9	9.4	8.3	152.6†	11.9	11.2	9.0	151.3†	11.7	10.2	9.7	150.9†	11.3	11.5	9.5	151.2†
4	10.6	10.4	8.4		12.4	11.0	9.4		14.3	10.5	10.5		12.2	10.8	9.7	
5	13.1	9.6	8.3	159‡	12.4	12.0	9.8	159‡	14.1	11.4	11.0	160‡	13.4	11.5	9.5	161‡
6	12.8	9.3	8.3		12.2	11.5	9.7		12.7	11.2	9.8		13.1	11.2	9.4	
7	12.5	9.6	8.7		12.3	10.6	9.0		13.7	11.7	10.0		12.9	11.3	9.4	
8	12.5	10.0	8.1		11.0	11.6	9.0		12.9	10.5	9.8		12.1	11.1	9.7	
9	12.2	9.5	8.1		11.5	11.7	9.4		11.5	11.3	9.7		11.9	11.4	9.8	
10	12.8	9.4	7.9		10.9	9.7	9.2		12.3	11.1	9.5		11.7	10.8	9.5	

† See Figure B9 for the definition of the leg numbers.

Table B41 – Weld Measurements for Specimen TNY-1

Measurement Number	Front Face					Back Face				
	Shear Leg (mm)	Tension Leg (mm)	45° Meas. (mm)	Leg Length (mm)	Gauge Length (mm)	Shear Leg (mm)	Tension Leg (mm)	45° Meas. (mm)	Leg Length (mm)	Gauge Length (mm)
1	13.5	12.9	11.0	76.3		13.8	14.1	11.1	76.4	
2	13.0	12.5	10.8	76.3		14.2	13.0	11.4	76.3	
3	12.8	11.9	11.4	76.3	16.2 (LVDT1)	14.9	12.7	11.4	76.3	17.2 (LVDT3)
4	13.2	11.9	10.5			14.3	12.8	11.0		
5	13.7	12.1	10.6		13.6 (LVDT2)	14.0	11.8	10.3		16.5 (LVDT4)
6	13.4	11.9	10.5			13.6	12.1	10.8		
7	13.4	12.0	10.2			13.0	11.8	9.8		
8	13.8	12.2	10.6			13.3	10.6	9.5		

Table B42 – Weld Measurements for Specimen TNY-2

Measurement Number	Front Face					Back Face				
	Shear Leg (mm)	Tension Leg (mm)	45° Meas. (mm)	Leg Length (mm)	Gauge Length (mm)	Shear Leg (mm)	Tension Leg (mm)	45° Meas. (mm)	Leg Length (mm)	Gauge Length (mm)
1	13.7	11.8	11.3	76.2		14.6	12.1	11.0	76.3	
2	14.5	12.5	11.7	76.2		13.9	12.6	10.6	76.3	
3	15.0	12.4	11.4	76.2	16.1 (LVDT1)	13.9	12.9	11.1	76.3	17.9 (LVDT3)
4	14.3	12.6	11.4			14.0	11.1	11.3		
5	13.9	11.5	11.6		15.1 (LVDT2)	14.4	11.2	10.5		17.2 (LVDT4)
6	13.5	11.7	11.4			13.6	12.5	11.0		
7	13.1	12.0	11.0			14.1	12.3	10.3		
8	13.1	11.8	11.0			13.9	11.8	9.8		

Table B43 – Weld Measurements for Specimen TNY-3

Measurement Number	Front Face					Back Face				
	Shear Leg (mm)	Tension Leg (mm)	45° Meas. (mm)	Leg Length (mm)	Gauge Length (mm)	Shear Leg (mm)	Tension Leg (mm)	45° Meas. (mm)	Leg Length (mm)	Gauge Length (mm)
1	14.8	11.8	10.8	76.3		13.1	12.3	10.6	76.3	
2	14.8	11.7	11.3	76.3		13.7	12.6	10.8	76.3	
3	14.7	11.8	10.6	76.4	17.3 (LVDT1)	13.0	12.7	10.0	76.3	15.9 (LVDT3)
4	13.9	11.9	10.8			13.6	12.5	10.8		
5	14.7	12.3	11.0		15.5 (LVDT2)	14.6	12.8	11.0		15.0 (LVDT4)
6	14.4	12.3	11.1			13.5	12.4	10.8		
7	15.0	12.3	10.8			14.0	12.5	11.0		
8	13.6	12.4	10.6			13.4	12.3	10.8		

Table B44 – MOFW Specimen Fracture Angles+

Specimen	Failure Side	Leg 1*				Leg 2				Leg 3			
		1	2	3	4	1	2	3	4	1	2	3	4
TF-1	Front	N/A	N/A	N/A	N/A	19	14	9	9	N/A	N/A	N/A	N/A
TF-1	Back	17	11	15	15	14	22	15	16	7	13	19	19
TF-2	Front	9	13	10	61	69	64	69	47	6	N/A	22	20
TF-2	Back	20	18	N/A	11	23	24	24	22	N/A	21	14	15
TF-3	Front	26	18	21	20	17	12	62	44	19	15	19	8
TF-3	Back	10	11	12	21	B.M.F†				18	20	14	15
TF-4	Front	19	18	20	21	19	23	15	20	12	N/A	N/A	6
TFa-1	Front	15	13	0	9	0	B.M.F.†			7	115	9	20
TFa-1	Back	19	46	10	29	29	22	22	30	51	14	13	5
TFa-2	Front	0	20	19	21	25	23	28	42	8	15	11	20
TFa-2	Back	N/A	35	75	90	76	14	29	26	N/A	34	32	84
TFa-3	Front	16	19	28	80	10	0	0	23	20	25	17	39
TFa-3	Back	14	6	7	8	43	0	0	0	28	8	6	13
TFa-4	Front	9	0	4	13	18	0	0	0	10	N/A	12	N/A
TFa-4	Back	3	13	N/A	23	22	0	0	0	32	36	24	30
TL50-1	Front	84	79	79	0	82	77	79	74	9	19	15	21
TL50-1	Back	83	78	69	59	66	77	68	73	13	12	11	9
TL50-2	Front	59	60	59	59	68	66	52	67	12	16	15	15
TL50-2	Back	78	67	63	45	70	67	62	67	10	16	15	16
TL50-3	Front	72	80	77	71	70	80	80	77	26	18	18	19
TL50-3	Back	27	35	27	31	81	78	71	62	19	24	21	20
TL50-4	Front	N/A	N/A	61	70	13	18	45	49	67	72	72	81
TL50-4	Back	56	66	82	86	19	24	14	19	80	76	70	65
TL50a-1	Front	85	72	67	70	69	63	67	55	52	47	47	54
TL50a-1	Back	70	52	55	66	74	77	49	55	45	39	27	38
TL50a-2	Front	84	75	54	68	65	66	60	54	90	52	52	46
TL50a-2	Back	80	50	49	48	87	85	73	68	35	11	31	53
TL50a-3	Front	78	57	70	61	63	52	47	65	32	34	32	N/A
TL50a-3	Back	79	65	70	67	22	34	34	25	64	56	52	62
TL50a-4	Front	61	61	N/A	62	64	64	69	63	90	77	N/A	63
TL50a-4	Back	65	68	64	71	23	23	28	35	67	67	N/A	61
TL100-1	Front	66	64	59	73	11	18	16	16	60	62	79	N/A
TL100-2	Front	70	64	64	81	13	11	15	75	76	70	77	72
TL100-3	Back	69	65	54	60	27	34	16	14	N/A	60	70	72

* See Figures B6 – B9 for leg numbers

† Base Metal Failure

+ All measurements are given in degrees and are equally spaced along the leg.

Table B44 continued – MOFW Specimen Fracture Angles+

Specimen	Failure Side	Leg 1*				Leg 2				Leg 3			
		1	2	3	4	1	2	3	4	1	2	3	4
TL100SP-1	Front	66	69	80	68	47	N/A	49	38	65	73	74	71
TL100SP-2	Front	64	57	N/A	64	24	29	33	35	44	43	39	55
TL100SP-2	Back	66	62	62	52	53	57	58	61	70	N/A	58	N/A
TL100SP-3	Front	59	68	67	57	61	56	53	50	64	70	75	67
TL100D-1	Back	45	60	61	67	25	23	24	22	58	70	75	76
TL100D-2	Back	52	65	60	59	58	75	50	N/A	53	46	63	57
TL100D-3	Back	78	80	70	65	90	69	22	76	67	N/A	45	51
TL50D-1	Front	N/A	N/A	54	59	55	14	15	29	44	N/A	N/A	39
TL50D-1	Back	26	28	33	51	23	23	20	28	53	68	65	66
TL50D-2	Front	28	60	66	74	54	14	13	44	56	47	30	22
TL50D-3	Front	21	24	29	44	17	20	60	65	60	64	64	58
TL50D-3	Back	60	67	N/A	57	34	37	41	41	N/A	N/A	63	63

* See Figures B6 – B9 for leg numbers

+ All measurements are given in degrees and are equally spaced along the leg.

Table B45 – Weld Penetration Plus Shear Leg Measurements+

Specimen	Failure Side	Leg 1*				Leg 2				Leg 3			
		1	2	3	4	1	2	3	4	1	2	3	4
TF-1	Front	N/A	N/A	N/A	N/A	16.0	16.7	16.6	18.2	N/A	N/A	N/A	N/A
TF-1	Back	16.6	16.9	19.6	19.3	17.7	15.2	18.0	18.4	17.4	15.8	16.0	16.6
TF-2	Front	14.5	13.8	12.6	14.1	15.9	14.4	16.9	17.5	14.1	14.1	15.2	13.1
TF-2	Back	14.6	15.5	13.7	11.6	15.8	15.9	14.9	15.3	14.9	14.9	15.9	14.5
TF-3	Front	14.7	14.6	17.9	16.6	17.4	15.2	17.5	17.7	16.9	14.6	15.5	16.7
TF-3	Back	12.3	14.1	12.5	14.1	14.7	13.8	13.5	16.3	12.5	13.7	15.6	14.3
TF-4	Front	15.7	16.0	14.4	14.9	17.0	19.5	27.7	17.8	14.6	16.9	17.4	14.5
TFa-1	Front	10.3	9.4	9.2	10.0	8.3	9.5	10.2	10.7	10.5	10.0	10.2	9.4
TFa-1	Back	8.5	9.3	8.6	9.0	9.3	10.1	10.7	11.0	9.4	9.0	8.9	8.5
TFa-2	Front	10.2	10.9	8.8	10.9	10.8	10.8	10.8	12.1	10.1	10.8	9.9	9.7
TFa-2	Back	10.6	11.6	10.8	12.0	13.5	13.2	12.6	13.0	12.4	10.7	11.4	10.4
TFa-3	Front	9.0	7.5	10.1	10.2	10.2	9.3	9.9	11.1	10.6	8.9	8.7	9.1
TFa-3	Back	9.4	9.5	11.5	9.8	10.6	11.1	10.1	11.4	10.7	9.8	9.4	10.1
TFa-4	Front	8.6	9.4	8.5	9.4	10.4	9.1	9.2	9.2	11.5	9.0	7.2	7.2
TFa-4	Back	8.5	9.8	10.1	11.4	11.6	9.5	8.9	11.9	9.2	8.4	8.8	8.3

+ All measurements are given in millimetres and are equally spaced along the leg.

* See Figures B6 – B9 for leg numbers

Table B45 continued – Weld Penetration Plus Shear Leg Measurements+

Specimen	Failure Side	Leg 1*				Leg 2				Leg 3			
		1	2	3	4	1	2	3	4	1	2	3	4
TL50-1	Front	11.8	12.8	16.1	17.2	18.9	16.9	16.0	14.5	18.0	17.8	18.6	18.0
TL50-1	Back	14.1	12.7	14.3	13.2	16.9	15.2	14.7	15.6	14.9	17.3	16.1	17.9
TL50-2	Front	15.3	14.7	15.7	17.5	14.4	15.9	16.5	17.2	17.7	17.1	17.4	15.6
TL50-2	Back	13.0	14.0	13.3	15.9	15.0	15.6	14.0	15.2	14.5	16.6	14.8	14.9
TL50-3	Front	12.3	13.7	13.7	13.9	16.0	15.0	14.6	14.5	16.2	14.6	15.7	15.0
TL50-3	Back	12.5	13.1	12.9	12.7	14.1	16.9	16.9	18.3	16.9	17.2	15.7	17.2
TL50-4	Front	13.8	13.5	14.0	15.0	17.2	19.1	20.2	16.7	17.3	17.8	19.4	18.4
TL50-4	Back	14.4	13.8	12.6	N/A	14.2	17.3	16.4	16.2	12.8	13.2	12.7	13.9
TL50a-1	Front	8.5	9.6	9.7	11.7	12.3	11.3	10.6	9.8	12.2	12.2	10.8	11.6
TL50a-1	Back	8.4	8.6	10.0	11.0	11.2	10.0	9.6	10.8	9.1	10.5	12.3	12.4
TL50a-2	Front	8.9	11.3	9.2	10.2	11.6	11.3	12.2	10.8	10.7	10.3	11.5	11.9
TL50a-2	Back	9.3	11.8	9.4	11.8	12.1	11.6	10.1	9.8	11.2	11.5	11.6	12.1
TL50a-3	Front	9.2	8.9	9.7	12.3	11.4	10.0	10.0	9.4	13.0	11.0	11.0	14.7
TL50a-3	Back	9.0	9.8	9.6	10.7	9.0	9.0	13.3	8.2	9.7	11.0	10.9	12.7
TL50a-4	Front	9.0	9.6	11.2	N/A	11.7	9.4	12.0	12.0	12.0	12.7	8.5	8.0
TL50a-4	Back	10.0	10.3	10.3	9.7	11.6	11.3	11.5	13.2	11.1	10.1	9.9	8.9
TL100-1	Front	17.0	16.9	15.8	15.7	18.5	18.2	17.6	20.0	14.4	16.4	14.0	14.3
TL100-2	Front	14.9	14.7	14.9	15.6	15.2	15.7	16.7	15.7	15.2	15.5	14.4	16.6
TL100-3	Back	14.3	13.8	14.9	12.6	15.8	15.5	15.5	15.6	11.6	12.6	12.1	11.5
TL100SP-1	Front	12.7	11.3	13.5	11.5	13.8	12.5	11.6	12.3	13.4	14.1	12.2	12.4
TL100SP-2	Front	12.6	16.2	N/A	14.4	12.5	10.9	11.6	13.5	11.3	12.7	N/A	14.4
TL100SP-2	Back	14.6	N/A	14.2	15.4	11.8	14.5	14.5	13.9	12.6	11.2	11.9	N/A
TL100SP-3	Back	14.3	13.8	14.9	12.6	15.8	15.5	15.5	15.6	11.6	12.6	12.1	11.5
TL100D-1	Back	12.7	14.9	14.7	13.7	15.2	16.6	16.6	15.7	11.8	15.9	14.2	13.4
TL100D-2	Back	12.2	11.9	14.6	13.0	14.0	13.0	14.1	13.3	14.5	15.0	13.8	13.8
TL100D-3	Back	15.5	14.9	17.2	15.7	14.8	14.7	14.8	14.3	15.6	18.6	16.9	15.7
TL50D-1	Front	13.4	13.4	N/A	15.5	14.1	15.3	12.1	14.1	N/A	17.9	17.9	18.9
TL50D-1	Back	13.2	12.7	N/A	15.7	14.7	16.6	15.1	16.8	17.4	15.8	N/A	16.7
TL50D-2	Front	12.9	12.3	13.0	13.4	14.1	15.4	14.1	14.3	14.2	13.2	14.1	13.5
TL50D-3	Front	16.6	16.9	16.7	N/A	17.6	18.2	18.3	17.9	13.9	13.5	12.0	15.2
TL50D-3	Back	15.3	16.8	17.0	17.8	16.5	17.2	17.9	17.7	21.0	22.3	20.3	19.1

+ All measurements are given in millimetres and are equally spaced along the leg.
* See Figures B6 – B9 for leg numbers

Table B46 – Fractured Throat Measurements[+]

Specimen	Failure Side	Leg 1[*]				Leg 2				Leg 3			
		1	2	3	4	1	2	3	4	1	2	3	4
TF-1	Front	N/A	N/A	N/A	N/A	10.1	11.7	10.0	12.2	N/A	N/A	N/A	N/A
TF-1	Back	10.0	10.7	11.9	11.0	11.2	10.8	11.5	12.2	13.1	10.3	9.3	8.2
TF-2	Front	N/A	N/A	10.9	N/A	N/A	N/A	N/A	N/A	12.0	N/A	9.0	9.6
TF-2	Back	8.8	10.5	8.3	N/A	9.5	9.3	9.2	9.6	N/A	8.8	9.5	8.2
TF-3	Front	9.6	10.0	11.2	11.8	10.6	8.5	N/A	N/A	10.8	8.9	10.4	10.5
TF-3	Back	N/A	N/A	N/A	8.0	13.0	13.5	13.7	15.1	N/A	7.2	10.0	8.7
TF-4	Front	9.4	9.2	9.2	8.9	9.5	9.5	11.9	11.8	9.2	10.3	12.3	12.0
TFa-1	Front	8.5	8.0	8.7	7.9	8.3	9.5	10.2	10.7	8.7	7.9	9.5	8.0
TFa-1	Back	5.7	5.7	7.2	5.1	5.9	6.2	6.5	6.0	6.4	7.1	7.3	7.3
TFa-2	Front	10.1	6.9	7.8	7.5	7.3	7.9	9.8	5.9	8.3	8.2	8.0	8.1
TFa-2	Back	8.0	6.4	6.1	N/A	N/A	8.2	7.7	5.5	N/A	6.1	5.3	7.7
TFa-3	Front	7.5	5.8	6.0	7.4	7.1	9.3	9.9	7.3	7.9	6.2	6.3	5.1
TFa-3	Back	7.3	7.0	8.8	8.7	6.0	8.9	8.5	8.2	6.6	7.6	7.2	8.2
TFa-4	Front	8.5	9.4	8.5	3.9	7.3	9.1	9.2	9.2	9.0	6.4	5.8	5.1
TFa-4	Back	8.5	9.4	6.6	7.4	9.3	9.5	8.9	11.9	6.1	5.8	5.9	5.0
TL50-1	Front	10.8	10.5	10.4	11.3	9.4	9.1	9.1	8.7	10.5	12.5	12.0	13.6
TL50-1	Back	10.7	9.1	9.5	9.3	8.8	10.0	9.2	9.4	11.3	11.0	10.0	10.8
TL50-2	Front	10.9	10.0	11.5	10.6	9.6	11.3	10.9	10.6	11.7	11.6	11.4	12.5
TL50-2	Back	9.9	8.9	11.8	11.7	8.9	9.5	9.4	10.0	12.0	10.8	11.3	12.1
TL50-3	Front	8.2	8.5	11.0	10.2	9.4	9.7	11.1	8.8	9.7	9.7	9.7	9.8
TL50-3	Back	10.0	9.3	7.9	10.5	10.8	10.9	9.9	10.4	9.9	11.0	10.3	11.6
TL50-4	Front	9.2	9.5	10.4	10.1	12.3	12.2	7.7	8.3	9.3	9.9	N/A	9.2
TL50-4	Back	10.9	10.6	10.1	N/A	9.3	9.2	10.6	9.7	10.2	10.5	10.4	10.0
TL50a-1	Front	6.8	7.2	6.9	7.9	7.2	7.9	7.2	7.4	6.6	7.0	5.8	6.0
TL50a-1	Back	7.0	7.1	7.1	7.0	7.2	7.0	7.1	10.0	5.9	8.0	6.5	5.7
TL50a-2	Front	6.8	6.3	6.2	7.7	7.1	7.1	6.9	7.0	6.3	6.4	5.8	7.9
TL50a-2	Back	7.0	6.8	6.6	7.0	7.8	7.2	7.1	8.1	6.5	5.7	10.0	7.0
TL50a-3	Front	6.5	6.2	6.9	7.1	6.4	6.1	7.0	7.0	6.9	6.6	7.2	7.9
TL50a-3	Back	6.9	6.9	7.0	7.1	6.3	7.3	8.0	7.0	6.8	5.5	6.3	6.6
TL50a-4	Front	8.7	8.0	6.9	6.7	7.1	6.5	6.4	7.2	8.4	9.0	7.2	7.6
TL50a-4	Back	7.8	7.5	8.1	7.0	7.4	7.3	7.5	7.4	6.7	7.3	6.8	6.5
TL100-1	Front	12.9	12.0	11.7	11.7	14.4	12.2	12.5	13.9	11.2	12.8	13.1	11.6
TL100-2	Front	10.4	9.1	9.4	10.0	13.0	13.0	N/A	10.1	10.1	10.8	10.3	10.2
TL100-3	Back	7.8	8.2	8.4	7.2	7.3	7.0	10.2	9.2	8.6	8.4	8.2	9.2

[+] All measurements are given in millimetres and are equally spaced along the leg.
[*] See Figures B6 – B9 for leg numbers

Table B46 continued – Fractured Throat Measurements+

Specimen	Failure Side	Leg 1*				Leg 2				Leg 3			
		1	2	3	4	1	2	3	4	1	2	3	4
TL100SP-1	Front	8.9	8.3	10.0	8.0	6.9	7.4	7.1	7.3	9.5	10.9	N/A	8.1
TL100SP-2	Front	9.3	10.6	9.3	9.2	9.1	8.3	8.5	7.9	8.8	9.4	9.9	9.6
TL100SP-2	Back	8.7	N/A	8.6	8.8	7.2	7.6	7.5	7.2	8.3	8.6	8.7	N/A
TL100SP-3	Front	8.5	11.2	10.3	8.1	7.0	7.0	7.1	6.6	6.4	10.1	10.6	7.7
TL100D-1	Back	9.6	10.8	11.4	10.3	10.8	10.5	10.0	11.7	11.6	10.7	10.6	9.8
TL100D-2	Back	9.2	10.2	12.1	11.1	8.2	N/A	8.8	9.1	12.5	12.9	N/A	11.0
TL100D-3	Back	10.8	12.2	11.6	11.2	12.6	10.5	11.3	10.0	12.1	12.2	12.8	11.8
TL50D-1	Front	10.1	10.2	N/A	11.0	10.2	11.3	9.8	10.5	N/A	11.5	11.5	12.0
TL50D-1	Back	10.1	10.4	N/A	11.2	11.6	11.4	10.9	12.3	11.1	10.5	N/A	12.2
TL50D-2	Front	10.0	10.7	11.6	11.4	9.4	9.9	N/A	10.6	N/A	12.1	10.9	11.1
TL50D-3	Front	11.3	10.2	10.3	N/A	9.4	9.1	12.2	12.0	13.2	12.3	11.9	12.3
TL50D-3	Back	N/A	11.3	9.9	10.9	10.1	9.0	9.3	9.1	11.9	12.4	12.0	11.5

+ All measurements are given in millimetres and are equally spaced along the leg.
* See Figures B6 – B9 for leg numbers

Table B47 – Longitudinal Specimen Fracture Angles+

Specimen	Failure Side	Leg 1* (Front Side Failure) or Leg 3 (Back Side Failure)					Leg 2* (Front Side Failure) or Leg 4 (Back Side Failure)				
		1	2	3	4	5	1	2	3	4	5
L100-1	Front	39	59	N/A	N/A	N/A	68	61	59	N/A	N/A
L100-2	Back	32	47	N/A	N/A	N/A	61	N/A	N/A	N/A	N/A
L100-3	Front	58	43	N/A	N/A	N/A	30	51	N/A	N/A	N/A
L100-3	Back	36	56	50	N/A	N/A	32	N/A	N/A	N/A	N/A
L100-4	Back	48	47	N/A	N/A	N/A	57	68	46	N/A	N/A
L100-5	Front	61	N/A	N/A	N/A	N/A	46	61	N/A	N/A	N/A
L100-5	Back	65	58	N/A	N/A	N/A	51	N/A	N/A	N/A	N/A
L100-6	Back	67	61	72	N/A	N/A	56	57	N/A	N/A	N/A
L150-4	Back	75	63	N/A	N/A	N/A	70	N/A	N/A	N/A	N/A
L150-5	Front	72	68	N/A	N/A	N/A	56	59	52	56	N/A
L150-5	Back	72	83	85	85	N/A	31	25	74	82	75
L150-6	Front	77	67	68	45	N/A	65	62	59	N/A	N/A

+ All angles are given in degrees and are equally spaced along the leg.
* See Figure B9 for leg numbers

Table B48 – Longitudinal Specimen Weld Penetration Plus Shear Leg Measurements+

Specimen	Failure Side	Leg 1* (Front Side Failure) or Leg 3 (Back Side Failure)					Leg 2* (Front Side Failure) or Leg 4 (Back Side Failure)				
		1	2	3	4	5	1	2	3	4	5
L100-1	Front	13.1	12.2	12.5	N/A	N/A	13.3	13.2	N/A	N/A	N/A
L100-2	Back	13.4	15.3	13.5	N/A	N/A	14.7	N/A	N/A	N/A	N/A
L100-3	Front	15.1	N/A	N/A	N/A	N/A	15.1	14.9	N/A	N/A	N/A
L100-3	Back	15.2	N/A	N/A	N/A	N/A	14.8	13.1	N/A	N/A	N/A
L100-4	Back	13.4	13.2	13.2	14.2	12.6	14.5	14.5	13.8	13.5	N/A
L100-5	Front	10.2	N/A	N/A	N/A	N/A	12.9	N/A	N/A	N/A	N/A
L100-5	Back	12.5	14.1	13.0	N/A	N/A	13.3	13.6	13.3	N/A	N/A
L100-6	Back	10.3	11.6	10.3	N/A	N/A	13.1	13.8	11.4	13.3	N/A
L150-4	Back	13.6	16.1	N/A	N/A	N/A	13.9	13.4	14.3	N/A	N/A
L150-5	Front	14.5	14.3	15.9	N/A	N/A	14.1	14.6	14.6	N/A	N/A
L150-5	Back	13.5	13.2	14.3	N/A	N/A	13.8	13.3	12.7	N/A	N/A
L150-6	Front	14.2	13.9	N/A	N/A	N/A	13.1	13.0	13.6	N/A	N/A

+ All measurements are given in millimetres and are equally spaced along the leg.
* See Figure B9 for leg numbers

Table B49 – Longitudinal Specimen Fracture Throat Measurements+

Specimen	Failure Side	Leg 1* (Front Side Failure) or Leg 3 (Back Side Failure)					Leg 2* (Front Side Failure) or Leg 4 (Back Side Failure)				
		1	2	3	4	5	1	2	3	4	5
L100-1	Front	10.5	11.4	10.6	N/A	N/A	11.0	11.2	N/A	N/A	N/A
L100-2	Back	11.4	11.0	11.0	N/A	N/A	10.1	N/A	N/A	N/A	N/A
L100-3	Front	11.8	N/A	N/A	N/A	N/A	12.3	12.4	N/A	N/A	N/A
L100-3	Back	12.6	N/A	N/A	N/A	N/A	13.5	12.5	N/A	N/A	N/A
L100-4	Back	8.1	8.7	8.4	9.4	8.8	10.2	10.0	9.6	9.5	N/A
L100-5	Front	8.7	N/A	N/A	N/A	N/A	10.1	N/A	N/A	N/A	N/A
L100-5	Back	8.8	11.8	10.4	N/A	N/A	8.5	9.2	9.0	N/A	N/A
L100-6	Back	10.5	10.4	10.8	N/A	N/A	9.2	9.2	9.6	11.2	N/A
L150-4	Back	11.7	11.1	N/A	N/A	N/A	11.1	10.7	10.8	N/A	N/A
L150-5	Front	10.0	10.9	12.3	N/A	N/A	10.8	12.1	12.1	N/A	N/A
L150-5	Back	9.9	10.6	11.3	N/A	N/A	11.3	10.8	11.1	N/A	N/A
L150-6	Front	9.0	10.2	N/A	N/A	N/A	11.5	10.8	12.0	N/A	N/A

+ All measurements are given in millimetres and are equally spaced along the leg.
* See Figure B9 for leg numbers

Table B50 – Transverse Specimen Fracture Angles+

Specimen	Failure Side	Measurement Number				
		1	2	3	4	5
TNY-1	Front	0	0	0	0	26
TNY-2	Front	0	0	0	21	22
TNY-3	Back	24	0	0	0	0

+ All angles are given in degrees and measurement locations are equally spaced.

Table B51 – Transverse Specimen Weld Penetration Plus Shear Leg Measurements+

Specimen	Failure Side	Measurement Number				
		1	2	3	4	5
TNY-1	Front	14.1	14.9	14.5	15.2	14.8
TNY-2	Front	15.4	15.6	15.3	16.2	14.2
TNY-3	Back	14.6	15.2	16.3	16.1	15.5

+ All measurements are given in millimetres and are equally spaced.

Table B51 – Transverse Specimen Fracture Throat Measurements+

Specimen	Failure Side	Measurement Number				
		1	2	3	4	5
TNY-1	Front	14.5	14.7	14.9	15.4	10.9
TNY-2	Front	15.4	15.6	15.3	11.4	11.5
TNY-3	Back	10.4	15.2	16.3	16.1	15.5

+ All measurements are given in millimetres are equally spaced.

APPENDIX C

Ancillary Test Results

Appendix C – Ancillary Test Results

This appendix contains the information collected from the six all-weld-metal coupons that were tested to characterize the filler metal used to fabricate the fillet weld connections tested in this research program. As mentioned in Chapter 3, the specimens were fabricated over two years, though all the specimens were fabricated with E70T-7 weld metal only. Because the weld metal came from two different heats, it was necessary to establish the properties of both heats. Three coupons were fabricated during each of the two years that the specimens were fabricated. The coupons that were fabricated during 2002 are designated "102" and the coupons fabricated during 2003 are designated as "103". All of the stresses shown in the following charts are calculated as engineering stress, i.e., the load on the coupon divided by the initial area. Table C1 gives the initial areas and the post-fracture areas. The initial cross-sectional areas were calculated from nine measurements of the diameter in the coupon test region. The post-fracture areas were calculated from six diameter measurements taken on both of the two fracture areas from each coupon. All of the diameter measurements were taken with a calliper.

Table C1 – Coupon Cross Sectional Areas

Specimen	Cross Sectional Area		
	Initial (mm^2)	Post-Fracture (mm^2)	Reduction (%)
102-1	126	101	19.7
102-2	126	83	34.3
102-3	126	73	41.8
103-1	126	109	13.7
103-2	127	111	12.4
103-3	128	103	19.1

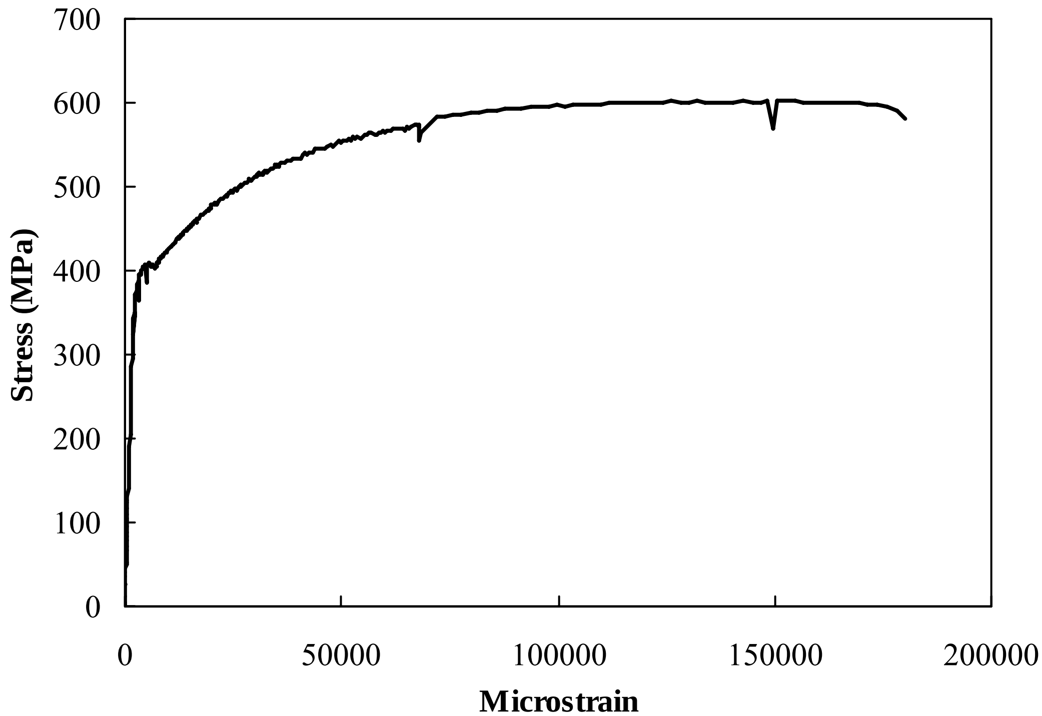

Figure C1 – Test Coupon 102-1 (2002)

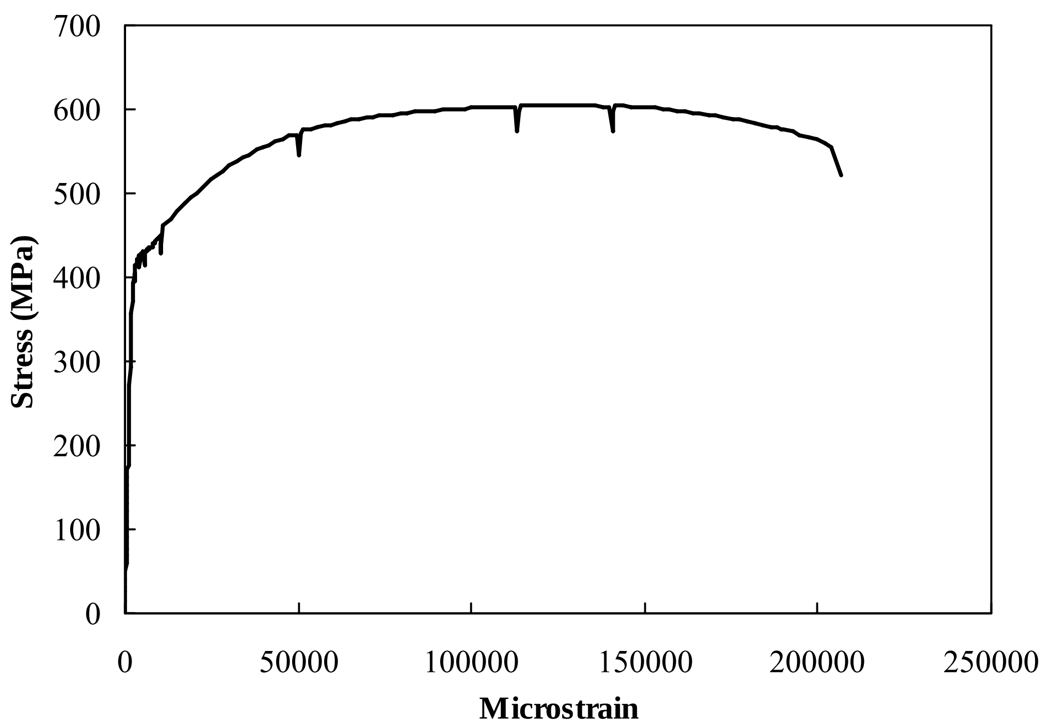

Figure C2 – Test Coupon 102-2 (2002)

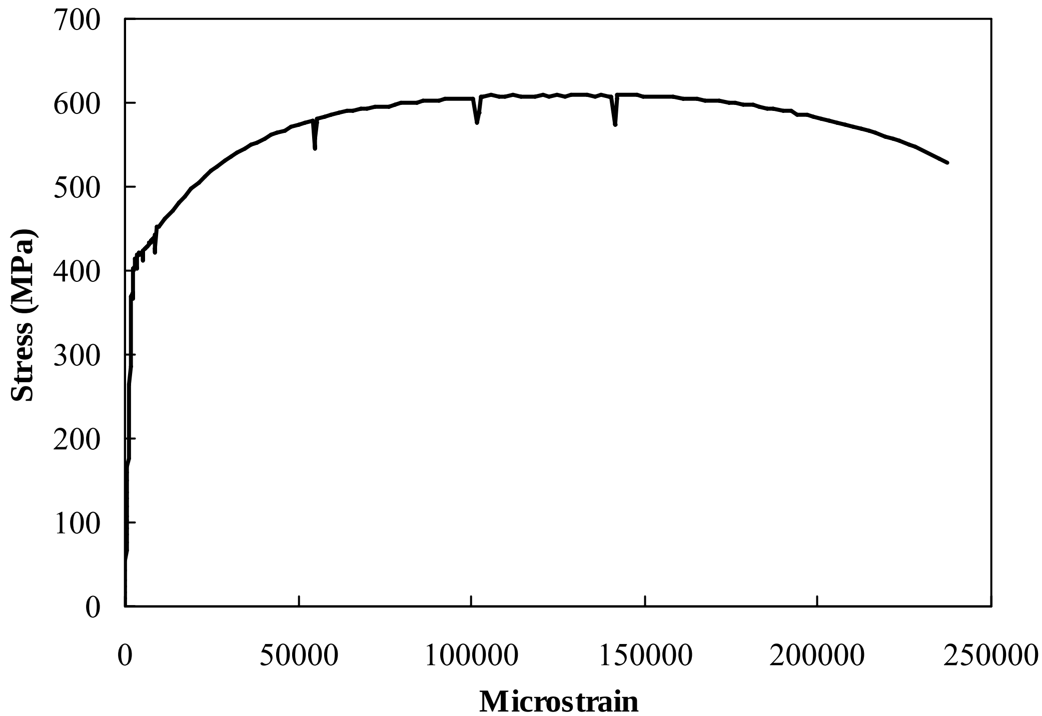

Figure C3 – Test Coupon 102-3 (2002)

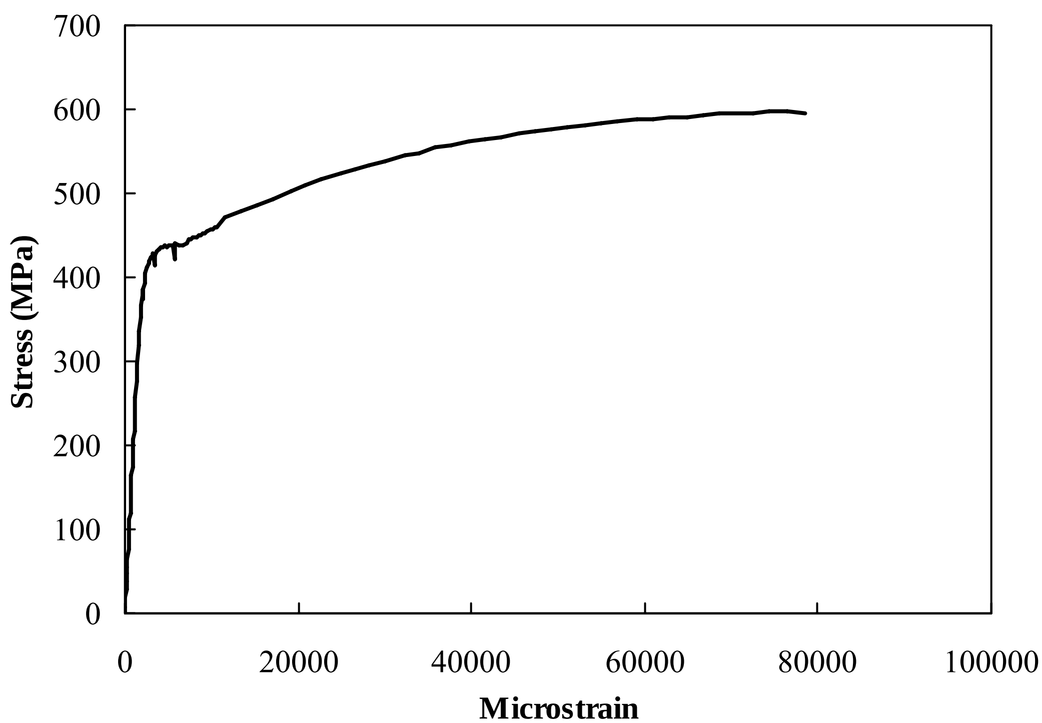

Figure C4 – Test Coupon 103-1 (2003)

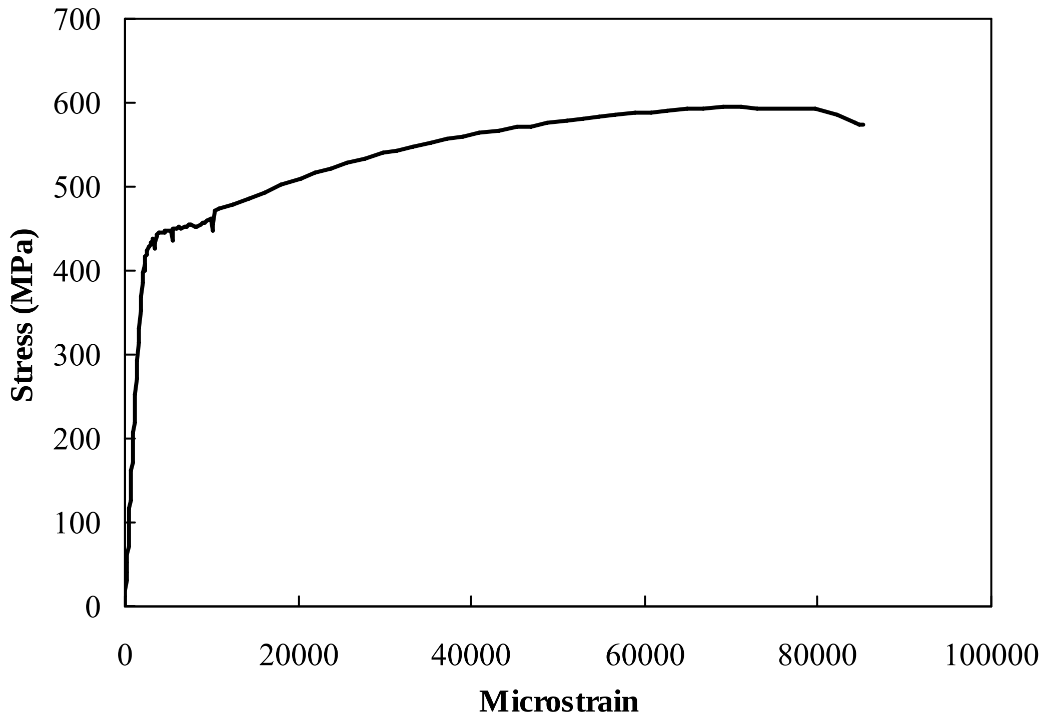

Figure C5 – Test Coupon 103-2 (2003)

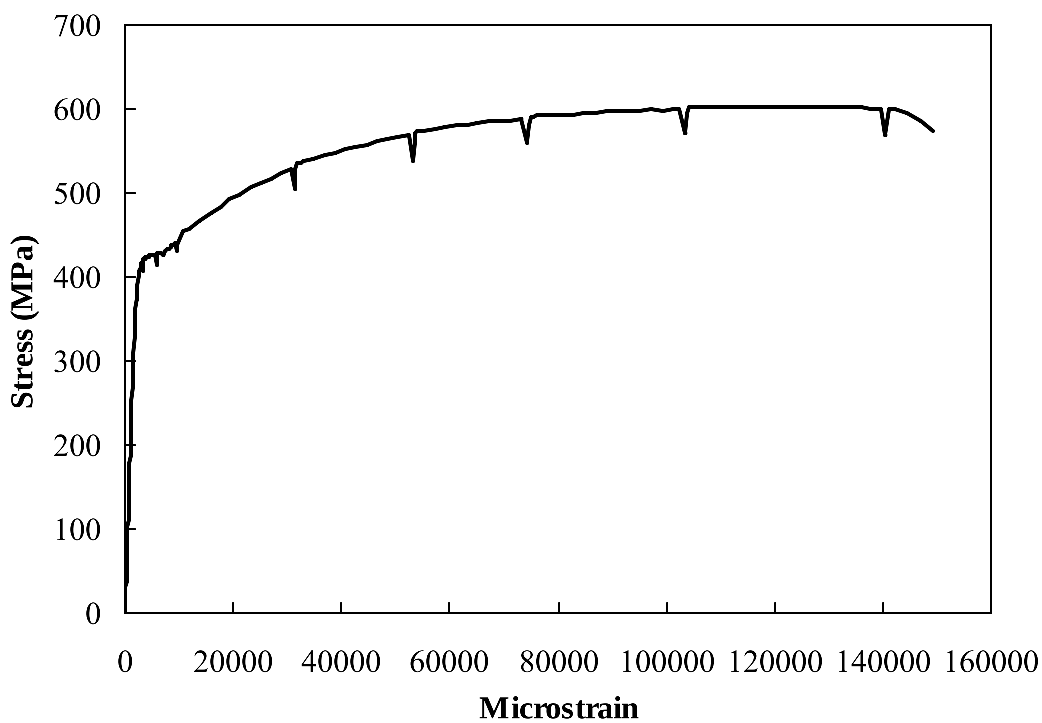

Figure C6 – Test Coupon 103-3 (2003)

APPENDIX D

Specimen Response Curves

Appendix D – Specimen Response Curves

All of the response curves obtained from testing are contained in this Appendix. The specimen response curves are given in the form of a chart as shown in Figure D1.

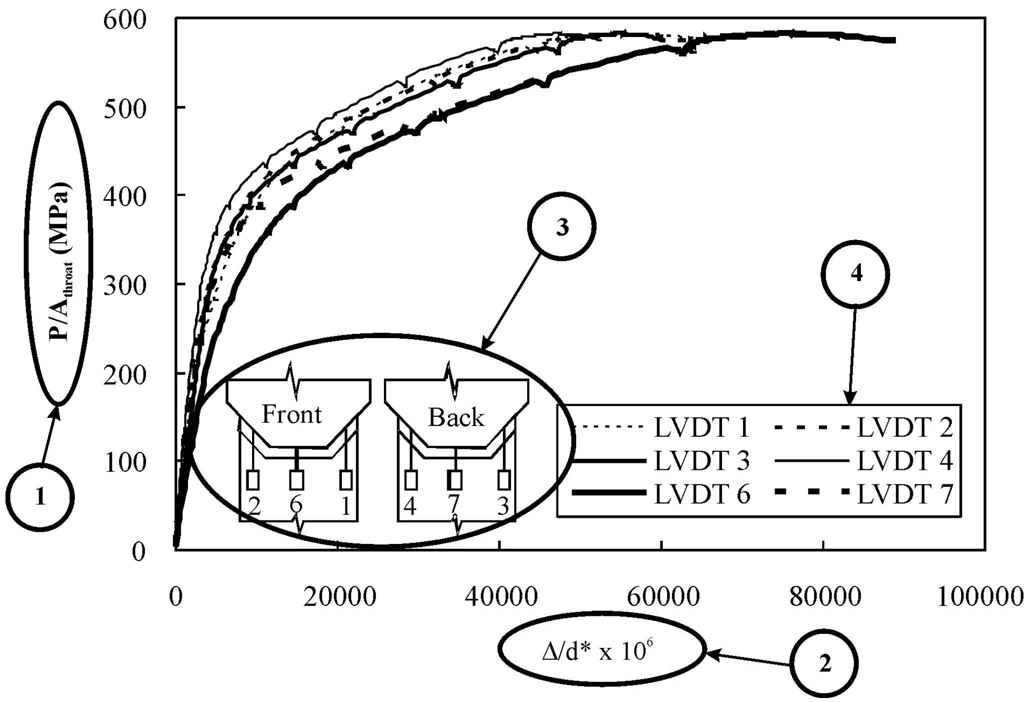

Figure D1 – Sample Response Curve

The four points shown in Figure D1 are described below. An understanding of these points is necessary to interpret properly the information presented in this appendix.

1. All of the charts in Appendix D have the test P/A_{throat} values plotted on the y-axis. The P/A_{throat} term is defined in Chapter 4.
2. All of the charts in Appendix D have the test Δ/d^* values plotted on the x-axis. The Δ/d^* values are then multiplied by 1×10^6 for the sake of clarity as the values of Δ/d^* are typically much less than one. The term Δ/d^* is defined in Chapter 4.
3. Both front and back views of the respective specimen are provided for each chart in order to give the location of the linear variable displacement transformers (LVDTs).
4. All six segment deformations are plotted as measured by the LVDTs. The key gives the information to distinguish between the displacement curves of each segment. The segment that is measured by a particular LVDT can be seen in the figure provided with each chart (as described in point 3 above).

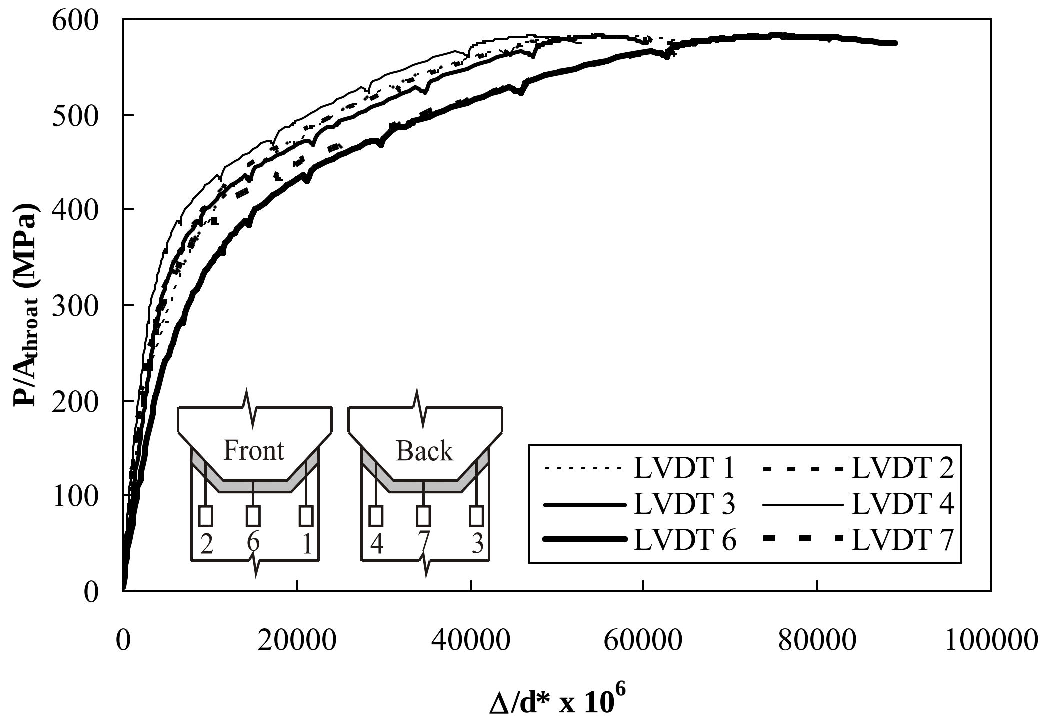

Figure D2 – Specimen TF-1 Response

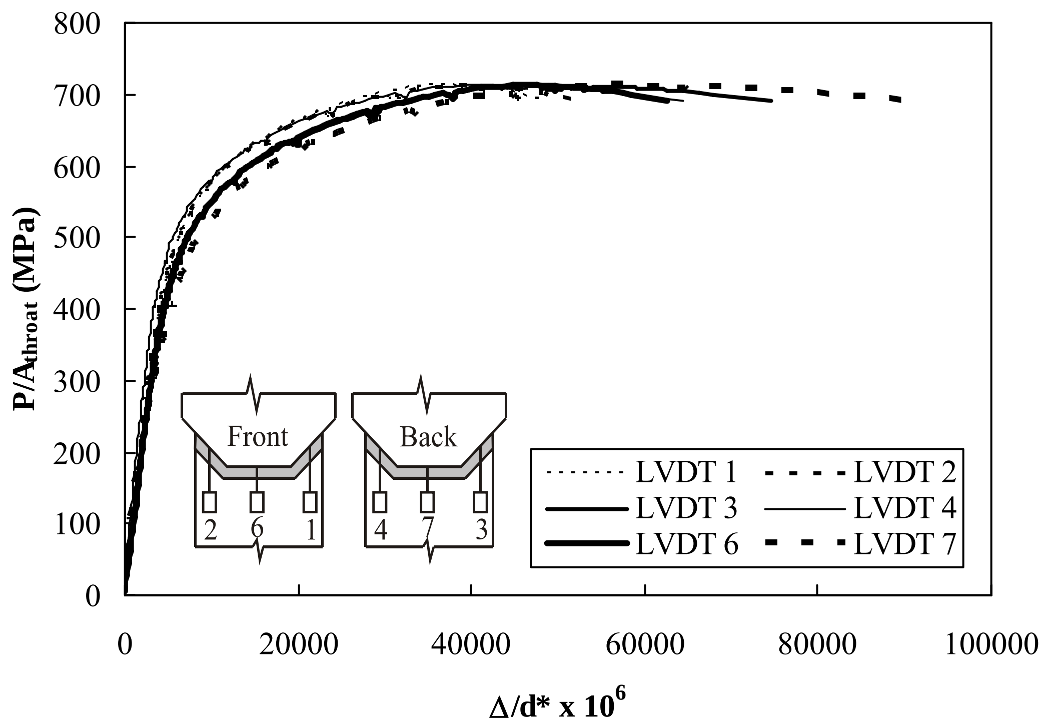

Figure D3 – Specimen TF-2 Response

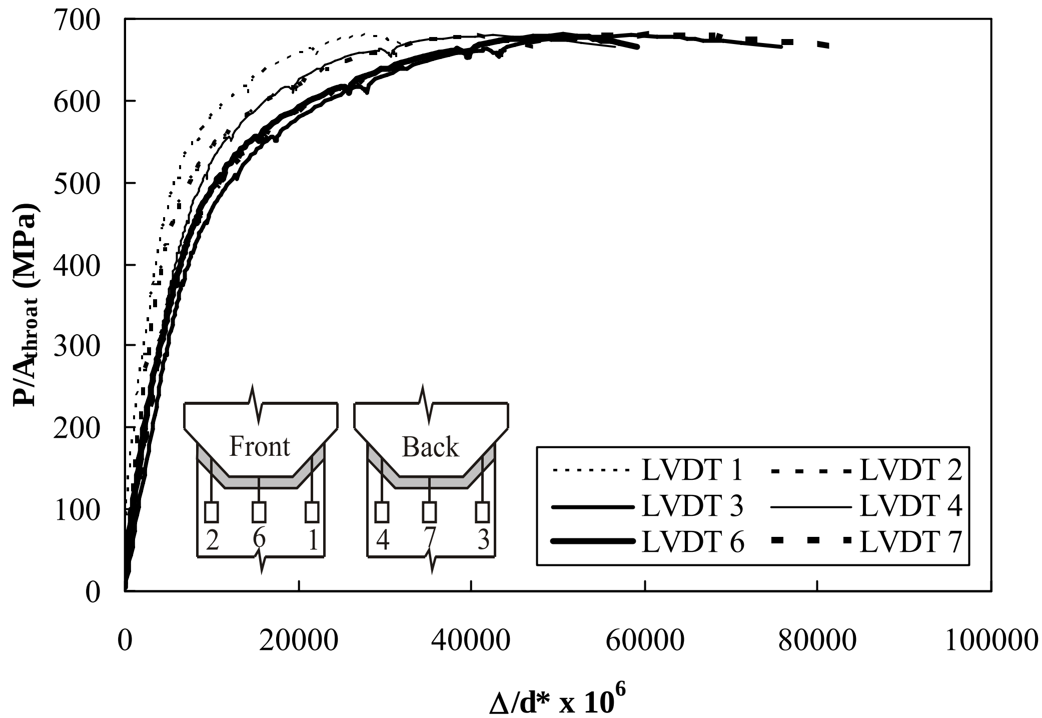

Figure D4 – Specimen TF-3 Response

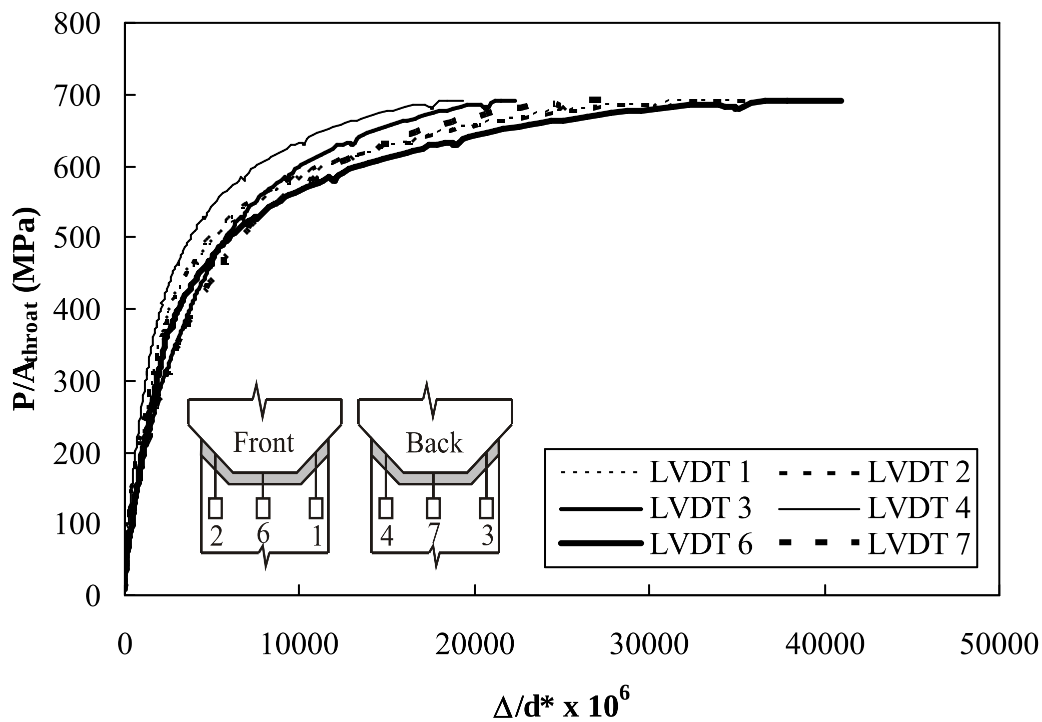

Figure D5 – Specimen TF-4 Response

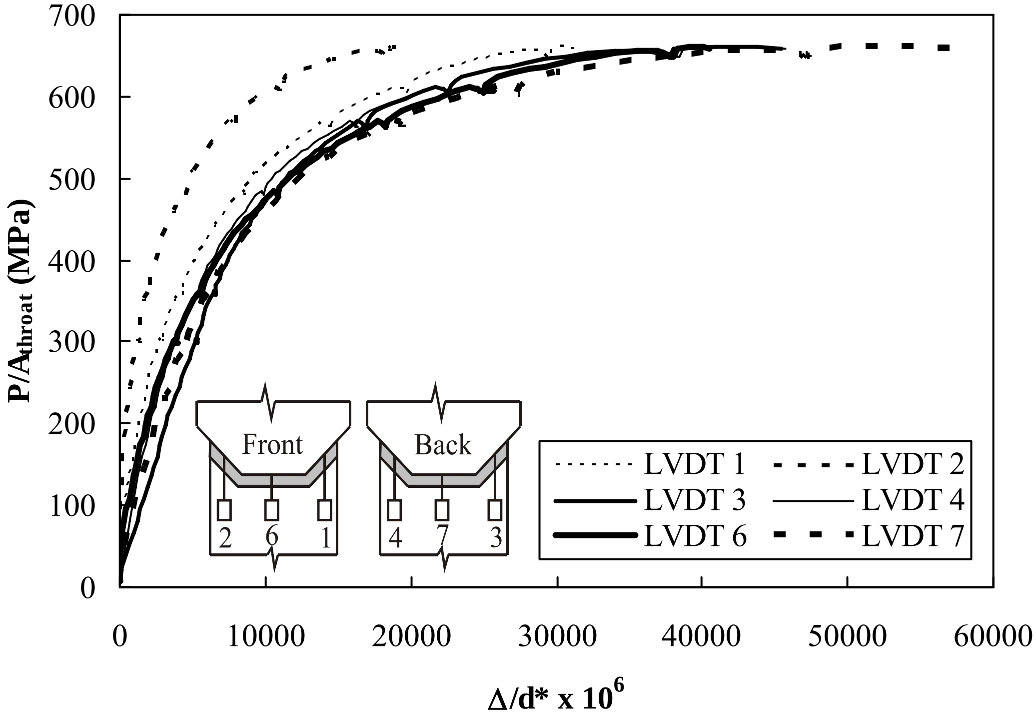

Figure D6 – Specimen TFa-1 Response

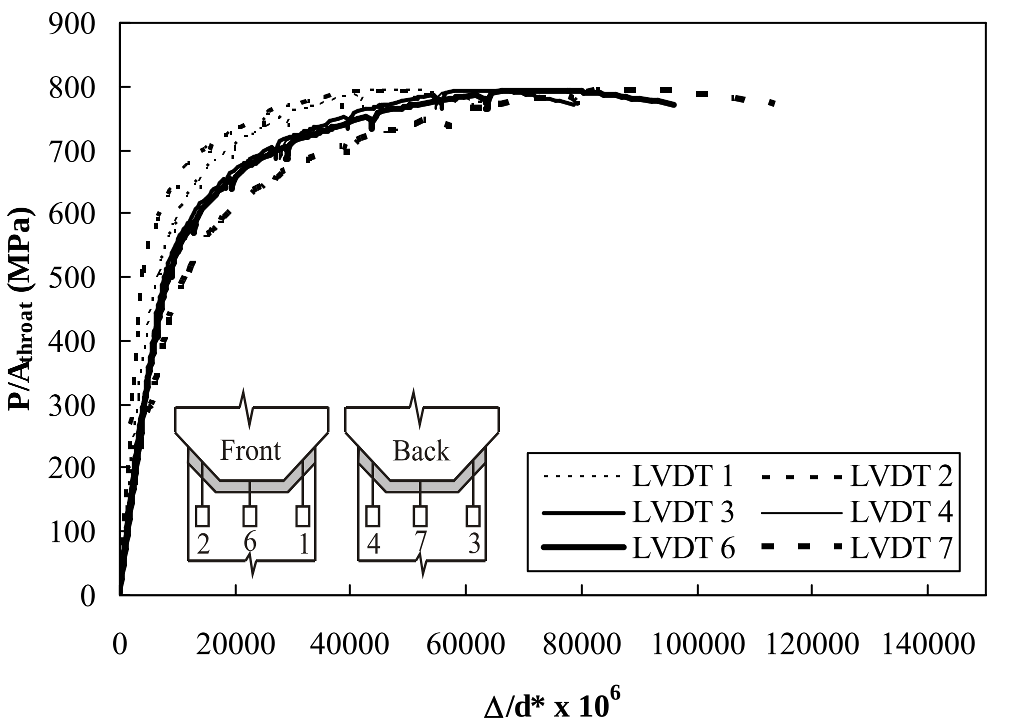

Figure D7 – Specimen TFa-2 Response

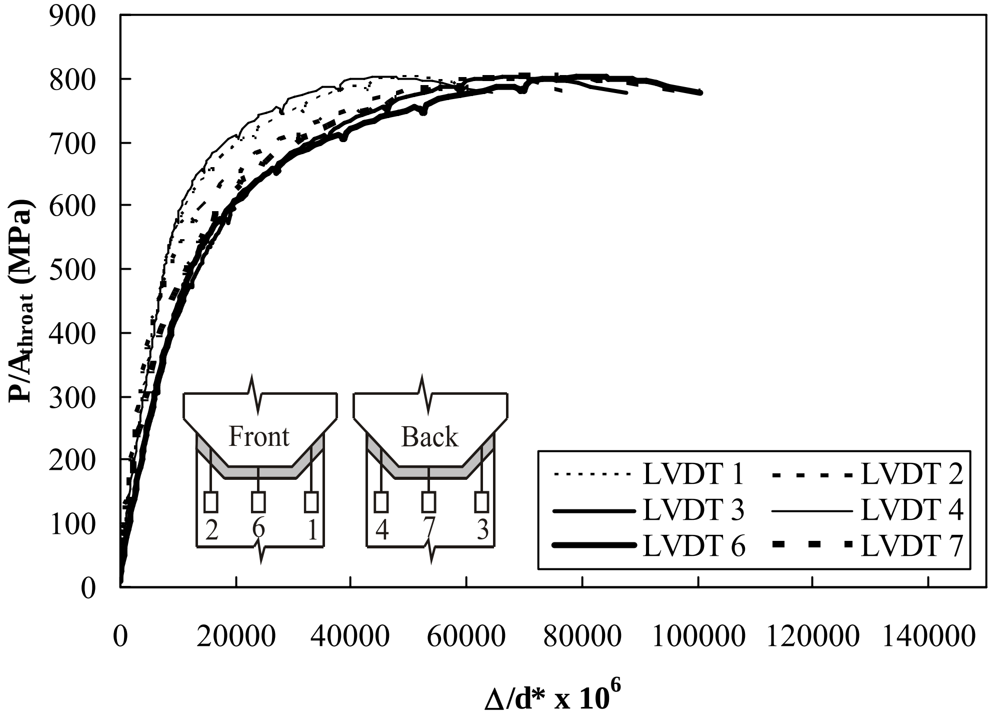

Figure D8 – Specimen TFa-3 Response

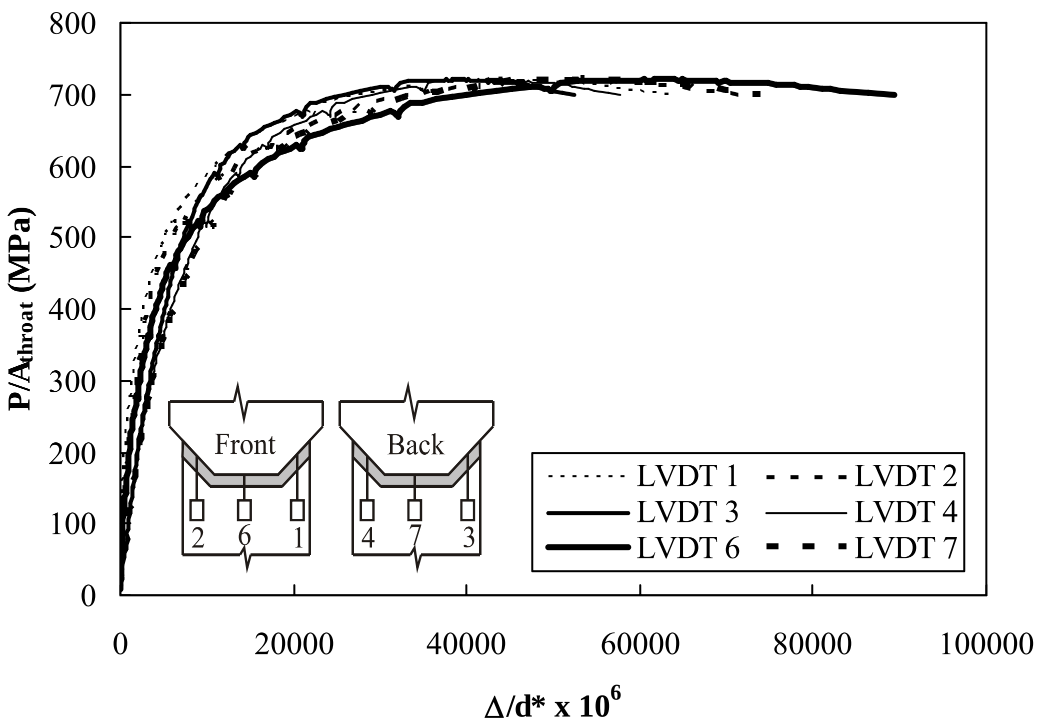

Figure D9 – Specimen TFa-4 Response

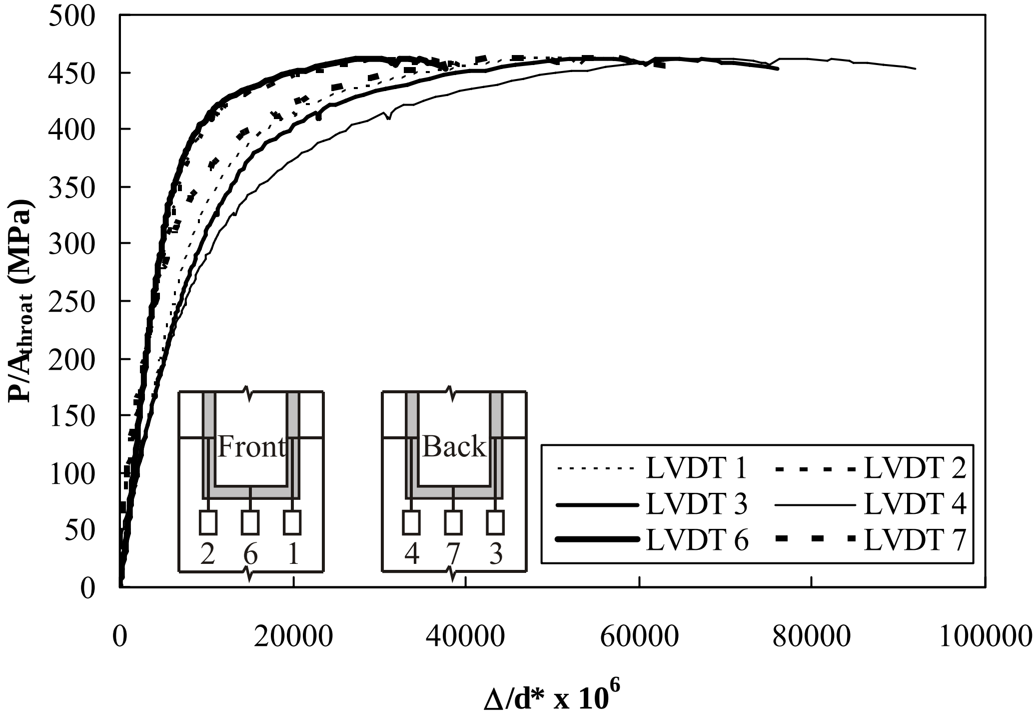

Figure D10 – Specimen TL50-1 Response

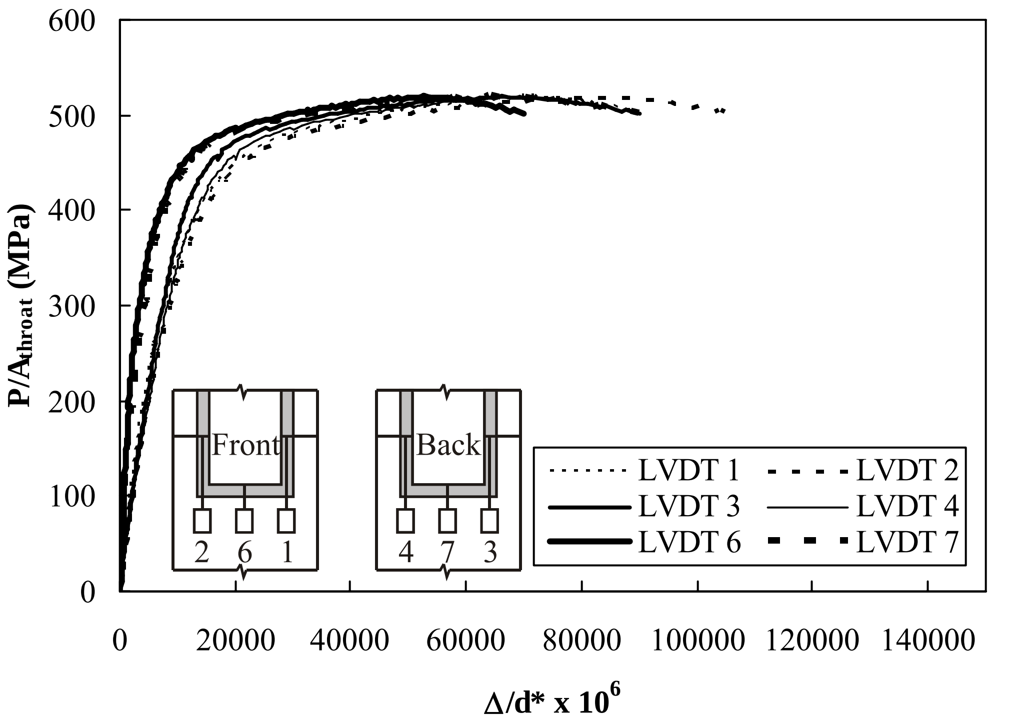

Figure D11 – Specimen TL50-2 Response

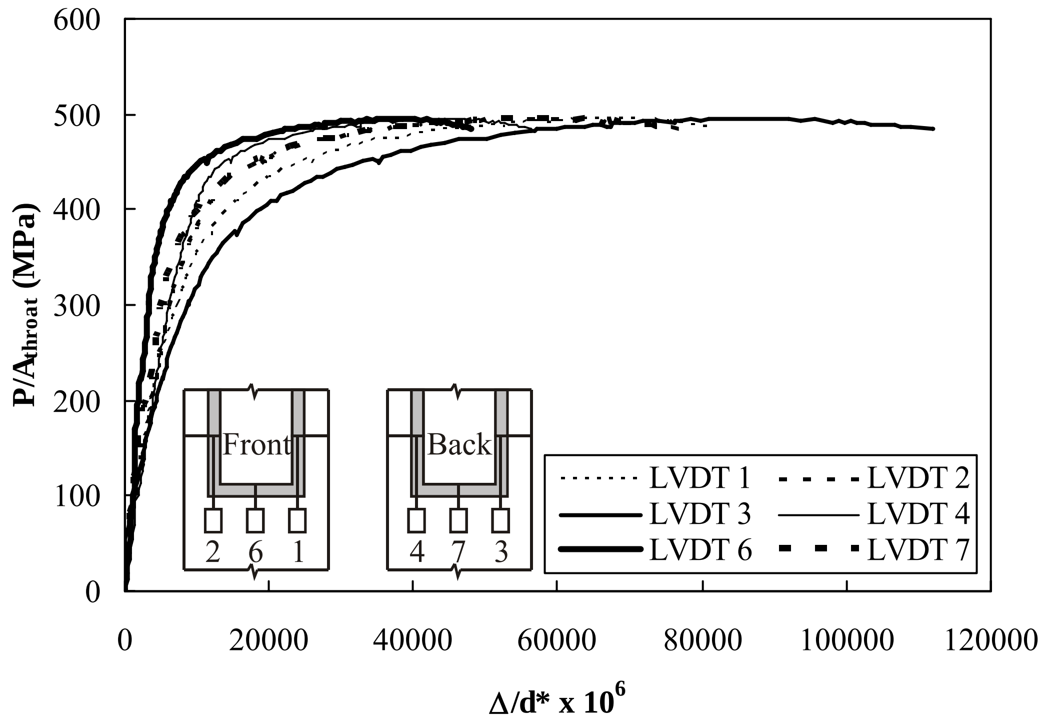

Figure D12 – Specimen TL50-3 Response

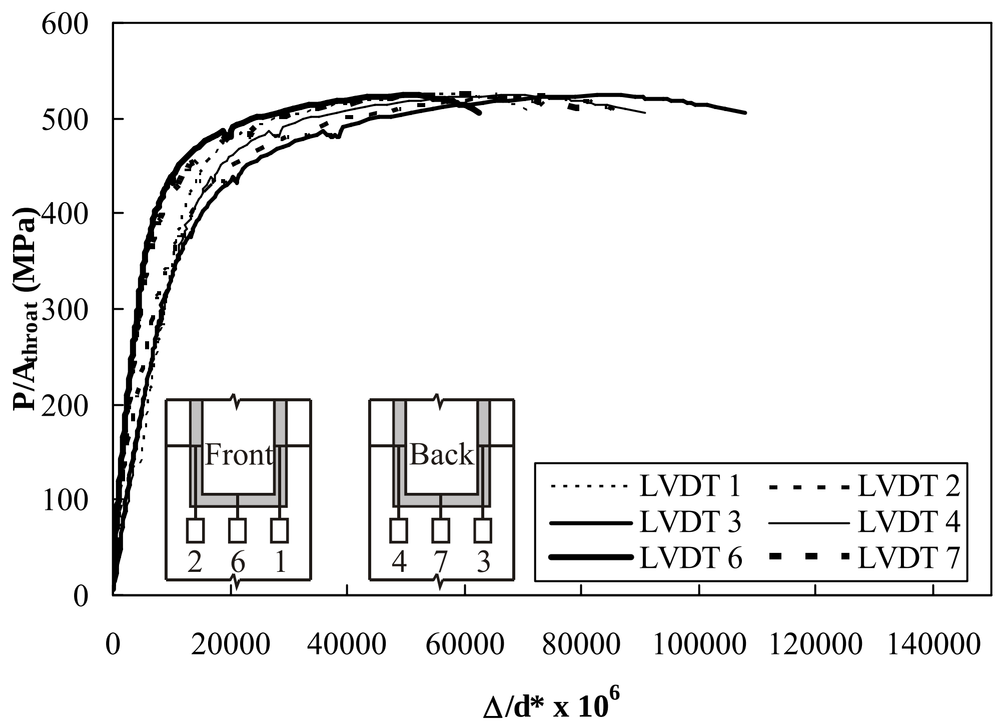

Figure D13 – Specimen TL50-4 Response

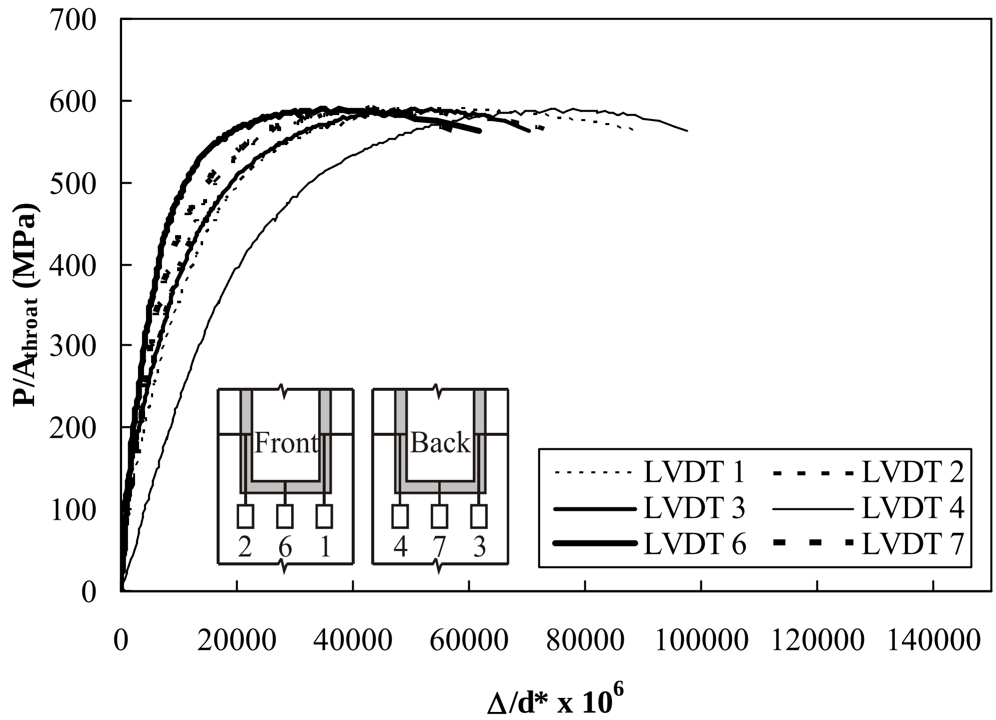

Figure D14 – Specimen TL50a-1 Response

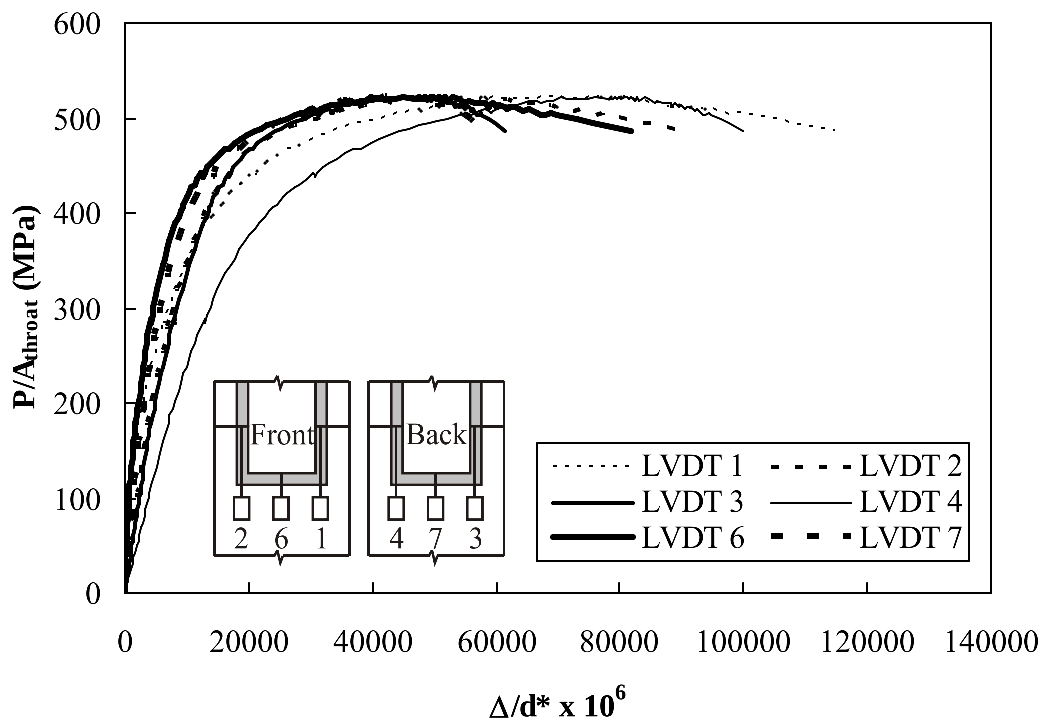

Figure D15 – Specimen TL50a-2 Response

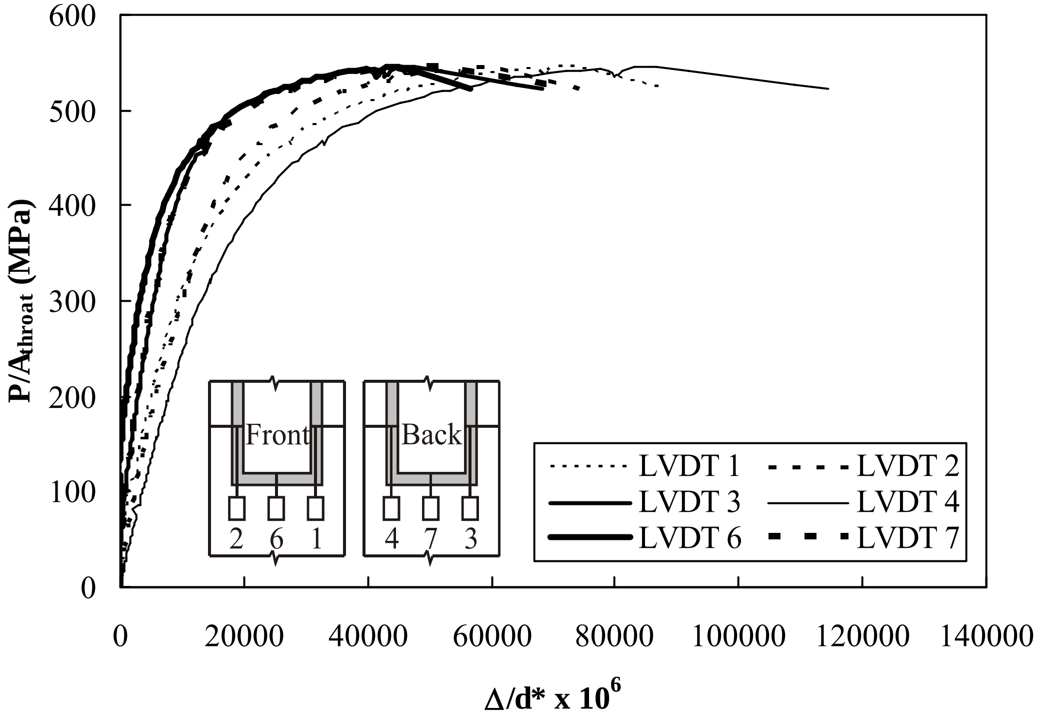

Figure D16 – Specimen TL50a-3 Response

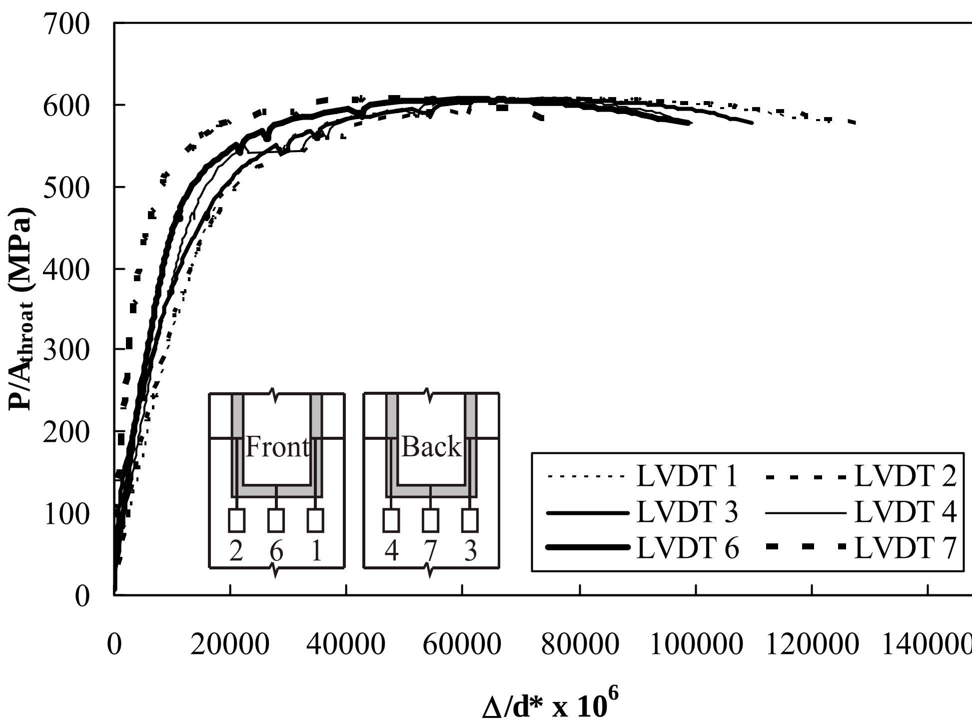

Figure D17 – Specimen TL50a-4 Response

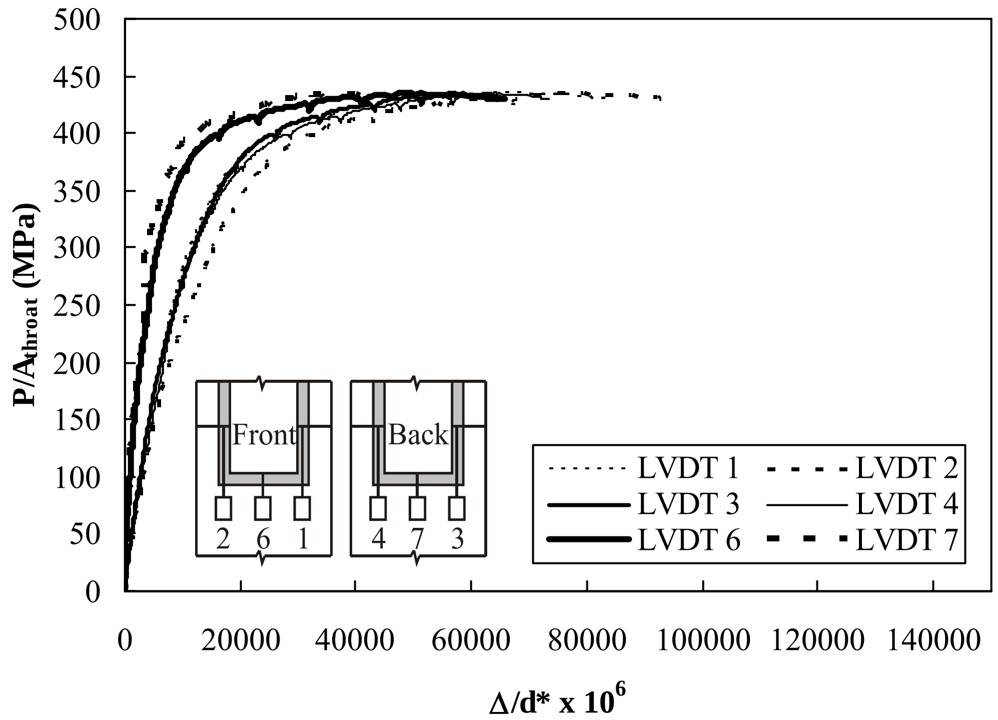

Figure D18 – Specimen TL100-1 Response

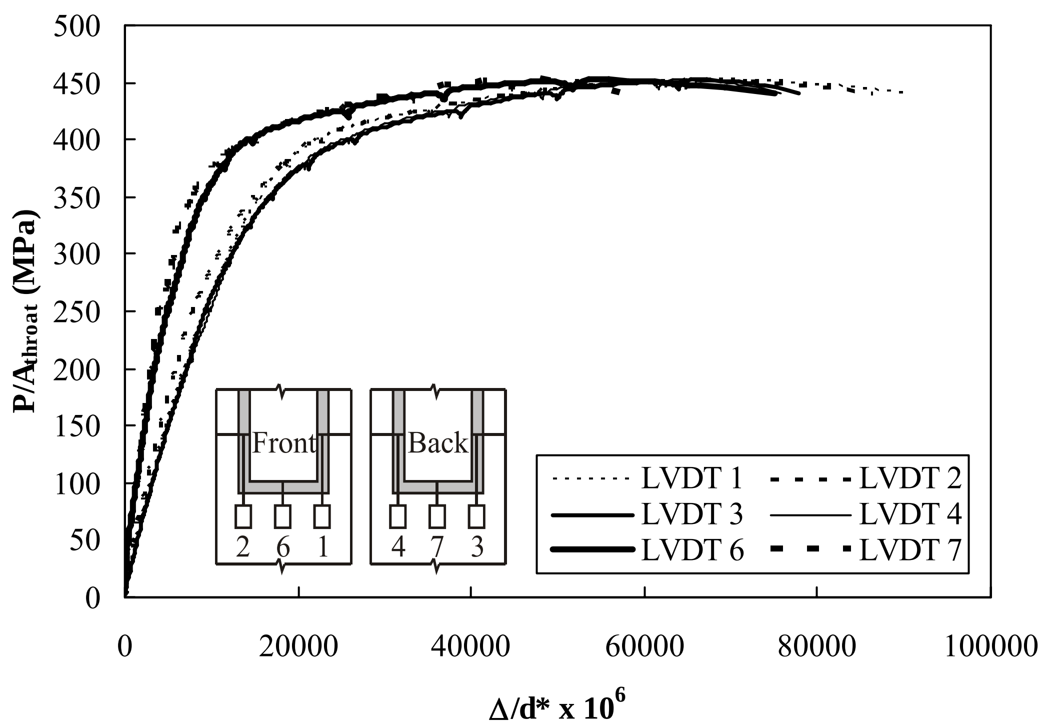

Figure D19 – Specimen TL100-2 Response

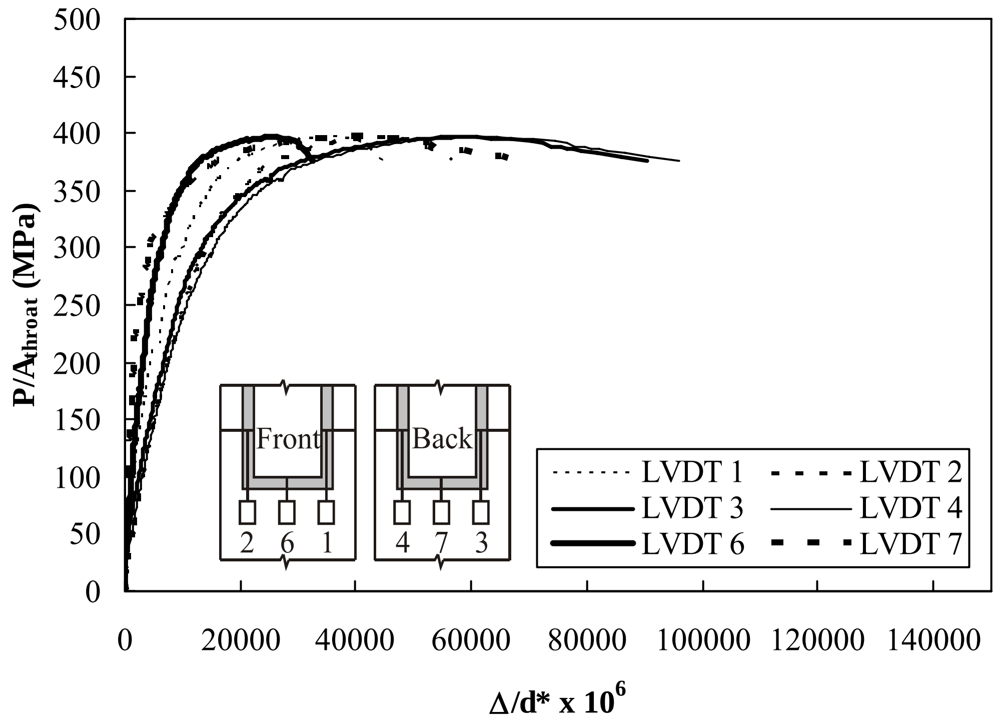

Figure D20 – Specimen TL100-3 Response

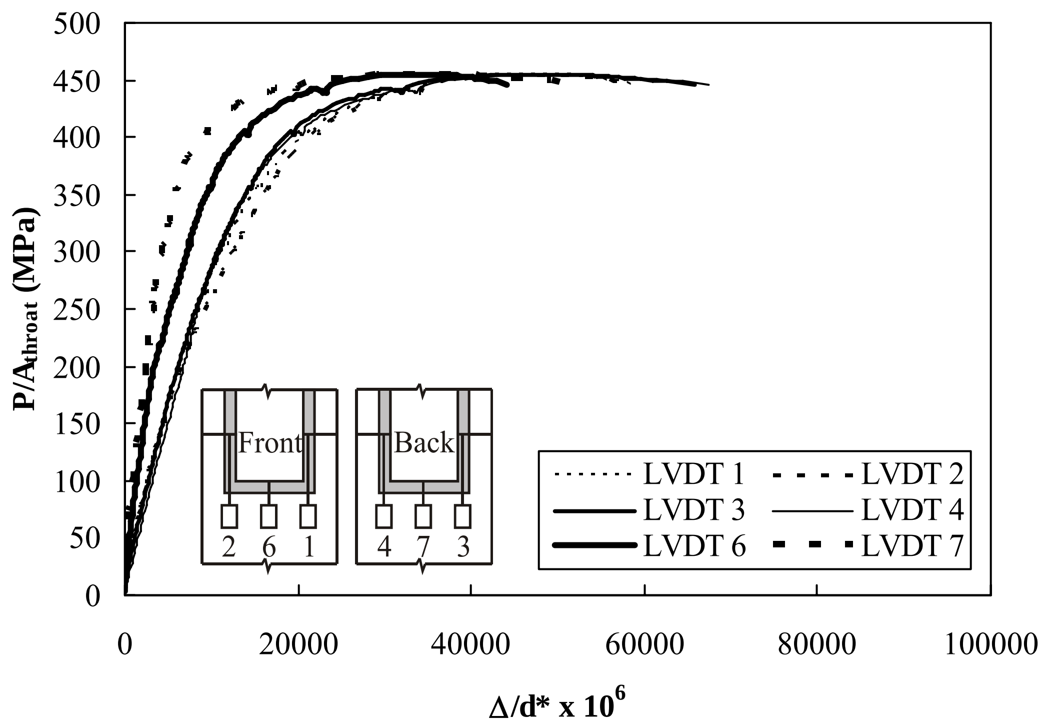

Figure D21 – Specimen TL100D-1 Response

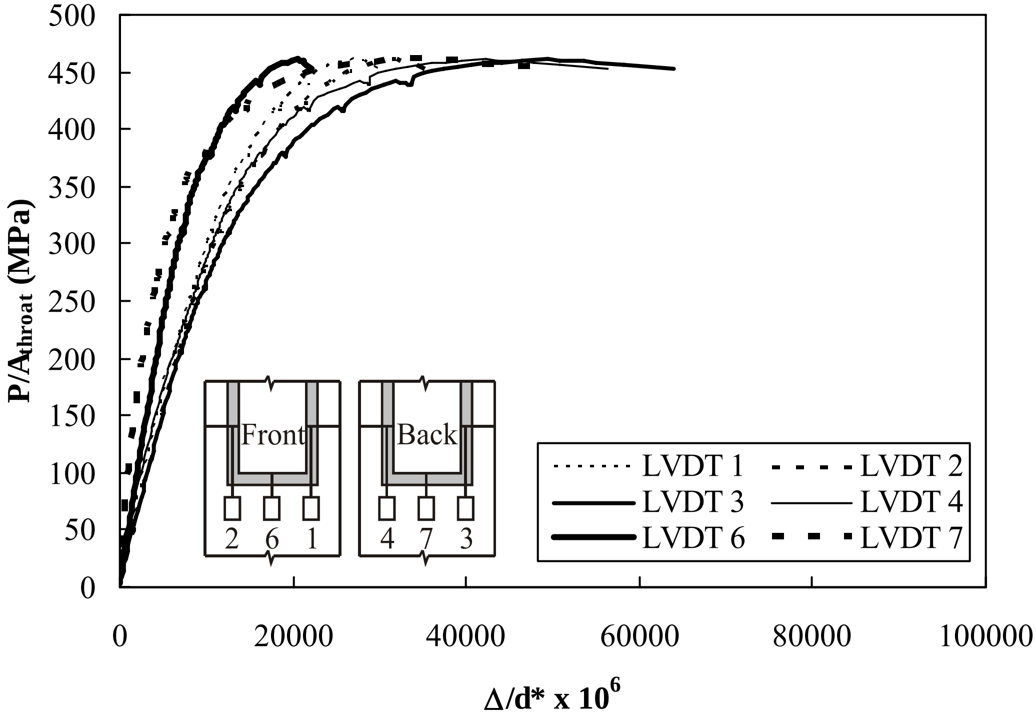

Figure D22 – Specimen TL100D-2 Response

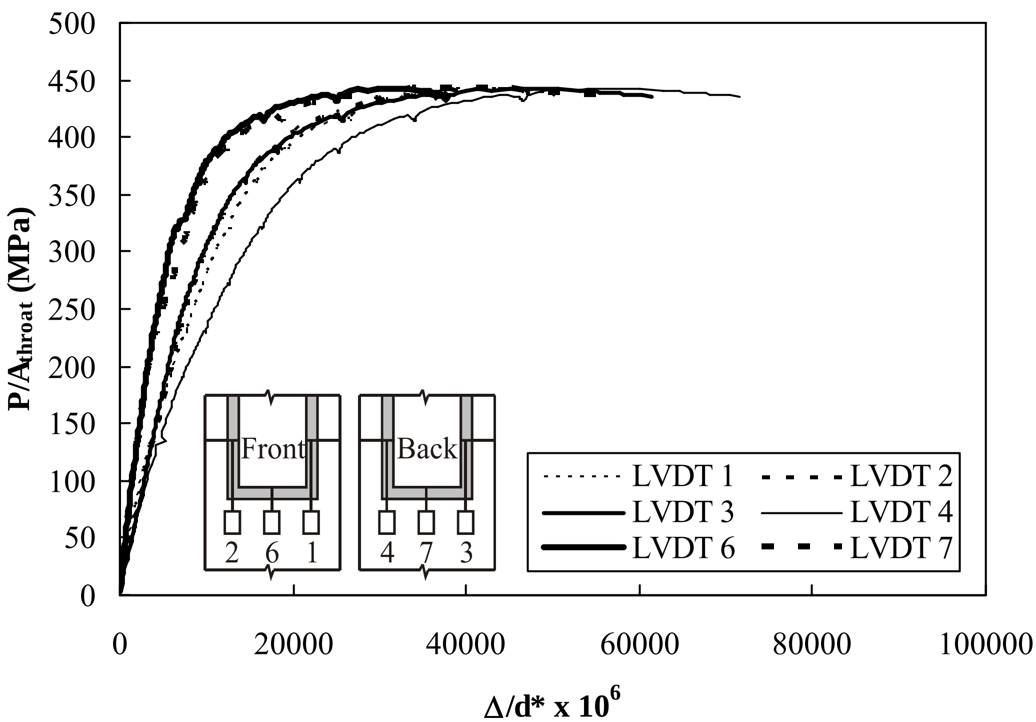

Figure D23 – Specimen TL100D-3 Response

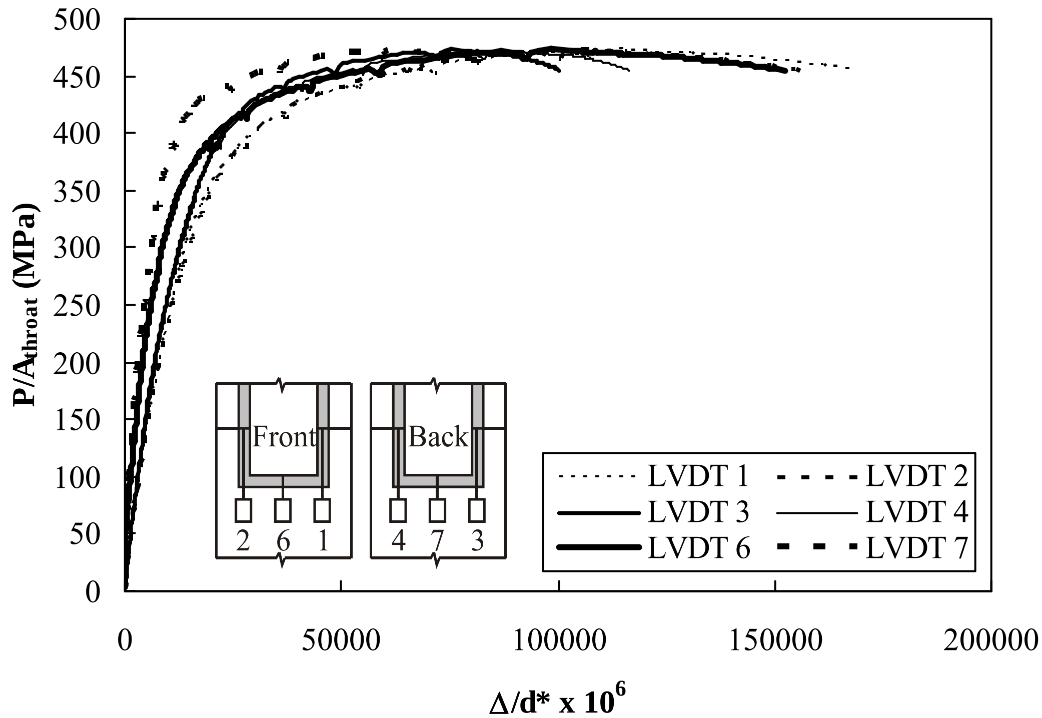

Figure D24 – Specimen TL100SP-1 Response

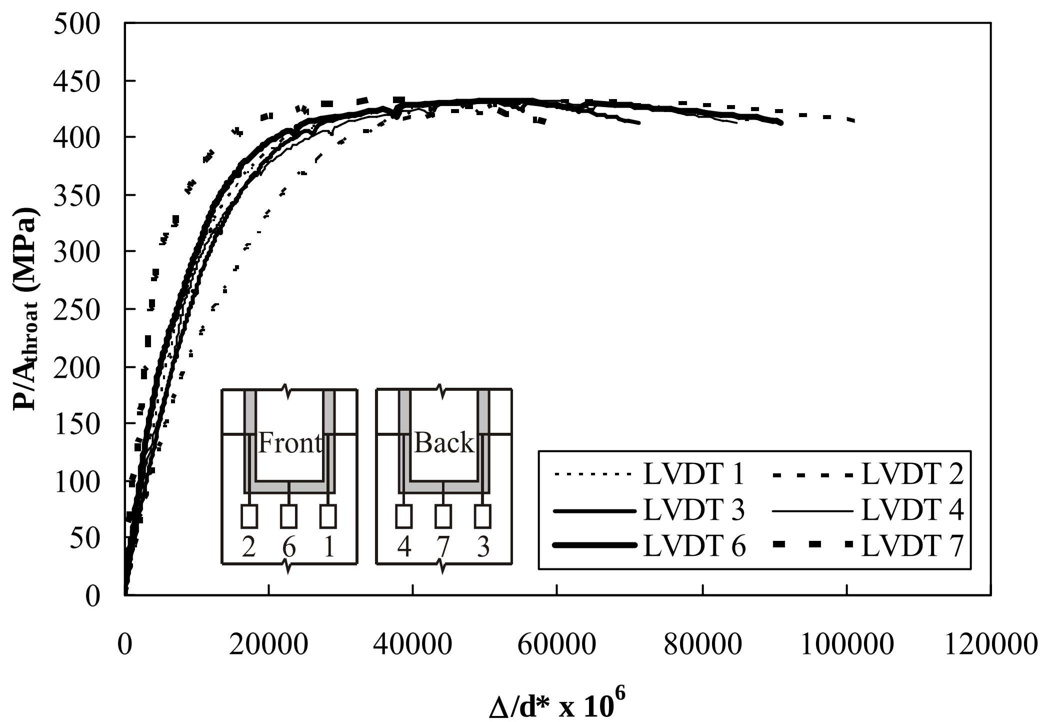

Figure D25 – Specimen TL100SP-2 Response

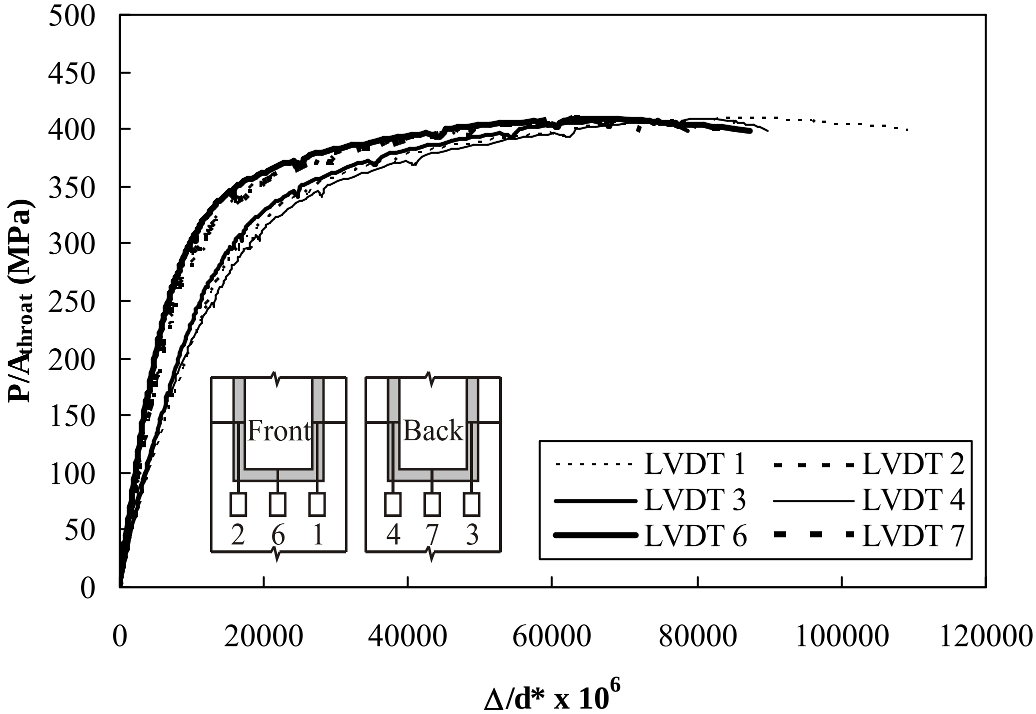

Figure D26 – Specimen TL100SP-3 Response

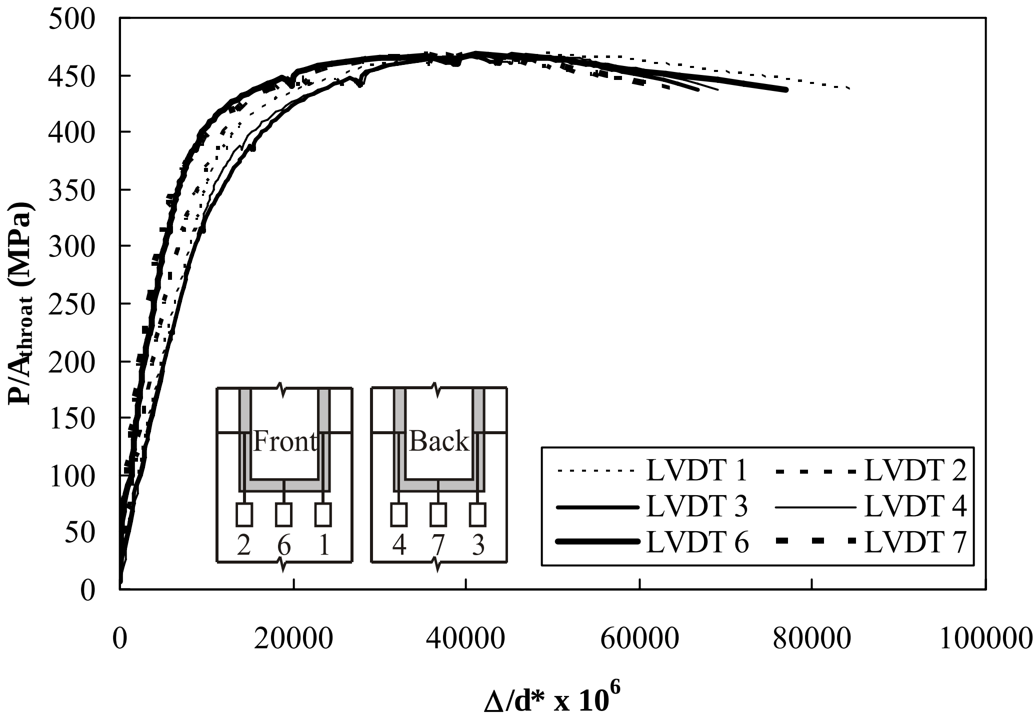

Figure D27 – Specimen TL50D-1 Response

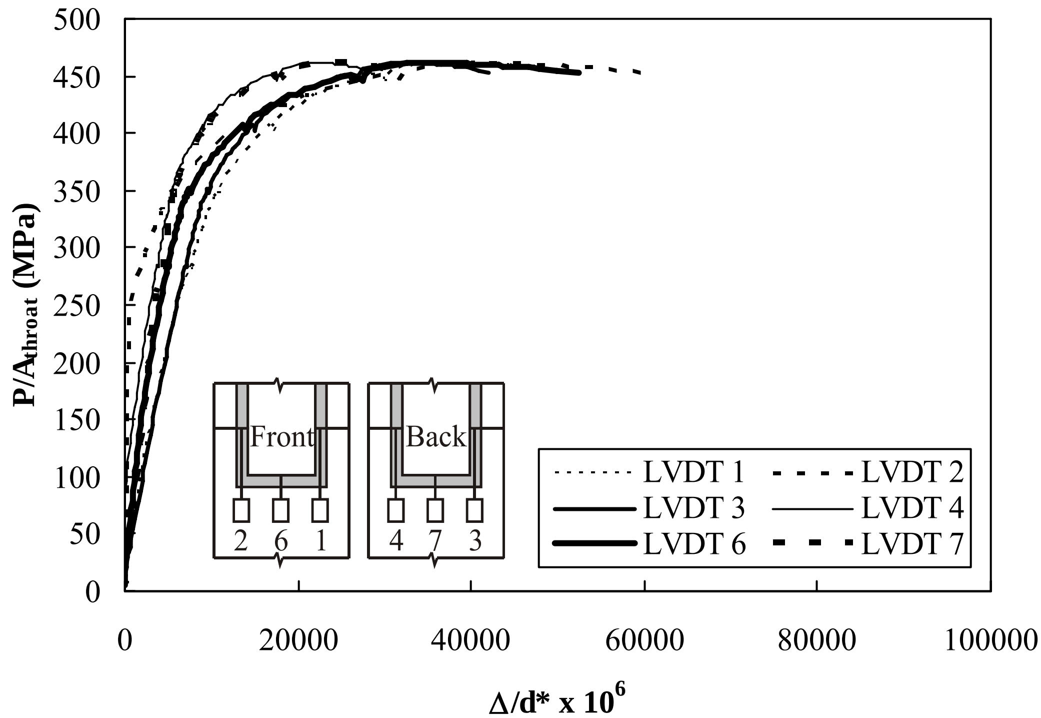

Figure D28 – Specimen TL50D-2 Response

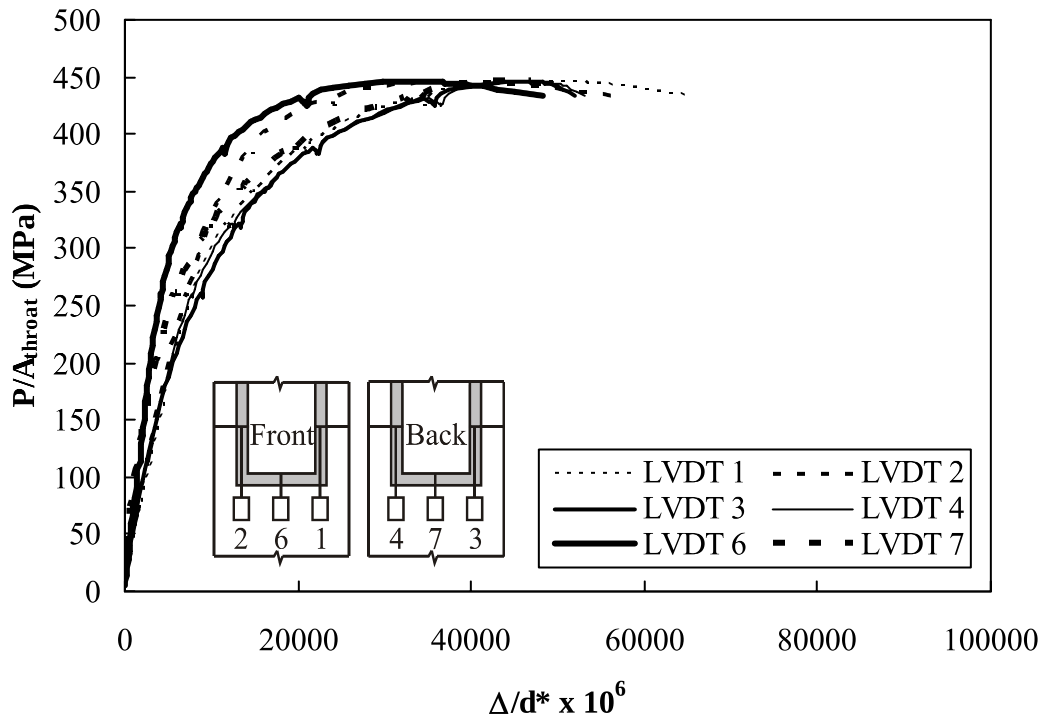

Figure D29 – Specimen TL50D-3 Response

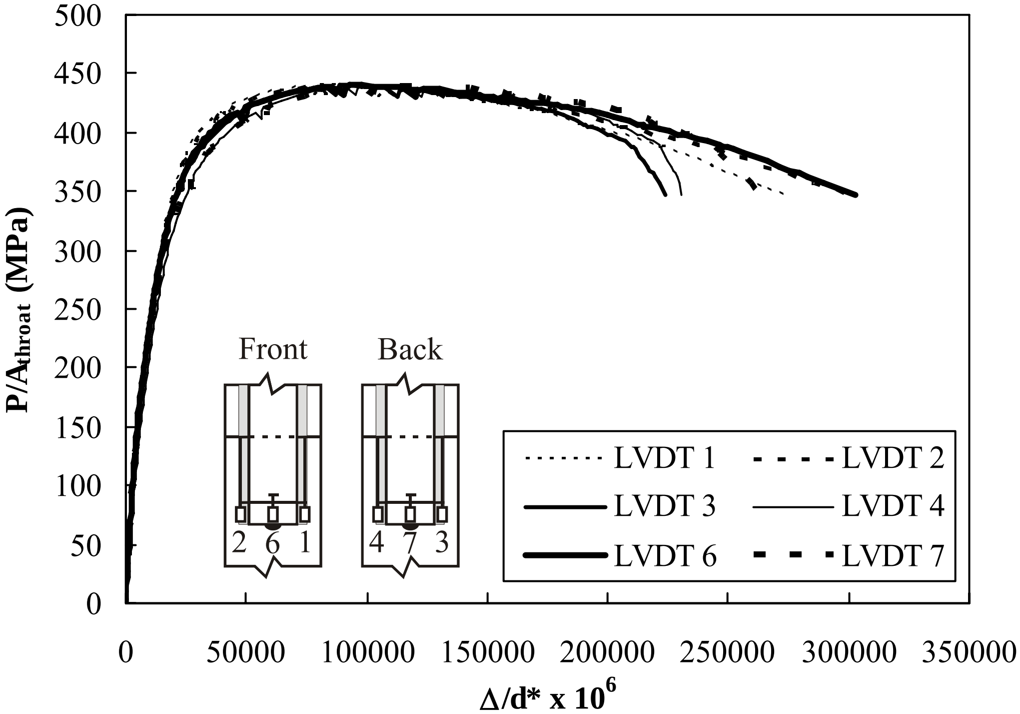

Figure D30 – Specimen L100-1 Response

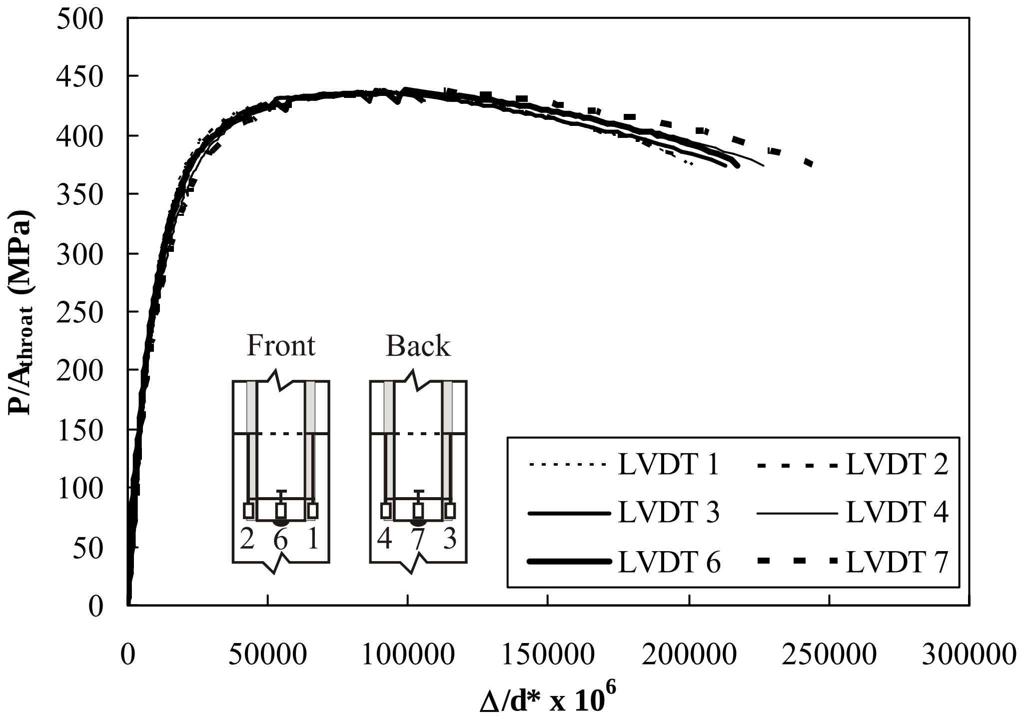

Figure D31 – Specimen L100-2 Response

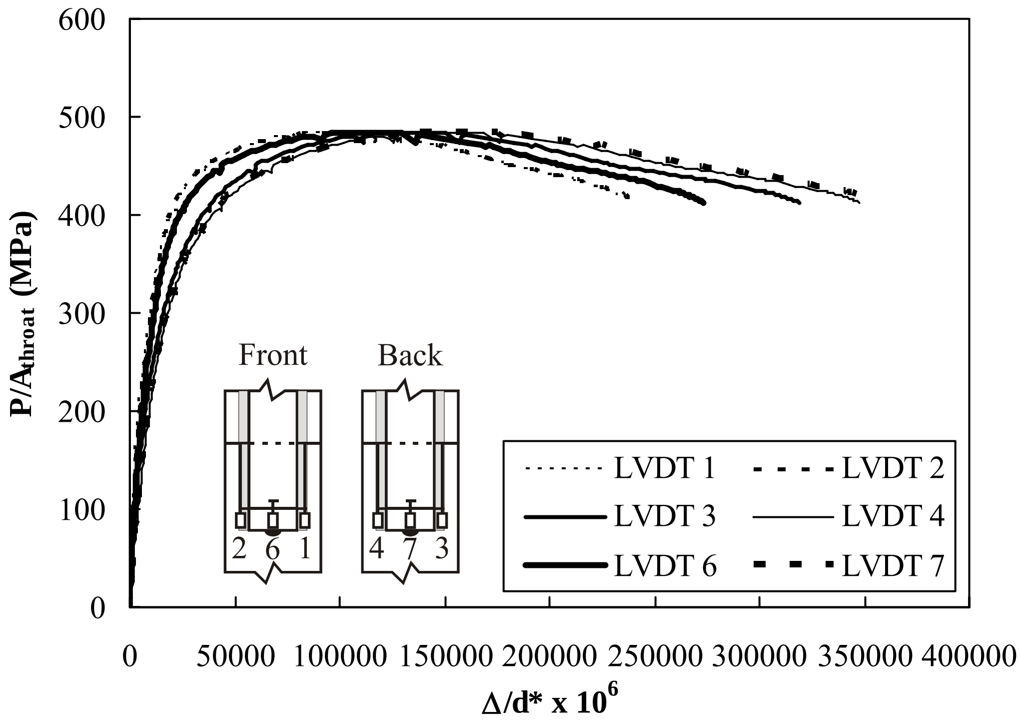

Figure D32 – Specimen L100-3 Response

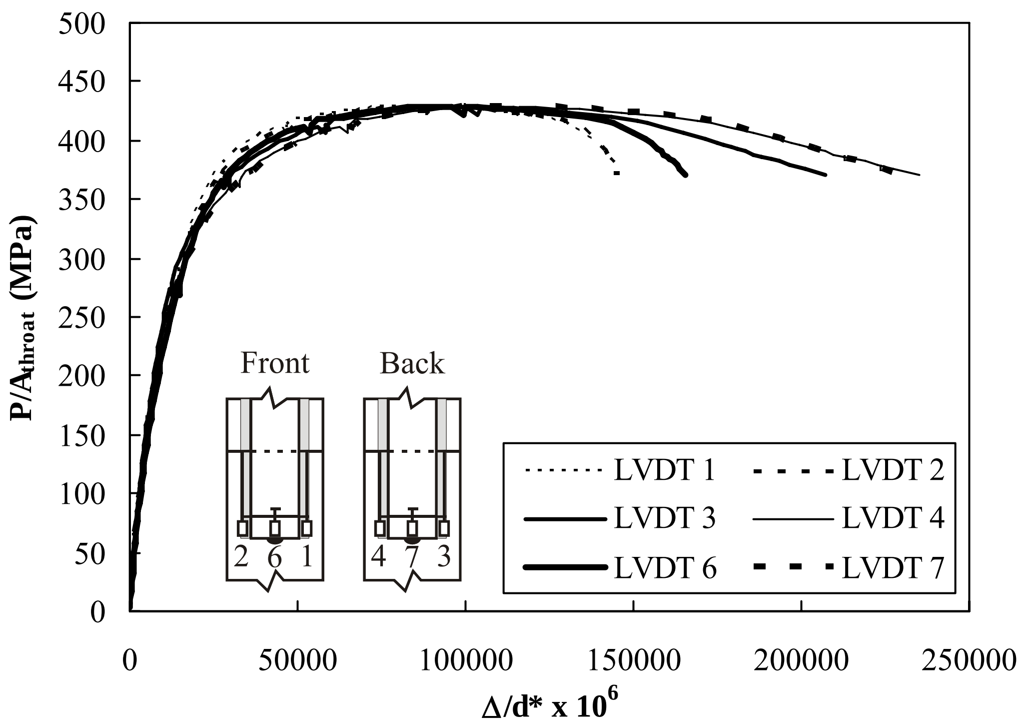

Figure D33 – Specimen L100-4 Response

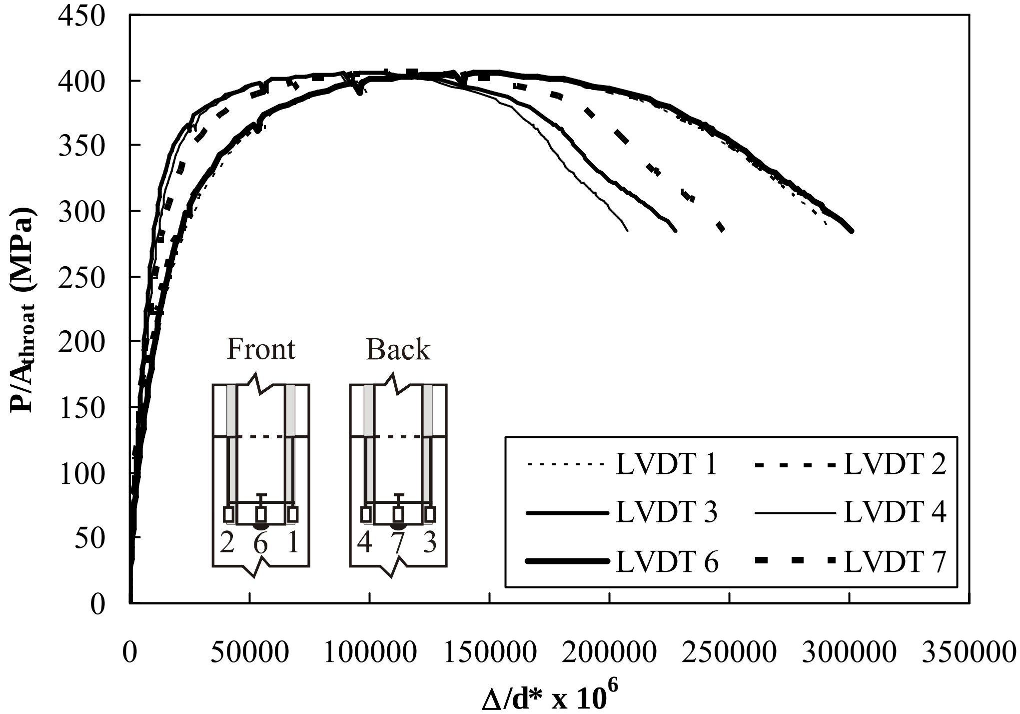

Figure D34 – Specimen L100-5 Response

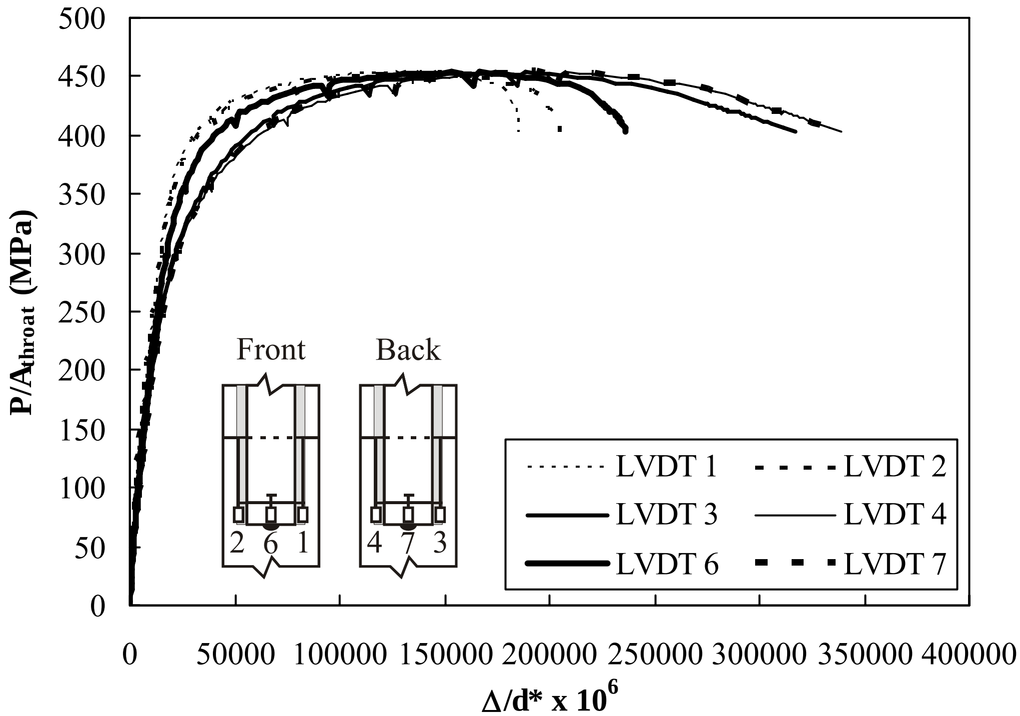

Figure D35 – Specimen L100-6 Response

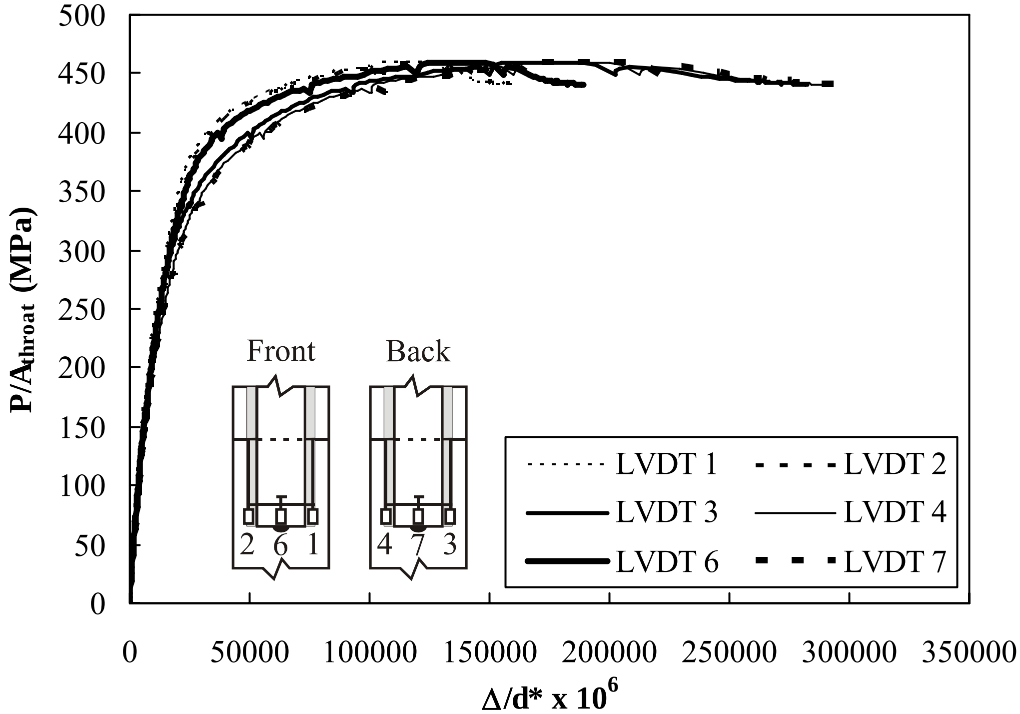

Figure D36 – Specimen L150-4 Response

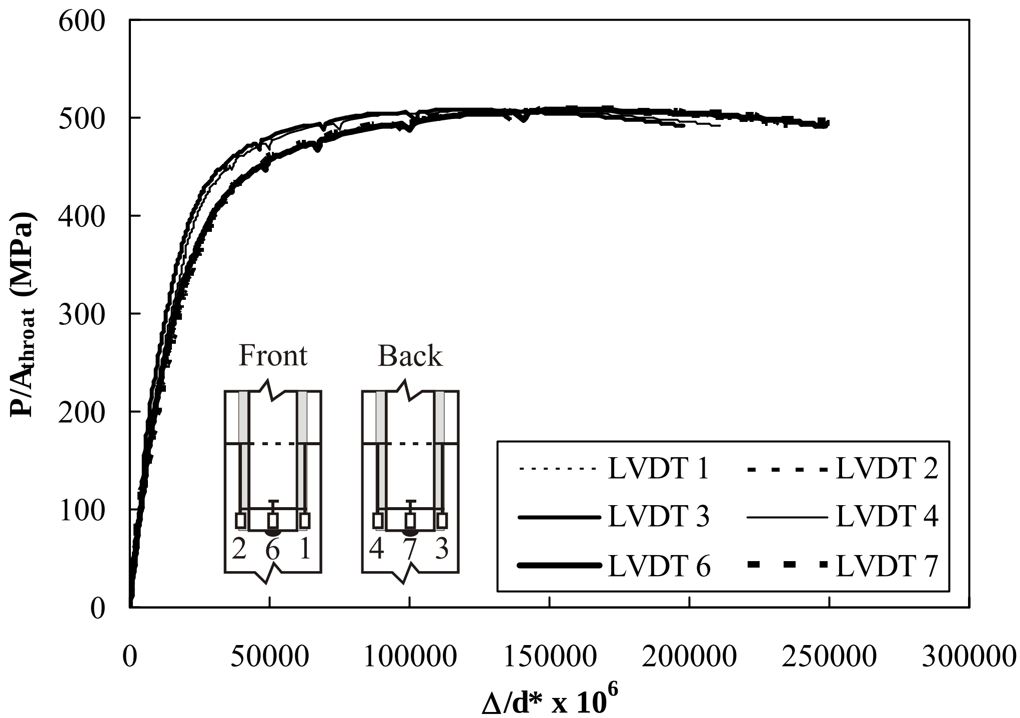

Figure D37 – Specimen L150-5 Response

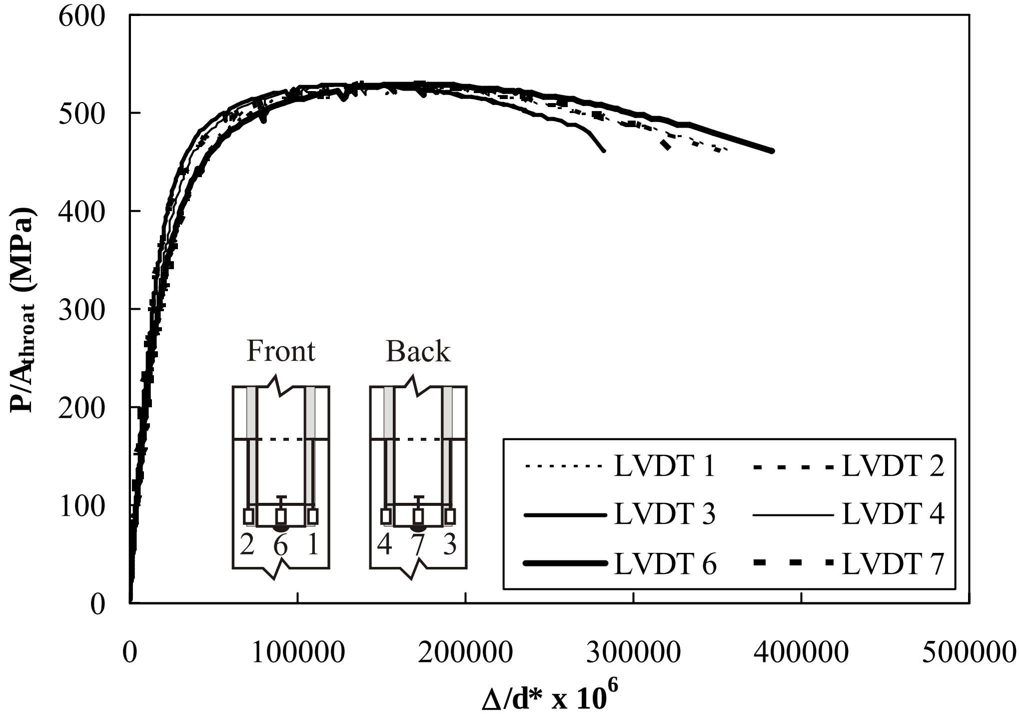

Figure D38 – Specimen L150-6 Response

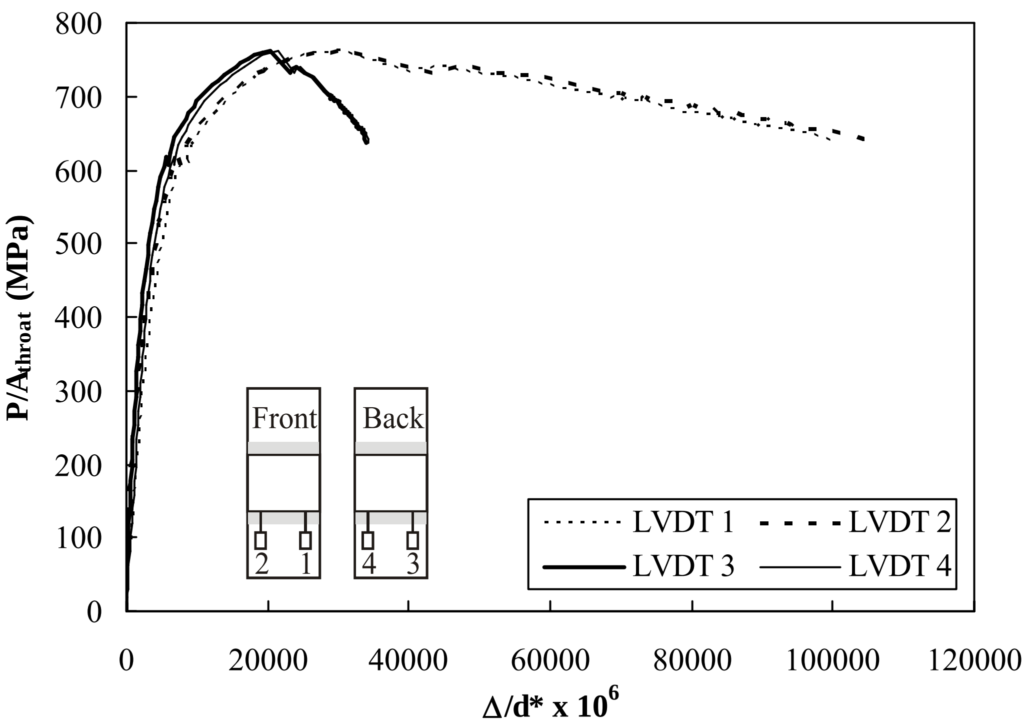

Figure D39 – Specimen TNY-1 Response

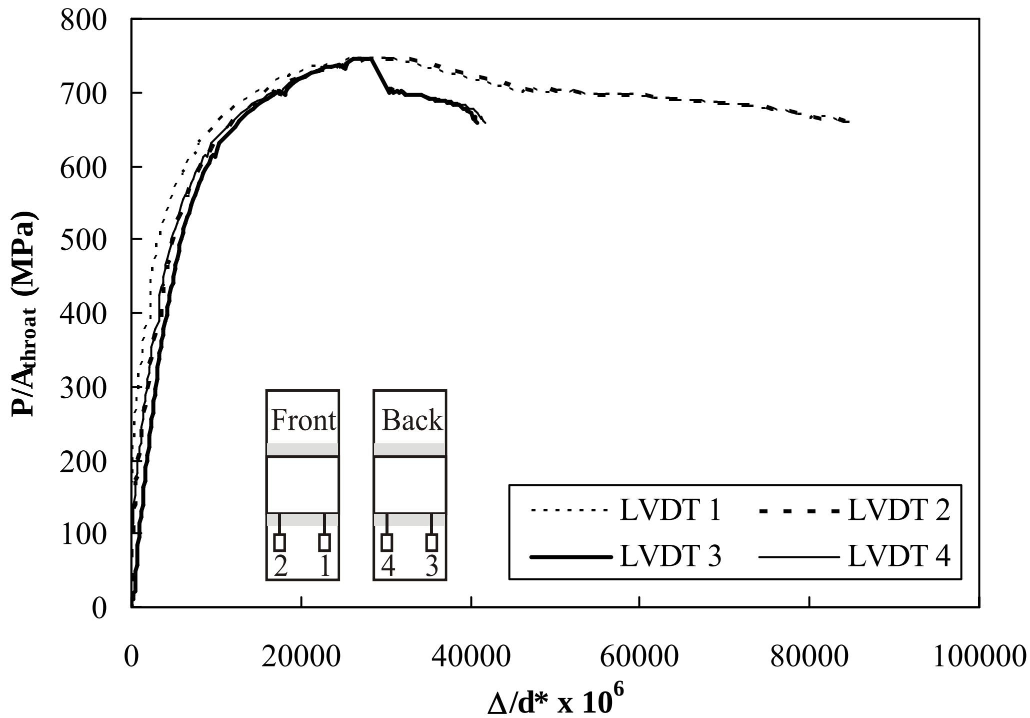

Figure D40 – Specimen TNY-2 Response

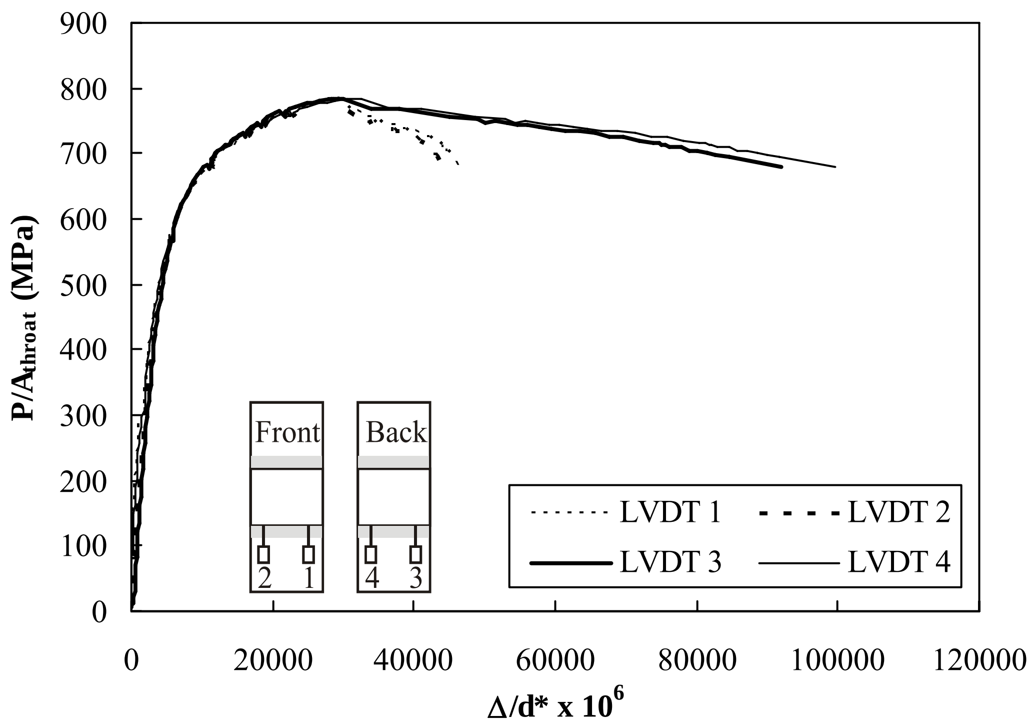

Figure D41 – Specimen TNY-3 Response

APPENDIX E

Low Temperature Tests

Appendix E – Low Temperature Tests

E.1 Introduction

In order to investigate the effect of low temperature on the response of multi-orientation fillet weld (MOFW) connections, three TL100 specimens were tested at -50°C. For the description of the TL100 specimens see Chapter 3 and Table 3.1. The specimens tested at low temperature are designated as TL100LT, but they were fabricated in the same way as the TL100 specimens.

Because low temperature is known to affect the ductility of fillet welds it was believed that MOFW connections would be affected by low temperature since their strength is already limited by ductility incompatibility. Tests by Ng *et al.* (2004a) confirmed that the ductility of transverse fillet welds was significantly reduced when the welds were subjected to low temperature. Three transverse fillet weld connections were tested by Ng *et al.* (2004a) at -50°C. These three connections had a mean ductility that was only 58% of the mean ductility of equivalent tests conducted at room temperature. Such a large decrease in ductility means that both the strength and the ductility of a MOFW connection could be significantly affected by low temperature.

The strength of a connection containing both transverse and longitudinal weld segments has been shown to be affected by a ductility incompatibility between the transverse and longitudinal weld. The effect of low temperature is to decrease the ductility of both segments, but the decrease in the transverse segment could be more critical. A decrease in ductility of the transverse segment would decrease the amount of ductility available to the longitudinal segment for developing its capacity. If this is the case, then testing the specimens at -50°C would amplify the ductility incompatibility effect that has been observed on tests at room temperature. Of course this assumes that only the ductility of the longitudinal fillet welds will be affected by low temperature, not the stiffness as well. If the stiffness is affected by low temperature then it would be difficult to tell whether or not temperature has an effect on ductility incompatibility as the proportion of the segment capacity that is developed varies with changes in stiffness.

Because the ductility incompatibility effect was expected to be accentuated under low temperatures, three MOFW connections were tested at -50°C. Unfortunately, the specimens did not fail in the expected manner. All three specimens failed in the lap plates (see Figures E1, E5, and E6). The failure is believed to be the result of a stress concentration and the low toughness of the lap plates as will be discussed later.

E.2 Testing Procedure

The low temperature test specimens were fabricated and measured in the same way as the TL MOFW specimens described in Chapter 3. The specimens were also tested in a similar manner to the TL specimens with the difference that they were tested at low temperature.

Once the specimens were measured, they were installed in the testing machine, as described in Chapter 3. The specimens were then instrumented with linear variable differential transformers (LVDTs) in an identical manner to the other TL specimens tested at room temperature. Two thermisters were then mounted to the lap plate of the specimen as shown in Figure E1(b). The thermisters were used to monitor the temperature of the test specimen throughout the tests.

A custom built cold temperature chamber was then fitted around the specimen. The chamber was built with rigid styrofoam insulation as shown in Figure E1(a). Dry ice was placed around the specimen (see Figure E1(c)) and fans were used to circulate air within the chamber and through the dry ice. This cooled the temperature to -50°C, where it was maintained within ±5°C for the entire test by turning the fans on or off.

Once the temperature was at -50°C, the test began. As with the rest of the test specimens, a concentric load was applied with a 6000 kN testing machine. The test continued until the lap plates fractured.

E.3 Test Results

The ultimate capacities of the three low temperature MOFW specimens are reported in Table E2. The procedure for normalizing the reported capacities, P_m/A_{throat} is identical to the procedure used in Chapter 4. The measured deformation of each weld for the measured values of P/A_{throat} is shown in Figures E2, E3, and E4.

E.4 Discussion

The fracture of the lap plates is believed to be caused by three factors. The first factor is the occurrence of a notch in the lap plate at the root of the fillet weld. The notch was created when the fillet welds were cut to separate the test portion from the reinforced portion of the fillet weld specimen (see Chapter 3). The notch provides a stress concentration at the root of the weld, which in turn provides a potential crack initiation point. The second factor that promoted the propagation of the crack through the lap plate is the existence of a shear lag effect. Because of the large thickness of the lap plates, the stress in the lap plates decreases significantly with increasing distance from the weld root, thus causing a stress concentration in the lap plates near the fillet welds, which is further amplified by the notch. The last factor which influences the fracture of the lap plate is the plate material itself. The plate material is classified as CAN/CSA-G40.21 350W, which does not have any notch toughness requirements at low temperature. A more suitable grade of plate for low temperature tests would be CAN/CSA-G40.21 350WT steel, which does have a low temperature notch toughness requirement. However, this plate was not chosen because of the potential mixing of weld and base metal during fabrication.

In an effort to prevent fracture of the lap plates, the notch was smoothed using small grinding and machining tools. An example of the smoothed notch is shown in Figure E7.

Though both specimens TL100LT-2 and TL100LT-3 had notches that were smoothed by grinding, this did not stop the lap plates from fracturing.

It should be noted that the low temperature specimens reached an average P_m/A_{throat} value that was 99% of the average P_m/A_{throat} reported for the TL100 specimens tested at room temperature (see Table 4.2). This is an indication that the ductility incompatibility effect was not amplified by low temperature. However, the fracture of the main plates would most likely cause the behaviour of the low temperature specimens to differ from the TL100 specimens. Thus, this data is not included in the reliability analysis.

Table E1 – Mean Measured Fillet Weld Leg Sizes of the Low Temperature Specimens

Specimen	Segment*	Front			Back		
		MPL Leg Size (mm)	LPL Leg Size (mm)	Segment Length (mm)	MPL Leg Size (mm)	LPL Leg Size (mm)	Segment Length (mm)
TL100LT-1	1	14.1	12.1	100.5	14.4	12.3	101.7
	2	17.2	11.6	77.9	18.1	12.0	76.9
	3	16.0	12.1	99.9	14.3	12.2	99.6
TL100LT-2	1	14.5	11.8	99.8	15.8	12.7	98.2
	2	16.4	12.2	77.2	18.5	13.9	76.0
	3	14.6	13.5	97.8	15.7	13.6	99.6
TL100LT-3	1	13.3	11.7	97.3	14.5	12.5	98.6
	2	14.9	12.2	77.2	17.5	12.2	78.8
	3	15.2	11.4	94.0	15.9	11.1	96.2

*See Figure 3.13

Table E2 – Low Temperature Specimen Capacities

Specimen	Ultimate Load (P_m) (kN)	Average Ultimate Load (kN)	Total Throat Area (A_{throat}) (mm^2)	P_m/A_{throat} (MPa)	Average P_m/A_{throat} (MPa)
TL100LT-1	2145	2195	5277	406	417
TL100LT-2	2300		5477	420	
TL100LT-3	2140		5038	425	

a) Cold Temperature Chamber

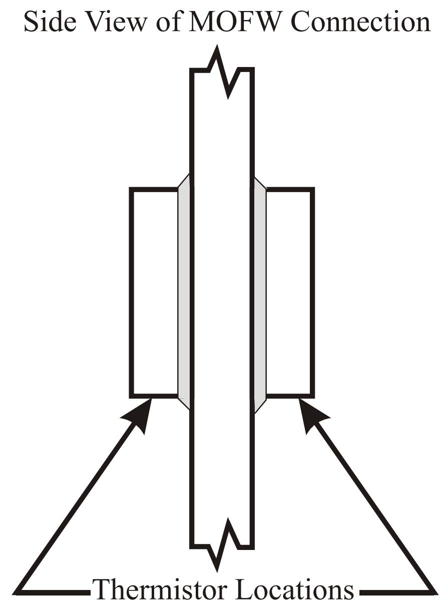

b) Instrumentation

c) Ice Surrounding Specimen

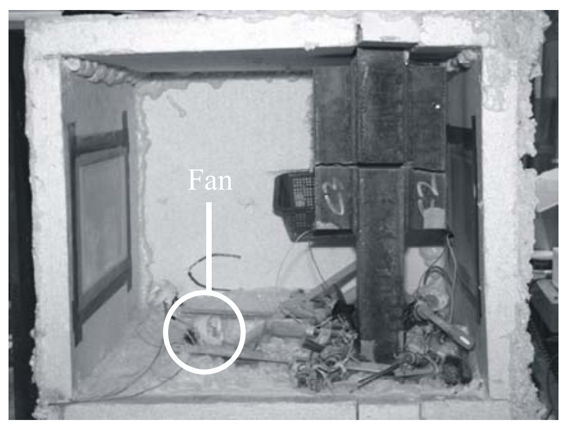

d) Fractured Specimen

Figure E1 – Low Temperature Test Setup

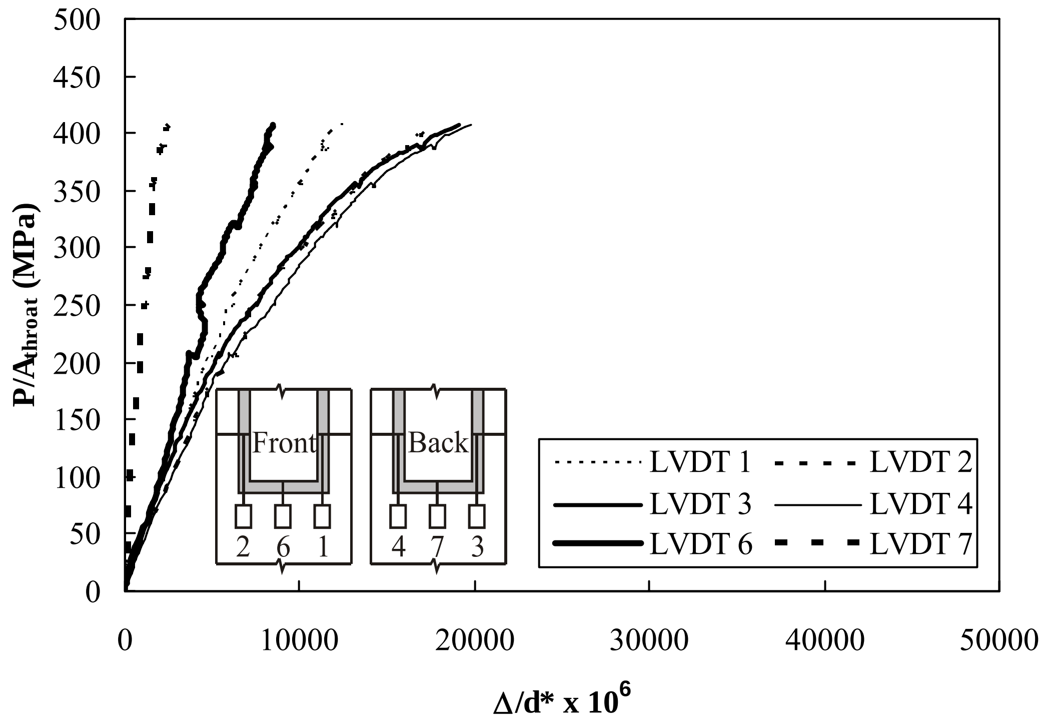

Figure E2 – Specimen TL100LT-1 Response

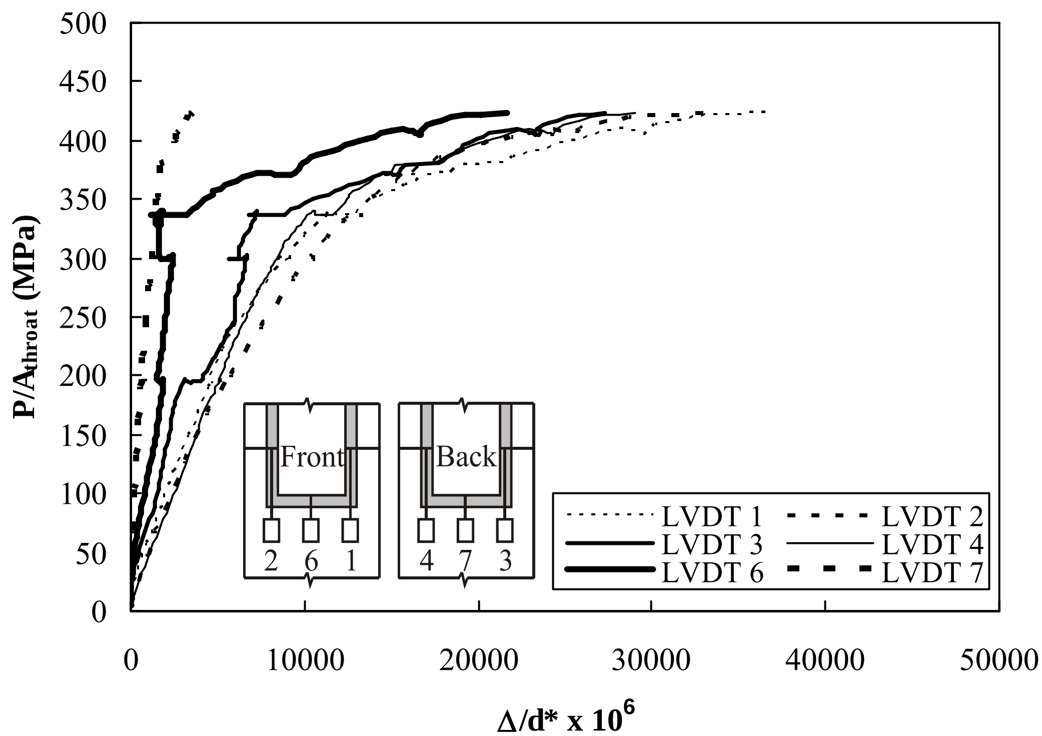

Figure E3 – Specimen TL100LT-2 Response

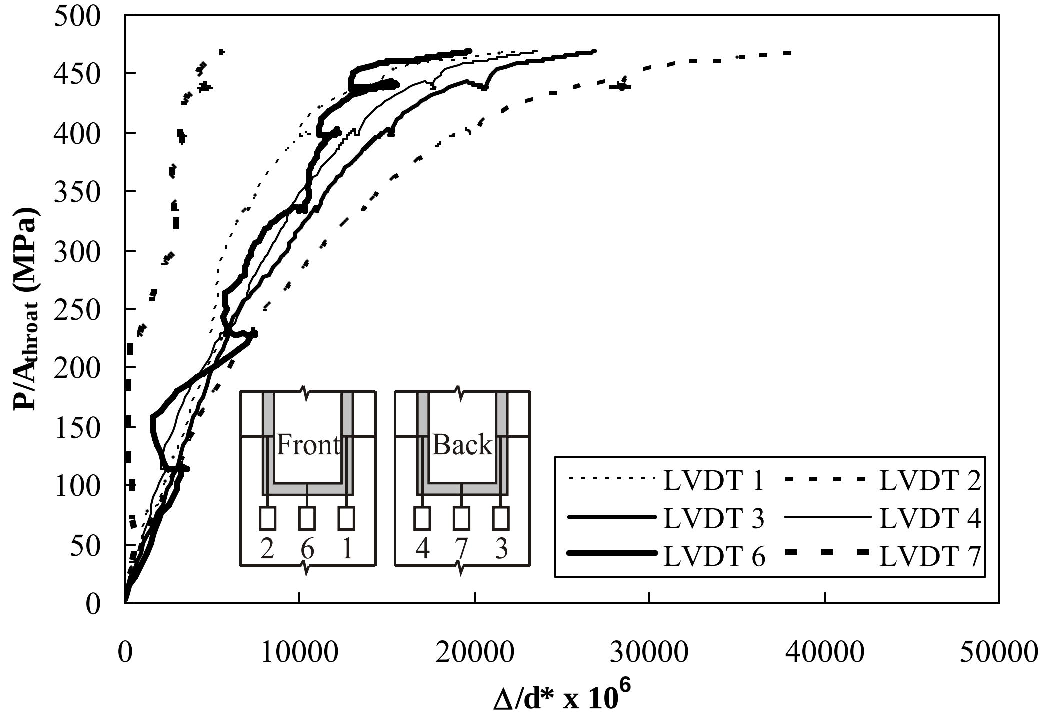

Figure E4 – Specimen TL100LT-3 Response

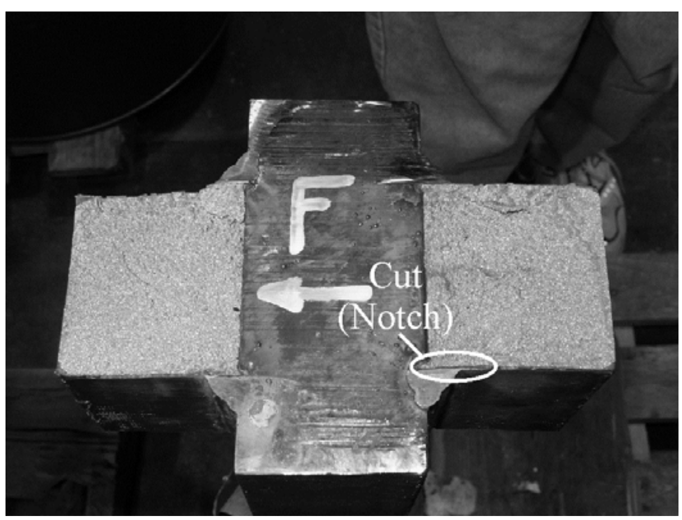

Figure E5 – Overview of Fracture Surface

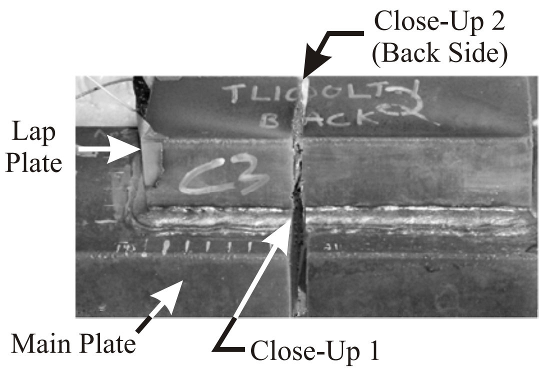

a) Fractured Specimen

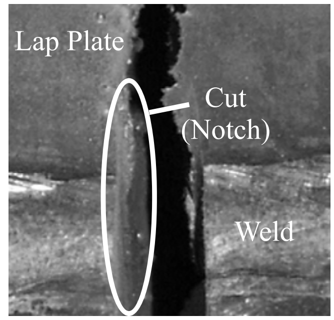

b) Close-Up 1

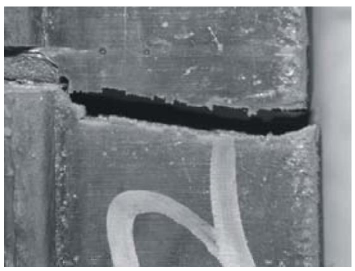

c) Close-Up 2

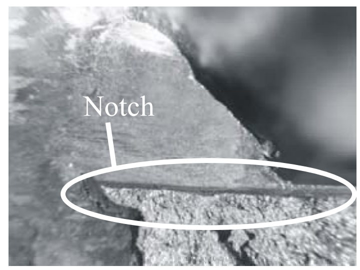

d) End View of Fillet Weld Showing Smooth Face from Cutting

Figure E6 – Origins of the Fracture

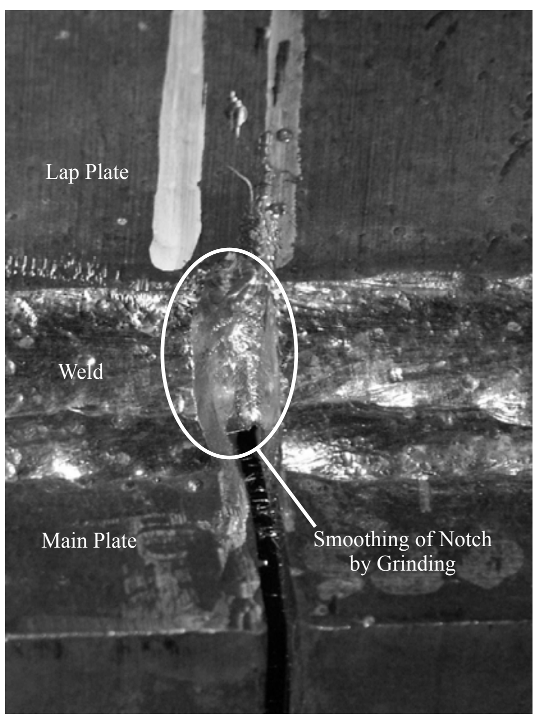

Figure E7 – Attempt at Mitigating the Effect of the Notch

APPENDIX F

Test Data From Other Research Programs

Test Data From Other Research Programs

This appendix presents a summary of the test data from Deng *et al.* (2003), Ng *et al.* (2002), and Miazga and Kennedy (1989) that have been used in this report. More information about these data can be obtained in the respective references.

Table F1 – 45° Test Results From Deng *et al.* (2003)

Specimen Designation	Specimen Identifier	Weld Location	Weld Failed? (Yes or No)	Ultimate Load P_u (kN)	Mean Shear Leg Size (mm)	Mean Tension Leg Size (mm)	Weld Length (mm)	Mean Strain at Pu
F1-1	E70T-4(H)S	Front	No	789	10.3	10.7	73.7	0.074
		Back	Yes		9.5	11.5	72.5	0.093
F1-2		Front	Yes	763	9.9	9.5	71.0	0.082
		Back	No		10.9	9.7	73.4	0.054
F1-3		Front	Yes	745	9.5	10.0	71.7	0.110
		Back	No		11.1	10.4	74.0	0.073
F2-1	E70T-7(H)S	Front	Yes	813	9.5	10.1	71.8	0.125
		Back	No		9.9	11.4	70.8	0.063
F2-2		Front	No	840	10.7	11.2	72.7	0.050
		Back	Yes		10.3	11.0	71.0	0.100
F2-3		Front	Yes	823	9.3	11.0	70.6	0.141
		Back	No		11.0	11.0	75.6	0.069
F3-1	E71T8-K6(H)S	Front	Yes	755	10.0	12.3	70.2	0.143
		Back	No		10.5	13.4	71.1	0.125
F3-2		Front	No	725	10.3	10.7	71.8	0.092
		Back	Yes		9.5	11.5	72.7	0.119
F3-3		Reinforced Welds Failed						

Table F2 – Longitudinal Test Results From Deng *et al.* (2003)

Specimen Designation	Specimen Identifier	Weld Location*	Weld Failed? (Yes or No)	Ultimate Load, P_u (kN)	Mean Shear Leg Size (mm)	Mean Tension Leg Size (mm)	Weld Length (mm)	Mean Strain at Pu
L1-1	E70T-4(H)S	Weld 1	No	731	10.6	11.4	49.6	0.115
		Weld 2	No		8.7	9.4	50.6	0.140
		Weld 3	Yes		10.5	10.6	49.3	0.173
		Weld 4	Yes		10.0	11.0	47.9	0.182
L1-2		Weld 1	Yes	762	11.3	11.5	49.9	0.156
		Weld 2	Yes		11.7	10.4	50.0	0.150
		Weld 3	No		11.0	9.6	50.4	0.146
		Weld 4	No		10.9	9.4	49.6	0.146
L1-3		Weld 1	Yes	740	10.8	11.5	48.3	0.140
		Weld 2	Yes		9.4	10.7	50.8	0.161
		Weld 3	No		10.8	10.1	49.5	0.139
		Weld 4	No		10.3	10.4	49.5	0.146
L2-1	E70T-7(H)S	Weld 1	No	830	10.9	12.0	48.0	0.147
		Weld 2	Yes		10.7	11.4	49.7	0.149
		Weld 3	No		10.8	11.3	49.6	0.152
		Weld 4	No		11.6	11.2	49.5	0.142
L2-2		Weld 1	No	805	10.3	11.0	48.9	0.129
		Weld 2	No		10.0	10.1	50.0	0.132
		Weld 3	No		12.3	11.0	49.9	0.100
		Weld 4	Yes		9.8	11.6	48.9	0.127
L2-3		Weld 1	No	802	11.2	11.9	49.8	0.100
		Weld 2	No		9.8	11.2	49.8	0.114
		Weld 3	Yes		10.5	11.8	46.6	0.154
		Weld 4	No		10.5	11.0	49.2	0.154

* See Figure F1 for Longitudinal Weld Locations

Table F2 continued – Longitudinal Test Results From Deng *et al.* (2003)

Specimen Designation	Specimen Identifier	Weld Location*	Weld Failed? (Yes or No)	Ultimate Load, P_u (kN)	Mean Shear Leg Size (mm)	Mean Tension Leg Size (mm)	Weld Length (mm)	Mean Strain at Pu
L3-1	E71T8-K6(H)S	Weld 1	Yes	743	10.0	11.9	49.3	0.224
		Weld 2	Yes		10.3	10.8	50.5	0.217
		Weld 3	Yes		9.8	10.7	48.9	0.188
		Weld 4	Yes		9.0	10.7	50.1	0.204
L3-2		Weld 1	No	700	9.5	12.2	48.3	0.151
		Weld 2	Yes		9.7	11.4	49.6	0.148
		Weld 3	No		9.6	12.0	50.3	0.179
		Weld 4	No		10.0	11.1	49.2	0.173
L3-3		Weld 1	Yes	750	9.3	11.3	50.9	0.198
		Weld 2	No		11.7	11.5	51.1	0.159
		Weld 3	No		10.7	10.2	52.1	0.181
		Weld 4	No		9.7	9.8	50.2	0.198

* See Figure F1 for Longitudinal Weld Locations

Table F3 – Test Data From Ng *et al.* (2002)

Specimen	Electrode Type	Fracture Side	Fracture Weld Length (mm)	Shear Leg (mm)	Tension Leg (mm)	Ultimate Load (kN)	Weld Metal UTS (MPa)	Average (Δ/d) at Ultimate Load
T1-1	E7014	Front	76.0	6.5	6.6	513	520	0.08
T1-2		Front	76.1	6.5	6.2	502	520	0.08
T1-3		Both	76.1	6.0	6.6	513	520	0.10
T2-1		Front	76.2	5.5	6.2	462	520	0.10
T2-2		Front	76.1	6.0	6.1	474	520	0.11
T2-3		Front	76.1	6.1	6.7	482	520	0.09
T3-1		Front	76.0	7.5	6.6	523	520	0.10
T3-2		Front	76.1	8.0	6.8	518	520	0.07
T3-3		Front	76.0	7.6	7.3	520	520	0.09
T4-1	E70T-4	Back	76.1	6.1	6.1	646	535	0.08
T4-2		Back	76.1	6.3	6.1	651	535	0.07
T4-3		Back	76.1	6.0	6.0	629	535	0.08
T5-1		Back	76.0	6.0	6.1	648	535	0.08
T5-2		Back	76.0	6.3	6.2	632	535	0.09
T5-3		Back	76.0	5.8	5.9	628	535	0.10
T6-1		Front	75.9	6.6	5.1	717	535	0.16
T6-2		Back	76.0	6.7	5.1	663	535	0.13
T6-3		Back	76.0	6.5	5.4	741	535	0.20
T7-1		Low Temperature Tests (Data Not Used)						
T7-2								
T7-3								
T8-1		Test Welds Did Not Fail						
T8-2		Back	75.5	6.5	7.3	683	562	0.20
T8-3		Front	76.3	6.5	7.8	713	562	0.23
T9-1		Back	76.1	8.6	5.8	806	562	0.15
T9-2		Back	76.0	8.3	6.1	809	562	0.19
T9-3		Front	76.0	8.3	6.1	829	562	0.24
T10-1		Front	76.0	7.7	6.6	740	562	0.10
T10-2		Back	76.1	8.2	6.3	794	562	0.11
T10-3		Back	76.0	8.6	6.6	757	562	0.06
T11-1	E70T-7	Front	76.1	6.4	6.7	695	605	0.13
T11-2		Back	76.0	7.1	6.8	680	605	0.08
T11-3		Front	76.2	6.5	7.2	655	605	0.09
T12-1		Back	76.1	7.8	5.4	745	605	0.12
T12-2		Back	75.9	7.8	5.1	769	605	0.12
T12-3		Front	76.1	7.5	6.2	783	605	0.16
T13-1		Front	75.9	6.7	5.2	607	584	0.06
T13-2		Test Welds Did Not Fail						
T13-3		Front	76.0	6.2	5.6	605	584	0.05

Table F3 cont. – Test Data From Ng *et al.* (2002)

Specimen	Electrode Type	Fracture Side	Fracture Weld Length (mm)	Shear Leg (mm)	Tension Leg (mm)	Ultimate Load (kN)	Weld Metal UTS (MPa)	Average (Δ/d) at Ultimate Load
T14-1	E70T-7	Back	76.0	8.7	6.9	769	652	0.08
T14-2		Back	76.1	8.7	6.7	778	652	0.11
T14-3		Front	76.0	7.9	6.9	709	652	0.10
T15-1		Front	76.1	6.8	6.7	781	652	0.06
T15-2		Front	76.0	7.4	7.3	760	652	0.07
T15-3		Front	76.1	7.2	7.0	766	652	0.06
T16-1	E70T7-K2	Back	76.2	7.7	7.5	769	592	0.31
T16-2		Test Welds Did Not Fail						
T16-3		Back	71.6	7.2	6.5	658	592	0.22
T17-1		Front	76.1	9.0	5.1	777	592	0.12
T17-2		Front	76.2	9.6	4.2	715	592	0.05
T17-3		Front	76.2	9.8	4.4	721	592	0.10
T18-1	E71T8-K6	Front	75.9	5.5	6.5	711	490	0.41
T18-2		Back	75.9	5.3	6.1	699	490	0.30
T18-3		Back	75.9	5.3	6.4	711	490	0.31
T19-1		Back	76.1	7.8	6.8	780	493	0.17
T19-2		Back	76.0	8.1	6.0	784	493	0.20
T19-3		Back	76.0	8.0	6.2	744	493	0.19
T20-1	E7014	Front	75.8	13.4	14.2	782	520	0.13
T20-2		Front	76.0	12.8	13.2	949	520	0.17
T20-3		Front	76.0	13.3	14.1	878	520	0.13
T21-1	E70T-4	Front	76.3	11.3	14.0	996	535	0.16
T21-2		Back	76.1	12.1	13.7	981	535	0.14
T21-3		Back	76.1	12.2	13.4	921	535	0.10
T22-1		Front	76.2	9.4	10.6	912	631	0.13
T22-2		Front	76.1	10.3	10.0	903	631	0.11
T22-3		Front	76.0	11.1	10.1	994	631	0.16
T23-1		Front	76.1	12.6	12.8	966	562	0.19
T23-2		Front	75.9	12.5	12.7	920	562	0.14
T23-3		Front	76.1	12.7	13.3	919	562	0.14
T24-1		Back	76.1	11.7	11.8	1014	562	0.20
T24-2		Back	76.0	12.0	11.4	1020	562	0.24
T24-3		Front	76.0	13.4	10.7	995	562	0.14
T25-1	E70T-7	Test Welds Did Not Fail						
T25-2		Front	76.0	12.3	11.8	999	605	0.11
T25-3		Back	76.0	13.3	10.9	1020	605	0.14
T26-1		Front	76.0	12.4	11.6	1060	605	0.17
T26-2		Back	76.1	12.7	11.2	1068	605	0.16
T26-3		Back	76.2	13.0	11.6	1062	605	0.13

Table F3 cont. – Test Data From Ng *et al.* (2002)

Specimen	Electrode Type	Fracture Side	Fracture Weld Length (mm)	Shear Leg (mm)	Tension Leg (mm)	Ultimate Load (kN)	Weld Metal UTS (MPa)	Average (Δ/d) at Ultimate Load
T27-1	E70T-7	Front	76.3	12.8	11.4	841	584	0.09
T27-2		Back	76.2	11.8	12.0	943	584	0.12
T27-3		Back	76.2	11.6	11.8	945	584	0.08
T28-1		Front	76.1	13.8	10.6	990	652	0.14
T28-2		Back	76.1	12.2	10.8	999	652	0.12
T28-3		Back	76.0	12.9	10.9	991	652	0.11
T29-1	E70T7-K2	Test Welds Did Not Fail						
T29-2		Test Welds Did Not Fail						
T29-3		Test Welds Did Not Fail						
T30-1		Test Welds Did Not Fail						
T30-2		Back	76.0	13.7	9.6	1073	592	0.19
T30-3		Front	76.0	12.3	10.4	1056	592	0.25
T31-1	E70T8-K6	Back	76.2	10.5	12.4	1036	490	0.27
T31-2		Back	76.2	10.7	12.1	1004	490	0.23
T31-3		Back	76.1	10.3	11.4	1014	490	0.21
T32-1		Back	76.2	12.2	12.7	1044	493	0.27
T32-2		Back	76.1	12.1	12.7	1049	493	0.24
T32-3		Front	76.0	10.5	12.9	1022	493	0.30

Table F4 – Test Data From Miazga and Kennedy (1989)

Specimen Designation	AWS Classification	Ultimate Load (kN)	Mean Leg Size (mm)	Measured Total Leg Length (mm)	Average (Δ/d) at Ultimate Load
90.1		421	5.3	200	0.19
90.2		431	5.3	200	0.19
90.3		407	5.3	201	0.19
75.1		466	5.1	215	0.14
75.2		451	5.0	211	0.11
75.3		471	5.1	210	0.17
60.1		568	5.1	230	0.11
60.2		566	5.1	231	0.10
60.3		559	5.0	226	0.10
45.1		447	5.4	204	0.08
45.2		433	5.1	200	0.08
45.3		419	5.1	196	0.08
30.1		614	5.3	294	0.08
30.2		626	5.5	302	0.07
30.3		610	5.3	296	0.08
15.1		484	5.2	306	0.06
15.2		477	5.1	313	0.05
15.3		482	5.1	311	0.07
00.1		513	4.9	316	0.06
00.2		487	5.2	309	0.06
00.3	E7014	483	5.2	315	0.07
90.11		789	9.1	197	0.07
90.12		807	9.3	200	0.05
90.13		791	9.2	200	0.08
75.11		822	9.2	211	0.07
75.12		810	9.1	207	0.06
75.13		805	9.2	209	0.07
60.11		895	9.4	226	0.05
60.12		892	9.7	229	0.04
60.13		894	9.9	228	0.05
45.11		842	9.4	272	0.05
45.12		858	9.5	279	0.05
45.13		861	9.2	279	0.04
30.11		980	9.4	296	0.05
30.12		968	9.2	296	0.05
30.13		989	9.7	294	0.04
15.11		773	8.8	300	0.06
15.12		724	9.2	294	0.04
15.13		815	9.1	294	0.07
0.11		752	9.5	300	0.05
0.12		825	9.1	321	0.05
0.13		787	9.2	316	0.04

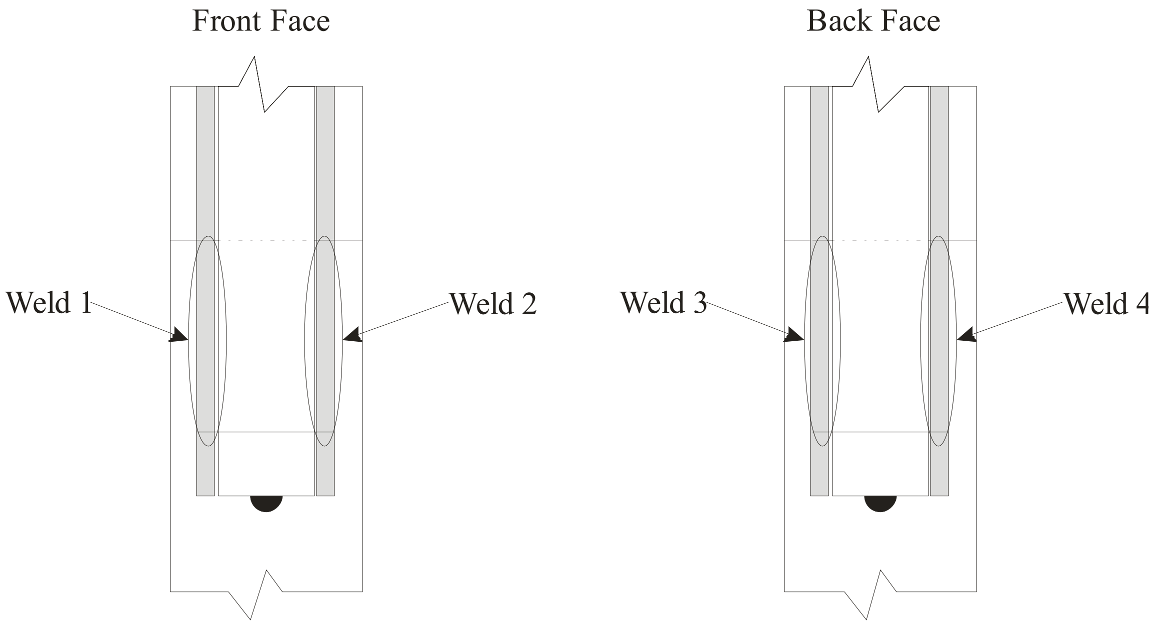

Figure F1 – Weld Locations for Longitudinal Weld Test From Deng *et al.* (2003)

Structural Engineering Reports

241. *Punching Shear Capacity of Slab-Column Connections with Steel-Fibre reinforcement under Lateral Cyclic Loading* by Sascha K. Schreiber and Scott D.B. Alexander, September 2001.

242. *Behaviour of Slabs with Fibre-Reinforced Polymer Reinforcement* by Carlos E. Ospina, Roger J.J. Cheng, and Scott D.B. Alexander, October 2001.

243. *Behaviour of Slab-Column Connections with Partially Debonded Reinforcement under Cyclic Lateral Loading* by M.A. Ali and S.D.B. Alexander, January 2002.

244. *Block Shear Behaviour of Coped Steel Beams* by Cameron R. Franchuk, Robert G. Driver, and Gilbert Y. Grondin, September 2002.

245. *Behaviour of Transverse Fillet Welds* by Anthony K.F. Ng, Robert G. Driver, and Gilbert Y. Grondin, October 2002.

246. *Analysis of Buried Pipelines with Thermal Applications* by Nader Yoosef-Ghodsi, and D.W. Murray, October 2002.

247. *Fracture of Wrinkled Energy Pipelines* by Das, S., Cheng, J.J.R., Murray, D.W., November 2002.

248. *Block Shear Behaviour of Bolted Gusset Plates* by Bino Baljit Singh Huns, Gilbert Y. Grondin, and Robert G. Driver, December 2002.

249. *Numerical Solutions for Pipeline Wrinkling* by Song, X., Cheng, J.J.R., Murray, D.W., January 2003.

250. *Behaviour of Steel Columns Reinforced with Welded Steel Plates* by Ziqi Wu and Gilbert Y. Grondin, February 2003.

251. *Effect of Loading Angle on the Behaviour of Fillet Welds* by Kam Deng, Gilbert Y. Grondin, and Robert G. Driver, March 2003.

252. *Experimental and Numerical Analysis of FPR Sheets Bonded to Concrete* by Ayman M.S. Kamel, Alaa E. Elwi, and J.J.R. Cheng, January 2003.

253. *Assessment and Rehabilitation of FC Girder* Bridges by Nadeem Khattak and J.J.R. Cheng, April 2003.

254. *Experimental and Numerical Investigation of Steel Plate Shear Walls* by M.R. Behbahanifard, G.Y. Grondin, and A.E. Elwi, September 2003.

255. *Strength and Behaviour of Multi-Orientation Fillet Weld Connections* by L. J. Callele, G.Y. Grondin, and R.G. Driver, October 2004.